LATVIJAS UNIVERSITĀTE
FIZIKAS UN MATEMĀTIKAS FAKULTĀTE

Tatjana Glaskova

Fizikas, astronomijas un mehānikas doktora studiju programmas studente

POLIMĒRU NANOKOMPOZĪTMATERIĀLU TERMOFIZIKĀLO UN MEHĀNISKO ĪPAŠĪBU EKSPERIMENTĀLĀ IZPĒTE UN MODELĒŠANA

Promocijas darbs

Zinātniskais vadītājs:

Dr. Sc. Ing. Andrejs Aņiskevičs

Polimēru mehānikas institūts

Latvijas Universitāte

Rīga, 2010

Saturs

Promocijas darba kopsavilkums latviešu valodā

LATVIJAS UNIVERSITĀTE
FIZIKAS UN MATEMĀTIKAS FAKULTĀTE

Tatjana Glaskova

Promocijas darba kopsavilkums
Promocijas darba veids: zinātnisku publikāciju kopa

POLIMĒRU NANOKOMPOZĪTMATERIĀLU TERMOFIZIKĀLO UN MEHĀNISKO ĪPAŠĪBU EKSPERIMENTĀLĀ IZPĒTE UN MODELĒŠANA

Doktora zinātniskā grāda iegūšanai fizikā

Apakšnozare: polimēru un kompozītmateriālu mehānika

Zinātniskais vadītājs:

Dr. Sc. Ing. Andrejs Aņiskevičs

Polimēru mehānikas institūts

Latvijas Universitāte

Rīga, 2010

Anotācija

Promocijas darbā ir apkopoti mehānisko un termofizikālo īpašību kompleksā pētījuma rezultāti epoksīda bāzes nanokompozītmateriāliem, kas ir izklāstīti zinātnisko rakstu kopas veidā.

Polimēri un kompozīti parasti ir pakļauti ārējo faktoru (temperatūra, mitrums, mehāniskās slodze utt.) ietekmei, kas izraisa laikā atkarīgo struktūras un īpašību maiņu, fizikālo un ķīmisko pārvērtību dēļ. Tādējādi, paredzot, kompozītmateriālu mehāniskās un termofizikālās īpašības, ir jāņem vērā pētījuma rezultāti par polimēra sveķu struktūras un īpašību atkarību no laika, ārējo faktoru iedarbībā.

Darba mērķis ir noteikt mitruma absorbcijas īpatnības un novērtēt absorbētā mitruma ietekmi uz mehāniskajām un termofizikālajām īpašībām epoksīda bāzes nanokompozītmateriāliem.

Šajā nolūkā vispirms eksperimentāli ir pētīta epoksīda saistvielu un to bāzes kompozītu mitruma absorbcijas kinētika plašā mitruma intervālā. Mitruma absorbcijas kinētikas raksturošanai ir veikta zināmo sorbcijas modeļu salīdzinošā analīze un analizētas to atbilstības īpatnības. Piedāvāts modelis, kas ņem vērā starpfāzes ietekmi, pamatojoties uz rezultātiem, kas iegūti nanokompozīta līdzsvara mitruma daudzumam. Pieņemts, ka šī slāņa blīvums ir zemāks nekā polimēra blīvums sakarā ar savstarpējas sasaistes atšķirību. Pierādīts, ka pildvielas daudzuma un, sekojoši, starpfāzes palielināšanās nosaka lielāku mitruma absorbciju kompozītmateriālos.

Epoksīdsveķu relatīvi augsta mitruma absorbcija izraisa to struktūras un īpašību izmaiņas laikā, kas noved pie kompozītu elastības īpašību pasliktināšanas. Kompozītmateriālu elastības raksturlielumi ir eksperimentāli pētīti, kā arī aprakstīti, izmantojot mikromehāniskos modeļus. Pierādīts, ka kompozītmateriālos polimēru sveķu elastības modulis ir atkarīgs no pildvielas satura un samazinās, pieaugot mitruma daudzumam. Ir sniegta pildvielas daļiņu morfoloģisko īpatnību (slāņveida struktūra un starpfāzes veidošanās) ievērošana kompozītmateriālā, un to ietekme uz kompozīta elastības raksturlielumiem.

Epoksīda sveķu un epoksīda sveķu-nanomāla kompozīta viskoelastīgā uzvedība ir analizēta pēc ilgtermiņa mitruma ietekmes. Termomehāniskās analīzes pielietošana ļauj noteikt pamata likumsakarības nanokompozīta stiklošanās temperatūrai ar dažādu pildvielas saturu un pie dažādiem mitruma daudzumiem. Eksperimentāli iegūtās nanokompozīta šļūdes un atslodzes līkņu saimes pie dažādām pildvielas un mitruma satura vērtībām ir aproksimētas, izmantojot Bolcmaņa-Volterra lineāro integrālo vienādojumu, ņemot vērā mitruma-laika analoģijas principu. Pierādīts, ka mitruma-laika redukcijas funkcija korelē ar nanokompozīta paraugu piespiestās elastības robežas un tilpuma izmaiņām pie mitrināšanas, kas norāda uz

nanokompozītmateriālu deformācijas viskoelastīgo raksturu, ko apstiprina termomehāniskās analīzes rezultāti.

Promocijas darba galvenie rezultāti ir publicēti 6 zinātniskajos rakstos [P] un 3 konferences krājumos [C], kā arī ir apspriesti 12 starptautiskās konferencēs.

Pētījumi ir veikti Latvijas Universitātes Polimēru mehānikas institūtā 2003.-2010. gadu periodā.

Saturs

1. Ievads, darba mērķis, un uzdevumi

Atzīts, ka visas cilvēces attīstības vēsture ir saistīta ar dažādu veidu kompozītmateriālu (KM) izgudrošanu, kas kļuva par tehnikas un civilizācijas attīstības stimulu. Pirmie ķieģeļi un keramika, kas ir parādījušies apm. 5000 gadu pirms mūsu ēras, tika pastiprināti ar akmeņiem vai salmiem. Senie podnieki savos produktos regulēja pat porainību. Pirmā gadu tūkstoša sākumā romieši izgudroja betonu, kas lielā mērā ietekmēja būvniecības un civilizācijas attīstību.

Pašlaik ir novērojama strauja zinātnes un tehnikas attīstība. Šai mūsdienu tehnikas attīstībai ir nepieciešami jauni materiāli ar uzlabotām īpašībām. Proti, ir vajadzīgi materiāli ar augstu ilgizturību, cietību, izturību pret siltumu, koroziju utt., kā arī šo īpašību kombinācijas. Galvenās polimēru kompozītu priekšrocības, salīdzinot ar tradicionālajiem materiālu veidiem (metāliem, keramiku, koksni u.c.), ir unikālā īpašību (izturības, deformācijas, trieciena, elastības, reoloģisko, adhēzijas, elektrisko, berzes, termofizikālo u.c.) kombinācija, kā arī iespēja kontrolēt materiāla īpašības, mainot sastāvu un ražošanas apstākļus.

Epoksīdsveķu mitruma absorbcija noved pie to laikā atkarīgās struktūras izmaiņām un, sekojoši, pie to īpašību pasliktināšanās. Lai samazinātu šo negatīvo mitruma ietekmi uz polimēru kompozītu funkcionālām, struktūras un mehāniskajām īpašībām, zinātnē un rūpniecībā liela uzmanība ir pievērsta polimēra-slāņainā silikāta nanokompozītmateriāliem (NK). Polimēra NK ietver dažāda veida saistvielas (termoplastus, reaktoplastus vai elastomērus), pildītas ar nelielu daudzumu (mazāk nekā 6% pēc masas) nano-izmēra (mazāk nekā 100 nm vismaz vienā dimensijā) daļiņām. Viena no vispievilcīgākajām un noderīgākajām īpašībām, kas nav pilnībā izpētīta līdz šim brīdim, ir materiālu lieliskā barjeras spēja ar ievērojami samazinātu mitruma un gāzu caurlaidību. Šī nosacījuma izpildei ir nepieciešams, lai silikātu plāksnītes ar lielu malu (garuma pret biezumu) attiecību tiktu sadalītas individuālās daļiņās un tad homogēni novietotas polimēru saistvielā [1]. Pilnīgā māla nanodaļiņu dispersitāte polimērā optimizē iespējamo pastiprinošo elementu skaitu slodzes izturēšanai un plaisu novirzīšanai. Māla milzīgās īpatnējās virsmas ($S \approx 800$ m^2/g) un polimēra saistvielas sasaiste veicina sprieguma pārnesi pastiprinājuma fāzei, rezultātā novedot pie stiprības un cietības uzlabojumiem [2].

Viena no spilgtākajām silikāta nanopildvielām ir montmorillonīts (MMT). Tas pieder pie minerālvielu filosilikātu (phyllosilicate) grupas, kas parasti veido mikroskopiskus kristālus. MMT, smektītu ģimenes elements ir 2:1 māls, kas nozīmē, ka to struktūru veido 2 četrskaldņu slāņi ar iesprausto starp tiem centrālo astoņskaldņu slāni. Daļiņām ir apaļa plākšņu forma ar vidējo biezumu viens nanometrs un diametru aptuveni viens mikrometrs. Pateicoties MMT nanodaļiņu, ar augstu garuma pret biezumu attiecību (turpmāk malu attiecību), sadalīšanai polimēru saistvielā, iegūtā sistēma var efektīvi darboties kā kompozīts ar anizotropām īpašībām

nanolīmenī. NK pievilcīgie raksturlielumi noder dažādos rūpnieciskos pielietojumos: automobiļu rūpniecībā (gāzes tvertnes, bamperi, iekšējie un ārējie paneļi), būvniecībā (ēkas daļas un celtniecības paneļi), aviācijas rūpniecībā (liesmas palēninātāja paneļi un augstās veiktspējas komponenti), elektrības un elektronikas pielietojumos (elektriskie komponenti un iespiedshēmu plates), pārtikas iepakojumu (taras un iesaiņojuma plēves) ražošanā [3, 4]. Polimēru KM ražošana un to īpašību izpēte pieder pie materiālzinātnes nozares. Tā ir viena no prioritārajām zinātnes nozarēm Latvijā ("Inovācijas materiāli un tehnoloģijas (nanostrukturētie daudzfunkcionālie materiāli un nanotehnoloģijas)") un pasaulē.

Plaši izmantotie kompozīta saistvielas epoksīda sveķi ir ļoti pievilcīgi, ņemot vērā to augsto izturību un stingrību, augsto siltuma pretestība, zemo gaistamību, šļūdi un rukumu, labu adhēziju ar metālu un keramiku. Tomēr epoksīda sveķu liels trūkums ir mitruma absorbcija, kas pasliktina kompozītu funkcionālās, struktūras un mehāniskās īpašības [5-7].

Ir svarīgi izpētīt NK mehāniskās, termiskās un barjeras īpašības un novērtēt to noturību pret vides faktoru iedarbību. Polimēra NK uzlabotā noturība varētu paplašināt to pielietošanas iespējas tehnikā un būvniecībā.

Polimēru struktūras un īpašību izmaiņas laikā, ārējo faktoru (temperatūra, mitrums, slodze, u.c.) iedarbībā, fizikālo un ķīmisko pārvērtību dēļ, izraisa izmaiņas KM struktūrā un īpašībās. Lai prognozētu cik lielā mērā izmainās KM struktūra un īpašības, ir jāizmanto pētījumu rezultāti polimēru struktūrai un īpašībām, kas, savukārt, ir atkarīgi no laika.

Parasti polimēru sveķu KM ir nehomogēna struktūra, veidojot starpfāzi ar noteiktu robežu netālu no pildvielas daļiņām. Starpfāzes blīvums var būt lielāks vai mazāks par polimēra blīvumu, sašūšanas un porainības pakāpes atšķirības dēļ. Tādējādi, pildvielas daļiņu morfoloģiskās īpatnības (slāņveida struktūra un starpfāzes veidošanās tuvu daļiņas robežai) var ietekmēt kompozīta īpašības: elastības un stiprības īpašības, mitruma absorbcijas kinētiku, izplešanās un sabrukuma raksturu.

Šī darba mērķis ir noteikt epoksīda sveķu un epoksīdsveķu-māla NK mitruma absorbcijas īpatnības un novērtēt absorbētā mitruma ietekmi uz NK mehāniskajām un termofizikālajām īpašībām.

Šim nolūkam ir noteikti sekojoši darba uzdevumi:

1. Noskaidrot eksperimentālās likumsakarības un modelēt epoksīda saistvielu un epoksīda-māla NK mitruma absorbcijas kinētiku plašā mitruma diapazonā;
2. Noteikt mitruma ietekmi uz epoksīda-māla NK un tā sastāvdaļu deformējamību, aprakstīt NK mehāniskās īpašības ar analītiskajiem modeļiem, ņemot vērā pildvielas daļiņu morfoloģiskās īpatnības, kā arī novērtēt mitruma ietekmi uz NK deformējamību, iekļaujot NK sastāvā silikāta nanodaļiņas;

3. Prognozēt ilgtermiņa šļūdi pētāmajiem materiāliem, izmantojot mitruma-laika analoģijas metodi, novērtēt retardācijas laika spektra un redukcijas funkcijas izmaiņas polimēram, iekļaujot sastāvā silikāta nanodaļiņas;

4. Noteikt termofizikālo un mehānisko īpašību sasaisti epoksīda-māla NK, tām absorbējot mitrumu, ar izmaiņām struktūrā deformēšanās procesā pie dažādām slodzes un temperatūras eksperimentālajām shēmām.

2. Pārskats par pašreizējām zinātniskajām atziņām epoksīda saistvielu un epoksīda bāzes-nanomāla kompozītu mehānisko un termofizikālo īpašību izpētē

Polimēru kompozītmateriāli ir bieži pakļauti mitruma ietekmei. Ūdens molekulas, kā arī zemmolekulārās vielas, spēj pārvietoties polimēra saistvielā un mainīt tās fizikālās īpašības. Galvenie parametri, kas nosaka mitruma absorbcijas mehānismu, ir polimēru ķīmiskais sastāvs un mikrostruktūra.

Epoksīda sveķu un to bāzes kompozītu mitruma absorbcija ir pietiekami labi izpētīta. Piedāvāti dažādi modeļi ūdens sorbcijas kinētikas aprakstīšanai [8-10]. Pieņemts, ka epoksīda sveķu mitruma absorbcija notiek difūzijas dēļ, saskaņā ar Fika (Fick) likumu [8, 11]. Šis modelis, kurš ir labi piemērots mitruma sorbcijai sākotnējā posmā, bieži vien ir neatbilstošs mitruma sorbcijas procesa aprakstīšanai kopumā. Mitruma absorbcija var aktivizēt dažādus procesus materiālos (ķīmiskās reakcijas, zemmolekulāro sastāvdaļu izskalošanās u.c.), kas, savukārt, ietekmē mitruma absorbcijas kinētiku. Tādējādi, katram pētāmajam materiālam, ir nepieciešams novērtēt dažādu mitruma pārneses modeļu pielietojamību, kā arī noteikt vispiemērotāko modeli ūdens sorbcijas eksperimentālo datu aprakstīšanai.

Absorbētā mitruma ietekmes samazināšanai uz polimēru kompozītu funkcionālām, struktūras un mehāniskajām īpašībām zinātnē un rūpniecībā liela uzmanība ir pievērsta polimēra-slāņainā silikāta NK. Tas saistīts ar šo materiālu izcilajām īpašībām un jaunām pielietošanas iespējām [12-14].

Pateicoties augstai dimensionālai anizotropijai un īpatnējai virsmai, silikāta slāņi darbojas kā efektīvas barjeras pret mitruma pārnesi cauri materiālam un izraisa molekulu trajektorijas garuma palielināšanos, difundējot polimēram cauri. Tā kā ūdens absorbcijas dēļ samazinās hidrofīlo polimēru elastības raksturlielumi, nanodaļiņu iekļaušana ūdens absorbcijas negatīvās ietekmes samazināšanai ir īpaši noderīga [6, 15-16]. Savukārt, mitruma absorbcijas samazināšanās ļauj pārvarēt iekšējos bojājumus un noved pie NK uzlabotās ilgtermiņa uzvedības.

Lai gan literatūrā ir daudz datu par polimēra-silikātu NK sintēzes metodēm, eksperimentiem un raksturojumiem, fundamentālie mehānismi nav pilnībā skaidri, tie ir nepietiekami apspriesti [17]. Tādēļ, NK ātrākai attīstībai un pielietošanai, ir nepieciešamas to labāka izpratnes un prognozēšanas iespējas.

Jāuzsver, ka divu komponenšu kompozītu efektīvas īpašības ir plaši izpētītas, ir izstrādāti un pielietoti dažādi mikromehānikas modeļi [18-25]. Šī veida modeļu pamatā ir elastīgs

risinājums bezgalīgai saistvielai ar vienu pildvielas daļiņu. Tomēr daudzi autori ieteica ievērot ne tikai divu pamatfāzu, bet arī to starpfāzes īpašības [20, 21].

Polimēra-māla NK struktūras hierarhiju var iedalīt vismaz divos stāvokļos: 1) pilnīgas eksfoliācijas stāvoklis māla plāksnītēm ar raksturīgiem parametriem – apaļo plākšņu biezumu un diametru; un 2) nepilnīgas eksfoliācijas stāvoklis māla plāksnītēm ar raksturīgiem parametriem – interkalētu (iestarpinātu) slāņu kopas biezumu un izmēriem plaknē [25]. Anizotropisko daļiņu malu attiecība un orientācija nosaka to pastiprinājuma pakāpi. Neskatoties uz to, ka ir diezgan grūti kontrolēt plakano daļiņu orientāciju kompozītmateriālu izgatavošanas procesā, to orientācijas reālais sadalījums var būt diezgan sarežģīts. Efektīvo elastīgo konstanšu noteikšanai NK, ar transversāli izotropiem silikātu slāņiem, ar koplanāru orientāciju, ir būtiska nozīme. Datus, kas ir iegūti šajā gadījumā, var izmantot kā orientējošos datus tālākai elastīgo īpašību analīzei kompozītam ar haotiski novietotām nanodaļiņām, ņemot vērā to orientācijas sadalījumu materiālā [25].

Ir jāievēro slāņveida silikāta anizotropija. Montmorillonīta māla atsevišķs slānis ir monoklīnais kristāls, kas sastāv no diviem silīcija četrskaldņu slāņiem un centrālā astoņskaldņu slāņa [22]. Ņemot vērā četrskaldņa sešstūra konfigurāciju divās četrskaldņu loksnēs un montmorillonīta māla slāņaino struktūru, pieņem, ka silikāta slāņu kopa ir transversāli izotropa vide. Interkalētā silikātu kompozīta gadījumā slāņaina struktūra paliek, bet, t. s., galerijas starp slāņiem ir aizpildītas ar polimēru. Vispārīgi šo gadījumu var uzskatīt kā transversāli izotropu vidi.

Interkalētā NK gadījumam var izmantot Halpina-Tsai (Halpin-Tsai) vienādojumus [25, 26], iegūtiem izotropai polimēra saistvielai, pildītai ar koplanāri novietotām transversāli izotropām cilindriskām daļiņām, ar patvaļīgu izmēru attiecību. Elastīgais risinājums ir iegūts kompozītam ar vienu šķiedru cilindra saistvielas apvalkā. Tas ir ievietots neierobežotā viendabīgā vidē, kura ir makroskopiski neatšķirama no kompozīta. Sprieguma un deformācijas komponenšu attiecībām ir jābūt novidējotām pa visu kompozītu. Formulas, precīziem elastības risinājumiem, kompozītam ar patvaļīgu daļiņu izmēru attiecību, iegūtas no līkņu aproksimācijas un ir apstiprinātas ar eksperimentālajiem mērījumiem.

Mehāniskajām parādībām, kas notiek polimēru kompozītu materiālos sorbcijas un izplešanās procesos, piemīt noteikta teorētiskā un praktiskā nozīme, taču tās ir nepietiekami izpētītas. Sevišķi NK, kas ir svarīgi augstās efektivitātes materiālu attīstīšanai. Piemēram, lielākajā daļā rakstu [2, 6, 14] ir parādītas māla NK uzlabotas mehāniskās, termofizikālās un barjeras īpašības, salīdzinot ar nepildītiem polimēriem. Tomēr nekāda informācija par tajos notiekošiem procesiem nav dota.

Līdz ar to ir būtiski noteikt attiecību starp māla-polimēru NK termofizikālajām un mehāniskajām īpašībām, mitruma absorbcijas procesā, un struktūras izmaiņām, kas notiek deformācijas procesā dažāda veida eksperimentos un pie dažādām temperatūrām.

Visbeidzot, mūsdienu materiālu, polimēru nanokompozītmateriālu, izmantošana dažādās tehnikas, būvniecības, kā arī elektronikas nozarēs, pieprasa ilgtermiņa deformējamības un izturības novērtēšanu dažādu vides faktoru apstākļos (slodze, paaugstinātā un/vai mainīgā temperatūra un mitrums). Tradicionālo KM (polimēru pildītu ar minerālvielu mikrodaļiņām, kompozītiem, pastiprinātiem ar oglekļa un stikla šķiedrām) ilgtermiņa deformējamības un izturības prognozēšanai ir pielietota sprieguma-laika, temperatūras-laika un mitruma-laika analoģijas metode [28, 29]. Šīs metodes pamatā ir laika reducēšana paātrinātu relaksācijas procesu pieauguma dēļ, palielinot slodzes līmeni, temperatūru un relatīvā mitruma saturu materiālā, ko raksturo redukcijas funkcija. Temperatūras-laika redukcijas funkcija, kas raksturo šļūdes ātruma izmaiņu temperatūras izmaiņas dēļ, NK ir augstāka, salīdzinot ar polimēru sveķiem.

Tādējādi, ir nepieciešama dažādu epoksīda sveķu un epoksīda-nanomāla kompozītu mehānisko un termofizikālo īpašību kompleksā izpēte par mūsdienu kompozītmateriālu noturību pret dažādiem vides faktoriem (temperatūra, mitrums, slodze, u.c.), kas ļaus novērtēt polimēru-nanomāla KM pielietošanas iespējas.

3. Pārskats par darbā izmantojamiem materiāliem un metodēm

Darbā ir izmantotas sekojošas termoreaktīvo polimēru saistvielas: 1) epoksīda sveķi ED 22, kas tika cietināti ar polietilēna poliamīdu un dispersi pildīti ar LiF kristāliem (pildvielas saturs 0,05, 0,11, 0,23, 0,28, 0,33, 0,38 un 0,46% pēc masas); 2) epoksīda sveķi Reapox 520; un 3) bisfenola epoksīda sveķi, kas tika cietināti ar polipropilēna oksīdu un pildīti ar montmorillonīta māla daļiņām (pildvielas saturs 2, 4 un 6% pēc masas).

Mitruma absorbcijas kinētika ir eksperimentāli pētīta ar sorbcijas metodi vidēs ar relatīvo mitrumu φ = 24, 34, 53, 77, 84 un 98%, izmantojot silikagelu un attiecīgi piesātinātu sāļu $MgCl_2$, $Mg(NO_3)_2$, NaCl, KCl, and K_2SO_4 šķīdumus. Nosakot izmaiņas pētāmo materiālu masā, absorbcijas eksperimentos ir izmantoti plāni plākšņveida paraugi. Tie nosaka sorbcijas norisi viendimensijas difūzijas režīmā. Paraugi tika novietoti mitrās vidēs istabas temperatūrā un tika regulāri nosvērti ar precizitāti 0,00005 g, izmantojot analītiskos svarus *Mettler Toledo XS 205DU*. Masas pieaugums $m(t)$-m_0 ir izmantots mitruma daudzuma noteikšanai mitruma absorbcijas laikā

$$w(t) = \frac{m(t) - m_0}{m_0} .$$

Pielietotas dažādas mehāniskās pārbaudes metodes: 1) kvazistatiskās stiepes eksperimenti, saskaņā ar LVS EN ISO 527 standartu, izmantojot Zwick 2,5 testēšanas mašīnu ar tvērēj spaiļu ātrumu 5 mm/min istabas temperatūrā; 2) šļūdes eksperimenti vienass stiepē, saskaņā ar ASTM D2990 standartu istabas temperatūrā, izmantojot šļūdes pārbaudes stendus ar sprieguma līmeni - pusi no stiepes stiprības, šļūdes eksperimentu ilgums - 7 st (slodze), 17 st (atslodze).

Pētāmo materiālu struktūras un īpašību izmaiņu noteikšanai sorbcijas procesā ir pielietotas sekojošās metodes: 1) diferenciāli skenējošās kalorimetrijas analīze, izmantojot ierīci *Mettler DSC 30* temperatūras diapazonā no -50 līdz 150 °C ar sildīšanas ātrumu 10 °C/min; 2) termogravimetrijas metode, izmantojot ierīci *Mettler TA 3000* temperatūras diapazonā 20-280 °C, ar sildīšanas ātrumu 10 °C/min; 3) diferenciālā termiskā analīze, izmantojot ierīci *UIP-70M*, paraugus sildot līdz 150 ^{o}C, ar sildīšanas ātrumu 2 ^{o}C/min; un 4) rentgena difrakcijas metodes analīze, izmantojot ierīci *DRON-3M*, ar $Cu_{K\alpha}$ starojumu, ar 0,1 ^{o} soli un impulsu savākšanas laiku 90 sek.

Visu NK paraugu caurspīdīgums liecina par labu pildvielas daļiņu dispersitāti (pildvielas daļiņu izmērs ir mazāks nekā redzamās gaismas viļņa garums (400-700 nm)). Pildvielas nanodaļiņu (montmorillonīta māla) struktūra ir papildus pētīta ar mikroskopijas metodēm, piemēram, skanējošo elektronu (SEM) un transmisijas (TEM) mikroskopiem.

4. Mitruma absorbcijas modelēšana kompozītmateriāliem

4.1. Sorbcijas modeļu pielietošana epoksīda sveķu mitruma absorbcijas kinētikas aprakstīšanai

[P2]

Kā iepriekš minēts, mitruma absorbcija epoksīdsveķiem izraisa laikā atkarīgas struktūras izmaiņas un tām sekojošo īpašību pasliktināšanos. Absorbētais mitrums materiālā var aktivizēt dažādus procesus. Tas, savukārt, ietekmē ūdens sorbcijas kinētiku (ķīmiskās reakcijas, zemmolekulāro komponenšu izskalošanās u.c.). Tāpēc katram pētāmajam materiālam ir nepieciešams novērtēt dažādu mitruma pārneses modeļu pielietojamību mitruma absorbcijas eksperimentālo datu aprakstīšanai un noteikt vispiemērotāko modeli.

Epoksīda sveķiem mitruma absorbciju bieži apraksta ar Fika modeli [9, 11, 27, 30]. Šajā modelī [8] ir pieņemts, ka absorbcija notiek tikai ūdens molekulu difūzijas dēļ un, saskaņā ar pirmo Fika likumu, difundējošās vielas plūsmas blīvums $\boldsymbol{j}$ ir tieši proporcionāls tā koncentrācijas gradientam C

$$\boldsymbol{j} = -D \operatorname{grad} C, \tag{4.1}$$

kur D ir difūzijas koeficients, kas raksturo mitruma absorbcijas ātrumu un ir neatkarīgs no mitruma koncentrācijas. Ņemot vērā masas saglabāšanas likumu, nestacionārā stāvoklī ir spēkā otrais Fika vienādojums. Viendimensijas difūzijas gadījumā gar x asi, kad parauga biezums ir mazāks nekā tā garums un platums, tas ir definēts kā

$$\frac{\partial C}{\partial t} = D \frac{\partial^2 C}{\partial x^2}, \tag{4.2}$$

kur C ir mitruma koncentrācija paraugā laika momentā t.

Vienādojuma (4.1) risinājumam plakanparalēlai plāksnei ar biezumu h pie sākuma C ($0 < x < h$, $t = 0$) = C_0 un robežnosacījumiem C ($x = 0$, $x = h$, $t > 0$) = C_∞ ir sekojoša izteiksme [8]

$$C(x,t) = C_\infty - 2\frac{(C_\infty - C_0)}{\pi}\sum_{k=1}^{\infty}\frac{\left(1-(-1)^k\right)}{k}\sin\left(\frac{\pi k}{h}x\right)\exp\left(-\left(\frac{\pi k}{h}\right)^2 Dt\right). \tag{4.3}$$

Integrējot vienādojumu (4.3) pa plāksnes biezumu, ir dabūta izteiksme mitruma daudzuma noteikšanai paraugā:

$$w(t) = w_\infty - 2\frac{(w_\infty - w_0)}{\pi^2}\sum_{k=1}^{\infty}\frac{\left(1-(-1)^k\right)^2}{k^2}\exp\left(-\left(\frac{\pi k}{h}\right)^2 Dt\right). \tag{4.4}$$

Šeit w_∞ ir robežmitruma daudzums paraugā. Šim modelim ir divi parametri: difūzijas koeficients D un robežmitruma daudzums w_∞. Ja sorbcijas līkni attēlot pret kvadrātsakni no

laika, tad diagrammas sākuma intervālu var aprakstīt ar taisni, kas iziet no koordināšu sākumpunkta [8]. Izmantojot eksperimentālos datus, difūzijas koeficientu var noteikt no šīs taisnes noliekuma:

$$D = \frac{\pi h^2}{16t} L^2, \tag{4.5}$$

kur $L = \frac{w(t) - w_0}{w_\infty - w_0}$ ir mitruma daudzuma $w(t)$-w_0 izmaiņas paraugā laika momentā t, kas ir normētas uz tās maksimālo vērtību.

Otrais modeļa parametrs ir robežmitruma daudzums. To parasti nosaka kā maksimālo, eksperimentāli sasniegto, mitruma daudzumu paraugos. Jāatzīmē, ka atbilstoši izteiksmei (4.4) šis maksimālais līmenis ir sasniegts tikai asimptotiski, kad $t \to \infty$. Tas noved pie kļūdas, nosakot w_∞. Attiecība starp difūzijas koeficientu, kas noteikts pēc izteiksmes (4.5) un vides relatīvo mitrumu φ epoksīda Reapox 520 paraugiem, ir parādīta Att. 4.1.

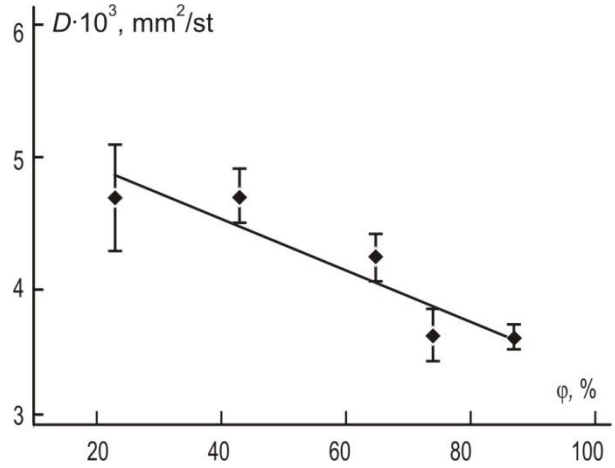

Att. 4.1. Difūzijas koeficients atkarībā no vides relatīvā mitruma.

Mitruma satura aprēķinu rezultāti pēc izteiksmes (4.4), kā arī eksperimentālie dati epoksīda Reapox 520 paraugiem, vidēs ar dažādu relatīvo mitrumu, ir parādīti Att. 4.2. Redzams, ka Fika modelis labi apraksta mitruma absorbcijas procesu atmosfērās ar zemu relatīvo mitrumu, bet, gadījumos, kad relatīvais mitrums pārsniedz 75%, mitruma sorbcijas process palēninās sorbcijas līknes vidējā daļā.

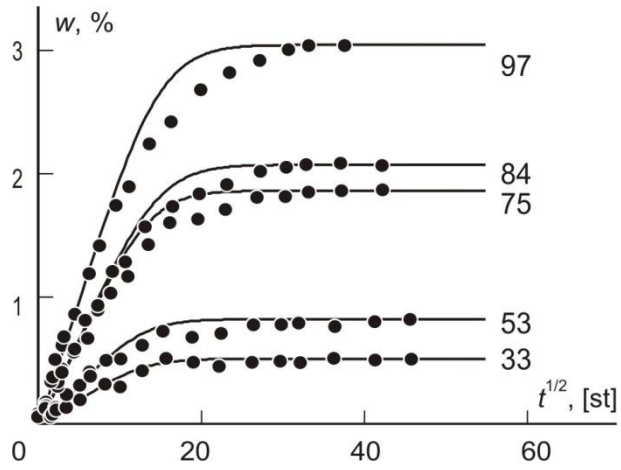

Att. 4.2. Paraugu masas izmaiņas laikā pie dažādām φ vērtībām (cipari uz līknēm): eksperimentālie dati (punkti) un aprēķins pēc Fika modeļa (4.4) (līknes).

Respektīvi, izmantojamā absorbcijas ātruma vērtība, aprēķinot mitruma daudzumu, ir pārspīlēta, jo modelī nav ņemta vērā mijiedarbība starp mitrumu un polimēru, izplešanās u.c. procesi, kas pavada mitruma absorbcijas procesu. Ir redzams, ka Fika modeļa atbilstība samazinās, palielinoties vides relatīvajam mitrumam, jo difūzijas mehānisms kļūst mazāk dominējošs. Citi mehānismi, piem., mijiedarbība starp polimēru un difundējošo vielu un/vai relaksācijas procesi, sāk ietekmēt mitruma pārnesi polimēros [31]. Lai izskaidrotu mitruma pārneses novirzi no klasiskās difūzijas mehānisma ar difūzijas koeficientu, kas ir neatkarīgs no mitruma koncentrācijas, jāpielieto alternatīvie mitruma absorbcijas modeļi, kas ņem vērā dažādas mitruma absorbcijas procesa īpatnības katrā atsevišķā gadījumā.

Džeikoba-Džonsa (Jacob's-Jones) modelī [9] pieņemts, ka materiāls sastāv no divām fāzēm ar dažādu blīvumu un attiecīgi ar dažādām sorbcijas īpašībām. Uzskata, ka abās fāzēs mitruma sorbcijas process notiek vienlaicīgi un pakļaujas Fika likumam. Ķīmisko saišu veidošanās starp ūdeni un polimēra molekulām nav ņemtas vērā.

Tādējādi, mitruma daudzumu katrā materiāla fāzē izsaka ar formulām

$$w_1(t) = w_{\infty 1} - 2\frac{(w_{\infty 1} - w_0)}{\pi^2}\sum_{k=1}^{\infty}\frac{\left(1-(-1)^k\right)^2}{k^2}\exp\left(-\left(\frac{\pi k}{h}\right)^2 D_1 t\right),$$

$$w_2(t) = w_{\infty 2} - 2\frac{(w_{\infty 2} - w_0)}{\pi^2}\sum_{k=1}^{\infty}\frac{\left(1-(-1)^k\right)^2}{k^2}\exp\left(-\left(\frac{\pi k}{h}\right)^2 D_2 t\right),$$

kuras satur četrus nezināmos parametrus, proti, katras fāzes robežmitruma daudzumu un difūzijas koeficientu. Rezultātā, summārais mitruma daudzums paraugā ir sekojošs:

$$w(t) = w_1(t) + w_2(t), \tag{4.6}$$

kur $w_1(t) = \frac{\Delta m_1}{m_0}$, $w_2(t) = \frac{\Delta m_2}{m_0}$; Δm_1, Δm_2 ir fāžu masas pieaugums.

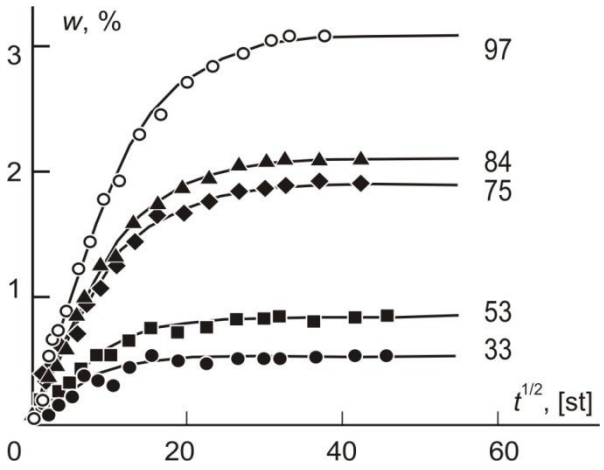

Att. 4.3. Paraugu masas izmaiņas laikā pie dažādām φ vērtībām (cipari uz līknēm): eksperimentālie dati (punkti) un aprēķins pēc vienādojuma (4.6) (līknes).

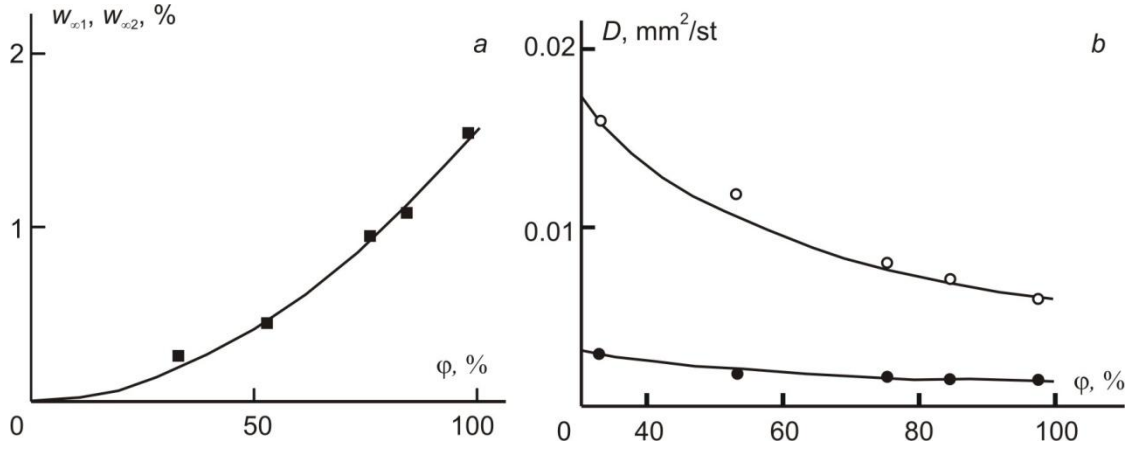

Att. 4.4. Fāžu sorbcijas izotermas (*a*) un difūzijas koeficienti D_1 (○) un D_2 (●) (*b*) atkarībā no φ.

Att. 4.3 ir parādīts aprēķins pēc vienādojuma (4.6), kas samērā labi apraksta eksperimentālos datus pie visām relatīvā mitruma vērtībām. Tas nozīmē, ka epoksīdsveķus var raksturot kā divfāžu materiālu. Zināms, ka epoksīdsveķi satur gan pietiekami homogēnus apgabalus ar blīvu telpisko tīklu, gan arī slikti sašūtos apgabalus, ko var uzskatīt par materiāla divfāžu struktūru. Kā tas ir redzams Att. 4.3, pieaugot vides relatīvajam mitrumam, sorbcijas līknes ir aprakstītas sliktāk, jo modelī nav ņemtas vērā iespējamās izmaiņas materiāla mikrostruktūrā mitruma absorbcijas dēļ. Tomēr to var izmantot, lai objektīvi novērtētu sorbcijas īpašības materiāliem ar nehomogēnu struktūru.

Att. 4.4 redzams, ka divu fāžu sorbcijas izotermas ir gandrīz vienādas. Savukārt, no Att. 4.4 seko, ka dažādās fāzēs difūzijas koeficients atšķiras vairākas reizes. Iespējams, ka tas atspoguļo reālo materiāla struktūru, apgabalus ar relatīvi zemu un augstu mitruma caurlaidību. Tādējādi, materiāla divu fāžu ievērošana, ļauj uzlabot sorbcijas līkņu aprakstu.

Pēdējais no promocijas darbā aprakstītajiem sorbcijas modeļiem, ir modelis ar laikā mainīgu difūzijas koeficientu [10]. Saskaņā ar šo modeli, sorbcijas laikā materiālā notiek dažādi

fizikālie procesi, galvenokārt, plastifikācijas un relaksācijas rakstura asociētas izmaiņas, kā arī novecošanās, papildus cietināšana u.c. Difūzijas koeficients ar laiku samazinās, pie tam proporcionāli tās pašreizējai vērtībai:

$$\frac{dD}{dt} = -\gamma D(t)\,.$$

Šī vienādojuma risinājums ir $D = D_0 e^{-\gamma t}$. Tātad modelis satur trīs parametrus: 1) difūzijas koeficientu sākuma laika momentā D_0, 2) robežmitruma daudzumu w_∞, un 3) koeficientu γ, kas raksturo difūzijas koeficienta izmaiņas ātrumu.

Mainīgā difūzijas koeficienta ieviešanai vienādojumā (4.2) pēc analoģijas ar D maiņu nestacionārā temperatūrā [32] ir izmantots modificēta laika princips:

$$dt^* = e^{-\gamma \cdot t} dt,\; t^* = \int_0^t e^{-\gamma \cdot t} dt = \frac{1 - e^{-\gamma \cdot t}}{\gamma}\,. \tag{4.7}$$

Tad difūzijas vienādojums ir izteikts sekojoši

$$\frac{\partial C}{\partial t^*} = D_0 \cdot \Delta C\,. \tag{4.8}$$

Izmantojot vienādojuma (4.2) risinājumu (4.4) un aizvietojot t ar t^*, saskaņā ar vienādojumu (4.7), ir iegūts vienādojuma (4.8) risinājums viendimensionālam gadījumam

$$w = w_\infty - \frac{2 \cdot (w_\infty - w_0)}{\pi^2} \sum_{k=1}^{\infty} \frac{(1 - (-1)^k)^2}{k^2} \cdot e^{-\lambda_k^2 \cdot F}\,, \tag{4.9}$$

kur $F = \frac{D_0}{\gamma}\left[1 - \exp\left(-\gamma \cdot t\right)\right], \lambda_k = \frac{\pi \cdot k}{a}$, F ir Furjē kritērijs, γ = 1/τ, un τ ir relaksācijas raksturīgais laiks. Sorbcijas līkņu apraksts ar izteiksmi (4.9) ir parādīts Att. 4.5.

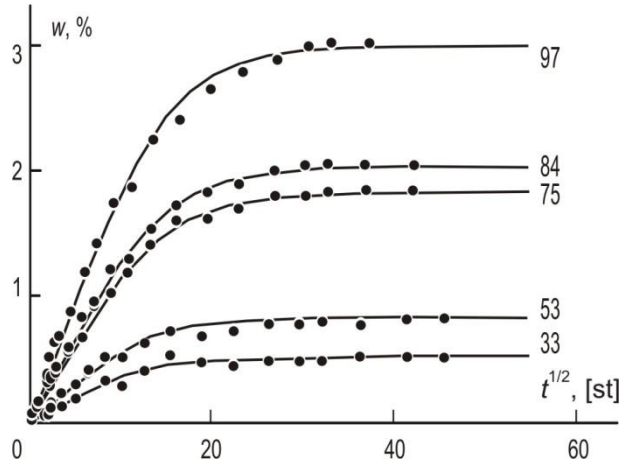

Att. 4.5. Sorbcijas eksperimentālo datu aproksimācija pēc modeļa ar laikā mainīgu difūzijas koeficientu pie dažādām φ vērtībām (cipari uz līknēm).

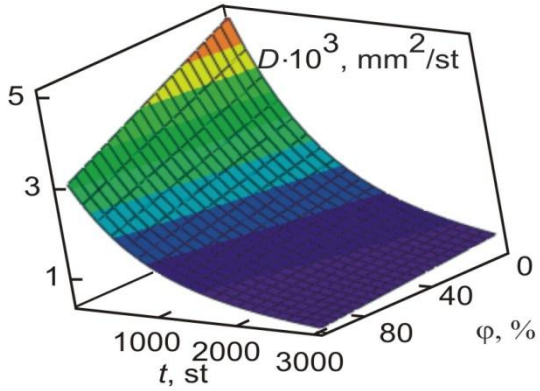

Att. 4.6. Difūzijas koeficients *D* atkarībā no laika *t* un vides relatīvā mitruma φ.

Difūzijas koeficienta *D* atkarība no laika un vides relatīvā mitruma ir dota Att. 4.6. Ir redzams, ka pie lieliem laikiem difūzijas koeficients tiecās pie bezgalīgi mazas vērtības, kas apraksta sistēmas piesātināto stāvokli. Mitruma absorbcijas laikā (aptuveni 450 st) pie φ = 98%, $D_0 = 3{,}61 \cdot 10^{-3}$ cm^2/st, un γ = 0,002, difūzijas koeficients samazinās 4-6 reizes. Kopumā, ņemot vērā to, ka modelim ir tikai trīs neatkarīgie parametri, tas ir samērā elastīgs un diezgan labi apraksta sorbcijas līknes (Att. 4.5).

Tādējādi, sorbcijas kinētikas aprakstīšanai vispiemērotākais ir modelis, kas ņem vērā divu fāžu veidošanos materiālā, un modelis ar laikā mainīgu difūzijas koeficientu. Šie modeļi diezgan labi apraksta eksperimentālos datus, kā arī satur salīdzinoši nelielu parametru skaitu, kas ļauj tos izmantot praktiski.

4.2. Epoksīda bāzes nanokompozīta mitruma absorbcija

[P3], [C1]

Daudzkomponenšu KM īpašības parasti diezgan sarežģītā veidā ir atkarīgas no sastāva un izgatavošanas apstākļiem. Tādēļ veiksmīgai KM īpašību prognozēšanai ir nepieciešams atsevišķi izpētīt materiāla katras sastāvdaļas īpašības, saglabājot nemainīgas materiāla paraugu izgatavošanas tehnoloģijas.

Mitruma daudzuma mērījumi NK paraugu sērijai ir veikti dažādos laika intervālos. NK epoksīda sveķu eksperimentāli noteiktais mitruma daudzums ir parādīts Att. 4.7 atkarībā no laika kvadrātsaknes. Katrs no šiem datu punktiem atbilst vidējai vērtībai ar vidējo kvadrātisko novirzi 4 paraugiem.

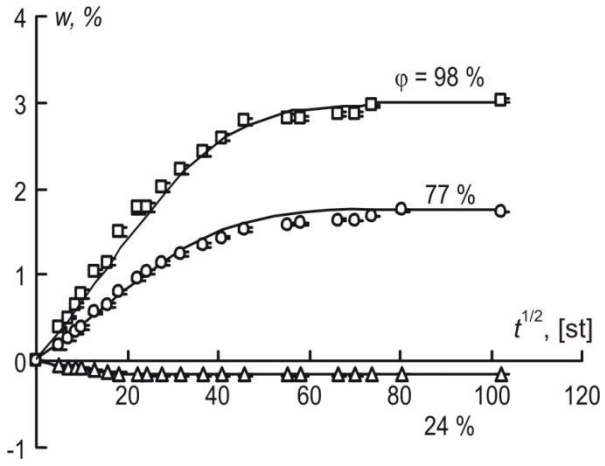

Att. 4.7. Eposkīda sveķu paraugu eksperimentāli noteiktas masas izmaiņas (punkti) atkarībā no kvadrātsaknes no laika pie dažādām φ vērtībām (cipari uz līknēm) un aprēķins pēc Fika modeļa (līnijas).

Att. 4.7 redzams, ka sorbcijas procesu epoksīda saistvielai var pietiekami labi aprakstīt ar Fika modeli visās vidēs. Līdzīgi rezultāti ir iegūti arī NK paraugiem, pie dažāda pildvielas satura. Jāatzīmē, ka NK difūzijas koeficients, kas iegūts no vienādojuma (4.5) ir neatkarīgs no vides relatīvā mitruma (skat. Att. 4.8). Vides ietvaros datu izkliede nepārsniedz 10% no difūzijas koeficienta vidējās vērtības. Eksperimentāli apstiprināts, ka sorbcijas process NK norit daudz lēnāk nekā tīrā (nepildītā) epoksīda saistvielā (kā parādīts Att. 4.8), pie augstākā pildvielas satura difūzijas koeficients samazinās par pusi, salīdzinot ar epoksīda saistvielas difūzijas koeficientu. Kā iepriekš minēts, šo parādību var izskaidrot ar silikātu plākšņu augsto malu attiecību, kas palielina ūdens molekulu trajektorijas izliekumu, mitrumam difundējot caur NK. Saskaņā ar līkumotā ceļa modeli, un, tā kā mitruma caurlaidība ir atkarīga no plākšņu tilpuma satura un malu attiecības, eksfoliētajam NK ir raksturīgs lielāks barjeras īpašību uzlabojums, nekā tradicionālajam kompozītam vai interkalētajam NK [7].

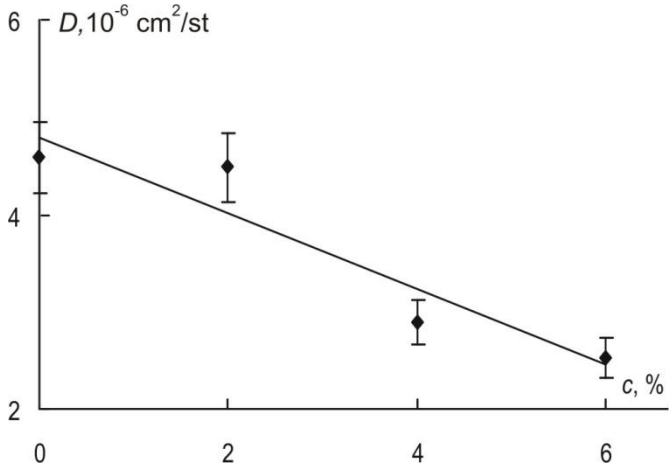

Att. 4.8. NK difūzijas koeficients pēc vienādojuma (4.5) atkarībā no pildvielas masas satura.

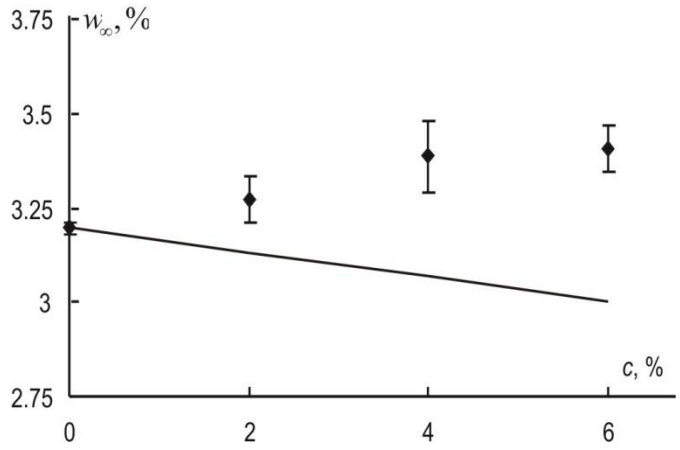

Att. 4.9. NK robežmitruma daudzums atkarībā pildvielas satura vidē ar relatīvo mitrumu 98% (punkti - eksperimentālo datu aproksimācijas rezultāts, līnija – aprēķins pēc vienādojuma (4.10).

NK robežmitruma daudzums w_∞^{NC} ietver sevī polimēra saistvielas w_∞^{ep} un pildvielas w_∞^f īpašības:

$$w_\infty^{NC} = w_\infty^{ep} \cdot (1-c) + w_\infty^f \cdot c\,. \qquad (4.10)$$

Maisījuma likumā masas izmantošana tilpuma vietā ir pamatota ar to, ka sorbcijas procesa beigās visi NK paraugi uzrādīja izplešanos aptuveni 3% pēc tilpuma piesātinājuma. Uzskatīts, ka hidrofīliem epoksīdsveķiem ir galvenais ieguldījums mitruma uzņemšanā, un pildvielas robežmitruma daudzums w_∞^f ir tuvs nullei, jo dabiski hidrofīlais MMT māls ir organiski apstrādāts.

NK robežmitruma daudzuma pieaugumu, palielinoties MMT saturam (redzams Att. 4.9), var izskaidrot ar starpfāzes satura pieaugumu. Starpfāzes mitruma sorbcijas īpašību novērtējums ir izveidots, izmantojot modificētu maisījuma likumu robežmitruma daudzumam

$$w_\infty^{NC} = w_\infty^{ep} \cdot (1-c-b) + w_\infty^i \cdot b\,, \qquad (4.11)$$

kur w_∞^i ir starpfāzes robežmitruma daudzums, b ir starpfāzes masas saturs. Starpfāzes iekļaušana maisījuma likumā ļauj novērst novirzi no aprēķina pēc (4.10) no eksperimentālo datu aproksimācijas rezultātiem. Tomēr jāatzīmē, ka vienādojums (4.11) satur 2 nezināmos parametrus (w_∞^i un b), kurus nevar noteikt neatkarīgi. Tādēļ pareizā analīze ir jābalsta uz starpfāzes mitruma ietilpības novērtējumu pēc formulas (4.10) un eksperimentālo datu starpību.

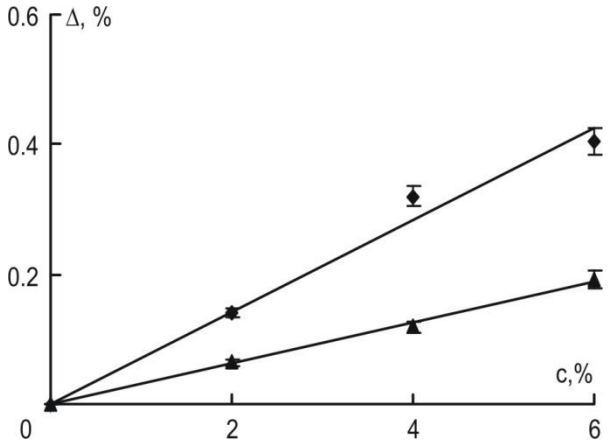

Att. 4.10. Novirze no eksperimentāliem datiem NK robežmitruma daudzumam un tā novērtējumu pēc maisījuma likuma (4.10) vidēs ar φ = 77 (▲) un 98 (◆) %.

Sagaidāms, ka vidē ar augstāko relatīvo mitrumu (augstāku absorbētā mitruma saturu) absorbētā mitruma daudzumu starpībai, kas ir noteikta eksperimentāli un prognozēta pēc formulas (4.10), ir jāpalielinās. Šo novērojumu apstiprina arī eksperimentu rezultāti (skat. Att. 4.10). Augstāks pildvielas saturs izraisa lielāku mitruma absorbciju un lielāku novirzi no maisījuma likuma, neņemot vērā starpfāzes sorbcijas īpašības. Vispārēji sakot, šī novirze, kas pārstāv starpfāzes mitruma saturu ir lineāri proporcionāla pildvielas saturam (Att. 4.10). Respektīvi, proporcionalitātes koeficienti atbilst NK starpfāzes sorbcijas ietilpībai uz 1% pildvielas.

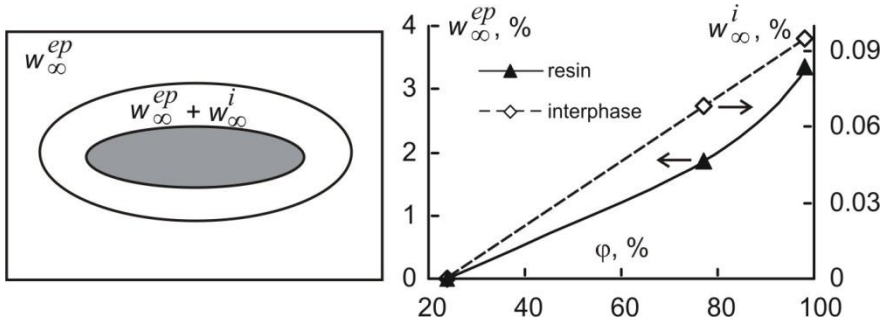

Att. 4.11. Shematisks atveidojums robežmitruma daudzuma sadalījumam kompozīta sistēmā ar vienu pildvielas daļiņu (*a*); un sorbcijas izoterma epoksīda sveķiem un starpfāzes slānim NK uz 1% pildvielas (*b*).

Līdzsvara stāvoklī attiecību starp mitruma daudzumu materiālā un apkārtējās vides līdzsvara relatīvo mitrumu var parādīt ar sorbcijas izotermu. Pieņemts, ka kopējais mitruma daudzums NK paraugu šķērsgriezumā ir sadalīts vienmērīgi un NK mitruma koncentrācija pakļaujas sorbcijas izotermai. Katrai relatīvā mitruma vērtībai sorbcijas izoterma norāda atbilstošo mitruma daudzumu dotā, nemainīgā temperatūrā. Sorbcijas procesu sarežģītības dēļ, kompozītmateriālu izotermas tradicionāli atšķiras no Henrija (Henry) likuma, uzrāda nelineāro raksturu, tādēļ katram pētāmajam materiālam tās ir jānovērtē eksperimentāli.

NK starpfāzes sorbcijas izotermu uz 1% MMT var noteikt pēc Att. 4.11. Kā iepriekš minēts, starpfāzes saturu NK no izteiksmes (4.11) nevar aprēķināt neatkarīgi. Tomēr ir iespējams novērtēt starpfāzes ietekmi uz NK sorbcijas īpašībām kopumā. Šos rezultātus var izmantot tālākai mitruma ietekmes analīzei uz NK mehāniskajām un termofizikālajām īpašībām. Attiecīgi mitruma saturu, kas atrodas gan saistvielā, gan NK starpfāzē, var prognozēt nevis no izteiksmes (4.10), bet ņemot vērā sekojošu kompozīta sistēmu

$$w_{\infty}^{NC} = w_{\infty}^{ep} \cdot (1-c) + w_{\infty}^{i} \cdot c\,, \tag{4.12}$$

kur abi parametri w_{∞}^{ep} and w_{∞}^{i} ir noteikti no Att. 4.11, kas ir epoksīda sveķu un starpfāzes sorbcijas izoterma. Šī sorbcijas izoterma un formula (4.12) ļauj aptuveni novērtēt papildus mitrumu NK vidē ar jebkuru relatīvo mitrumu un jebkuru pildvielas saturu. Līdz ar to ir pierādīts, ka sorbcijas procesu NK var aprakstīt ar Fika modeli pie visiem māla saturiem vidēs ar jebkuru no apskatāmiem relatīviem mitrumiem. Pamatojoties uz rezultātiem, ko iegūst attiecībā uz NK mitruma īpašībām, var secināt, ka mitrumu necaurlaidīgo māla nanodaļiņu izmantošana ir lietderīga mitruma negatīvas ietekmes samazināšanai uz NK īpašībām. Tas ļauj izmantot modificētus epoksīda sveķus ekspluatācijas apstākļos ar augstāku relatīvo mitrumu. Absorbētā mitruma ietekme uz epoksīda-māla NK mehāniskajām un termofizikālajām īpašībām ir apspriesta nākamajās nodaļās.

5. Epoksīda bāzes kompozītmateriālu mehānisko īpašību raksturošana

5.1. Stiprības un elastības īpašības

[P1], [P4], [P6], [C1]

Lai novērtētu pildvielas un absorbētā mitruma ietekmi uz stiepes elastības moduli un izturību epoksīda sveķu un ar mikrodaļiņām (LiF kristāli) un nanodaļiņām (MMT) pildītu epoksīdsveķu mehāniskā uzvedība ir pētīta kvazistatiskos stiepes eksperimentos. Piem., Att. 5.1 ir parādītas sprieguma-deformācijas līknes epoksīda sveķu un NK paraugiem ar pildvielas saturu c = 6%, sākotnēji uzturētiem līdz piesātinājuma stāvoklim, vidēs ar mitrumu 24, 77 un 98%. Pārējo NK paraugu (ar pildvielas saturu 2 un 4%) sprieguma-deformācijas līknes ir līdzīgas ar Att. 5.1 uzrādītajām līknēm ar stipri izteiktu piespiestās elastības robežu.

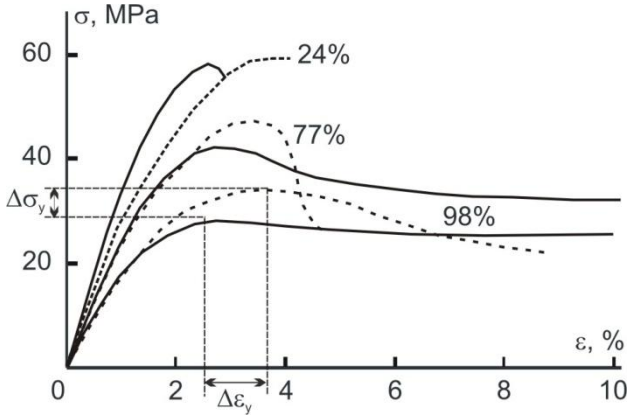

Att. 5.1. Tipiskas sprieguma-deformācijas līknes pie pastāvīgā deformācijas ātruma (5 mm/min) epoksīda saistvielai (pārtraukta līnija) un NK ar c = 6% (nepārtraukta līnija) pie dažādām φ vērtībām (cipari uz līknēm).

Kā izriet no Att. 5.2, epoksīda sveķu pildīšana ar MMT nanodaļiņām noveda pie elastības moduļa pieauguma sausajam materiālam aptuveni par 30% un piespiestās elastības robežas sprieguma un deformācijas samazināšanās par apm. 1/3. Mitruma satura pieauguma dēļ, samazinās gan epoksīdsveķu, gan NK elastības modulis un piespiestās elastības robežas spriegums, savukārt, piespiestās elastības robežas deformācijai ir apm. tāda pati vērtība. Sausajiem NK paraugiem (pie φ = 24%) sabrukuma raksturs bija daudz trauslāks nekā mitrinātajiem (pie φ = 98%). Turklāt sauso paraugu stiepes stiprība divreiz pārsniedza mitrināto paraugu stiprību. Starpvērtības ir iegūtas NK paraugiem vidē ar φ = 77%.

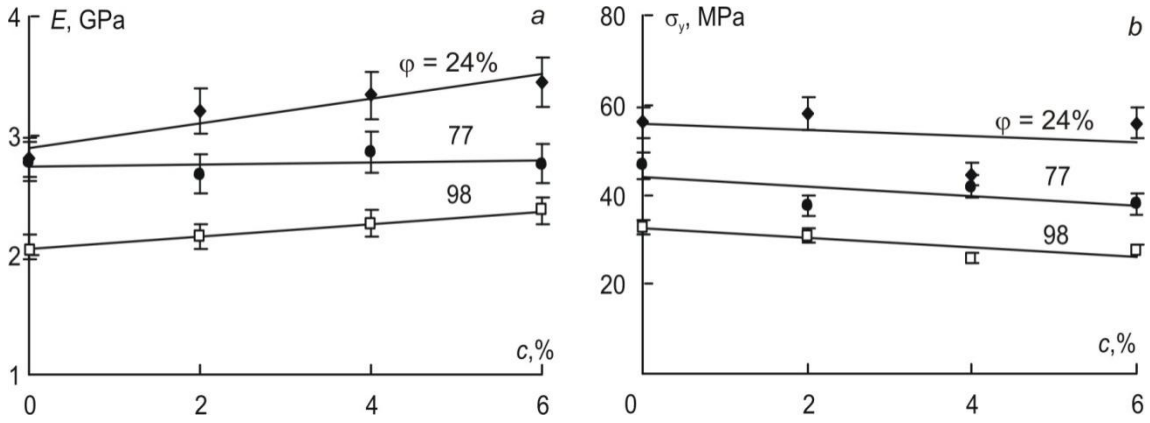

Att. 5.2. NK elastības modulis (*a*) un piespiestās elastības robežas spriegums (*b*) atkarībā no pildvielas masas satura pie dažādām φ vērtībām (cipari uz līknēm).

Līdz ar to absorbētā mitruma dēļ, gan nepildītam epoksīdam, gan NK ar c = 6% ir novērota gandrīz identiska elastības moduļa samazināšanās par 1 GPa un stiepes stiprības samazināšanās par 25 MPa. Lai gan pašas elastības moduļa un stiprības vērtības ir uzlabotas attiecībā pret pildvielas saturu, mitruma saturam palielinoties (vidēs no 24 līdz 98%), nanodaļiņu pozitīvā ietekme nav konstatēta.

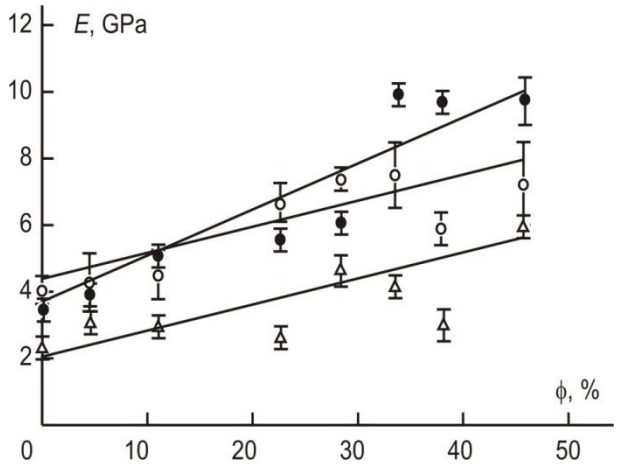

Att. 5.3. KM eksperimentāli noteiktais elastības modulis sākotnējā (o) un mitrinātā (Δ) stāvoklī, un pēc mitrināšanās-žāvēšanas cikla (●) atkarība no pildvielas tilpuma satura ϕ.

Att. 5.3 parāda mitruma ietekmi uz eksperimentāli iegūto elastības moduli epoksīda sveķiem, pildītiem ar dažādu LiF kristālu saturu. Kā izriet no attēla datiem, palielinoties pildvielas tilpuma saturam ϕ, palielinās arī KM elastības modulis - nosacīti sākotnējā stāvoklī pie $\phi \leq 0{,}33$, piesātinātā stāvoklī pie visām ϕ vērtībām, un pēc mitrināšanas- žāvēšanas cikla pie $\phi \leq 0{,}38$. Līdz ar to ir pieņemts, ka pildvielas dēļ, polimēra struktūra un īpašības mainās. To var izskaidrot ar starpfāzes veidošanos, kuras īpašības atšķiras no polimēra saistvielas īpašībām. Tādēļ, aprakstot KM elastības īpašības, ir svarīgi ņemt vērā pildvielas daļiņu morfoloģiskās

īpatnības nosacīti sākotnējā stāvoklī. Tad jānovērtē absorbētā mitruma ietekme uz KM struktūru un īpašībām pie dažāda pildvielas satura.

5.2. NK elastības īpašību modelēšana, ievērojot MMT māla slāņaino struktūru

[P4]

NK uzvedība un īpašības ir atkarīgas ne tikai no tā struktūras komponenšu īpašībām, bet arī no materiāla mikrostruktūras: pildvielas daļiņu dispersitātes un orientācijas, kā arī no savstarpējās pildvielas daļiņu un polimēru saistvielas mijiedarbības [33].

Tomēr viens no galvenajiem parametriem, kas ietekmē NK uzvedību, ir pildvielas daļiņu dispersitātes efektivitāte polimēru saistvielā [34].

Viens no veidiem, kā pārbaudīt māla nanodaļiņu morfoloģiskās īpatnības šķīdumā, pirms to ievietošanas polimēra saistvielā, ir to dispersitātes novērošana ar TEM. Tipisks TEM attēls māla nanodaļiņu acetona suspensijā ir parādīts Att. 5.4*a*.

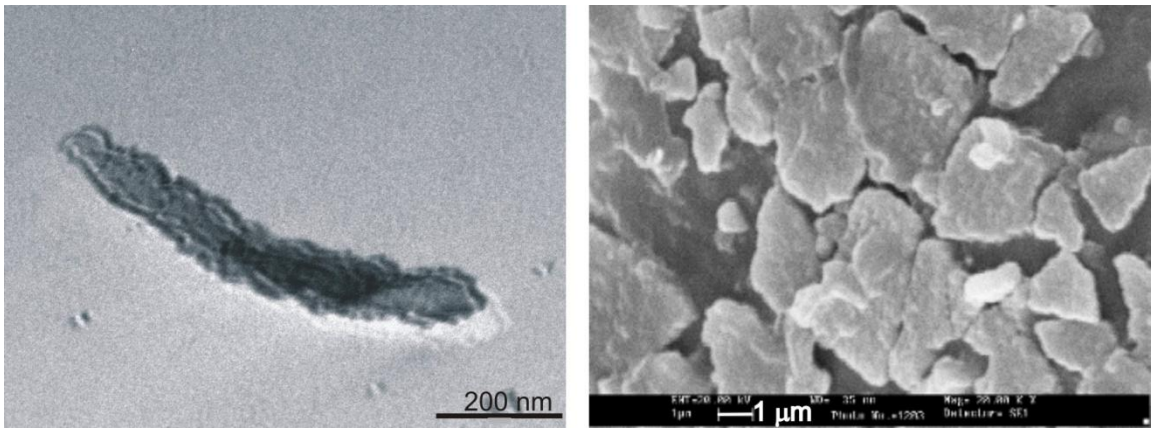

Att. 5.4. Tipiski TEM attēli māla nanodaļiņu acetona suspensijā. Nanomāls ir attēlots melnā krāsā (*a*); NK ar c = 2% sabrukuma virsmas SEM attēls (*b*).

No Att. 5.4*a* ir redzams, ka novērotais agregāts ir māla plāksnīšu kopa ar slāņveida struktūru un daļiņu augstu malu (garums pret biezumu) attiecību. No Att. 5.4*a* plākšņu kopas malu attiecība ir aptuveni vienāda ar 7.

Turklāt pildvielas daļiņu plākšņveida formu var apstiprināt NK ar c = 2% sabrukuma virsmas SEM attēli (Att. 5.4*b*). Ir redzams, ka pildvielas agregātu transversālais izmērs ir daudz mazāks nekā gareniskajā virzienā.

Ir mēģināts attiecināt mitrinātā NK efektīvo stiepes elastības moduli uz to struktūras komponenšu īpašībām. Jāuzsver, ka, ņemot vērā reālo KM sarežģīto struktūru, teorētiski var iegūt tikai salīdzinošus rezultātus [18].

Eksfoliētā NK gadījumam ir izmantoti Halpina-Tsai (Halpin-Tsai) vienādojumi [25, 26], kas iegūti izotropai polimēra saistvielai pildītai ar transversāli izotropām cilindriskām daļiņām ar

patvaļīgu malu attiecību (5.1). Elastīgs risinājums iegūts kompozītam ar vienu ar šķiedru, apvilktu ar saistvielas cilindru. Tas ir ievietots neierobežotā, viendabīgā vidē, kas makroskopiski neatšķiras no kompozīta. Sprieguma un deformācijas attiecības komponenti ir novidējoti pa visu kompozītu. Formulas precīziem elastības risinājumiem kompozītam ar patvaļīgu daļiņu izmēru attiecību iegūtas no līkņu aproksimācijas un ir apstiprinātas ar eksperimentālajiem mērījumiem.

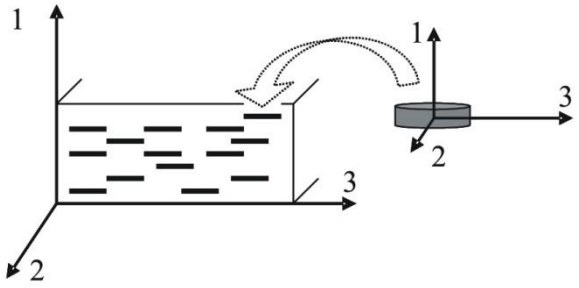

Att. 5.5. Cilindrisko pildvielas daļiņu shematisks attēlojums polimēra saistvielā.

Pilnīgi eksfoliētai kompozīta sistēmai Halpina-Tsai vienādojumi elastības moduļu noteikšanai ir sekojoši:

$$E_1 = E_m \frac{1+2\eta_1\varphi}{1-\eta_1\varphi}, \tag{5.1}$$

$$E_2 = E_3 = E_m \frac{1+2A_f\eta_2\varphi}{1-\eta_2\varphi}, \tag{5.2}$$

kur

$$\eta_1 = \frac{R_1-1}{R_1+2}, R_1 = \frac{E_{f1}}{E_m},\ \eta_2 = \frac{R_2-1}{R_2+2A_f}, R_2 = \frac{E_{f2}}{E_m}.$$

Vienādojumos (5.1)-(5.2) E_1, E_2, E_3 ir KM elastības moduļi, E_m ir saistvielas elastības modulis un E_{f1}, E_{f2} – ir pildvielas elastības modulis asu virzienos, saskaņā ar Att. 5.5; A_f ir plāksnītes malu attiecība (A_f > 1 jo cilindriskām plāksnītēm tā ir vienāda ar diametra attiecību pret biezumu); ϕ ir pildvielas daļiņu tilpuma saturs, ko parasti nosaka no formulas

$$\phi = \frac{c}{\rho_f} \cdot \frac{1}{\left(\frac{c}{\rho_f} + \frac{(1-c)}{\rho_m}\right)},$$

kur c ir pildvielas masas saturs, ρ_f un ρ_m ir attiecīgi pildvielas un saistvielas blīvums.

Gadījumā, kad pildvielas daļiņu eksfoliācija ir nepilnīga, uzskatīts, ka KM sastāv no saistvielas un pseidodaļiņām (atsevišķo plākšņu kopām) [22]. Att. 5.6 ir redzama pildvielas pseidodaļiņas shēma, kuru veido plākšņu kopa. N ir plākšņu skaits kopā, L – plāksnītes garums (platums), t - biezums, s – starpplākšņu attālums.

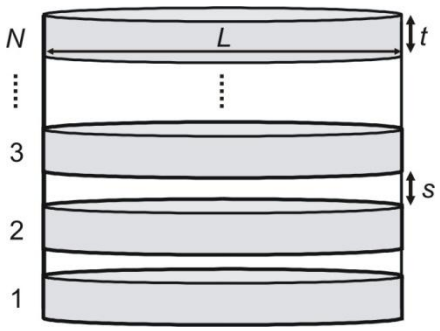

Att. 5.6. Pseidodaļiņas attēlojums (plākšņu kopa).

Nepilnīgās eksfoliācijas gadījumam Halpina-Tsai vienādojumus var modificēt un rezultātā iegūt izteiksmes NK elastības moduļiem:

$$E_1 = E_m \frac{1+2\eta_1'\varphi'}{1-\eta_1'\varphi'}, \tag{5.3}$$

$$E_2 = E_3 = E_m \frac{1+2A_f'\eta_2'\varphi'}{1-\eta_2'\varphi'}, \tag{5.4}$$

kur

$$\eta_1' = \frac{R_1'-1}{R_1'+2}, R_1' = \frac{E_{p1}}{E_m},\ \eta_2' = \frac{R_2'-1}{R_2'+2A_f'}, R_2' = \frac{E_{p2}}{E_m}.$$

Šeit A_f' ir plākšņu kopas malu attiecība, ϕ' - plākšņu kopu tilpuma saturs, R' - plākšņu kopas elastības moduļa attiecība pret saistvielas elastības moduli. Plākšņu kopas elastības moduļus dažādos asu virzienos var aprēķināt, izmantojot tiešo un apgriezto maisījuma likumu

$$E_{p1} = \frac{V_{ps}}{\frac{V_p}{E_{f1}} + \frac{V_{ip}}{E_m}}$$

un

$$E_{p2} = \frac{E_{f2}V_p + E_m V_{ip}}{V_{ps}},$$

kur V_p ir plākšņu tilpums, V_{ip} - starpplākšņu telpas tilpums, V_{ps} - plākšņu kopas tilpums. Izmantojot vienkāršos ģeometriskus pieņēmumus, ka katra plākšņu kopa sastāv no N plāksnēm ar biezumu t, garumu L un starpplākšņu attālumu s, ir iegūtas formulas plākšņu kopas elastības moduļa noteikšanai

$$E_{p1} = \frac{E_{f1}E_m\left(Nt + (N-1)s\right)}{E_m Nt + E_{f1}(N-1)s}$$

un

$$E_{p2} = \frac{E_{f2} Nt + E_m (N-1)s}{Nt + (N-1)s}.$$

Vienādojumu parametriem ir iegūtas attiecīgās formulas plākšņu kopas malu attiecībai A_f', plākšņu kopas tilpuma saturam ϕ' un plākšņu kopas elastības moduļa attiecībai pret saistvielas elastības moduli E_r' [22]:

$$A_f' = \frac{A_f}{N}\left(\frac{1}{1+\left(1-\frac{1}{N}\right)\frac{s}{t}}\right),$$

$$\phi' = \phi\left(1+\left(1-\frac{1}{N}\right)\frac{s}{t}\right),$$

$$R_1' = R_1\frac{1+\left(1-\frac{1}{N}\right)\frac{s}{t}}{1+R_1\left(1-\frac{1}{N}\right)\frac{s}{t}}, \quad R_2' = \frac{R_2}{1+\left(1-\frac{1}{N}\right)\frac{s}{t}} + \frac{\left(1-\frac{1}{N}\right)\frac{s}{t}}{1+\left(1-\frac{1}{N}\right)\frac{s}{t}}.$$

Izmantojot zināmās vērtības saistvielas elastības modulim, vidēs ar dažādu relatīvo mitrumu, no vienādojumiem (5.3) un (5.4) var noteikt NK elastības moduli. Montmorillonīta māla plāksnītēm elastības moduļa vērtības sākās no 40 GPa [35] plākšņu šķērsvirzienā līdz 180 GPa [25, 36] plākšņu garenvirzienā, pamatojoties uz literatūras datiem, slāņveida struktūras māla minerāliem, alumīnija oksīda, silīcija dioksīda un to savienojumu empīriskām attiecībām starp moduli un blīvumu, kā arī elastības moduli un plākšņu biezumu, ko iegūst simulācijas procesā. Šeit ir pieņemts, ka pildvielas elastības moduļiem ir sekojošas vērtības: E_{f1} = 55 GPa, $E_{f2} = E_{f3}$ = 180 GPa; pildvielas plākšņu malu attiecība A_f = 50, plākšņu skaits kopā N mainās no 1 līdz 6, s/t = 1.

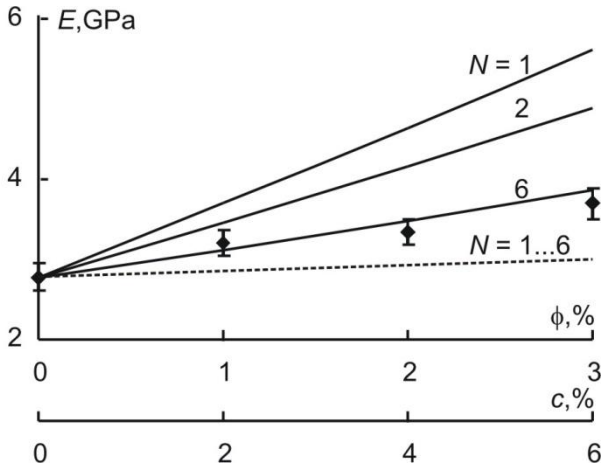

Att. 5.7. NK elastības modulis atkarībā no pildvielas tilpuma satura. Aprēķins pēc izteiksmes (5.1) (nepārtraukta līnija) un (5.3) (pārtraukta līnija) pie dažāda elementāro slāņu skaita *N* (cipari uz līknēm) plākšņu kopā. Punkti – eksperimentālie dati pie φ = 24%.

Aprēķina rezultāti pēc izteiksmes (5.1) ir salīdzināti ar kvazistatiskās stiepes eksperimentālajiem datiem paraugiem, kas ir uzturēti sausā vidē (φ = 24%) (Att. 5.7). Redzams, ka NK elastības moduļa aprēķina rezultāti ar eksfolietām pildvielas daļiņām ir lielāki nekā eksperimentāli iegūtas vērtības. Plākšņu skaita palielināšana dod iespēju iegūt labāku datu aprakstu. Tie ir salīdzinoši rezultāti, jo modelī ir pieņemts, ka pildvielas daļiņas polimēra saistvielā ir novietotas koplanāri. No otras puses aprēķins pēc izteiksmes (5.4) (apakšējā robeža) ir daudz zemāks nekā eksperimentu rezultāti. Tas nozīmē, ka māla plāksnīšu reālais orientācijas sadalījums atrodas starp šiem robežstāvokļiem un var būt diezgan sarežģīts.

Tomēr, izmantojot iegūtos rezultātus, tos pašus parametrus *N, t, s,* mitrinātam NK, ir iespējams novērtēt polimēra saistvielas struktūras izmaiņas, mitruma absorbcijas dēļ.

Rezultātā mitrinātā NK elastības moduļa novērtēšana pēc (5.3) atšķiras no eksperimentāli iegūtajiem rezultātiem (skat. Att. 5.8). Kā redzams, ņemot vērā plākšņu kopas slāņveida struktūru palielinot plākšņu skaitu kopā līdz 6, ir uzlabots eksperimentālo datu aprēķina rezultāts. To var izskaidrot ar izmaiņām plākšņu kopas elastības īpašībās. Lai gan mitrumu necaurlaidīgo māla plāksnīšu elastības modulis nav atkarīgs no mitruma daudzuma, saistvielas fāze, kas atrodas starpplākšņu telpā, var absorbēt mitrumu. Tādēļ plākšņu kopu elastības īpašības ir atkarīgas no absorbētā mitruma daudzuma un izraisa mitrinātā NK elastības moduļa būtisku samazināšanos (Att. 5.8).

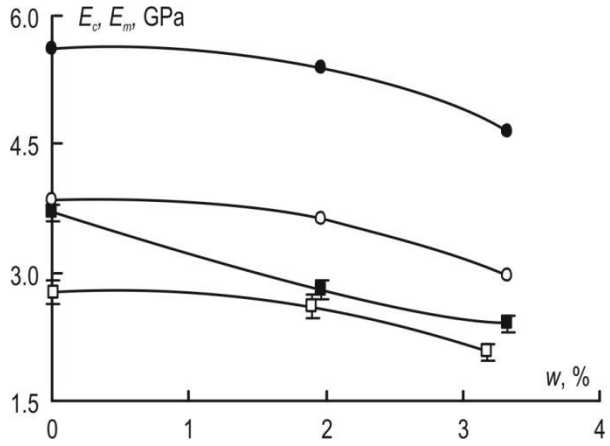

Att. 5.8. Epoksīda saistvielas un NK ar c = 6% elastības modulis atkarībā no absorbētā mitruma daudzuma. Eksperimentālie dati (NK ar c = 6% (■), epoksīda saistvielai (□)), aprēķins pēc izteiksmes (5.3) NK ar c = 6% un N = 1 (●) un N = 6 (○).

Par piemēru izmantojot NK ar c = 6%, var redzēt, ka elastības moduļa izmaiņas, mitruma ietekmes dēļ, pierāda, ka mitrums, kas atrodas starpplākšņu telpā, būtiski ietekmē KM elastības moduli. Lielāks pildvielas saturs noved pie augstākā starpplākšņu telpas satura, kā rezultātā parādās lielākā mitruma absorbcija un lielākas izmaiņas NK īpašībās, kas ir jutīgas pret mitrumu.

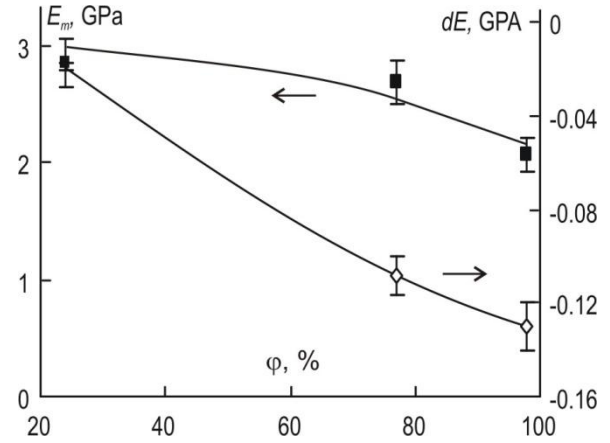

Att. 5.9. Epoksīda saistvielas elastības modulis (■) un normētā uz 1% masas pildvielas saturu novirze no NK elastības moduļa (◊) atkarībā no vides relatīvā mitruma.

No izotermas, kas ir parādīta Att. 5.9, seko piedāvātā mitruma un pildvielas ietekmes analīze uz epoksīda-MMT NK deformējamību, ņemot vērā pildvielas daļiņu morfoloģiskās īpatnības. Izmantojot šo attēlu, ir iespējams novērtēt NK elastības moduli pie jebkura pildvielas satura vidē ar jebkuru relatīvo mitrumu. Sakarā ar mitruma absorbciju NK elastības modulis ievērojami samazinās. Pieaugot pildvielas saturam epoksīda sveķu elastības moduļa vērtības uzlabojās. Neskatoties uz to, ka MMT daļiņām nav pozitīvās ietekmes uz NK elastības moduli, mitruma absorbcijas dēļ (vidēs ar relatīvo mitrumu no 24 līdz 98%), epoksīdsveķus, kas ir modificēti ar mitrumu necaurlaidīgām cietām MMT māla nanodaļiņām var rekomendēt pielietošanai vidēs ar augstāku ekspluatācijas relatīvo mitrumu.

5.3. NK elastības īpašību modelēšana, ievērojot starpfāzes veidošanos

[C2]

Silikātu plākšņu novietojumu polimēra saistvielā var nosacīti iedalīt trīs kategorijās: agregātos, interkalētās slāņveida kopās un eksfoliētās atsevišķās plāksnītēs. Šajā apakšnodaļā ir aprakstīts pēdējais gadījums, un, galvenokārt, ir uzsvērta starpfāzes problēma. Eksfoliētas plāksnes ir modelētas kā transversāli izotropi sferoīdi ar mazu apgriezto malu attiecību (mazās ass attiecība pret lielo, turpmāk tekstā proporcijas parametrs), kas ir vienāda ar apm. 0,015.

Tā kā īpaša uzmanība ir pievērsta starpfāzes īpašību un NK adhēzijas efektivitātes novērtēšanai, NK elastības īpašību aprēķināšanai ir pielietotas formulas haotiski orientētām transversāli izotropiem sferoīdiem ar mazu apgrieztu malu attiecību. Parādīts [21], ka pie maza pildvielas tilpuma satura Norrisa (Norris) tuvinātās izteiksmes [19] tilpuma un bīdes moduļiem diezgan labi korelē ar Mori-Tanakas (Mori-Tanaka) izteiksmēm, kas ir plaši pielietotas NK īpašību aprakstam. Šīs aptuvenās izteiksmes ir sekojošas

$$K = K_1 + \frac{4}{9}\cdot\phi\cdot\left(\chi\frac{\pi}{8}\frac{3-4\cdot\nu_1}{\mu_1\cdot(1-\nu_1)} + \frac{1}{\mu_2}\frac{1-\nu_2}{1+\nu_2}\right)^{-1}, \tag{5.5}$$

$$\mu = \mu_1 + \frac{1}{15}\cdot\phi\cdot\left(\chi\frac{\pi}{8}\frac{3-4\cdot\nu_1}{\mu_1\cdot(1-\nu_1)} + \frac{1}{\mu_2}\frac{1-\nu_2}{1+\nu_2}\right)^{-1} + \frac{2}{5}\cdot\phi\cdot\left(\chi\frac{\pi}{16}\frac{7-8\nu_1}{\mu_1\cdot(1-\nu_1)} + \frac{1}{\mu_2}\right)^{-1}, \tag{5.6}$$

kur ϕ ir pildvielas tilpuma saturs, χ ir pildvielas daļiņas asu attiecība, K, μ un ν ir attiecīgi KM tilpuma un bīdes moduļi, un Puasona (Poisson) koeficients. Indeksi 1 un 2 ir attiecīgi saistvielas un pildvielas īpašības. Parametrs χ ir definēts kā pildvielas daļiņas biezuma attiecība pret tās diametru un māla plāksnīšu gadījumā tas ir daudz mazāks par 1.

Skaitliskos aprēķinos saistvielas un pildvielas tilpuma un bīdes moduļu vērtības ir izvēlētas tā, lai tās atspoguļotu tipiskās epoksīda sveķu un montmorilonīta māla īpašības. Pieņemts, ka polimēra saistvielas elastības modulis un Puasona koeficients: E_1 = 3,45 GPa un ν_1 = 0,35. Kā iepriekš minēts, literatūrā parasti pieņem, ka MMT elastības moduļi garenvirzienā ir intervālā no 140 [21] līdz 180 GPa [15, 25, 36]. Šajā darbā uzskatīts, ka E_2 = 180 GPa, $\nu_2 = 0.2$ un proporcijas parametrs ir vienāds ar 0,015.

Aprēķinot KM moduļus no formulām (5.5) un (5.6), elastības moduli var noteikt pēc izteiksmes

$$E = \frac{9\cdot K\cdot\mu}{3\cdot K+\mu} \tag{5.7}$$

Starpfāze ir ieviesta kā apgabals ar īpašību gradientu pildvielas daļiņu tuvumā. Nanolīmenī ir izskatītas vienas daļiņas un starpfāzes elastības īpašības. Ir ņemta vērā arī adhēzijas efektivitāte starpfāzes apgabalā. Iepriekš [27] pierādīts, ka starpfāzes veidošanas rezultātā absorbcijas eksperimentos palielinās robežmitruma daudzums, kā rezultātā ir novērota būtiska NK elastības moduļa samazināšanās. Pie tam analītiskā aprēķina rezultāti gan NK elastības, gan sorbcijas īpašībām ir augstāki, nekā eksperimentāli iegūtie rezultāti. Tādēļ secina, ka starpfāzes elastības īpašības ir zemākas par saistvielas elastības īpašībām.

Pieņemta sekojoša pildvielas daļiņas-starpfāzes-saistvielas sistēmas izteiksme tilpuma modulim

$$K(x,k,R_f)=\begin{cases} K_2 \text{ if } 0 \le x \le R_f \\ K_1 \cdot \left(1-\dfrac{(K_2-K_1)}{K_2}\cdot \exp\left(\dfrac{-(x-R_f)}{k\cdot R_f}\right)\right) \text{if } R_f \le x \le R_i(k,R_f) \\ K_1 \text{ pretējā gadījumā} \end{cases} \tag{5.8}$$

kur x ir koordināte viendimensionālā gadījumā, k - adhēzijas efektivitāte, R_f - pildvielas daļiņas biezums. Adhēzijas efektivitāte mainās no 0 līdz 1 un raksturo pildvielas un saistvielas mijiedarbības spēku. Starpfāzes biezums R_i ir definēts kā attālums no pildvielas daļiņas līdz saistvielas materiālam ar novirzi no saistvielas īpašībām $\delta = 0.1\%$. To var aprēķināt no formulas

$$R_i(k,R_f) = R_f - R_f \cdot k \cdot \ln\left(\delta \frac{\delta \cdot K_2}{(K_2-K_1)}\right).$$

Formulas NK bīdes modulim ir iegūtas pēc analoģijas ar formulām NK tilpuma modulim.

Att. 5.10 ir parādītas tilpuma moduļa izmaiņas sistēmai, kas sastāv no pildvielas, starpfāzes un saistvielas materiāliem. Ir izmantoti četri dažādi pildvielas saturi, kas atbilst eksperimentālajām vērtībām. No attēla ir redzams, ka, pildvielas saturam palielinoties, palielinās arī starpfāzes biezums. Tas noved pie efektīvā tilpuma moduļa samazināšanos attiecībā uz sistēmu kopumā.

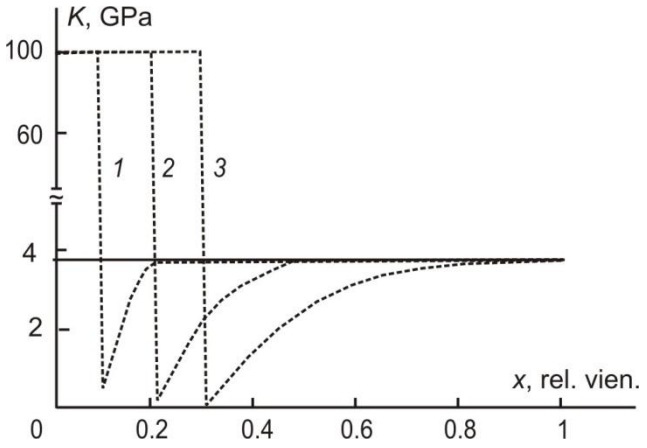

Att. 5.10. Trīsfāzu sistēmas tilpuma modulis dažādam pildvielas saturam R_f = 1, 2 un 3% (cipari uz līknēm) un taisna līnija – nepildīta saistviela, k = 0.3.

Turklāt adhēzijas efektivitāte būtiski ietekmē starpfāzes biezumu un tādā veidā samazina elastības moduļa vērtību, līdz ar R_i pieaugumu. Starpfāzes biezuma atkarība no pildvielas satura un adhēzijas efektivitātes ir parādīta Att. 5.11. Ir skaidri redzams, ka, palielinoties pildvielas saturam vai pildvielas daļiņu biezumam, palielinās arī starpfāzes biezums, sasniedzot maksimālo vērtību pie augstākās adhēzijas efektivitātes, kad k = 1.

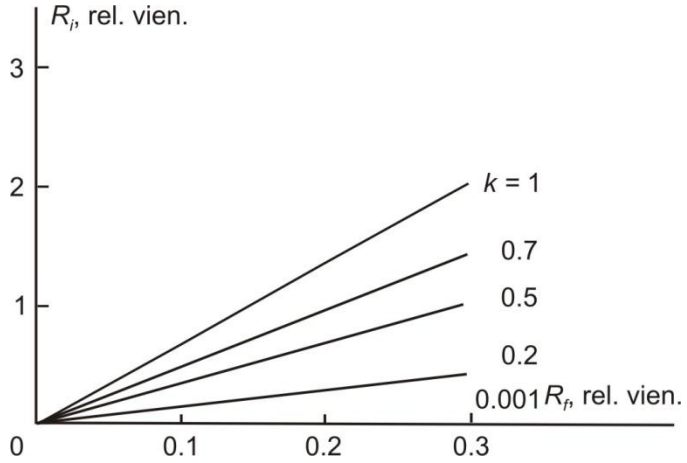

Att. 5.11. Starpfāzesu biezums atkarībā no pildvielas daļiņas biezuma dažādām adhēzijas efektivitātes vērtībām.

Pēc tam moduļu iegūtās izteiksmes ir vidējotas pa visu sistēmu kvazidaļiņas nemainīgu īpašību iegūšanai pēc formulām

$$\bar{K}(k,R_f)=\frac{1}{x_{\max}}\cdot\int_0^{R_i(k,R_f)}K(x,k,R_f)dx\,, \tag{5.9}$$

$$\bar{\mu}(k,R_f)=\frac{1}{x_{\max}}\cdot\int_0^{R_i(k,R_f)}\mu(x,k,R_f)dx\,. \tag{5.10}$$

Šie elastības raksturlielumi ir izmantoti, lai novērtētu NK elastības moduli, ņemot vērā adhēzijas efektivitāti un kvazidaļiņas ar novidējotām īpašībām. Elastības moduli nosaka, izmantojot labi zināmu attiecību starp elastības raksturlielumiem

$$\bar{E}(k,R_f)=\frac{9\cdot\bar{K}(k,R_f)\cdot\bar{\mu}(k,R_f)}{3\cdot\bar{K}(k,R_f)+\bar{\mu}(k,R_f)}. \qquad (5.11)$$

Galīgais rezultāts, attiecībā uz KM elastības moduli, ir parādīts Att. 5.12. Iepriekš minēts, ka starpfāzes elastības modulis ir zemāks, nekā polimēra saistvielā. Kā redzams no šī attēla, adhēzijas efektivitāte ievērojami ietekmē KM elastības īpašības un pazemina efektīvo elastības moduli. Interesanti atzīmēt, ka, pieaugot adhēzijas efektivitātei, starpfāzes biezums palielinās un, tādējādi, palielinās arī pildvielas kvazidaļiņu saturs. Vidējošana pa pildvielas daļiņas biezumu rezultējās monotoni augošā funkcijas atkarībā no pildvielas satura.

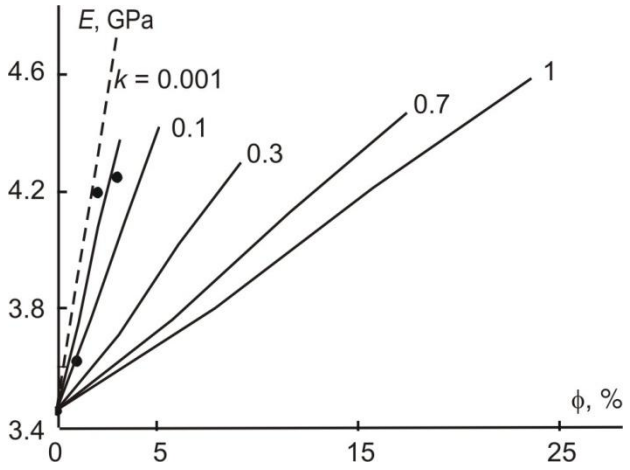

Att. 5.12. Efektīvais elastības modulis atkarībā no pildvielas tilpuma satura (punkti – eksperimentālie dati, pārtraukta līnija – aprēķins pēc formulas (5.7), nepārtraukta līnija – aprēķins pēc formulas (5.11)).

Tādējādi, KM tilpuma un bīdes moduļu aprakstīšanai ir izmantotas Norrisa izteiksmes haotiski orientētām plāksnītēm, kuras var pielietot pie maziem pildvielas saturiem, kad pildvielas daļiņas nepārklājas. Vispirms, nosacīti, nanolīmenī ir noteiktas kvazidaļiņu īpašības, ņemot vērā adhēzijas efektivitāti un dažādu pildvielas saturu. Jāatzīmē, ka pildvielas daļiņu elastības modulis garenvirzienā ir dominējošs parametrs šajos aprēķinos. Tā kā literatūrā ir maz datu par MMT elastības konstantēm var secināt, ka, mainot šīs vērtības, var iegūt labāku eksperimentālo datu atbilstību.

Saskaņā ar teorētiskā apraksta rezultātiem, izmantojot Norrisa izteiksmes, var diezgan labi aprakstīt kvazistatiskās stiepes rezultātus. Tomēr šī apraksta rezultāti ir augstāki, ko var izskaidrot ar parametru precīzo vērtību (piem., MMT māla elastīgo konstanšu un proporcijas parametra) trūkumu. Viena no iespējām, kā izskaidrot šo novirzi, ir ievest starpfāzi. Ņemot vērā adhēzijas efektivitāti un augstu pildvielas daļiņu virsmu, NK gadījumā ir iegūts diezgan liels kvazidaļiņu saturs. Tādēļ starpfāzes biezums un adhēzijas efektivitāte var ievērojami ietekmēt

NK mehānisko uzvedību un tādēļ šie parametri ir jāievēro. Šī daudzlīmeņu analīze dod iespēju novērtēt pildvielas un starpfāzes īpašību ietekmi un saturu uz NK efektīvajiem elastības īpašībām. Tomēr polimēri nav elastīgas cietas vielas un tiem ir raksturīga arī viskoelastīgā uzvedība, tādēļ ir svarīgi izpētīt arī NK viskoelastīgās īpašības, kas ir apskatītas nākamajā nodaļā.

6. Epoksīda bāzes nanokompozīta viskoelastīgās īpašības

[P6], [C3]

Polimēra bāzes NK dažādu veidu pielietošanai ir īpaši svarīgi novērtēt pielietojamo materiālu ilgtermiņa deformējamību un izturību, dažādu vides faktoru ietekmes apstākļos (slodze, paaugstinātā un/vai mainīgā temperatūra, un mitrums) [37, 38]. Polimēru pildīšana ar mitrumu necaurlaidīgām MMT plāksnītēm var ietekmēt NK kopējās viskoelastīgās īpašības un rezultātā samazināt NK padevīgumu mitruma absorbcijas procesā. Šajā nodaļā ir apspriesta un analizēta mitrināto NK paraugu viskoelastīgā uzvedība, pie dažāda pildvielas satura.

NK šļūdes slodzes un atslodzes režīmā ir iegūtas padevīguma līkņu saimes paraugiem ar dažādu pildvielas saturu un dažādām absorbētā mitruma daudzuma vērtībām *w*. Šo līkņu aprakstīšanai ir izmantots Bolcmaņa-Volterra (Boltzmann-Volterra) lineārais integrālais vienādojums

$$\varepsilon(t) = \frac{\sigma(t)}{E} + \frac{1}{E}\int_0^t K(t-s)\sigma(s)ds \tag{6.1}$$

ar šļūdes kodolu eksponenšu summas veidā:

$$K(t) = \sum_{i=1}^{n} \frac{b_i}{\tau_i} e^{-\frac{t}{\tau_i}}, \tag{6.2}$$

kur, τ_i, un b_i, i = 1, ..., n, ir retardācijas laiku spektrs. Saskaņā ar mitruma-laika analoģijas principu,

$$t = t' a_w, \tag{6.3}$$

kur $a_w(w)$ ir mitruma-laika redukcijas funkcija, kas raksturo izmaiņas retardācijas spektrā, izmainoties mitruma daudzumam materiālā.

Gadījumā, kad spriegums mainās pēc likuma

$$\sigma(t) = \sigma_0 H(t) - \sigma_0 H(t-t_0), \tag{6.4}$$

kur t = 0 un t_0 ir attiecīgi slodzes un atslodzes laika momenti, un $H(t)$ ir Hevisaida pakāpju funkcija, padevīgumam $I(t) = \frac{\varepsilon(t)}{\sigma_0}$ ir iegūta sekojoša izteiksme

šļūdes slodzes režīmam pie $t<t_0$,

$$I(t) = \frac{1}{E} + \frac{1}{E}\sum_{i=1}^{n} b_i \left(1 - e^{-\frac{t a_w}{\tau_i}}\right), \tag{6.5}$$

šļūdes atslodzes režīmam pie $t>t_0$,

$$I(t) = \frac{1}{E}\sum_{i}^{n} b_i e^{-\frac{t a_w}{\tau_i}} \left(e^{\frac{t_0 a_w}{\tau_i}} - 1 \right). \qquad (6.6)$$

Mitruma-laika redukcijas funkcija ir izvēlēta attiecīgā veidā

$$\ln a_w = \alpha_1 w + \alpha_2 w^2 . \qquad (6.7)$$

Šādas funkcijas bieži pielieto epoksīda saistvielām un epoksīda bāzes KM [39].

Īstermiņa šļūdes slodzes (7,5 st) rezultāti sausajam (nemitrinātam) materiālam liecina, ka NK šļūdes padevīguma līknes paraugiem ar pildvielas saturu $c = 0$ un 4% gandrīz sakrīt, izņemot momentāno padevīgumu $I_0 = 1/E$ (Att. 6.1*a*). Pildvielas satura ietekme parādās saistībā ar momentānā padevīguma pieaugumu. Pētāmo materiālu mitrināšana noveda pie ievērojamā šļūdes padevīguma pieauguma (Att. 6.1*a*). Acīmredzot, tas saistīts ar to, ka materiāls ir tuvu viskoelastīgajam stāvoklim.

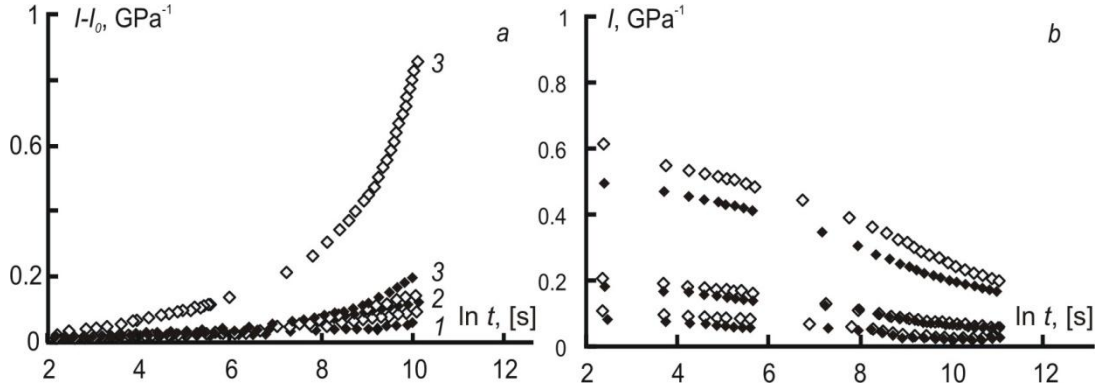

Att. 6.1. NK padevīguma līknes pildvielas saturam $c = 0$ (♦) un 4 (◊)%, φ = 24 (*1*), 77 (*2*) un 98% (*3*) šļūdes slodzes (*a*) un atslodzes režīmā (*b*).

Šļūdes eksperimenti parādīja, ka pēc 17 st novērošanas, šļūdes atslodzes deformācija laika gaitā vēl turpināja samazināties (skat. Att. 6.1*b*). Tas nozīmē, ka var uzskatīt, ka šļūdes deformācijas ir atgriezeniskas. Lai pārbaudītu šo pieņēmumu, ir nepieciešams, lai modeļa parametri, kas ir noteikti no šļūdes slodzes rezultātiem, būtu piemērojami arī šļūdes atslodzes rezultātiem un otrādi. Tad retardācijas laiku spektrus τ_i, b_i, $i = 1,\ldots, n$ (6.2) un mitruma-laika redukcijas funkciju (6.7), NK ar dažādu pildvielas saturu var noteikt no šļūdes atslodzes eksperimentu rezultātiem. Katrai pildvielas satura c vērtībai, no šļūdes atslodzes padevīguma līkņu saimes, atbilstoši dažādam mitruma daudzumam w, ir aproksimētas ar vienādojumu (6.6), saskaņā ar (6.7). Aproksimācija ir veikta, izmantojot SIMPLEX algoritmu, programmā FORTRAN, un mazāko kvadrātu metodi novirzei starp aprēķinu un eksperimentu rezultātiem. Retardācijas laiku sākotnējās vērtības ir izvēlētas ar vienādu soli logaritmiskajā skalā, t.i., 1, 10, 100, utt., un šļūdes kodola eksponenciālo funkciju (6.2) skaits ir $n = 7$. Mērķa funkcijas

minimizācijas laikā tika noraidīti summēšanas locekļi ar pirmsekponentes reizinātāja koeficientu ar kārtu 10^{-3} un mazāk. Rezultātā, vienādojumā (6.2) ir palikušas tikai četras eksponentes.

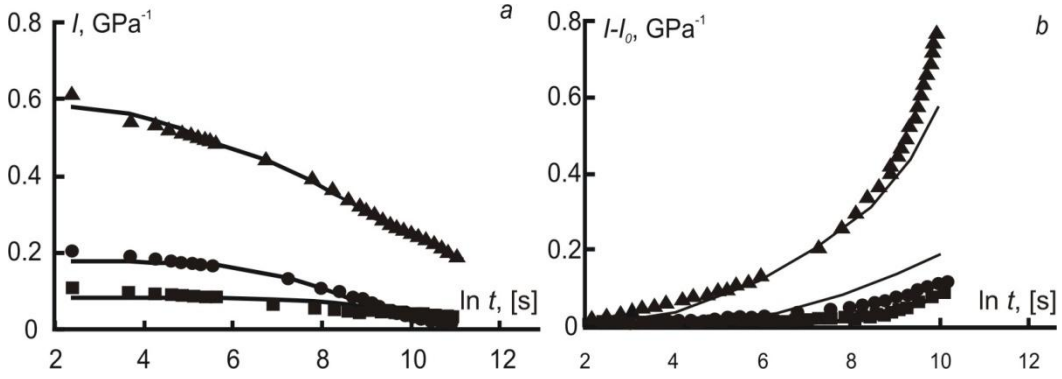

Att. 6.2. NK eksperimentāli noteiktās padevīguma līknes šļūdes atslodzes (*a*) un slodzes režīmā (*b*) pildvielas saturam *c* = 4%pie *w* = 0 (■), 2,04 (●), un 3.52% (▲), to aproksimācija ar izteiksmi (6.6), saskaņā ar (6.7) (*a*), un aprēķins pēc izteiksmes (6.5), saskaņā ar (6.7) (*b*).

Piemēram, Att. 6.2*a* ir parādītas aproksimētas šļūdes atslodzes padevīguma līknes NK ar pildvielas saturu *c* = 4%. Izmantojamā modeļa atbilstības pārbaude parādīja šļūdes slodzes eksperimentu apmierinošu aprakstu (Att. 6.2*b*). Retardācijas laiku spektri un mitruma-laika redukcijas funkcija NK ar dažādu pildvielas saturu, iegūti no padevīguma līkņu aproksimācijas, ir attiecīgi doti Att. 6.3 un Att. 6.4. Redzams (Att. 6.3), ka retardācijas laiku spektri NK ar *c* = 2 un 4% gandrīz neatšķiras no saistvielas spektra: tām ir kopīgā amplitūdas apliecēja. Tomēr NK ar *c* = 6% šie spektri atšķiras: retardācijas laiki palielinās, bet to intensitāte nedaudz samazinās. Tā rezultātā spektra apliecēja ir plakanāka, salīdzinot ar spektru apliecēju saistvielai un NK pie *c* < 6%.

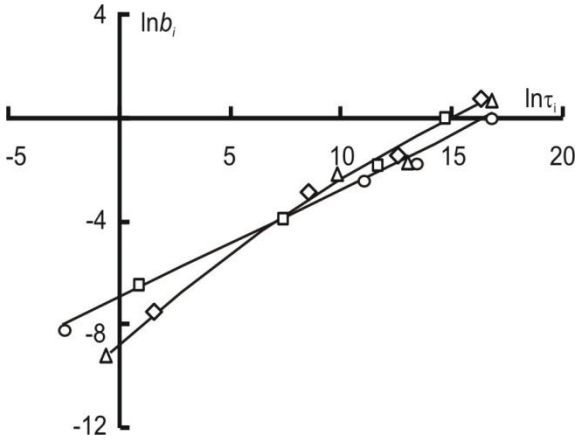

Att. 6.3. Retardācijas laiku spektri NK ar *c* = 0 (◊), 2 (□), 4 (Δ), un 6% (○).

Mitruma-laika redukcijas funkcijas NK ar dažādu pildvielas saturu (skat. Att. 6.4) ir nelineāras, ieliektas līnijas, kas raksturo arvien lielāku absorbētā mitruma ietekmi, palielinoties mitruma daudzumam materiālā. Mitruma-laika redukcijas funkciju salīdzinājums, NK ar dažādu *c*, liecina, ka mazs pildvielas saturs (*c* = 2%) vājina mitruma ietekmi uz KM saistvielas

viskoelastīgām īpašībām. Iespējams, ka tas ir saistīts ar pildvielas daļiņu un saistvielu makromolekulu mijiedarbību un tai sekojošu fizikālo saišu veidošanos. Iespējams, ka kāda daļa no absorbētā mitruma atrodas starpfāzes slānī [27]. Pieaugot pildvielas saturam, mitruma ietekme uz KM saistvielas viskoelastīgajām īpašībām palielinās, un pie c = 6% kļūst vienāda ar tīras saistvielas mitruma-laika redukcijas funkciju. Tādējādi, pildvielas daļiņas atslābina NK saistvielas struktūru, un relaksācijas procesu ātrums lielo laiku apgabalā samazinās.

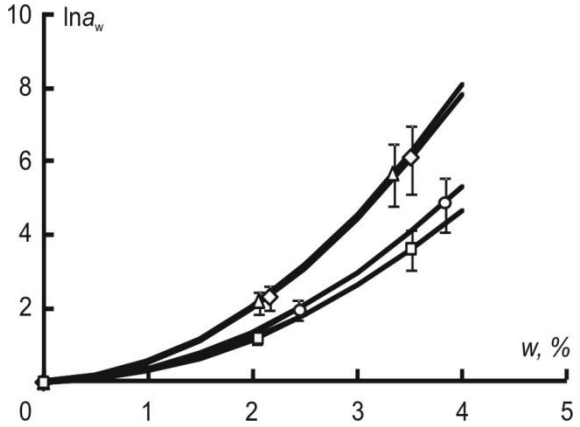

Att. 6.4. Mitruma-laika redukcijas funkcijas NK ar c = 0 (◊), 2 (□), 4 (Δ), un 6% (○), iegūtas no šļūdes atslodzes līkņu saimes aproksimācijas pēc izteiksmēm (6.6) un (6.7) materiālam ar dažādu mitruma daudzumu.

NK robežmitruma daudzuma ietekme uz viskoelastīgajām īpašībām izpaužas piespiestās elastības robežas sprieguma izmaiņās, kas izriet no kvazistatiskajiem stiepes eksperimentiem (skat. Att. 5.2*b*). Saskaņā ar Eiringa (Eyring) vienādojumu, piespiestās elastības robežas (augšējā plūstamības robeža spriegumam) atkarībai no deformācijas ātruma ir sekojoša izteiksme

$$\sigma_{v.e.} = A + B \ln \dot{\varepsilon} . \tag{6.8}$$

Ņemot vērā viskoelastības relaksācijas raksturu $\dot{\varepsilon}\tau_i = const_w$,

$$\ln \frac{\dot{\varepsilon}_1}{\dot{\varepsilon}_0} = \ln \frac{\tau_i^0}{\tau_i^1} = -\ln a_w , \tag{6.9}$$

t.i., piespiestās elastības robežas izmaiņām jākorelē ar redukcijas funkciju. Šī korelācija tiešām eksistē: NK ar dažādu pildvielas saturu, piespiestās elastības robežas izmaiņas ir tieši proporcionālas mitruma-laika redukcijas funkcijai (Att. 6.5). Šī korelācija var kalpot par pamatu alternatīvajai mitruma-laika redukcijas funkcijas noteikšanai, proti, izmantojot kvazistatisko eksperimentu rezultātus pastāvīgas deformācijas ātruma režīmā.

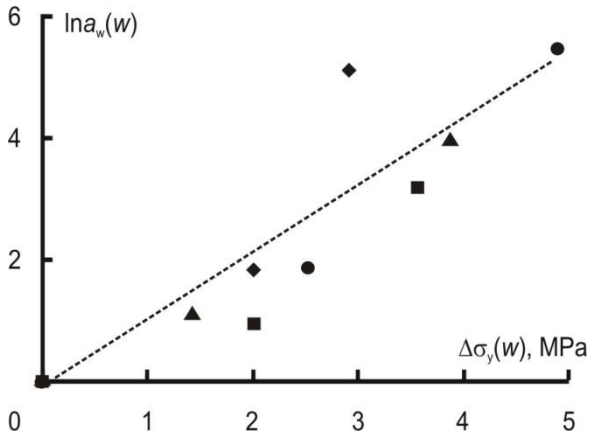

Att. 6.5. Mitruma-laika redukcijas funkcijas (6.7) korelācija ar augšējās plūstamības robežas sprieguma izmaiņām kvazistatiskos stiepes eksperimentos NK ar c = 0 (♦), 2 (■), 4 (▲), un 6% (●).

Pastāv alternatīvs veids redukcijas funkcijas noteikšanai – no tilpuma deformācijas [39]. Pieņemot, ka nepildīta polimēra saistviela ir izotropa, tilpuma izplešanās deformācija ir $\frac{\Delta V}{V_0} = 3\varepsilon_h$ un, izmantojot attiecību starp redukcijas funkciju un tilpuma izmaiņām [40],

$$\ln a_w = \frac{1}{f_0^2}\frac{\Delta V}{V_0}\frac{1}{1+\frac{1}{f_0}\frac{\Delta V}{V_0}}, \qquad (6.10)$$

ir dabūta mitruma-laika redukcijas funkcija (Att. 6.4), kas atbilst šļūdes eksperimentos noteiktai pie f_0 = 0.062.

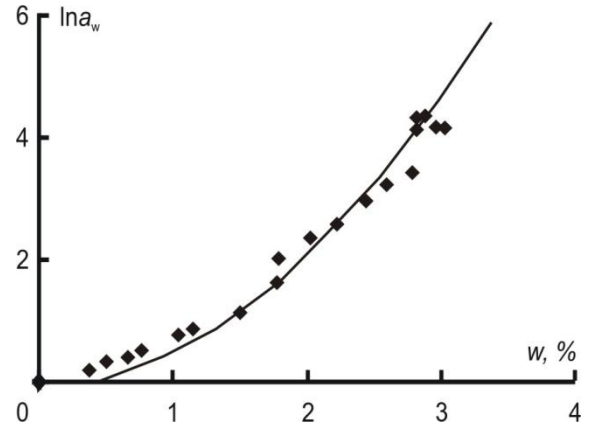

Att. 6.6. Mitruma-laika redukcija epoksīda saistvielai: punkti – aprēķins pēc formulas (6.10), ņemot vērā izplešanās deformācijas un mitruma daudzumu sakarību; līnija – šļūdes atslodzes līkņu saimes aproksimācija, kas dota Att. 6.4.

Tādējādi, pamatojoties uz mitruma-laika analoģijas principu, ir iegūta epoksīda saistvielas mitruma-laika redukcijas funkcija, kas korelē ar paraugu tilpuma izmaiņām mitrināšanas laikā. Tas ļauj novērtēt redukcijas funkciju no paraugu izplešanās rezultātiem. Savukārt, noteiktā mitruma-laika redukcijas funkcijas korelācija ar piespiestās elastības robežas izmaiņām norāda uz NK paraugu ar dažādu mitruma daudzumu, deformācijas viskoelastīgo raksturu.

Polimēru KM viskoelastīgās īpašības ir pilnībā saistītas ar apkārtējās vides apstākļiem (temperatūru, mitrumu). Palielinoties temperatūrai, molekulāro pārkārtojumu frekvence pieaug, bet retardācijas laiki samazinās. Tādējādi, NK paraugu, absorbējot mitrumu, uzvedība atšķiras. Tas izpaužas arī NK stiklošanās temperatūras atšķirībā. Epoksīda bāzes NK termofizikālo īpašību īpatnības un to sasaiste ar struktūras izmaiņām mitrināšanas procesā ir apspriestas nākamajā nodaļā.

7. Epoksīda bāzes NK termofizikālās īpašības un struktūras izmaiņas pie mitrināšanas

[P5], [C3]

NK paraugu fāzes un relaksācijas pāreju īpatnības ir izpētītas, izmantojot termomehāniskās analīzes metodi (TMA), bez ārējās slodzes. Tipiskas TMA līknes NK paraugiem, izturētiem līdz piesātinājuma stāvoklim vidēs ar relatīvo mitrumu no 24 līdz 98%, ir attēlotas Att. 7.1. Redzams, ka visiem NK, tostarp arī tiem, kas atrodas vidē ar mitrumu 77%, TMA līknēm pastāv šaurs temperatūras apgabals (5-10^{o}C) ar strauju deformācijas rakstura izmaiņu, kad sildīšanas laikā paraugu izplešanās pie temperatūras T_1 ir aizstāta ar saraušanos. Pēc tam, pie temperatūras T_2, tikpat ātri sākas jauns deformācijas pieaugums. Šādas atkarības ir raksturīgas amorfiem polimēriem, kuros, izejot caur stiklošanās temperatūru T_g, diezgan ātri notiek kristalizācija, kas noved pie materiāla sacietēšanās. Tālāk spontāni sākas izveidoto kristalītu kušana, kas izraisa TMA līkņu kāpumu.

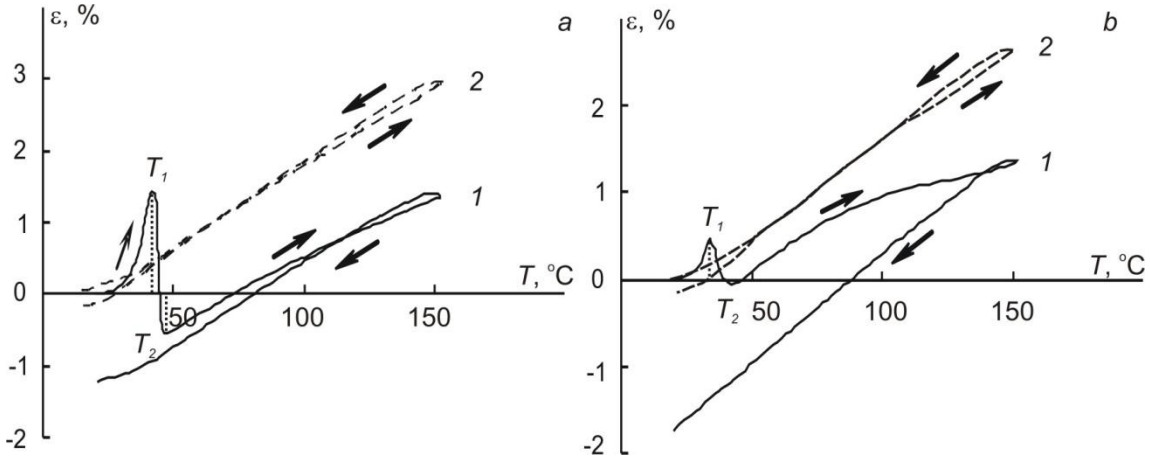

Att. 7.1. TMA līknes NK paraugiem ar c = 4%, φ = 24% (*a*) un 98% (*b*) (sildīšanas-dzesēšanas kārtas numurs (*1*, *2*)).

NK saistvielas sarukums ir saistīts ar kristalizāciju, kas ir eksperimentāli apstiprināts ar pārbaudes eksperimentiem, paraugus vairākkārt sildot līdz 70 ^{o}C un dzesējot līdz 20 ^{o}C. Att. 7.2 ir parādītas triju sildīšanas-dzesēšanas ciklu TMA līknes, kas liecina, ka katrā ciklā kristalizācijas procesā ir novērots paraugu rukums un tam sekojošais kausēšanas process, ar spontānu paraugu pagarinājumu. Līdz ar to, norādītajā temperatūras apgabalā 20-70 ^{o}C pārstrukturēšanas procesi polimēra saistvielā notiek atgriezeniski, kristalizācija sākas pie T_1 = 41-45 ^{o}C, un kušana pie T_2 = 46-50 °C.

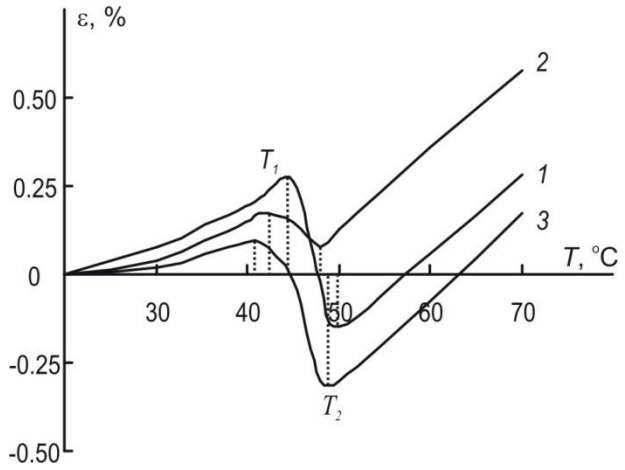

Att. 7.2. TMA līknes epoksīda saistvielai pie φ = 24% (sildīšanas-dzesēšanas kārtas numurs (*1*, *2*, *3*)).

Savukārt, rentgena struktūras analīze apstiprina, ka pēc paraugu sākotnējās atlaidināšanas, pie temperatūras 80 ^{o}C un tai sekojošās žāvēšanas vidē ar relatīvo mitrumu 24%, saistvielā ir saglabāta kristāliskā fāze (skat. Att. 7.3 difraktogrammu *1*). MMT nanodaļiņu iekļaušana NK sastāvā (difraktogrammu *2*), izraisa NK epoksīda saistvielas kristāliskā refleksa (intensitātes maksimuma) parametru izmaiņu. Piem., tā izraisa starpplākšņu attāluma *d* pieaugumu un līdz ar to iekšējā sprieguma izmaiņas NK.

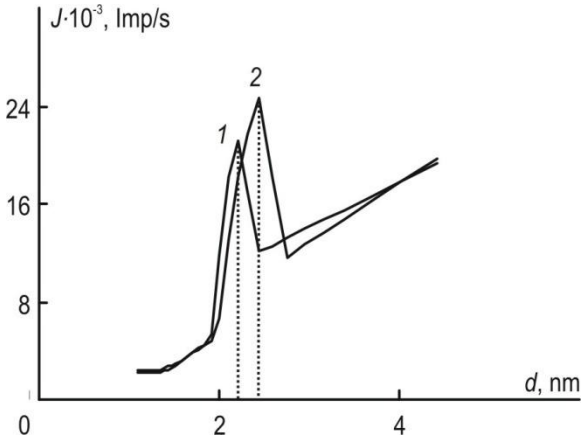

Att. 7.3. Difraktogrammas NK paraugiem ar *c* = 0% (*1*) un 6% (*2*).

Eksistē zināmas grūtības stiklošanās temperatūras T_g noteikšanā no TMA līknēm, jo stiklošanās temperatūras sasniegšana ir priekšnosacījums NK saistvielas kristalizācijai. Pieņemts, ka atstiklošanas un kristalizācijas procesa sākumposms norit gandrīz vienlaicīgi. Tādēļ pieņemts, ka TMA-līknēm deformācijas maksimālā temperatūra T_1 (Att. 7.1), kas raksturo kristalizācijas temperatūru, atbilst arī stiklošanās temperatūrai T_g. Tādējādi, pielietojot TMA analīzi, NK ar dažādu pildvielas saturu mitruma ietekmē, parādīts (Att. 7.4), ka NK stiklošanās temperatūra samazinās no 45 līdz 35 °C, pieaugot mitruma daudzumam NK, savukārt, NK stiklošanās temperatūra, attiecībā uz pildvielas saturu, vidēs ar vienādu relatīvo mitrumu, mainās nenozīmīgi.

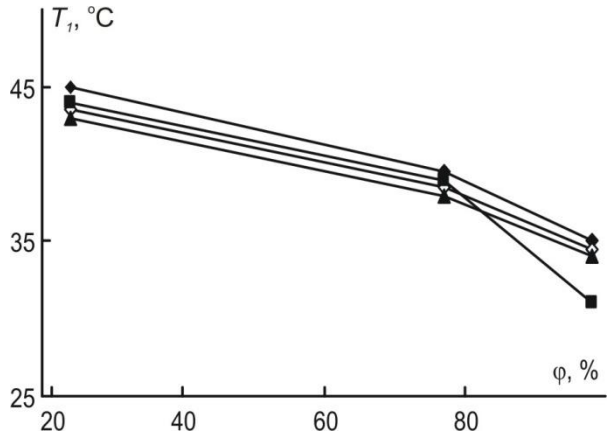

Att. 7.4. Stiklošanās temperatūras atkarība no vides relatīvā mitruma NK ar c = 0 (♦), 2 (◊), 4 (▲), un 6% (■).

Vājš pildvielas pastiprināšanas efekts, iespējams, ir saistīts ar zemu polimēra makromolekulu un pildvielas daļiņu starpķēžu mijiedarbību, kā arī ar iespējamu pildvielas daļiņu aglomerāciju [14]. Savukārt, epoksīda sveķu un NK stiklošanās temperatūras samazināšanās ar mitruma daudzuma pieaugumu (skat. Att. 7.4) liecina, ka absorbētais mitrums plastificē materiālu, t.i., veicina polimēra makromolekulu mijiedarbības intensitātes samazināšanos un segmentu mobilitātes pieaugumu, kas izraisa relaksācijas procesu paātrinājumu. Epoksīda sveķu un NK stiklošanās temperatūra ir novirzīta temperatūras apgabalā, kas tikai par 10-20 °C atšķiras no istabas temperatūras, t.i., temperatūras, kurā notiek mehāniskie eksperimenti. Tādēļ slodze var izraisīt epoksīda saistvielas pāreju uz viskoelastības apgabalu, kuram ir raksturīgas lielas deformācijas. Dotā epoksīda saistviela ar palielināto mitruma daudzumu atrodas pārejas apgabalā no stiklveida uz viskoelastīgo stāvokli.

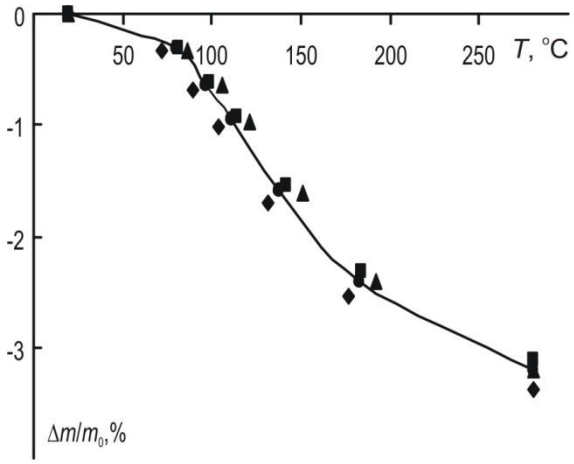

Att. 7.5. Masas zudumi NK paraugiem ar c = 0 (♦), 2 (■), 4 (▲), un 6% (●) pie φ = 98%.

Termogravimetriskās analīzes masas zudumu līknēs (skat. Att. 7.5) ir redzams, ka temperatūras apgabalā 80-170 ^{o}C, masas zudumu process notiek ātrāk. Tas labi atbilst termiskās izplešanās koeficienta samazināšanai. Maksimālie masas zudumi ir novērojami paraugiem,

uzturētiem vidē ar relatīvo mitrumu 98%. Piem., NK ar c = 6% masas zudumi pie T = 150 ^{o}C ir 1,5%, bet saistvielai tie ir 2% pie tādiem pašiem nosacījumiem. Tomēr noteikta masas zudumu atkarība no pildvielas satura nav novērota. Vēl lielākā temperatūras palielināšana izraisa masas zudumu ātruma samazināšanos. Vadoties pēc gandrīz lineāras savstarpējās mitruma daudzuma un masas zudumu atkarības (Att. 7.6), var secināt, ka NK paraugu, sildīšanas laikā līdz 280 ^{o}C, dominē mitruma desorbcijas process.

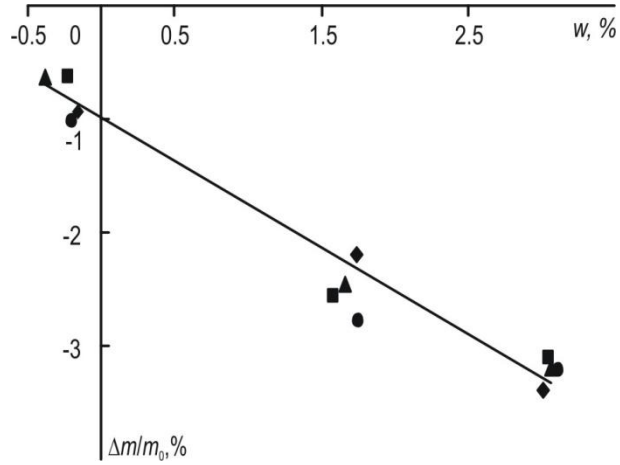

Att. 7.6. Mitruma daudzums NK paraugos ar c = 0 (♦), 2 (■), 4 (▲), un 6% (●) atkarībā no masas zudumiem sildīšanas laikā.

Noteicot attiecību starp NK termofizikālajām īpašībām un struktūras izmaiņām, TMA analīze ir pielietota epoksīda bāzes NK paraugiem pēc kvazistatiskiem stiepes (Att. 5.1) un šļūdes eksperimentiem (Att. 6.1). Šim nolūkam paraugi, mitrinātie vidē ar φ = 98%, tika iepriekš deformēti kvazistatiskajā režīmā, kad $\dot{\varepsilon}$ = const un šļūdes režīmā, kad σ = const, kamēr pilnīgi viss parauga darba platums nonāca „kakliņā". Tad paraugi tika izgriezti stiepšanas gareniskajā un šķērsvirzienā. Analizējot TMA līknes (Att. 7.7*a*), ir redzams, ka šo NK paraugu termiskās izplešanās savstarpēji perpendikulāros virzienos ievērojami atšķiras. Ir novērotas termomehānisko raksturlielumu anizotropas izmaiņas. Līdzīgi rezultāti ir iegūti arī NK paraugiem pēc šļūdes eksperimentiem. NK paraugiem, kas ir izgriezti stiepšanas virzienā gan pēc kvazistatiskās stiepes, gan pēc eksperimentiem šļūdē, ir skaidri redzama TMA līkņu līdzība (Att. **7.7***b*). Piem., stiklošanās temperatūras apgabalā to lineārie izmēri strauji samazinās. Tomēr paraugi, kas ir orientēti šļūdes režīmā (līkne *2*), saraujas lielākā mērā, un process turpinās šaurākā temperatūras diapazonā, nekā paraugiem, orientētiem kvazistatiskajā stiepē (līkne *1*). Temperatūrai sasniedzot 37 ^{o}C (šļūdes režīmā orientētiem paraugiem) un 64 ^{o}C (kvazistatiskajā stiepes režīmā orientētiem paraugiem), tikpat ātri kā rukumam, sākās spontānais paraugu izplešanās process.

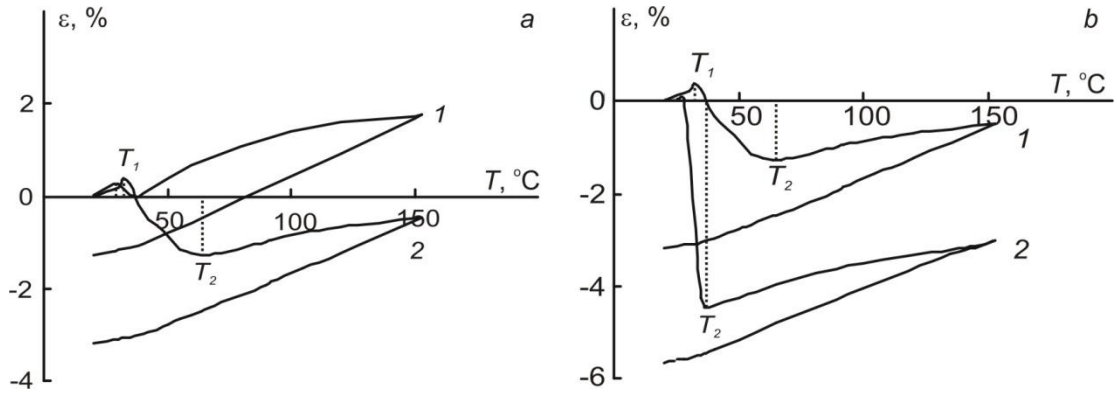

Att. 7.7. TMA līknes NK paraugiem, izgrieztiem paraugu šķers- (*1*) un gareniskajā (*2*) stiepšanas virzienā kvazistatiskajā stiepē (*a*) un paraugiem, izgrieztiem gareniskajā stiepšanas virzienā kvazistatiskajā stiepē (*1*) un šļūdē (*2*) (*b*).

No TMA līkņu salīdzinājuma neslogotajiem NK paraugiem (Att. 7.1*b*), ir redzams, ka orientēto paraugu kristalizācija sākas pie zemākas temperatūras. Savukārt, rukuma vērtība, kas ir proporcionālā polimēra saistvielas kristāliskuma pakāpei, ir daudz lielāka nekā slogotiem paraugiem. Tas ir izskaidrojams ar to, ka orientācijas laikā notiek ievērojama NK struktūras pārkārtošanās, un, tādējādi, tā pāreja uz kristālisko struktūru ir krietni atvieglota. Sekojot kristalizācijai, fibrillu agregātu izmēri nav pilnībā atgūti NK paraugos. Tajā pašā laikā, TMA līknes paraugiem, izgrieztiem orientācijas pretējā virzienā, pēc kvazistatiskajiem stiepes un šļūdes eksperimentiem, rezultāti liecina, ka tās gandrīz sakrīt attiecībā uz deformējamības izmaiņas raksturu un tās vērtību. Otrā cikla paraugu TMA līknes liecina, ka neslogotiem paraugiem, eksistē tikai viena pāreja, kas ir saistīta ar NK atstiklošanos.

Rentgena struktūras analīzes dati korelē ar struktūras izmaiņām NK pie lielām deformācijām. Att. 7.8 ir parādītas meridiāna un ekvatora difraktogrammas NK paraugiem, slogotiem līdz sabrukšanai. Redzams, ka mazo leņķu apgabalā ekvatora difraktogrammā ir novērojams maksimums, ko izraisa kristāliskās fāzes eksistence. Tajā pašā laikā tas nav novērojams meridiāna difraktogrammai. To var izskaidrot ar to, ka, stiepšanas procesā, materiāls iegūst gandrīz pilnībā fibrilētu orientētu struktūru, kas noved pie raksturīgas mikroplaisu pazušanas. Acīmredzot, notiek mikroplaisu savienošana, tādēļ meridiāna difraktogrammā nav novērota difūzā izkliede.

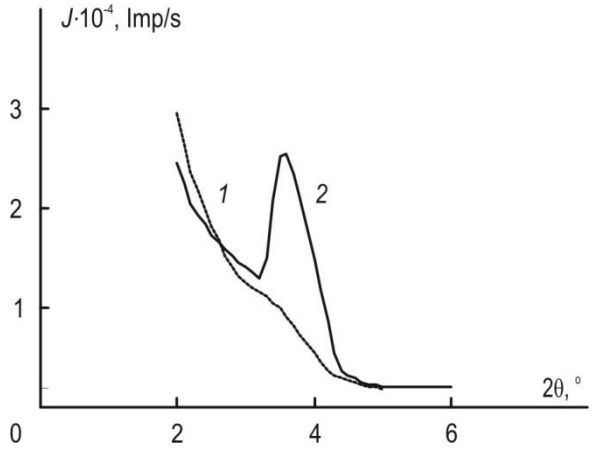

Att. 7.8. Difraktogrammas iepriekš deformētiem NK paraugiem ar *c* = 6%, izgrieztiem no "kakliņa" apgabala: meridiāns (*1*); ekvators (*2*).

No iepriekš minētajiem datiem izriet, ka NK nelīdzsvarotās struktūras termomehāniskās uzvedības īpatnības, pēc stiepšanas, lielā mērā nosaka sākotnējais saistvielas daudzums. Tas nonāk orientētā stāvoklī, kurā veidojas fibrillu agregāti un mikroplaisas. Izmaiņas notiek stiklošanās temperatūras apgabalā un tādēļ tiem ir virsmolekulārais raksturs. NK paraugus sildot, fibrillas iegūst lielāku mobilitāti, un notiek koagulācijas procesi. Tas noved pie fibrillu savstarpējās dezorientācijas un starpfāzes apgabalu samazināšanos, kas makroskopiski parādās kā NK rukums.

Šī nodaļa noslēdz kompleksu mehānisko un termofizikālo īpašību izpēti epoksīda bāzes NK, pildītam ar MMT nanodaļiņām, pie tā mitrināšanas. Noteikta termofizikālo un mehānisko īpašību sasaiste ar struktūras izmaiņām, kas ir novērota epoksīda bāzes NK paraugu mitrināšanas un deformācijas procesos. Tā ir ir noteikta pie dažādiem slodzes pielikšanas režīmiem un dažādām temperatūrām. Darba galvenie secinājumi un rezultāti, kā arī to praktiskā nozīme un zinātniskā novitāte, ir apspriestas un analizētas nākamajā nodaļā.

8. Darba galvenie rezultāti, praktiskā nozīme, un zinātniskā novitāte

Dažādu epoksīda sveķu un epoksīdsveķu-māla nanokompozīta kompleksās sorbcijas, mehāniskās un termofizikālo īpašību izpētes galvenie rezultāti ir sekojoši:

1. Pētāmā epoksīda-māla nanokompozīta absorbcija ir pietiekami labi aprakstīta ar Fika modeli pie visiem pildvielas saturiem 0-6% pēc masas, un vidēs ar relatīvo mitrumu 24, 77, un 98%. Eksperimentāli ir pierādīts, ka sorbcijas process NK norit daudz lēnāk nekā epoksīda saistvielas paraugos, un NK ar augstāko pildvielas saturu difūzijas koeficients samazinās par pusi, salīdzinot ar difūzijas koeficientu epoksīda saistvielai. Māla nanodaļiņas darbojas kā efektīvas barjeras pret mitruma pārnesi. Robežmitruma daudzuma pieaugums, kas ir novērots NK ar pildvielas satura pieaugumu, ir izskaidrots ar starpfāzes satura pieaugumu. Ir noteikta īpatnējā starpfāzes sorbcijas ietilpība NK uz 1% pildvielas un iegūta starpfāzes sorbcijas izoterma.
2. Konstatēta būtiska mitruma ietekme uz mehāniskajām īpašībām. Absorbētais mitrums ievērojami plastificē kompozītu, izmainot tā sabrukuma raksturu. Mitrināto kompozītu stiepes stiprība samazinās divas reizes. Gan mitrinātu epoksīda saistvielas, gan NK ar dažādu pildvielas moduli elastības modulis samazinās aptuveni par 1/3, salīdzinot ar nosacīti sākotnējo stāvokli.
   2.1. Pildvielas morfoloģisko īpatnību ietekmes novērtēšanai, attiecībā uz NK elastības īpašībām, ir modificēti Halpina-Tsai vienādojumi slāņveida silikāta plāksnīšu gadījumam. Šie vienādojumi ir pielietoti NK efektīvo elastības moduļu noteikšanai, NK paraugiem ar dažādu mitruma daudzumu. Vienādojuma parametri, kas ir iegūti paraugiem no sausās vides, ir izmantoti mitrinātu NK paraugiem, kas dod iespēju novērtēt polimēra saistvielas struktūras, izmaiņas, mitruma absorbcijas dēļ.
   2.2. Starpfāzes ietekmes novērtēšanai uz NK elastības īpašībām, ir iegūtas izteiksmes epoksīda-māla NK tilpuma un bīdes moduļiem, modificējot Norrisa izteiksmes izotropai saistvielai ar haotiski orientētām plāksnītēm. Vispirms, nanolīmenī ir novērtētas kvazidaļiņu īpašības, ņemot vērā adhēzijas efektivitāti, pie dažāda pildvielas satura. Tad epoksīdsveķi ir pildīti ar šīm kvazidaļiņām un ir piemērots mikromehānikas modelis epoksīda-māla NK elastības īpašību noteikšanai. Šī nano- un mikrolīmeņu analīze ļauj novērtēt pildvielas un starpfāzes īpašību un satura ietekmi uz NK efektīvajām elastības īpašībām kopumā.
3. Epoksīda sveķu un NK viskoelastīgo īpašību atkarība no absorbētā mitruma daudzuma ir aprakstīta, balstoties uz mitruma-laika analoģijas principu.
   3.1. Retardācijas laiku spektri NK ar pildvielas saturu 6% atšķiras no retardācijas laiku spektra epoksīda saistvielai: retardācijas laiki palielinājās, bet to intensitāte nedaudz

samazinās. Mitruma-laika redukcijas funkcijas vērtība NK ar pildvielas saturu 2% ir mazāka, salīdzinot ar epoksīda sveķiem. Pildvielas saturam palielinoties vēl vairāk, redukcijas funkcijas parametri palielinās.

3.2. Konstatēts, ka mitruma-laika redukcijas funkcija korelē ar NK piespiestās elastības izmaiņām, kas norāda uz deformācijas viskoelastīgo raksturu, NK paraugiem ar dažādu mitruma daudzumu.

3.3. Noteikta epoksīda sveķu mitruma-laika redukcijas funkcijas un tilpuma izmaiņu korelācija, kas ļauj novērtēt mitruma-laika redukcijas funkciju no paraugu izplešanās datiem.

4. NK mitruma absorbcija izraisa materiāla plastifikāciju un stiklošanās temperatūras samazināšanos par 10 ^{o}C. Mitruma ietekmes dēļ, ir būtiski mainījies NK deformācijas mehānisms. Mitrinātiem NK paraugiem ir novērotas lielas deformācijas un orientētu apgabalu veidošanās („kakliņš"), stiepšanas procesā. Termiskā izplešanās ievērojami atšķiras NK paraugiem, izgrieztiem savstarpēji perpendikulāros virzienos pēc stiepes kvazistatiskiem un šļūdes eksperimentiem. Ir novērotas termomehānisko raksturlielumu anizotropas izmaiņas. Rentgenstruktūras analīzes dati korelē ar NK struktūras izmaiņām pie lielām deformācijām.

5. Mitruma necaurlaidīgu māla nanodaļiņu ar augstām mehāniskajām īpašībām iekļaušana kompozīta sastāvā nesamazina absorbētā mitruma negatīvo ietekmi uz NK mehāniskajām īpašībām. Bet, tā kā epoksīda sveķu elastības moduļa vērtība ir uzlabota atkarībā no pildvielas satura līdz 20%, epoksīda sveķus, pildītus ar necaurlaidīgām cietām montmorillonīta māla nanodaļiņām, var rekomendēt pielietošanai vidēs ar augstāku ekspluatācijas relatīvo mitrumu.

Dažādu epoksīda sveķu un to bāzes kompozītu sorbcijas, mehānisko un termofizikālo īpašību kompleksās izpētes **praktisko nozīmi** raksturo iegūtie rezultāti jauno kompozītmateriālu noturības novērtēšanai, dažādu apkārtējās vides faktoru (temperatūra, mitrums, slodze, u.c.) iedarbībā. Šie rezultāti ļauj novērtēt iespējamus pielietojumus nanomāla kompozītmateriāliem vides faktoru iedarbībā, kas var paplašināt polimēru kompozītu materiālu pielietošanu būvniecības un tehnoloģijas nozarēs. Tā kā kompozītu pielietošana dažādās dzīves sfērās kļūst nenovēršama, neatjaunojamo dabas resursu zuduma dēļ, KM pielietošanas efektivitātei un drošībai ir jābūt garantētām ar pareizu ekspluatācijas īpašību izpēti dažādu faktoru iedarbībā.

Šī darba ietvaros ir izvirzītas sekojošas tēzes, kurām ir **zinātniskā novitāte**:

1. Epoksīda-māla NK mitruma absorbcijas modelēšanā un sorbcijas īpašības noteikšanā ir svarīgi ņemt vērā saistvielas nehomogenitāti un starpfāzes veidošanos;

2. Halpina-Tsai vienādojumu modificēšana izotropai polimēra saistvielai ar transversāli izotropām cilindriskām daļiņām, ar patvaļīgu malu attiecību un haotisko pildvielas daļiņu orientāciju, ļauj novērtēt KM tilpuma un bīdes moduļus. Tā rezultātā noteikts epoksīda-māla NK

efektīvais elastības modulis, ņemot vērā pildvielas morfoloģiskās īpatnības (pildvielas daļiņu slāņveida struktūru un nehomogēnas starpfāzes veidošanos);

3. Konstatētā NK mitruma-laika redukcijas funkcijas korelācija ar piespiestās elastības izmaiņām un tilpuma izmaiņām, mitrināšanās dēļ, norāda uz deformācijas viskoelastīgo raksturu NK paraugiem, ar dažādu mitruma daudzumu, kas ļauj to novērtēt, pamatojoties uz paraugu izplešanās datiem.

4. Noteiktas NK termomehānisko raksturlielumu anizotropas izmaiņas, savstarpēji perpendikulāros virzienos, pēc stiepes kvazistatiskiem un šļūdes eksperimentiem, labi korelē ar rentgena struktūras analīzes datiem.

Promocijas darba galvenie rezultāti ir publicēti 6 zinātniskajos rakstos [P] un 3 konferenču materiālos [C], kā arī apspriesti 12 starptautiskajās konferencēs (konferenču tēzes nav iekļautas promocijas darbā).

9. Atsauces

1. *Fornes T. D., Yoon P. J., Hunter D. L., Keskkula H., Paul D. R.* Effect of organoclay structure on nylon 6 nanocomposite morphology and properties. Polymer, 2002, Vol. 43, No. 22, p. 5915-5933.
2. *LeBaron P., Wang Z., Pinnavaia T. J.* Polymer-layered silicate nanocomposites: an overview. Applied Clay Science, 1999, Vol. 15, No. 1, p. 11-29.
3. *Gay D., Hoa A., Tsai S.* Composite materials. Design and applications. CRC Press, 2003, 503 p.
4. Roco M. Broader social issues of nanotechnology. Journal of Nanoparticle Research, 2003, Vol. 5, No. 3-4, p. 181-189.
5. *Aniskevich K., Glaskova T., Janson Yu.* Elastic and sorption characteristics of an epoxy binder in a composite during its moistening. Mechanics of Composite Materials, N. Y., Kluwer Academic/Plenum Publishers, 2005, Vol. 41, No. 4, p. 341-350.
6. *Vlasveld D., Groenevold J., Bersee H., Mendes E., Pichen S. J.* Analysis of the modulus of polyamide-6 silicate nanocomposites using moisture controlled variation of the matrix properties. Polymer, 2005, Vol. 46, No. 16, p. 6102-6113.
7. *Kim J.-K., Hu Ch., Woo R. S. C., and Sham M.-L.* Moisture barrier characteristics of organoclay-epoxy nanocomposites. Composites Science and Technology, 2005, Vol. 65, No. 5, p. 805-813.
8. *Crank J.* The Mathematics of Diffusion, Oxford, 1956, 224 p.
9. *Maggana C. and Pissis P.* Water sorption and diffusion studies in an epoxy resin system. Journal of Polymer Science. Part B — Polymer Physics, 1999, Vol. 37, No. 11, p. 1165-1182.
10. *Andrikson G. A., Mochalov V. P., and Aniskevich A. N.* Principle of modified time scale for tasks of nonstationary moisture diffusion in polymer materials. Mekh. Kompoz. Mater., 1980, Vol. 16, No. 1, p. 153-170.
11. *Xiao G. Z. and Shanahan M. E. R.* Swelling of DGEBA/DDA epoxy resin during hygrothermal ageing. Polymer, 1998, Vol. 39, No. 14, p. 3253-3260.
12. *Koo J. H.* Polymer nanocomposites. McGraw-Hill, 2006.
13. *Ajayan P. M., Schadler L. S., Braun P. V.* Nanocomposite science and technology. Wiley, 2003.
14. *Yasmin A., Luo J. J., Abot J. L., Daniel I. M.* Mechanical and thermal behaviour of clay/epoxy nanocomposites. Composites Science and Technology, 2006, Vol. 66, No. 14, p. 2415-2422.
15. *Maksimov R. D., Gaidukov S., Zicans J., and Jansons J.* Moisture permeability of a polymer nanocomposite containing unmodified clay. Mechanics of Composite Materials, 2008, Vol. 44, No. 5, p. 505-514.
16. *Glaskova T., Aniskevich A.* Moisture effect on deformability of epoxy/montmorillonite nanocomposite. Journal of Applied Polymer Science, 2010, Vol. 116, No. 1, p. 493-498.
17. *Wang J., Pyrz R.* Prediction of the overall moduli of layered silicate-reinforced nanocomposites – part I: basic theory and formulas. Composites Science and Technology, 2004, Vol. 64, No.7-8, p. 925-934.
18. *Christensen R. M.* A critical evaluation for a class of micromechanics models. Journal of Mechanics and Physics of Solids, 1990, Vol. 38, p. 379-404.
19. *Norris A. N.* The mechanical properties of platelet reinforced composites. International Journal of Solids and Structures, 1990, Vol. 26, p. 663-674.
20. *Odegard G. M., Clancy T. C., Gates T. S.* Modeling of the mechanical properties of nanoparticle/polymer composites. Polymer, 2005, Vol. 46, p. 553-562.
21. *Wang J., Pyrz R.* Prediction of the overall moduli of layered silicate-reinforced nanocomposites-part II: analyses. Composites Science and Technology, 2004, Vol. 64, p. 935-944.

22. *Bicerano J.* Prediction of polymer properties. 3d ed., Marcel Dekker, 2002, 756 p.
23. *Giannelis E.* Polymer layered silicate nanocomposites. Advanced materials, 1996, Vol. 8, p. 29-35.
24. *Pal R.* Mechanical properties of composite of randomly oriented platelets. Composites: Part A, 2008, Vol. 39, p. 1496-1502.
25. *Maksimov R. D., Gaidukov S., Kalnins M., Zicans J., Plume E.* A nanocomposite based on styrene-acrylate copolymer and native montmorillonite clay. Part 2. Modeling of the elastic properties. Mechanics of Composite Materials, 2006, 42, p. 163-172.
26. *Halpin J. C., Kardos J. L.* The Halpin-Tsai equations: a review. Polymer Engineering and Science, 1976, Vol. 16, No. 5, p. 344-352.
27. *Glaskova T., Aniskevich A.* Moisture absorption by epoxy/montmorillonite nanocomposite. Composites Science and Technology, 2009, Vol. 69, No.15-16, p. 2711-2715.
28. *Ferry J. D.* Viscoelastic properties of polymers. John Wiley & Sons. New York, 1961, 218 p.
29. *Perez C. J., Alvarez V. A., Vazquez A.* Creep behaviour of layered silicate/starch-polycaprolactone blends nanocomposites. Materials Science and Engineering A, 2008, Vol. 480, No. 1-2, p. 259-265.
30. *Glaskova T. I., Guedes R. M., Morais J. J., Aniskevich A. N.* A comparative analysis of moisture transport as applied to an epoxy binder. Mechanics of Composite Materials, 2007, Vol. 43, No. 4, p. 377-388.
31. *Bond D. A.* Moisture diffusion in a fiber-reinforced composite. Pt.I. Non-Fickian transport and the effect of fiber spatial distribution. Journal of Composite Materials, 2005, Vol. 39, No. 23, p. 2113-2129.
32. *Weitsman Y.* Diffusion with time-varying diffusivity with application to moisture sorption in composites. Journal of Composite Materials, 1976, Vol. 10, p. 193-204.
33. *Masenelli-Varlot K., Chazeau L., Gauthier C., Bogner A., Cavaillé J.Y.* The relationship between the electrical and mechanical properties of polymer–nanotube nanocomposites and their microstructure. Composites Science and Technology, 2009, Vol. 69, p. 1533-1539.
34. *Tsai J., Sun T.* Effect of platelet dispersion on the load transfer efficiency in nanoclay composites. Journal of Composite Materials, 2004, Vol. 38, p. 567-579.
35. *Chen B., Evans J. R. G.* Elastic moduli of clay platelets. Scripta Materialia, 2006, Vol. 54, p. 1581-1585.
36. *Anthoulis G. I., Kontou E.* Micromechanical behavior of particulate polymer nanocomposites. Polymer, 2008, Vol. 49, p. 1934-1942.
37. *Luo J.-J., Daniel I. M.*. Characterization and modeling of mechanical behavior of polymer/clay nanocomposites. Composites Science and Technology, 2003, Vol. 63, p. 1607–1616.
38. *Starkova O., Yang J., Zhang Zh.* Application of time-stress superposition to non-linear creep of polyamide 66 filled with nanoparticles of various sizes. Composites Science and Technology, 2007, Vol. 67, p. 2691-2698.
39. *Aniskevich K., Krastev R., Hristova Yu.* Effect of long-term exposure to water on viscoelastic properties of an epoxy-based composition. Mechanics of Composite Materials, 2009, Vol. 45, No. 2, p. 137-144.
40. *Aniskevich A. N., Yanson Yu. O., Aniskevich N. I.* Creep of epoxy binder in a humid atmosphere. Mechanics of Composite Materials, 1992, Vol. 28, No.1, p. 12-18.

10. Publikāciju un konferenču materiālu saraksts

10.1. Promocijas darbā iekļaujamās publikācijas žurnālos

[P1] *Aniskevich K., Glaskova T., Janson Yu.* Elastic and sorption characteristics of an epoxy binder in a composite during its moistening. Mechanics of Composite Materials, N. Y., Kluwer Academic/Plenum Publishers, 2005, Vol. 41, No. 4, p. 341-350.

[P2] *Glaskova T. I., Guedes R. M., Morais J. J., Aniskevich A. N.* A comparative analysis of moisture transport models applied to epoxy binder. Mechanics of Composite Materials, N. Y., Kluwer Academic/Plenum Publishers, 2007, Vol. 43, No. 4, p. 377-388.

[P3] *Glaskova T., Aniskevich A.* Moisture absorption by epoxy/montmorillonite nanocomposite. Composites Science and Technology, 2009, Vol. 69, p. 2711-2715.

[P4] *Glaskova T., Aniskevich A.* Moisture effect on deformability of epoxy/montmorillonite nanocomposite. Journal of Applied Polymer Science, 2010, Vol. 116, No. 1, p. 493-498.

[P5] *Faitel'son E. A., Glaskova T. I., Korkhov V. P., Aniskevich A. N.* Structural changes in a clay-containing nanocomposite with a different moisture content caused by its deformation. Journal of Engineering Physics and Thermophysics, 2010, Vol. 83, No. 3, p. 443-451.

[P6] *Aniskevich K. K., Glaskova T. I., Aniskevich A. N., and Faitelson Ye. A.* Effect of moisture on the viscoelastic properties of epoxy-clay nanocomposite. Mechanics of Composite Materials, 2010, in press.

10.2. Promocijas darbā iekļaujamie konferenču materiāli (conference proceedings)

[C1] *Aniskevich A., Glaskova T., Spacek V., Sviglerova P.* Effect of moisture sorption on deformability of epoxy/montmorillonite nanocomposite. Proceedings of European conference on Composite Materials, 2006, CD, No. 90.

[C2] *Glaskova T., Aniskevich A.* Modeling of effective elastic properties of composite material containing nanoparticles with an inhomogeneous interphase. Proceedings of European Conference on Composite Materials, 2008, CD, No. 1454.

[C3] *Glaskova T., Aniskevich A.* Creep behavior of epoxy/clay nanocomposite. Proceedings of International Conference on Composite Materials, 2009, CD, No. F1:14.

10.3. Konferenču tēzes

1. *Glaskova T., Aniskevich K., Korkhov V.* Structure and properties of epoxy resin in filled composite during its moistening. Baltic Polymer Symposium, November 24-25, 2004, Kaunas, Lithuania. Book of abstracts p. 28.
2. *Glaskova T., Aniskevich A., Spacek, V., Sviglerova P*. Effect of moisture sorption on the mechanical properties of epoxy/montmorillonite nanocomposite. Mechanics of Composite Materials, May 29-June 2, 2006, Riga, Latvia. Book of abstracts p. 58.
3. *Aniskevich A., Glaskova T., Spacek V., Sviglerova P.* Effect of moisture sorption on deformability of epoxy/montmorillonite nanocomposite. 12-th European conference on Composite Materials, August 29 – September 1, 2006, Biarritz, France. Book of abstracts p. 101.
4. *Glaskova T., Aniskevich A., Starkova O., Merijs Meri R., Zicans J.* Mechanical performance of organo-clay-epoxy nanocomposite under moisture effect. Baltic Polymer Symposium, September 20-22, 2006, Riga, Latvia. Book of abstracts p. 51.
5. *T. Glaskova, A. Aniskevich, Yu. Jansons.* Organoclay-epoxy nanocomposite: properties modeling including interphase layer. ICSAM - The international Conference on Structural

Analysis of Advanced Materials, September 2-6, 2007, Patras, Greece. Book of abstracts p. 42.

6. *T. Glaskova, A. Tuchs, A. Aniskevich.* Modeling of volume-dependent properties of disperse filled composite material considering inhomogeneous interphase. Baltic Polymer Symposium, May 13-16, 2008, Otepaa, Estonia. Book of abstracts p. 65.
7. *E. A. Faitelson,T. I. Glaskova, A. N. Aniskevich, and V. P. Korhov.* Thermomechanical properties of epoxy/clay nanocomposite depending on filler and moisture content. Mechanics of Composite Materials, May 26-30, 2008, Riga, Latvia. Book of abstracts p. 84.
8. *T. Glaskova, A. Aniskevich*. Modeling of effective elastic properties of composite containing nanoparticles with an inhomogeneous interphase. European Conference on Composite Materials, June 2-5, 2008, Stockholm, Sweden. CD, No. 1454.
9. *T. Glaskova, A. Aniskevich, R. M. Guedes, and J. J. Morais*. Application of moisture absorption theories for epoxy resin system. Duracosys'08 (Durability Analysis of Composite Systems), July 16-18, 2008, Porto, Portugal. Book of abstracts p. 119, 120.
10. *T. Glaskova, A. Tuchs, A. Aniskevich.* Modeling of nanocomposite scalar properties taking into account inhomogeneity of the interphase. Functional materials and nanotechnologies, March 31-April 3, 2009, Riga, Latvia. Book of abstracts p. 190.
11. *T. Glaskova, A. Aniskevich.* Creep behavior of epoxy/clay nanocomposite. 17th International Conference on Composite Materials, July 27-31, 2009, Edinburgh, United Kingdom. CD.
12. *T. Glaskova, K. Aniskevich, A. Aniskevich*. Creep behavior of epoxy/clay nanocomposite. Mechanics of Composite Materials, May 24-28, 2010, Riga, Latvia. Book of abstracts p. 71.

11. Dalība pētniecisko projektu realizācijā

1. "Inovatīvi strukturāli integrēti kompozītmateriāli: dizains, iegūšanas un pārstrādes tehnoloģijas, ilgmūžība". Valsts pētījumu projekts materiālzinātnē, 2005.-2008.g. Projekta vadītājs Habil. Dr. Sc. Ing., LZA akadēmiķis *Juris Jansons*.
2. "Nanokompozītu ar neelastīgu matricu deformatīvo un stiprības īpašību izpēte". LZP grants No. 05.1933, 2006.-2010. g. Projekta vadītājs Habil. Dr. Sc. Ing., LZA akadēmiķis *Juris Jansons*.
3. "Jauno zinātnieku grupas izveide modernu dispersi pildīto polimēru kompozītmateriālu mehānisko un fizikālo īpašību izpētei nano-, mezo- un mikrolīmenī". Latvijas Universitātes pētījumu projekts No. Y2-ZP119-100, 01.06.-30.11.2009. Projekta vadītāja Dr. Phys. *Olesja Starkova*.
4. "Atbalsts doktora studijām Latvijas Universitātē". ESF projekts No. 20092009/0138/1DP/1.1.2.1.2/09/IPIA/VIAA/004, 01.10.2009.-31.09.2010.
5. "Cilvēkresursu piesaiste moderno kompozītmateriālu kompleksiem pētījumiem". ESF projekts No. 2009/0209/1DP/1.1.1.2.0/09/APIA/VIAA/114, 01.12.2009.-30.11.2012. Projekta vadītājs Habil. Dr. Sc. Ing., LZA akadēmiķis *Juris Jansons*.

Pateicības

Es vēlētos izteikt sirsnīgu pateicību savam zinātniskajam vadītājam Dr Sc. Ing. *Andrejam Aņiskevičam,* Polimēru mehānikas institūta (PMI) direktoram un mūsu laboratorijas vadītājam Habil. Dr. Sc. Ing *Jurim Jansonam,* Dr. Phys. *Oļesjai Starkovai* un Dr Sc. Ing. *Mauro Zarrelli*, kā arī pārējiem kolēģiem no PMI un CNR par jūsu ieguldījumu manu prasmju un zināšanu attīstībā.

Esmu bezgalīgi pateicīga arī L `ORÉAL Baltic (stipendija „Sievietēm zinātnē" ar UNESCO Latvijas Nacionālās komitejas un Latvijas Zinātņu akadēmijas atbalstu) un Eiropas Sociālajam fondam (projekti „Atbalsts doktorantūras studijām Latvijas Universitātē" un „Cilvēkresursu piesaiste moderno kompozītmateriālu kompleksiem pētījumiem") par sniegto finansiālo atbalstu visos promocijas darba tapšanas etapos.

Un visbeidzot pēdējo, bet milzīgu PALDIES es gribu izteikt manai ģimenei un draugiem par viņu nenovērtējamo atbalstu un bezgalīgo pacietību. Pateicoties manam vecākajam brālim, kuram pirmā izglītība bija fizika, es kādreiz biju nolēmusi studēt fiziku. Rezultātā es vēl joprojām ar lielu baudu veicu zinātniskos pētījumus. Mani vecāki un mans vīrs arī iedvesmoja mani strādāt efektīvāk un paveikt vairāk, lai viņi būtu priecīgi par mani ☺.

Promocijas darba kopsavilkums angļu valodā

UNIVERSITY OF LATVIA
FACULTY OF PHYSICS AND MATHEMATICS

Tatiana Glaskova

Summary of Doctoral Thesis
Type of work: collection of scientific papers

EXPERIMENTAL AND THEORETICAL INVESTIGATION OF THERMOPHYSICAL AND MECHANICAL PROPERTIES OF POLYMER NANOCOMPOSITES

Submitted for Doctoral Degree in Physics

Subbranch: Mechanics of Polymer and Composite Materials

Scientific supervisor:

Dr. Sc. Ing. Andrey Aniskevich

Institute of Polymer Mechanics

University of Latvia

Riga, 2010

Abstract

The doctoral thesis generalizes results of complex research of mechanical and thermophysical properties of epoxy-based nanocomposites and is presented as a set of scientific papers.

Polymers and composites are usually exposed to influence of external factors (temperature, humidity, mechanical loading, etc.) which cause a time-dependent change of their structure and properties due to physical and chemical transformations. Thus, predicting mechanical and thermophysical properties of composite materials, it is necessary to consider results of research about structure and properties time-dependent variability of polymer resins under the influence of external factors.

The aim of the work is to establish features of moisture absorption and to estimate influence of the absorbed moisture on mechanical and thermophysical properties of epoxy based nanocomposites.

For this purpose at first the kinetics of moisture absorption of epoxy matrix and composites on their basis was experimentally investigated in a wide interval of humidity. For the description of moisture absorption kinetics the comparative analysis of known sorption models is denoted and features of their application are analyzed. The model considering influence of an interphase is offered based on the results obtained for equilibrium moisture content for the nanocomposite. The density of this layer is assumed to be lower than for polymer resin owing to distinction of cross-linking. It is shown that the increase of filler content and consistently interphase leads to greater moisture absorption of composite materials.

Relatively high moisture absorption of epoxy resins causes changes in their structure and properties in time and there is subsequent deterioration of elastic properties of composites. Elastic characteristics of composite materials are investigated experimentally and are described by means of micromechanical models. It is shown that elastic modulus of polymer resin in a composite material depends on filler content and decreases with the increase of moisture content. The consideration of morphological features of filler particles (presence of layered structures and formation of an interphase) in a composite material and their influence on elastic characteristics of composite in whole is presented.

Viscoelastic behavior of epoxy resin and epoxy-nanoclay composite are analyzed after long-term influence of moisture. Application of thermomechanical analysis allowed establishing the basic regularities for glass transition temperature for nanocomposite with different filler and moisture contents. The experimentally obtained sets of creep and creep recovery curves for nanocomposite with different filler and moisture contents are approximated by means of the linear integral equation of Boltzmann-Volterra, considering a principle of moisture-time analogy.

It is shown that function of a moisture-time reduction correlates with change of a yield stress and volumetric change of nanocomposite samples during moistening that indicates viscoelastic character of deformation of nanocomposites and is confirmed by results of dilatometry.

Main results of doctoral thesis are published in 6 scientific articles [P] and 3 conference proceedings [C], and also reported at 12 international conferences.

The investigations were carried out at the Institute of Polymer Mechanics, University of Latvia, in 2003 – 2010.

Table of contents

1. Introduction, aim, and tasks of the work

It's well recognized that all history of mankind development is connected with the invention of some kind of composite materials (CM) which have become a push to technics and civilization development. The very first bricks and the pottery which have appeared app. 5000 years BC contained the crushed stones or reinforcing straw. Ancient potters regulated even porosity of the products. In the beginning of the first millennium Romans have invented the concrete which to high extent influenced building and civilization development.

The present time is remarkable for high rates of scientific and technical progress. The rapid development of modern technics demands more and more new materials having advanced properties. Materials having high durability, hardness, heat and corrosion resistance etc. and a joint combination of these properties are required. The main advantages of polymer composites over traditional kinds of materials (metals, ceramics, wood etc.) is a unique combination of properties (strength, deformation, impact, elastic, rheological, adhesive, electric, frictional, thermophysical etc.) and also a possibility to control material properties changing composition and conditions of manufacture.

Moisture absorption of epoxy resins leads to their time-dependent change in their structure and subsequent deterioration of properties. In order to minimize this negative effect of moisture on functional, structural, and mechanical properties of polymer composites the scientific and industrial interest is devoted to polymer/layered silicate nanocomposites (NC). Polymer NC include different types of matrix (thermoplastic, thermosets, or elastomers) filled with small quantity (less than 6% by weight) of nanosized (less than 100 nm at least in one dimension) particles. The excellent barrier capability with significantly reduced permeability of moisture and gases is one of the most attractive and useful properties that have not been fully explored in the past. The key to such performance rests in the ability to exfoliate and disperse individual, high-aspect ratio silicate platelets within the polymer matrix [1]. The complete dispersion of clay nanolayers in a polymer optimizes the number of available reinforcing elements for carrying an applied load and deflecting cracks. The coupling between the tremendous specific surface area of the clay ($S \approx 800$ m^2/g) and a polymer matrix facilitates stress transfer to the reinforcement phase, allowing for such tensile and toughening improvements [2].

One of the most prominent silicate nanofillers is montmorillonite (MMT). It belongs to phyllosilicate group of minerals that typically form in microscopic crystals. MMT, a member of the smectite family, is a 2:1 clay, meaning that it has 2 tetrahedral sheets sandwiching a central octahedral sheet. The particles are plate-shaped with an average thickness of one nanometer and diameter of approximately one micrometer. Due to dispersion of MMT nanoparticles with high

length to thickness ratio in polymer matrix, the obtained system can effectively operate as composite with anisotropic properties at nanolevel that is particularly useful for different applications. The attractive characteristics suggest a variety of industrial applications for NC: automotive (gas tanks, bumpers, interior and exterior panels), constructions (building sections and structural panels), aerospace (flame retardant panels and high performance components), electrical applications and electronics (electrical components and printed circuit boards), food packaging (containers and wrapping films) [3, 4]. The production and investigation of polymers composites belongs to material science area that is one of priority areas in Latvia („Innovation materials and technologies (nano-structured multifunctional materials and nanotechnologies)") and worldwide.

Epoxy resins widely used as composite matrix are very attractive due to their high strength and stiffness, high temperature resistance, low volatility, creep and shrinkage, good adhesion to metal and ceramic substrates. Nevertheless epoxy resins have a major drawback of moisture absorption, which in turn degrades the functional, structural and mechanical properties of the composites [5-7].

It is essential to investigate mechanical, thermal and barrier properties of NC and to estimate their steadiness to environmental effects. The improved stability of polymer NC could broaden their application in techniques and construction.

Change of structure and properties of polymers in time due to physical and chemical transformations under the influence of external factors (temperature, humidity, loading, etc.) leads to change of structure and properties of composite materials. The forecast of such changes is necessary to formulate basing on investigation results of time-dependent variability of structure and properties of polymers.

Usually polymer resins in a composite material are non-uniform, forming an interphase with more or less expressed border near the filler particles. The density of interphase could be above or below density of polymer resin owing to distinction of cross-linking and porosity degree. Thus morphological features of filler particles (layered structure and presence of interphase near the border of particles) could influence properties of a composite: elasticity characteristics, durability, and kinetics of moisture absorption, swelling and fracture character.

Therefore the aim of the work is to establish features of moisture absorption and to estimate influence of the absorbed moisture on mechanical and thermophysical properties of epoxy resins and epoxy-clay NC.

For this purpose the following objectives have been set:

1. To ascertain experimental regularities and to model the kinetics of moisture absorption of investigated epoxy resins and epoxy-clay NC in a wide range of humidity;

2. To establish effect of moisture on deformability of epoxy-clay NC and its components, to describe mechanical properties of NC by means of analytical models taking into account filler morphological peculiarities and to verify effect of moisture on deformability of NC incorporating silicate nanoparticles;

3. To forecast long-term creep of investigated materials using method of moisture-time analogy and to estimate change of retardation time spectrum and reduction function of polymer resin by addition of silicate nanoparticles;

4. To establish the interrelation of thermophysical and mechanical characteristics of epoxy-clay NC, having absorbed moisture, with the structural changes accompanying deformation at various schemes of loading and temperatures.

2. Overview of current scientific verities for investigation of mechanical and thermophysical properties of epoxy resins and epoxy-based nanoclay composites

Composite materials based on polymers are frequently exposed to a humid environment. Water molecules, as well as low-molecular substances, are able to move in a polymeric binder and change its physical properties. The key parameters determining the mechanism of moisture sorption are the chemical composition and microstructure of the polymers.

The moisture sorption in epoxy resins and composites based on them is investigated rather well. Different models have been suggested for describing the water sorption kinetics [8-10]. It is usually assumed that the moisture sorption in epoxy resins proceeds by diffusion according to Fick's law [8, 11]. Such a model, which suits well the initial stage of moisture sorption, is often inadequate for describing the moisture sorption process as a whole. The moisture sorption can activate different processes in a material, which, in turn, affect the water sorption kinetics (chemical reactions, leaching of low-molecular components, etc.). Therefore, for each investigated material it is necessary to estimate the applicability of different moisture transport models to describing experimental data on water sorption in epoxy binders and to determine the most adequate ones.

In order to minimize the negative effect of moisture on functional, structural, and mechanical properties of polymer composites the scientific and industrial interest devoted to polymer/layered silicate nanocomposites due to their outstanding properties and possible novel applications have resulted in numerous studies [12-14].

Owing to high shape-anisotropy and surface of the exfoliated silicate layers they act as efficient barriers against moisture transport through the material and cause an increase in the path length for molecules diffusing through the polymer. Since absorption of water reduces the elastic characteristics of hydrophilic polymers, the addition of nanoparticles to minimize the negative effects of water uptake is particularly useful [6, 15-16]. The reduction of moisture absorption in turn can suppress the internal damage and progress to improved long-term performance of the NC.

Although there have been numerous material syntheses, tests and characterizations of layered silicate-filled NC in the literature, the fundamental mechanisms are not fully clear and are rarely discussed [17]. Therefore a better understanding and prediction ability is significant in accelerating development and application of NC.

It should be emphasized that effective properties of two-phase composites have been extensively studied and various micromechanical models have been developed [18-25]. The

basis of these micromechanics models is elastic solution of an infinite matrix containing one inclusion. Nevertheless many authors proposed that apart from two base phases there is an interphase between particle and matrix and its properties should be taken into account [20, 21].

In the structural hierarchy of polymer-clay NC at least two states can be assigned: 1) state of total exfoliation of clay platelets with characteristic parameters as thickness and dimensions in the plane of platelets; and 2) state of incomplete exfoliation of clay platelets and characteristic parameters as thickness and dimensions in the plane of intercalated layered stacks [25]. The aspect ratio and orientation of anisometric particles determine their reinforcement degree. Nevertheless, it is difficult to control the orientation of plane particles during processing of composite and the real distribution of their orientation could be rather complex, the determination of the effective elastic constants of transversely isotropic layers of a NC with coplanar orientation of such particles is of great importance. The data obtained in this case could serve as initial for a further analysis of the elastic properties of a composite with disoriented nanoparticles taking into account their orientational distribution in the material [25].

Another point is that anisotropy of the layered silicate should be considered. A single layer of montmorillonite clay is a monoclinic crystal composed of two silica tetrahedral sheets and a central octahedral sheet [22]. Taking into account the hexagonal configuration of the tetrahedrons in the two tetrahedral sheets and layered structure of montmorillonite clay it could be assumed that a stack of the silicate layers is a transversely isotropic medium. For the case of intercalated silicate in composite, the layered structure remains while the galleries between layers are filled with polymer. This case also could be represented as transversally isotropic medium from an overall point of view.

Halpin-Tsai equations [25, 26] obtained for isotropic polymer matrix filled with coplanar transversally isotropic cylindrical particles of arbitrary aspect ratio could be used for the case of exfoliated NC. The elastic solution was obtained for the composite consisted of a single fiber encased in a cylinder of matrix, both embedded in an unbounded homogeneous medium, which is macroscopically indistinguishable from the composite. The relations between the stress and strain components have to be averaged throughout the composite. The obtained formulas are curve fitted to exact elasticity solutions and confirmed by experimental measurements in order to get the solution for composite filled with particles of arbitrary aspect ratio.

The mechanical phenomena taking place in the process of sorption and swelling in polymer composite materials, while being of certain theoretical and practical interest, have been studied slightly, especially for nanocomposite that are of interest in developing high-efficiency materials. For example, for clay-containing NC exhibiting improved mechanical, thermal, and

barrier properties compared to unfilled polymers, the majority of papers [2, 6, 14] presented results without conclusions about the processes proceeding in them.

Therefore it is significant to establish the relation between the thermophysical and mechanical characteristics of the clay-containing NC that has absorbed the moisture and the structural changes attending the deformation process under different kinds of load and at different temperatures.

Finally the use of modern materials – nanocomposites on the basis of a polymer resin in different areas of techniques, constructions, and also in electronics demands the estimation of long-term deformability and durability in the conditions of influence of different environmental factors (loading, raised and/or variable temperature and/or humidity). For the forecasting of long-term deformability and durability of conventional composite materials: polymers filled with microparticles of minerals, and also reinforced with carbon and glass fibers, the method of stress-time, temperature-time and moisture-time analogies is applied [28, 29]. This method is based on reduction of time by means of acceleration of relaxation processes at increase in level of loading, temperatures, and relative moisture content inside the material, characterized by reduction function. The function of temperature-time reduction which characterizes change of creep rate at change of temperature, for NC is higher in comparison with polymer resin.

Thus the complex research of mechanical and thermophysical properties of various epoxy resins and epoxy-nanoclay composite is necessary in order to determine the steadiness of modern composite materials to different environmental factors (temperature, humidity, loading, etc.) that will allow estimating possible applications of nanoclay composite materials.

3. Overview of materials and methods used within the work

The following thermosetting polymers are investigated in the work: 1) epoxy resin ED-22, hardened by polyethylene polyamine and filled with disperse crystal filler LiF (filler content 0.05, 0.11, 0.23, 0.28, 0.33, 0.38, and 0.46% by weight); 2) epoxy resin Reapox 520; and 3) bisphenol A epoxy resin, hardened by polypropylene oxide filled with particles of montmorillonite clay (filler content 2, 4 and 6% by weight).

Kinetics of moisture sorption is experimentally investigated using sorption method in atmospheres with relative humidity φ = 24, 34, 53, 77, 84 and 98% using desiccators with silica gel and saturated solution of salts $MgCl_2$, $Mg(NO_3)_2$, NaCl, KCl, and K_2SO_4 respectively. Specimens in the form of thin plates are used in order to measure the percentage of weight change due to moisture absorption as a one-dimensional diffusion mode. The specimens are placed then into the humid atmospheres at room temperature and periodically weighed with accuracy 0.00005 g using *Mettler Toledo XS 205DU*. The mass increment $m(t)$-m_0 is used to find the moisture content during sorption

$$w(t) = \frac{m(t) - m_0}{m_0} .$$

The investigations are performed by various mechanical methods: 1) quasistatic tension tests according to LVS EN ISO 527 standard by the use of *Zwick 2.5* testing machine with a crosshead rate of 5 mm/min at room temperature; and 2) creep in uniaxial tension according to ASTM D2990 standard by the use of creep-test bench at stress level equal to half of tensile strength for 7 h and recovery tests for 17 h for the specimens at room temperature.

The changes of structure and properties of investigated materials are studied by means of 1) differential scanning calorimetric analysis using *Mettler DSC 30* for temperature range from -50 to 150 °C at heating rate 10 °C/min; 2) thermogravimetry using *Mettler TA 3000* device for temperature range 20–280 ^{o}C at heating rate was 10 ^{o}C⁄min; 3) differential thermal analysis using *UIP-70M* device with specimens heated to 150 ^{o}C at heating rate 2 ^{o}C⁄min with subsequent cooling; and 4) X-ray diffraction analysis using *DRON - 3M* device with photography in transmitted light on CuK_α radiation. Scanning of angular intervals was carried out with a 0.1 ^{o} step and with a pulse collection time in each step of 90 sec.

The homogeneity of the filler particles' dispersion in polymer resin is approved by the transparency of all NC specimens. Additional microscopy methods such as scanning electron (SEM) and transmission electron microscopy (TEM) are applied for the micro structural analysis.

4. Modeling of moisture sorption of composite materials

4.1. Application of sorption models to kinetics of moisture sorption of epoxy resins

[P2]

As it was mentioned before moisture absorption of epoxy resins leads to the time-dependent change in the structure and subsequent deterioration of properties. Absorbed moisture can activate different processes in a material, which, in turn, affect the water sorption kinetics (chemical reactions, leaching of low-molecular components, etc.). Therefore, for each investigated material it is necessary to estimate the applicability of different moisture transport models to describing experimental data on water sorption in epoxy binders and to determine the most adequate ones.

Moisture sorption by epoxies is usually [9, 11, 27, 30] described by Fick's model. In this model [8], it is assumed that moisture sorption occurs only by diffusion, and, according to the first Fick's law, the diffusate flow density $\boldsymbol{j}$ is directly proportional to the gradient of its concentration C

$$\boldsymbol{j} = -D \operatorname{grad} C, \tag{4.1}$$

where D is the diffusivity describing the rate of moisture sorption, which is independent of moisture concentration. For a non-stationary state, with account of the mass conservation law, the second Fick's equation is valid. For the case of one-dimensional diffusion along the x axis, when the specimen thickness is smaller than its length and width, it has the form

$$\frac{\partial C}{\partial t} = D \frac{\partial^2 C}{\partial x^2}, \tag{4.2}$$

where C is the moisture concentration in the specimen at the instant of time t.

The solution to Eq. (4.1) for a plane-parallel plate of thickness h, with initial C ($0 < x < h$, $t = 0$) = C_0 and boundary C ($x = 0$, $x = h$, $t > 0$) = C_∞ conditions, is the series [8]

$$C(x,t) = C_\infty - 2\frac{(C_\infty - C_0)}{\pi}\sum_{k=1}^{\infty}\frac{\left(1-(-1)^k\right)}{k}\sin\left(\frac{\pi k}{h}x\right)\exp\left(-\left(\frac{\pi k}{h}\right)^2 Dt\right). \tag{4.3}$$

Integrating Eq. (4.3) across the plate thickness, we come to an expression for determining the moisture content in the specimen:

$$w(t) = w_\infty - 2\frac{(w_\infty - w_0)}{\pi^2}\sum_{k=1}^{\infty}\frac{\left(1-(-1)^k\right)^2}{k^2}\exp\left(-\left(\frac{\pi k}{h}\right)^2 Dt\right). \tag{4.4}$$

Here, w_∞ is the equilibrium moisture content in the specimen. The model considered contains two material characteristics as parameters: the diffusivity D and the equilibrium

moisture content w_∞. In numerous studies [e.g., 8], it is shown that, if the sorption curve is drawn on a diagram whose abscissa axis is $\sqrt{t}$, the initial section of this diagram will be a straight line passing through the origin of coordinates. Then, using experimental data, the diffusivity can be determined from its inclination:

$$D = \frac{\pi h^2}{16t} L^2, \tag{4.5}$$

where $L = \dfrac{w(t) - w_0}{w_\infty - w_0}$ is the change in the moisture content $w(t)$-w_0 in the specimen by the instant of time t, normalized to its maximum value.

The second parameter of the model – the equilibrium moisture content – as a rule, is found experimentally as the maximum achieved moisture content in the specimen. It should be noted here that, according to Eq. (4.4), this maximum is achieved only asymptotically at $t \to \infty$, which in practice leads to an error in determining w_∞. The relation between the diffusivity found by Eq. (4.5) and φ of the environment is shown in Figure 4.1 for Reapox 520 epoxy resin specimens stored in atmospheres with relative humidity φ = 33, 53, 75, 84 and 97%.

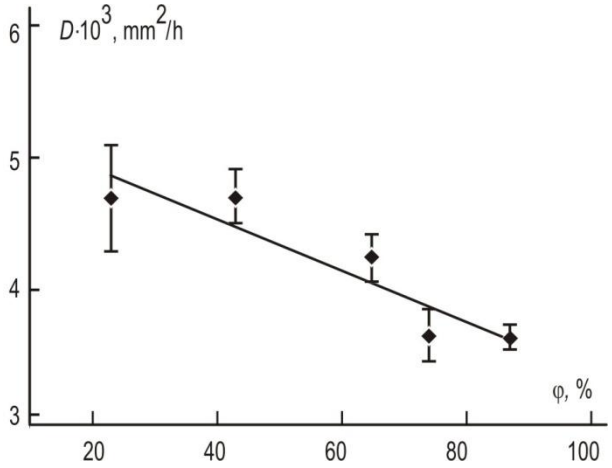

Figure 4.1. Diffusivity in relation to the relative humidity of environment.

The results from calculating the moisture content for Reapox 520 epoxy resin by Eq. (4.4) and experimental data for atmospheres of various humilities are shown in Figure 4.2. It is clear that the Fick's model describes well the process of moisture sorption in a low-humidity atmosphere, but when the relative humidity exceeds 75%, the moisture sorption process slows down in the middle part of sorption curve.

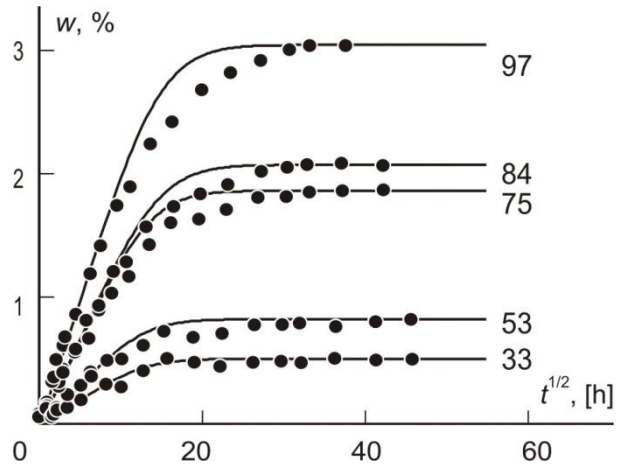

Figure 4.2. Changes in specimen mass with time at different values of φ (numbers next to the curves): experimental data (dots) and calculations by Fick's model (4.4) (curves).

In other words, the value of moisture sorption rate used in calculating the moisture content is overestimated, since the model disregards the processes of interaction between the moisture and polymer, swelling, etc., which accompany the process of moisture sorption. It is seen that the adequacy of Fick's model declines with increasing relative humidity of environment, since the diffusion mechanism becomes less dominating, and other mechanisms, such as the interaction between the polymer and the diffusate and/or relaxation processes, start to affect the moisture transport in the polymer [31]. The alternative models of moisture sorption which should be used to explain the deviation of moisture transport in polymers from the classical diffusion mechanism with the diffusivity independent of moisture concentration, take into account different subtle differences in the moisture sorption process in each particular case.

In the model known as the Jacob's–Jones model [9], it is assumed that the material consists of two phases of different density and, accordingly, different sorption properties. It is taken that the moisture sorption process in both the phases proceeds simultaneously and obeys Fick's law. The possibility of formation of chemical bonds between water and polymer molecules is neglected.

Accordingly, the moisture content in each phase of the material is expressed by the formulas

$$w_1(t) = w_{\infty 1} - 2\frac{(w_{\infty 1} - w_0)}{\pi^2}\sum_{k=1}^{\infty}\frac{\left(1-(-1)^k\right)^2}{k^2}\exp\left(-\left(\frac{\pi k}{h}\right)^2 D_1 t\right),$$

$$w_2(t) = w_{\infty 2} - 2\frac{(w_{\infty 2} - w_0)}{\pi^2}\sum_{k=1}^{\infty}\frac{\left(1-(-1)^k\right)^2}{k^2}\exp\left(-\left(\frac{\pi k}{h}\right)^2 D_2 t\right),$$

which contain four unknown parameters, namely the equilibrium moisture content and diffusivity of each of the phases. As a result, the total moisture content in the specimen is

$$w(t) = w_1(t) + w_2(t) \qquad (4.6)$$

where $w_1(t) = \frac{\Delta m_1}{m_0}$, $w_2(t) = \frac{\Delta m_2}{m_0}$; Δm_1, Δm_2 are the mass increments of the phases.

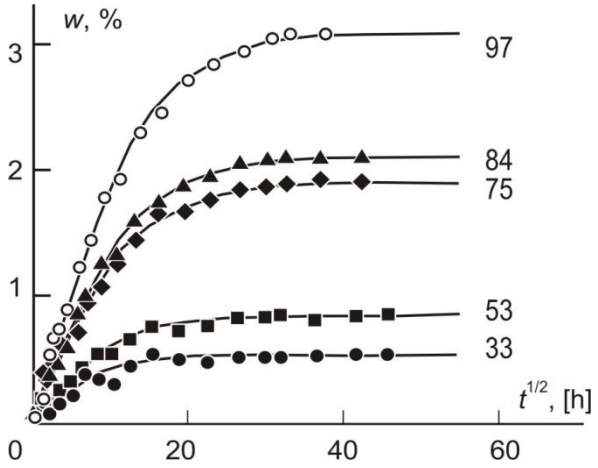

Figure 4.3. Changes in the mass of specimens with time at different values of φ (numbers next to the curves): experimental data (dots) and calculations by Eq. (4.6) (curves).

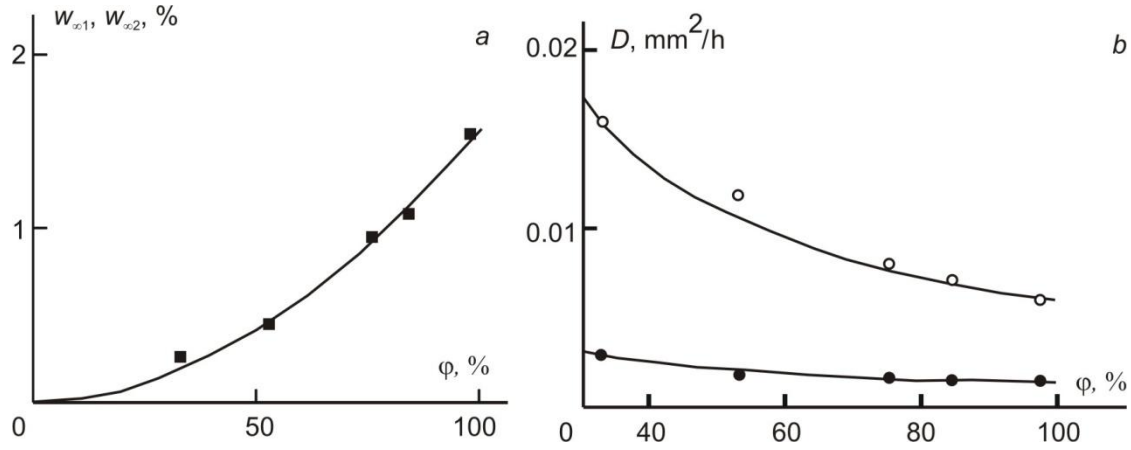

Figure 4.4. Sorption isotherms (*a*) and diffusivity (*b*) of the phases D_1 (○) and D_2 (●) in relation to φ.

The calculation by Eq. (4.6), presented in Figure 4.3, agrees with experimental data rather well for all the atmospheres considered, which means that the epoxy resin is two-phase. It is known that epoxy resins contain both areas with a sufficiently perfect and dense spatial network and poorly cross-linked regions, which can be regarded as a two-phase structure of the material. This model does not take into account possible changes in the material microstructure during the sorption process, which can be expressed in a worse description of sorption curves with increasing relative humidity of environment, as seen from Figure 4.3. Nevertheless, it can be used for an objective estimation of sorption characteristics of materials with a nonuniform structure.

As seen from Figure 4.4 sorption isotherms of two phases are almost equal. In turn, it follows from Figure 4.4 that, the diffusivity in the different phases differs several times. Probably, this reflects the real material structure with areas of relatively small and high

permeabilities. The account of two-phase nature of the system allows improving the description of the sorption curve.

The last sorption model presented in the thesis is a model with a time-dependent diffusivity [10]. According to this model, owing to the physical processes going on in the material (primarily, the plasticization and associate changes in the relaxation character, as well as aging, aftercure, etc.), the diffusivity decreases with time in proportion to its current value:

$$\frac{dD}{dt} = -\gamma D(t) .$$

The solution of this equation is $D = D_0 e^{-\gamma t}$. This model contains three parameters — the diffusivity at the initial instant of time D_0, the equilibrium moisture content w_∞, and the coefficient γ describing the rate of change in diffusivity.

To reduce the diffusion equation to Eq. (4.2) with a constant diffusivity D, the principle of modified time is used, by analogy with the change in D under a nonstationary temperature [32]:

$$dt^* = e^{-\gamma \cdot t} dt,\ t^* = \int_0^t e^{-\gamma \cdot t} dt = \frac{1 - e^{-\gamma \cdot t}}{\gamma} . \tag{4.7}$$

Then, the diffusion equation takes the form

$$\frac{\partial C}{\partial t^*} = D_0 \cdot \Delta C . \tag{4.8}$$

Using the earlier-found solution (4.4) to Eq. (4.2) and replacing t with t^*, according to Eq. (4.7), the solution to Eq. (4.8) for the one-dimensional case has the form

$$w = w_\infty - \frac{2 \cdot (w_\infty - w_0)}{\pi^2} \sum_{k=1}^{\infty} \frac{(1 - (-1)^k)^2}{k^2} \cdot e^{-\lambda_k^2 \cdot F} , \tag{4.9}$$

where $F = \frac{D_0}{\gamma}\left[1 - \exp\left(-\gamma \cdot t\right)\right], \lambda_k = \frac{\pi \cdot k}{a}$, F is the Fourier criterion, $\gamma = 1/\tau$, and τ is the characteristic time of relaxation. A description of the sorption curve by Eq. (4.9) is shown in Figure 4.5.

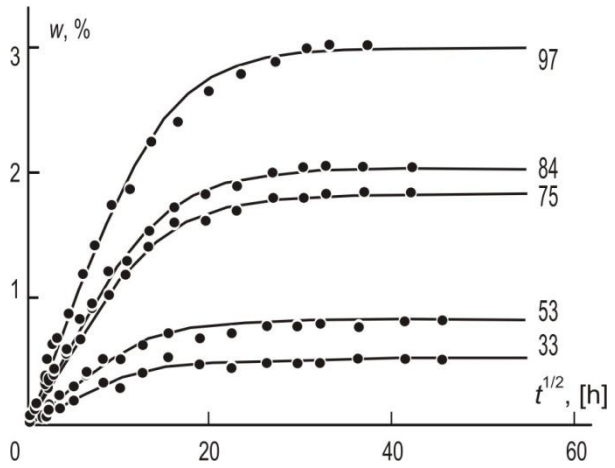

Figure 4.5. Approximation of experimental sorption data according to the model with a time-variable diffusivity for different φ (numbers next to the curves).

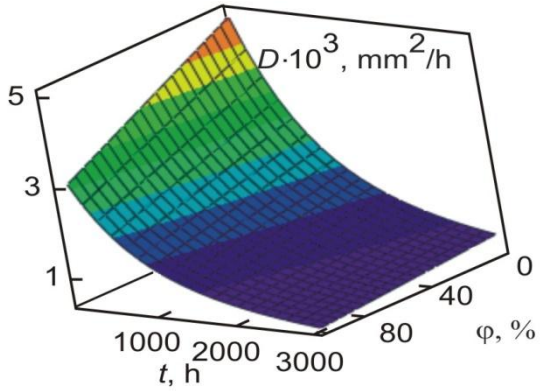

Figure 4.6. Diffusivity *D* as a function of time *t* and the relative humidity φ of environment.

The diffusivity *D* as a function of time and the relative humidity of environment is shown in Figure 4.6. It is seen that, at great times, the diffusivity tends to an infinitesimal value, which describes the saturated state of the system. During moisture sorption (for about 450 h) at φ = 98%, $D_0 = 3.61 \cdot 10^{-3}$ cm^2/h, and γ = 0.002, the diffusivity decreased 4-6 times. In general, due to the presence of three parameters, the model is relatively flexible and can describe the sorption curves rather well (Figure 4.5).

Thus the most suitable for describing the sorption kinetics are found to be the model taking into account the two-phase nature of materials and the model with a variable diffusivity. These models give results agreeing rather well with experimental data and in addition contain a relatively small number of parameters, which make them more acceptable in practical applications.

4.2. Moisture sorption by epoxy-based nanocomposite

[P3], [C1]

Properties of multi-component composite materials, as a rule, depend on composition and conditions of their manufacture in a very complicated manner. Therefore for successful forecasting of composite materials' properties it is necessary to investigate properties of each material component separately having equally manufactured material samples.

A series of moisture content measurements of the specimens was executed at different time intervals. The experimental values of moisture content for NC with filler mass fraction c = 0% are plotted in Figure 4.7 versus the square root of time. Each of these data points corresponds to the mean value with mean deviation of 4 specimens.

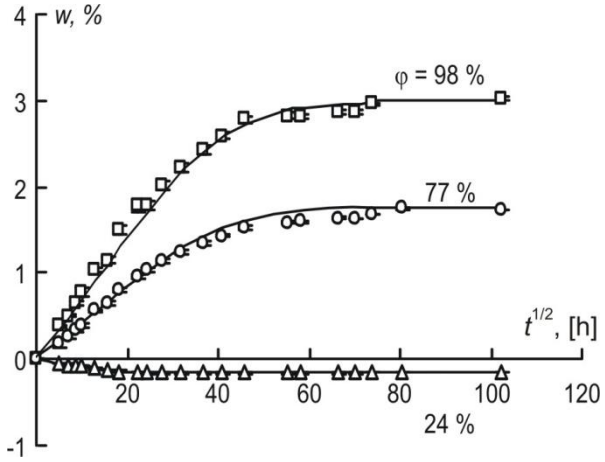

Figure 4.7. The percentage of experimental weight gain (dots) in relation to square root of time in hours for NC with c = 0% in atmospheres with φ (numbers on the curves) and evaluation by Fick's model (solid lines).

From Figure 4.7 it is obvious that sorption process could be described by Fick's model with good agreement for all contents of MMT and in all atmospheres. It should be mentioned that the diffusion coefficients of NC obtained by Eq. (4.5) are independent on relative humidity of atmosphere (see Figure 4.8). The scattering within the atmosphere of equal humidity doesn't exceed 10% of average value. It was experimentally confirmed that sorption process in NC passes much more slowly than in pure epoxy resin (as shown in Figure 4.8), for the highest filler content diffusivity reduces about half of diffusivity as for neat epoxy resin. As it was mentioned above this phenomenon takes place owing to the extremely high aspect ratio of silicate platelets, which increased the tortuosity of the water molecules' path of while moisture diffuses into the NC. According to the tortuous path model and since the moisture permeability is a function of volume fraction and aspect ratio of the platelets the exfoliated NC is more preferred to conventional or intercalated composites in terms of the barrier characteristics [7].

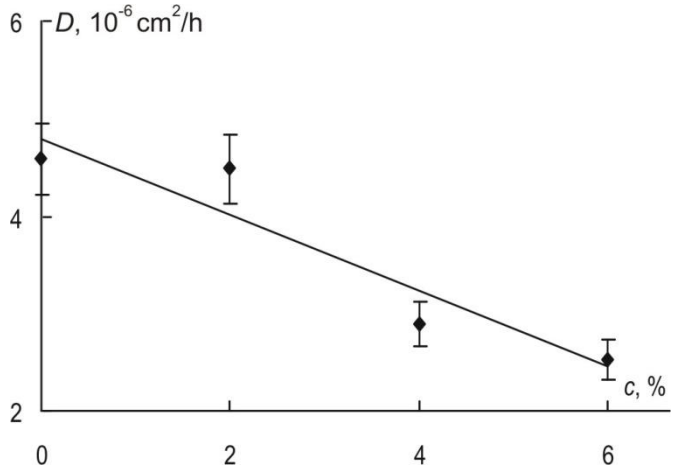

Figure 4.8. Diffusion coefficient of NC evaluated by Eq. (4.5) in relation to filler weight content.

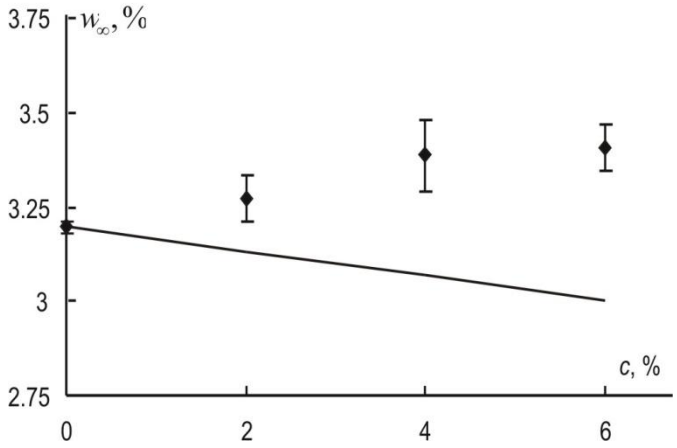

Figure 4.9. Equilibrium moisture content in relation to filler weight fraction in atmosphere with 98% RH (dots - approximation of experimental data, line - evaluation by Eq. (4.10).

The equilibrium moisture content of NC w_∞^{NC} involves the equilibrium moisture content of the NC components: of polymer resin w_∞^{ep} and of filler w_∞^f, accordingly:

$$w_\infty^{NC} = w_\infty^{ep} \cdot (1-c) + w_\infty^f \cdot c\,. \tag{4.10}$$

The use of mass was chosen as a reference in the rule of mixture instead of volume since all the NC specimens revealed swelling of about 3% by volume at the end of the saturation. It is considered that hydrophilic epoxy resin has the main contribution to the moisture uptake and equilibrium moisture content of the filler w_∞^f is close to zero since naturally hydrophilic MMT clay has been organically treated.

The increase of equilibrium moisture content with the increase of MMT weight content in NC (shown in Figure 4.9) could be caused by growth of interphase mass content. The estimation of interphase moisture sorption characteristics is created using modified rule of mixture for equilibrium moisture content

$$w_\infty^{NC} = w_\infty^{ep} \cdot (1-c-b) + w_\infty^i \cdot b\,, \tag{4.11}$$

where w_∞^i is equilibrium moisture contents of interphase, *b* is interphase fraction by mass. Such addition of interphase around the filler particles allows preventing the deviation of evaluation by Eq. (4.10) from results of approximation using experimental data. Nevertheless Eq. (4.11) contains 2 unknown parameters (w_∞^i and *b*), that can't be determined independently. That's why the proper analysis is based on the attributing capacity of moisture absorption of the interphase to the deviation between evaluation by Eq. (4.10) and experimental results.

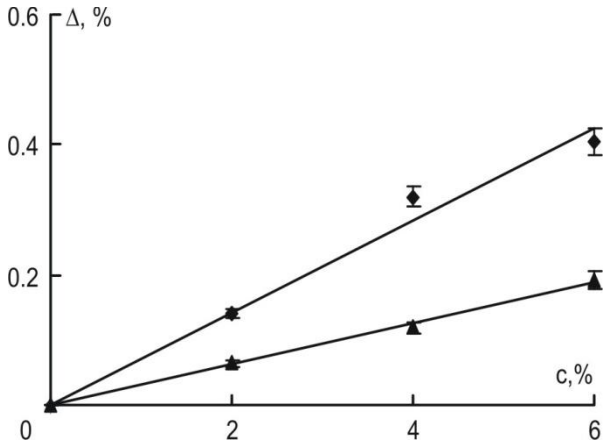

Figure 4.10. Deviation between experimental data of equilibrium moisture content of NC and estimation of it by mixture rule (4.10) for atmosphere with φ = 77 (▲) and 98 (◆) % RH.

Moreover it should be expected that for atmosphere with higher relative humidity (higher content of absorbed moisture) the difference between the amount of absorbed moisture content measured by experiments and predicted by Eq. (4.10) should increase. This observation is further supported by experiments as shown in Figure 4.10. The higher content of filler leads to greater moisture absorption and greater deviation from estimation by mixture rule without consideration of sorption characteristics of interphase. The general idea is that this deviation that represents moisture content in interphase is linear proportional on filler content (as shown in Figure 4.10). It means that coefficients of proportionality correspond to sorption capacity of interphase in NC per 1% of filler.

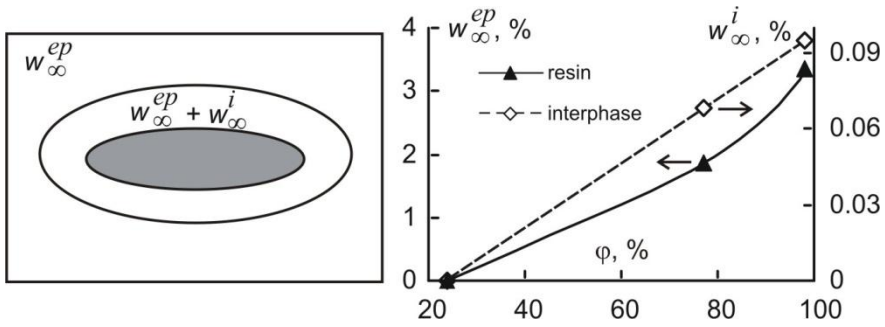

Figure 4.11. Schematic representation of equilibrium moisture content distribution within composite system of one particle (*a*) and sorption isotherm of epoxy resin and interphase in NC per 1% of clay by weight (*b*).

At equilibrium the relationship between moisture content in material and equilibrium relative humidity of surrounding atmosphere can be displayed by sorption isotherm. It is estimated that the total moisture content is distributed homogeneously by the section of the NC specimens and according to sorption isotherm for the moisture concentration in NC. For each humidity value, a sorption isotherm indicates the corresponding moisture content at a given, constant temperature. Because of the complexity of sorption processes in composite materials, the isotherms traditionally deviate from Henry's law, exhibit nonlinear behavior and should be measured experimentally.

The sorption isotherm of interphase in NC per 1% of clay could be estimated from Figure 4.11. As it was mentioned before the content of interphase in NC couldn't be predicted independently from Eq. (4.11). Nevertheless it's possible to estimate the effect of the interphase on sorption properties of NC in whole. These results could be used for further analysis of the moisture effect on mechanical and thermal properties of NC. Respectively moisture content which exists both in matrix and in interphase of NC could be predicted instead of Eq. (4.10) for given composite system

$$w_{\infty}^{NC} = w_{\infty}^{ep} \cdot (1-c) + w_{\infty}^{i} \cdot c\,, \tag{4.12}$$

where both w_{∞}^{ep} and w_{∞}^{i} are determined from Figure 4.11, which represents the sorption isotherm of epoxy resin and interphase. This sorption isotherm and formula (4.12) allow approximate estimation of additional moisture content of NC in atmosphere of any relative humidity and any filler content.

Hence it is shown that sorption process could be described by Fick's model with good agreement for all contents of clay and all atmospheres. Based on the results obtained by relating moisture on properties of NC it could be concluded that the addition of impenetrable clay nanoparticles is useful for the reduction of negative effect of moisture on properties of NC allowing the application of modified epoxy resin in environments with higher-operating relative humidity. The effect of absorbed moisture on mechanical and thermophysical properties of epoxy-clay NC is thoroughly discussed in the following chapters.

5. Mechanical characterization of epoxy-based composite materials

5.1. Strength and elastic properties

[P1], [P4], [P6], [C1]

The mechanical behavior of neat epoxy resin and epoxy resin filled with microparticles (crystals of LiF) and nanoparticles (MMT) was studied in quasistatic tensile tests for the revealing of filler and absorbed moisture influence on tensile elastic modulus and strength of composite materials. For instance Figure 5.1 shows stress-strain curves of epoxy resin and NC with filler content c = 6% specimens being preliminary sustained to an equilibrium condition in atmospheres with humidity 24, 77 and 98%. Stress-strain curves of the other NC (with filler content 2 and 4%) look similarly to curves presented in Figure 5.1 having strongly pronounced limit of forced elasticity.

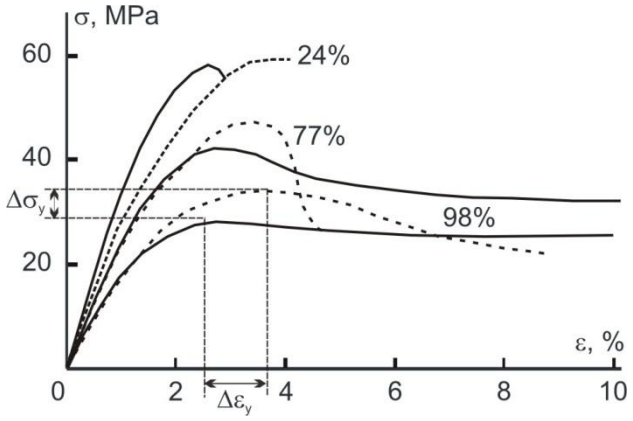

Figure 5.1. Typical stress-strain curves at a fixed rate of deformation (5 mm/min) for neat epoxy resin (dotted line) and NC with c = 6% (solid line) and different φ (numbers on the curves).

As it is clear from Figure 5.2 filling of epoxy resin with MMT nanoparticles leaded to increase in elastic modulus of dry material approximately by 30% and to reduction of upper yield stress and yield strain app. by 1/3. The increase of moisture content both in epoxy resin and in NC resulted in reduction of elastic modulus and yield stress; while yield strain has almost the same value. Dry (sustained in atmosphere with φ = 24%) specimens failed in more brittle manner than moistened ones (sustained in atmosphere with φ = 98%). Durability of the former specimens twice exceeded durability of the latter. Intermediate values of durability are obtained for NC specimens sustained in atmosphere with φ = 77%.

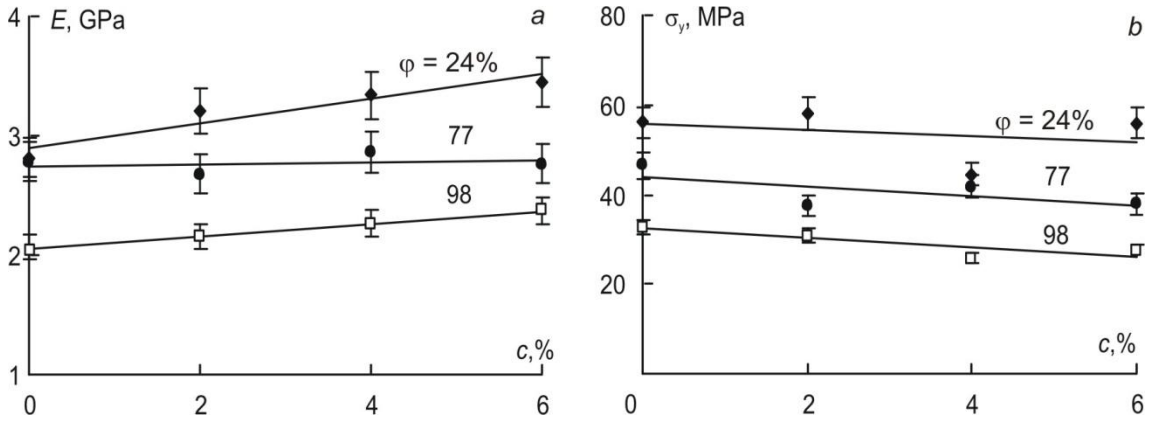

Figure 5.2. Elastic modulus (*a*) and yield stress (*b*) of NC in relation to the filler weight content for different φ (numbers on the curves).

Consequently due to absorbed moisture both pure resin and NC with c = 6% show almost same degradation as for elastic modulus by 1 GPa and for tensile strength by 25 MPa, respectively. It should be noted that though the values themselves of elastic modulus and strength are improved with respect to filler content, the positive effect as moisture content increases (in atmosphere from 24% RH till 98% RH) was not established.

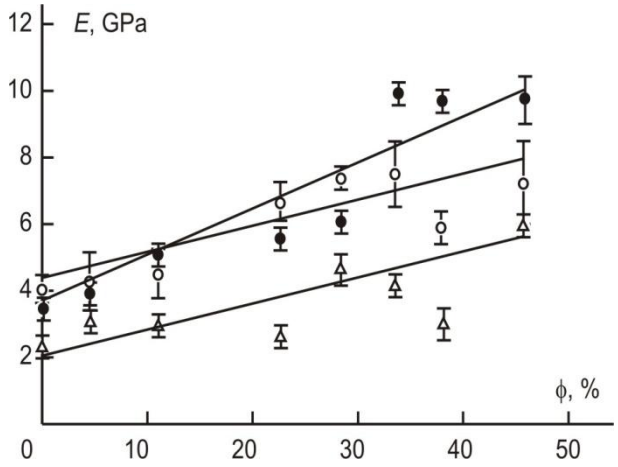

Figure 5.3. Experimental elastic moduli E of the CM in the initial (o) and moisture saturated (Δ) states and after a moistening-drying cycle (●) in relation to the filler volume content ϕ.

Figure 5.3 demonstrates moisture effect on experimentally obtained elastic modulus of epoxy resin filled with different content of LiF crystals. As follows from the data in the figure an increase in the elastic modulus with increasing ϕ is observed for the CM in the conditionally initial state at $\phi \leq 0.33$, in the saturated state at all the values of ϕ considered, and after a moistening-drying cycle at $\phi \leq 0.38$. Thus it is assumed that the structure and properties of polymer resin changes upon filling. This could be explained by the presence of interphase having properties different from the properties of the polymer resin in the bulk. That's why upon modeling of elastic properties of CM it is important to take into account morphological

properties of filler particles in the conditionally initial state and then to estimate effect of absorbed moisture on structure and properties of CM having different filler content.

5.2. Modeling of elastic properties considering layered structure of MMT clay

[P4]

The behavior and properties of NC are dependent not only on properties of its structural components, but also on the material microstructure: the dispersion and orientation of filler particles, and the interactions between filler particles and polymer matrix [33].

Nevertheless one of the main parameters that affect the behavior of the nano-system is the effectiveness of dispersion of filler particles within the polymer matrix [34].

One way to check the morphological peculiarities of clay nanoparticles in a solvent, before incorporating them to a matrix, is to observe their dispersion by TEM. A typical image of acetone suspension of clay nanoparticles is shown in Figure 5.4*a*.

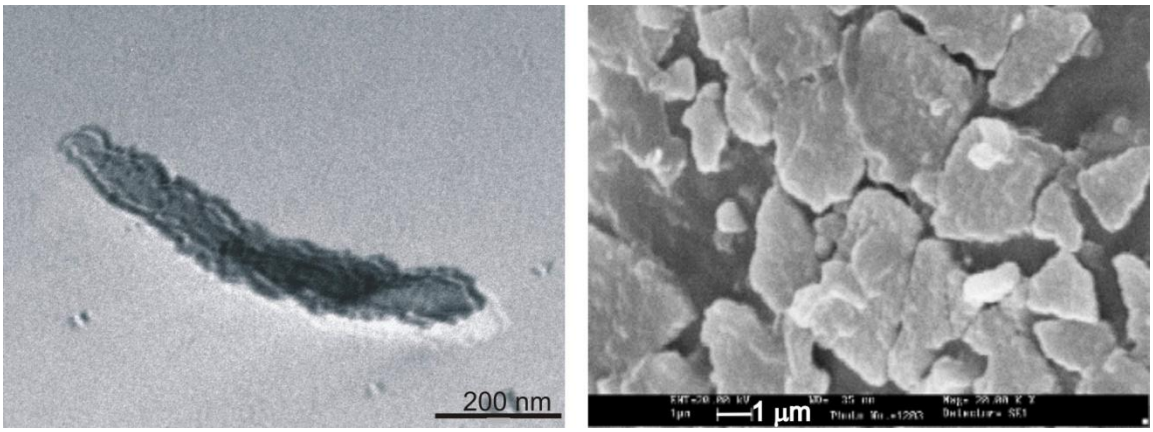

Figure 5.4. Typical TEM image of acetone suspension of clay nanoparticle. The nanoclay appears in black (*a*); SEM micrograph of fracture surface of NC with c = 2% (*b*).

It is obvious from the Figure 5.4*a* that the observed aggregate should be a stack of clay platelets having layered structure and high aspect (diameter to thickness) ratio (50). The aspect ratio of the platelet stack as observed from Figure 5.4 is about 7.

Moreover the platelet shape of the filler particles could be confirmed by SEM micrograph (Figure 5.4*b*) of fracture surface of NC specimen with c = 2%. It could be seen that the transversal dimension of the filler aggregates is much smaller than longitudinal ones.

Efforts are being made to relate effective tensile elastic modulus of moistened NC with properties of its structural components. It should be emphasized that taking into account complicated structure of real composite material, only evaluative results could be obtained theoretically [18].

Halpin-Tsai equations [25, 26] obtained for isotropic polymer matrix filled with coplanar transversally isotropic cylindrical particles of arbitrary aspect ratio (5.1) are used for the case of exfoliated NC. The elastic solution was obtained for the composite consisted of a single fiber encased in a cylinder of matrix, both embedded in an unbounded homogeneous medium which is macroscopically indistinguishable from the composite. The relations between the stress and strain components were averaged throughout the composite. The obtained formulas were curve fitted to exact elasticity solutions and confirmed by experimental measurements in order to get the solution for composite filled with particles of arbitrary aspect ratio.

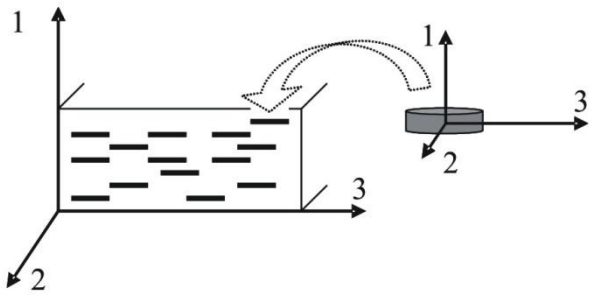

Figure 5.5. Schematic representation of cylindrical filler particles embedded in polymer matrix.

For a completely exfoliated system Halpin-Tsai equations for elastic moduli of NC take form:

$$E_1 = E_m \frac{1+2\eta_1\varphi}{1-\eta_1\varphi}, \tag{5.1}$$

$$E_2 = E_3 = E_m \frac{1+2A_f\eta_2\varphi}{1-\eta_2\varphi}, \tag{5.2}$$

where

$$\eta_1 = \frac{R_1 - 1}{R_1 + 2}, R_1 = \frac{E_{f1}}{E_m},\ \eta_2 = \frac{R_2 - 1}{R_2 + 2A_f}, R_2 = \frac{E_{f2}}{E_m}.$$

In the equations (5.1)-(5.2) E_1, E_2, E_3 are elastic moduli of given composite, E_m is elastic modulus of matrix and E_{f1}, E_{f2} – elastic modulus of filler for axes' directions shown in Figure 5.5; A_f is the aspect ratio of platelet ($A_f > 1$ since it equals to the diameter divided by thickness for cylindrical platelets); ϕ is the volume fraction of filler particles and is determined by formula

$$\phi = \frac{c}{\rho_f} \cdot \frac{1}{\left(\frac{c}{\rho_f} + \frac{(1-c)}{\rho_m}\right)},$$

where c is filler weight content, ρ_f and ρ_m are filler and matrix density, accordingly.

If the exfoliation is incomplete the composite system is considered to consist of matrix and pseudo particles (stacks of individual platelets) [22]. Figure 5.6 shows scheme of filler particles

that are forming a stack (a pseudo particle). *N* is the number of platelets per stack, *L* – length (width), *t* – thickness of the platelet, *s* – inter-platelet spacing.

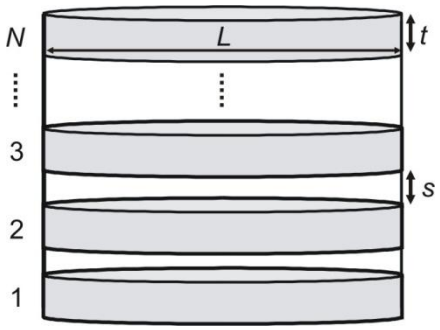

Figure 5.6. Representation of pseudoparticle (platelet stack).

For the case of incomplete exfoliation Halpin-Tsai equations are modified and get form:

$$E_1 = E_m \frac{1+2\eta_1'\varphi'}{1-\eta_1'\varphi'}, \tag{5.3}$$

$$E_2 = E_3 = E_m \frac{1+2A_f'\eta_2'\varphi'}{1-\eta_2'\varphi'}, \tag{5.4}$$

where

$$\eta_1' = \frac{R_1'-1}{R_1'+2}, R_1' = \frac{E_{p1}}{E_m},\ \eta_2' = \frac{R_2'-1}{R_2'+2A_f'}, R_2' = \frac{E_{p2}}{E_m}.$$

Here A_f' is the aspect ratio of platelet stack, ϕ' is the volume fraction of platelet stacks, R' is the ratio of platelet stack elastic modulus to elastic modulus of the matrix. Elastic moduli of platelet stack in different axes' directions could be calculated using direct and reverse rules of mixture

$$E_{p1} = \frac{V_{ps}}{\frac{V_p}{E_{f1}} + \frac{V_{ip}}{E_m}}$$

and

$$E_{p2} = \frac{E_{f2}V_p + E_m V_{ip}}{V_{ps}},$$

where V_p is volume of platelets, V_{ip} is volume of inter-platelet spacing, V_{ps} is volume of platelet stacks. Using simple geometrical assumptions (each platelet stack consists of *N* platelets of thickness *t*, length *L* and located at inter-platelet spacing *s*) the formulas for elastic moduli of platelet stack take form

$$E_{p1} = \frac{E_{f1}E_m\left(Nt + (N-1)s\right)}{E_m Nt + E_{f1}(N-1)s}$$

and

$$E_{p2} = \frac{E_{f2} Nt + E_m (N-1)s}{Nt + (N-1)s}.$$

Accordingly following formulas for aspect ratio of platelet stack A_f', volume fraction of platelet stacks ϕ' and ratio of platelet stack elastic modulus to elastic modulus of the matrix E_r' were obtained for model parameters [22]:

$$A_f' = \frac{A_f}{N}\left(\frac{1}{1+\left(1-\frac{1}{N}\right)\frac{s}{t}}\right),$$

$$\phi' = \phi\left(1+\left(1-\frac{1}{N}\right)\frac{s}{t}\right),$$

$$R_1' = R_1\frac{1+\left(1-\frac{1}{N}\right)\frac{s}{t}}{1+R_1\left(1-\frac{1}{N}\right)\frac{s}{t}}, \quad R_2' = \frac{R_2}{1+\left(1-\frac{1}{N}\right)\frac{s}{t}} + \frac{\left(1-\frac{1}{N}\right)\frac{s}{t}}{1+\left(1-\frac{1}{N}\right)\frac{s}{t}}.$$

Using known values of elastic modulus of matrix in atmospheres with different relative humidity it is possible to determine elastic moduli of NC by equations (5.3) and (5.4). The elastic moduli of montmorillonite clay platelets are ranging from 40 GPa [35] (in transverse direction of platelet) to 180 GPa [25, 36] (in longitudinal direction of platelet) based on the literature values for layered-structure clay minerals, an empirical modulus-density relation for alumina, silica and their compounds and values obtained by simulation for the product of elastic modulus and thickness of the platelets. In the current study elastic moduli of filler are assumed to be E_{f1} = 55 GPa, $E_{f2} = E_{f3}$ = 180 GPa, aspect ratio of filler platelet A_f = 50, number of platelets per stack N is changed from 1 to 6, s/t = 1.

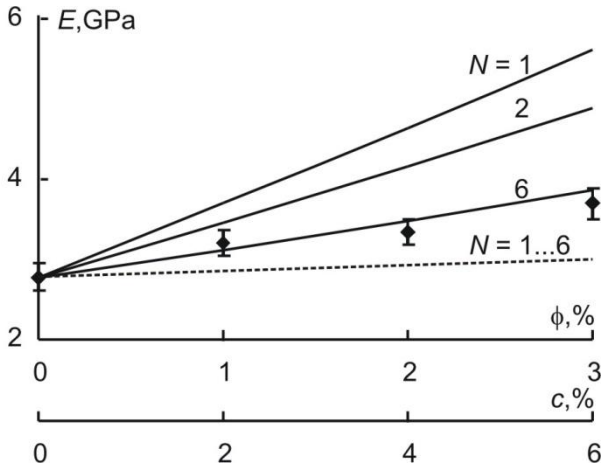

Figure 5.7. Elastic modulus of NC versus filler volume content. Evaluation by (5.1) (solid line) and (5.3) (dashed line) for different number of elementary layers *N* (numbers on the curves) in a platelet stack. Dots – experimental data for φ = 24% RH.

Comparing results of evaluation by Eq. (5.1) with experimental data of quasistatic tensile tests of specimens conditioned in dry atmosphere (φ = 24% RH) provided in Figure 5.7 it is obvious that evaluation results for elastic modulus of NC with exfoliated filler particles are higher than experimental ones. Increasing the number of platelets per stack gives the opportunity to get better agreement between them. Although it's rather arguably since it is assumed in the model that filler particles obey coplanar orientation in polymer matrix. On the other hand evaluation by Eq. (5.4) (low bound) is much lower than experimental results even for the case of exfoliated platelets. It means that real orientation distribution of clay platelets is somewhere in between these limits and could be rather complicated.

Nevertheless using obtained results (the same parameters *N*, *t*, *s*) for moistened NC it is possible to estimate structural changes of the polymer resin due to moisture absorption.

The resulting evaluation of elastic modulus of moistened NC by Eq. (5.3) shows the deviation from results obtained experimentally (see Figure 5.8). As it can be seen taking into account platelet stack layered structure (increasing the number of platelets in stack till 6) improves the congruence of results with experimental data. Apparently it could be described by the change of elastic properties of the platelet stacks. It should be emphasized that while elastic modulus of impermeable clay platelets is not dependent on moisture content, the matrix phase that is located in the inter-platelet spacing absorbs moisture. Therefore the elastic properties of the platelet stacks are dependent on absorbed moisture content and cause more significant decrease of moistened NC elastic modulus as presented in Figure 5.8.

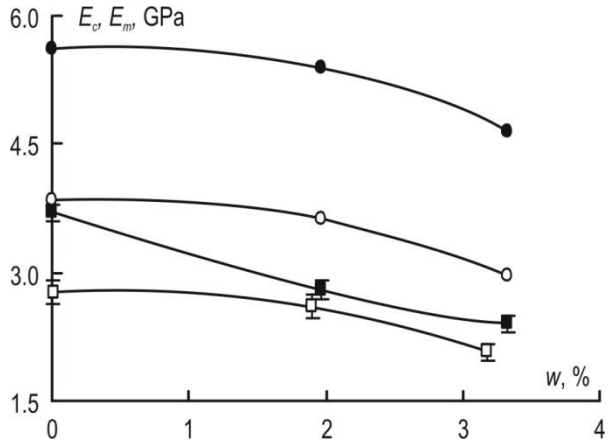

Figure 5.8. Elastic modulus of epoxy resin and NC with c = 6% in relation to the absorbed moisture content. Experimental data (NC with c = 6% (■), epoxy resin (□)), evaluation by (5.3) for NC with c = 6% and N = 1 (●) and N = 6(○).

The change of elastic modulus under effect of moisture e. g. NC with c = 6% proves that moisture which exists in the inter-platelet spacing significantly influences the elastic modulus. Logically enough, the higher content of filler leads to higher content of inter-platelet spacing and as a result to greater moisture absorption and greater change of NC properties that are sensitive to moisture.

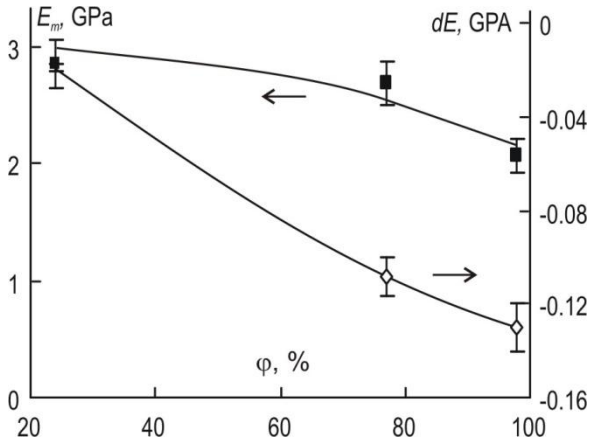

Figure 5.9. Elastic modulus of epoxy resin (■) and normalized to 1% wt of filler deviation of NC elastic modulus (◊) in relation to the relative humidity of the atmosphere.

The isotherm shown in Figure 5.9 concludes the proposed analysis of moisture and filler effect on deformability of epoxy/MMT NC taking into account filler morphological peculiarities. Using this figure it's possible to estimate NC elastic modulus of any filler content in atmosphere with any relative humidity. It is obvious that due to moisture absorption NC elastic modulus is substantially decreased. Since the value of elastic modulus of epoxy resin is improved with respect to filler content in spite of no positive effect for the decrease of elastic modulus of NC due to moisture absorption (in atmosphere from 24 till 98% RH) epoxy resin modified by

impenetrable stiff MMT clay nanoparticles could be applied in environments with higher-operating relative humidity.

5.3. Modeling of elastic properties considering formation of interphase

[C2]

As pointed out before the silicate platelets could be dispersed in the polymer in three ways: in aggregates, as in intercalated layered NC and in exfoliated platelets. In the current work only the last case was considered due to primary emphasis on the interphase problem. The exfoliated platelets were represented as transversally isotropic spheroids with low aspect ratio that is equal to app. 0.015.

Since special attention is given to the evaluation of interphase problem and efficiency of adhesion in NC appropriate formulas for the elastic properties of NC filled with randomly oriented transversally isotropic spheroids with zero small aspect ratio will be applied. Wang [21] showed that for the small filler volume fractions Norris approximate expressions [19] for bulk and shear moduli of composite material reinforced with isotropic oblate spheroids with small aspect ratio agree well with explicit Mori-Tanaka expressions which are widely applied for the prediction of NC properties. These approximate expressions can be written as

$$K = K_1 + \frac{4}{9}\cdot\phi\cdot\left(\chi\frac{\pi}{8}\frac{3-4\cdot\nu_1}{\mu_1\cdot(1-\nu_1)}+\frac{1}{\mu_2}\frac{1-\nu_2}{1+\nu_2}\right)^{-1}, \tag{5.5}$$

$$\mu = \mu_1 + \frac{1}{15}\cdot\phi\cdot\left(\chi\frac{\pi}{8}\frac{3-4\cdot\nu_1}{\mu_1\cdot(1-\nu_1)}+\frac{1}{\mu_2}\frac{1-\nu_2}{1+\nu_2}\right)^{-1}+\frac{2}{5}\cdot\phi\cdot\left(\chi\frac{\pi}{16}\frac{7-8\nu_1}{\mu_1\cdot(1-\nu_1)}+\frac{1}{\mu_2}\right)^{-1}, \tag{5.6}$$

where ϕ is filler volume fraction, χ is aspect ratio of filler, K, μ and ν are the bulk, shear moduli and Poisson ratio of composite, respectively. Indices 1 and 2 represent matrix and filler properties. The aspect ratio χ is defined as filler particle's thickness related to its diameter and is for the case of NC filled with clay platelets much smaller than 1.

In the numerical calculations, the bulk and shear moduli of the matrix and filler are chosen in such way that they reflect the typical properties of epoxy resin and montmorillonite silicate, respectively. Therefore, the Young's modulus and Poisson's ratio of the matrix are considered to be E_1 = 3.45 GPa and ν_1 = 0.35. The elastic modulus is also experimentally determined value. Unfortunately there is lack of the complete elastic constants of montmorillonite silicate. As it was mentioned above in the literature it is usually assumed that elastic modulus in the longitudinal direction is ranging from 140 GPa [21] to 180 GPa [15, 25, 36]. In this work it is assumed that E_2 = 180 GPa and ν_2 = 0.2. The aspect ratio is chosen to be about 0.015.

Then the calculated values of formulas (5.5) and (5.6) are used to evaluate the elastic modulus by the equation

$$E = \frac{9 \cdot K \cdot \mu}{3 \cdot K + \mu} \tag{5.7}$$

The interphase was introduced as a region with gradient of properties nearby the interface of matrix and filler particles. At nanolevel the elastic properties of one single particle containing interphase were considered. The effect of adhesion efficiency was taken into account in the region of the interphase. Previously [27] it was shown that existence of interphase results in increase of equilibrium moisture content during sorption experiments and as a result a significant decrease of elastic moduli was observed. Since the analytical evaluation for both elastic and sorption properties was higher than that for experimental results it was concluded that interphase has elastic properties lower than the matrix and this conclusion will be used in current work.

The expression of the bulk modulus for the system of filler particle-interphase-matrix is assumed to follow the formula

$$K(x,k,R_f) = \begin{cases} K_2 \text{ if } 0 \le x \le R_f \\ K_1 \cdot \left(1 - \dfrac{(K_2 - K_1)}{K_2} \cdot \exp\left(\dfrac{-(x - R_f)}{k \cdot R_f}\right)\right) \text{if } R_f \le x \le R_i(k,R_f) \\ K_1 \text{ otherwise} \end{cases} \tag{5.8}$$

where x is the coordinate in one-dimensional approach, k is the efficiency of adhesion, R_f is the thickness of the filler particle. The adhesion efficiency is varying from 0 to 1 and expresses the strength of interaction between filler and matrix. The thickness of interphase R_i is denoted as the distance from filler particle to the matrix material with the deviation from matrix properties $\delta = 0.1\%$ and is evaluated by formula

$$R_i(k,R_f) = R_f - R_f \cdot k \cdot \ln\left(\delta \frac{\delta \cdot K_2}{(K_2 - K_1)}\right).$$

The similar formulas could be written for the shear modulus.

Figure 5.10 shows the change of bulk modulus within the system of filler-interphase-matrix material. Four different filler contents corresponding to experimental ones are used in the analysis. It is evident from the figure that increasing filler radius the thickness of the interphase increases. This leads to decrease of effective bulk modulus for the system in whole.

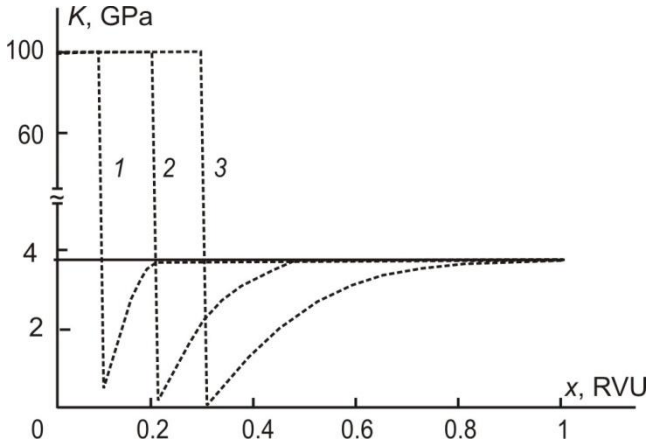

Figure 5.10. Bulk modulus of the 3-phase system for different filler contents R_f = 1, 2 and 3% (numbers on the curves) and constant line – neat resin, k = 0.3.

Moreover the adhesion efficiency strongly influences the thickness of the interphase and in this way lowers the value of the elastic moduli with the increase of R_i. The dependence of interphase thickness on the filler thickness and adhesion efficiency is shown in Figure 5.11. It is clearly seen that with the increase of filler content or thickness of filler particle the thickness of interphase increases reaching maximal value for the highest adhesion efficiency k = 1.

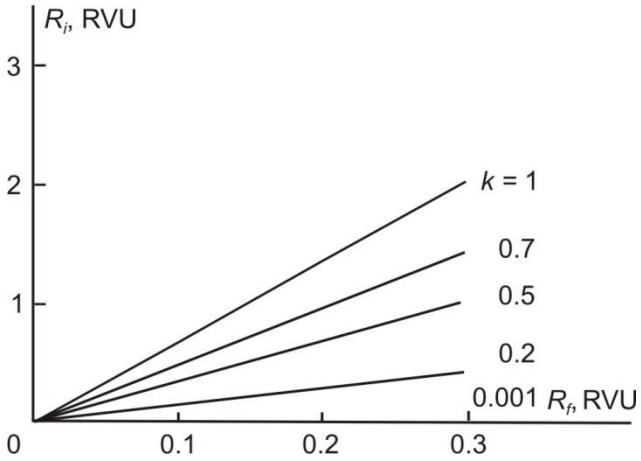

Figure 5.11. Thickness of the interphase vs. thickness of filler particle for different values of adhesion efficiency.

Then the derived variations of moduli were averaged for system of filler particle-interphase in order to get quasi-particle with constant properties using formulas

$$\bar{K}(k,R_f)=\frac{1}{x_{\max}}\cdot\int_0^{R_i(k,R_f)}K(x,k,R_f)dx\,, \tag{5.9}$$

$$\bar{\mu}(k,R_f)=\frac{1}{x_{\max}}\cdot\int_0^{R_i(k,R_f)}\mu(x,k,R_f)dx\,. \tag{5.10}$$

These elastic characteristics were used to evaluate the elastic modulus of NC taking into account degree of adhesion and presence of quasi-particles with averaged properties. The elastic modulus is determined by well known relation between elastic characteristics

$$\bar{E}(k,R_f)=\frac{9\cdot\bar{K}(k,R_f)\cdot\bar{\mu}(k,R_f)}{3\cdot\bar{K}(k,R_f)+\bar{\mu}(k,R_f)}. \qquad (5.11)$$

The final result for the elastic modulus of the composite is showed in Figure 5.12. As it was mentioned before the elastic moduli in the interphase were assumed to be lower than that of the matrix. As seen from the figure adhesion efficiency greatly influences elastic properties of the composite and lowers the effective elastic modulus. It is interesting to notice that with the increase of adhesion efficiency the thickness of the interphase increases and so the content of the quasi-filler particles grows as well. Nevertheless the averaging by the diameter of the particle gives results which are monotonically growing functions in dependence of filler content.

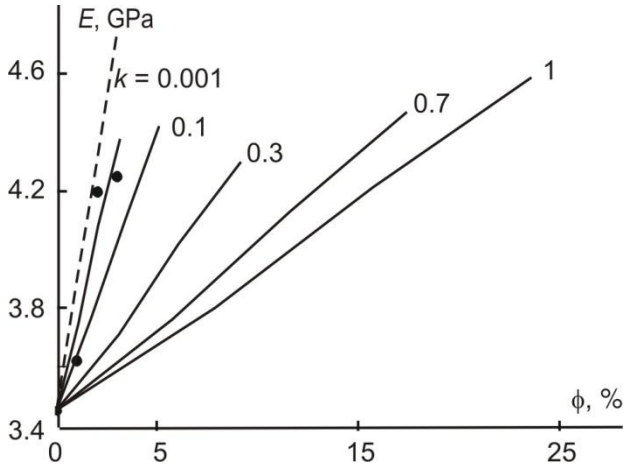

Figure 5.12. Effective elastic modulus in relation to the filler volume content (dots – experimental data, dotted line - evaluation by Eq. (5.7), solid lines – evaluation by Eq. (5.11)).

The expressions for the bulk and shear moduli of the composite were presented using expressions of Norris for randomly oriented platelets which are suitable for low filler contents. First the properties of quasi-particle were estimated at nanolevel considering efficiency of adhesion at different filler contents. It should be noted that the stiffness of filler particles in the direction of major axis is the dominating parameter in these calculations. Since the literature data for the elastic constants of montmorillonite is incomplete it could be concluded that these values could be varied in order to get better agreement with the experimental data.

According to the results obtained in the work the theoretical prediction using expressions of Norris describes the results of quasistatic tensile test quite well. Nevertheless the results of this prediction are higher which can be described by the lack of precise values of parameters like elastic constants and aspect ratio of montmorillonite clay. The possibility to describe this deviation is to introduce interphase. It is clear that taking into account adhesion efficiency and

high surface of filler particles quite high content of quasi-particles is obtained in the case of NC. That's why the thickness of the interphase and adhesion efficiency can greatly influence the mechanical behavior of the NC and should be considered. This analysis at nano- and microlevels provides possibility to estimate the effect of filler and interphase properties and content on effective elastic properties of NC in whole. However polymers are not elastic solids and they behave as viscoelastic materials and therefore viscoelastic properties of NC have to be investigated as described in the following chapter.

6. Viscoelastic properties of epoxy-based nanocomposite

[P6], [C3]

For different kinds of application of NC on the basis of a polymer resin the estimation of long-term deformability and durability in the conditions of influence of different environmental factors (loading, raised and/or variable temperature and/or humidity) is of particular importance [37, 38]. Addition of moisture impenetrable MMT platelets should affect overall viscoelastic properties of NC and result in decrease in NC compliance during moisture absorption process. The viscoelastic behavior of moisture saturated NC specimens with different filler content is an objective of the study and is analyzed in this chapter.

To describe the family of creep and creep recovery curves of NC with different filler content at various values of moisture content *w*, the Boltzmann-Volterra linear integral equation was used

$$\varepsilon(t) = \frac{\sigma(t)}{E} + \frac{1}{E}\int_0^t K(t-s)\sigma(s)ds \tag{6.1}$$

with the creep kernel as a sum of exponents:

$$K(t) = \sum_{i=1}^{n} \frac{b_i}{\tau_i} e^{-\frac{t}{\tau_i}}, \tag{6.2}$$

where, τ_i, and b_i, i = 1, ..., n, is the spectrum of retardation times. According to the principle of moisture-time analogy,

$$t = t' a_w, \tag{6.3}$$

where $a_w(w)$ is the function of moisture-time reduction, describing variations in the spectrum of retardation times with changes in the relative moisture content in the material.

If the stress varies according to the law

$$\sigma(t) = \sigma_0 H(t) - \sigma_0 H(t-t_0), \tag{6.4}$$

where t = 0 and t_0 are the instants of loading and unloading, respectively, and $H(t)$ is the Heaviside function, the compliance $I(t) = \frac{\varepsilon(t)}{\sigma_0}$ has the following expression

for the creep at $t<t_0$,

$$I(t) = \frac{1}{E} + \frac{1}{E}\sum_{i=1}^{n} b_i \left(1 - e^{-\frac{t a_w}{\tau_i}}\right), \tag{6.5}$$

for the creep recovery at $t>t_0$,

$$I(t) = \frac{1}{E}\sum_{i}^{n} b_i e^{-\frac{t a_w}{\tau_i}} \left(e^{\frac{t_0 a_w}{\tau_i}} - 1 \right). \qquad (6.6)$$

The function of moisture-time reduction was chosen in the form

$$\ln a_w = \alpha_1 w + \alpha_2 w^2 . \qquad (6.7)$$

Such functions were used earlier for epoxy binders and composites based on them [39].

The results of short-term (7.5 h) creep of dry (nonmoistened) materials showed that creep compliance curves for NC with filler content c = 0 and 4% almost coincide (except for instantaneous compliance $I_0 = 1/E$) (Figure 6.1*a*). That is the filler effect appears in relation of instantaneous compliance to filler content. Moistening of investigated material leads to remarkable increment in creep compliance (Figure 6.1*a*). Obviously this is caused by case that material is close to viscoelastic state.

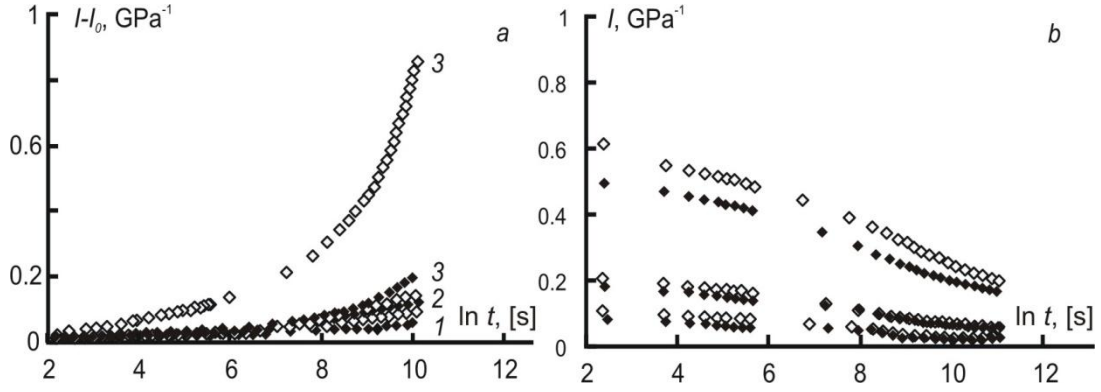

Figure 6.1. Compliance curves of the NC with the filler content c = 0 (♦) and 4 (◊)% for φ = 24 (*1*), 77 (*2*) and 98% (*3*) in creep (*a*) and creep recovery (*b*).

The creep recovery experiments revealed that after 17 h of observation the creep recovery strain still continued to decrease with time (Figure 6.1*b)*. In other words, there is a reason to believe that the creep deformations are reversible. To verify this assumption, it is necessary that the model parameters determined from the results of creep tests could be applied to the case of creep recovery or vice versa. The spectra of retardation times τ_i, b_i, i = 1,…, n (6.2) and the function of moisture-time reduction (6.7) of the NC with different filler content can be found from the results of creep recovery tests. For each value of c, the family of compliance curves in creep recovery corresponding to different levels of moisture content w was approximated by Eq. (6.6) with account of Eq. (6.7). The approximation was performed using the SIMPLEX algorithm in FORTRAN. The objective function was specified as the root-mean-square deviation of the calculation from experiment. The initial values of retardation times were chosen at uniform steps in the logarithmic scale, i.e., 1, 10, 100, etc.; the number of exponential functions in creep kernel (6.2) was n = 7. During minimization of the objective function, the summands

whose pre-exponential multiplier was of the order of magnitude 10^{-3} and smaller were rejected, and only four exponents remained in Eq. (6.2).

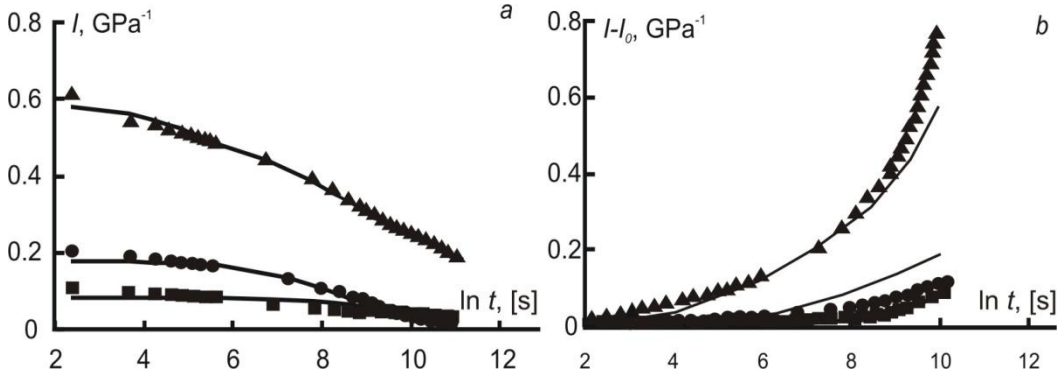

Figure 6.2. Experimental compliances in creep recovery (*a*) and creep (*b*) of the NC with c = 4% at w = 0 (■), 2.04 (●), and 3.52% (▲), their approximations by Eq. (6.6) with account of Eq. (6.7) (*a*), and calculations by Eq. (6.5) with account of Eq. (6.7) (*b*).

As an example, Figure 6.2*a* presents the approximated compliance curves in creep recovery for the NC with a filler content of 4%. The verification of applicability of the model used showed a satisfactory description of creep experiments (Figure 6.2*b*). The spectra of retardation times and the function of moisture-time reduction of NC with different filler content obtained from the approximation are given in Figure 6.3 and Figure 6.4, respectively. The spectra of retardation times for the NC with c = 2 and 4% (Figure 6.3) practically do not differ from the spectrum for the binder in a block: they have a common amplitude envelope. However, at c = 6%, these spectra differ: the retardation times increase, but the intensity slightly decreases. As a result, the spectrum envelope is more flat than that for the binder in a block and the NC at c < 6%.

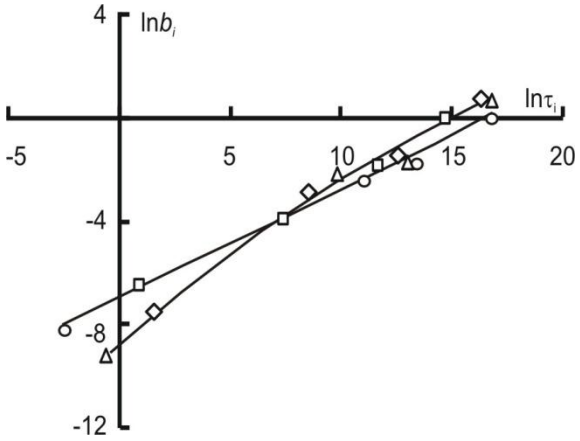

Figure 6.3. Spectra of retardation times of the NC at c = 0 (◊), 2 (□), 4 (Δ), and 6% (○).

The functions of moisture-time reduction of the NC with different filler content (Figure 6.4) are nonlinear, and their graphs are concave lines describing the growing influence of the absorbed moisture as its content in the material increases. A comparison of the functions of

moisture-time reduction of the NC at different values of c shows that the addition of a small amount of filler (c = 2%) weakens the influence of moisture on the viscoelastic properties of the binder in the CM. Probably, this is caused by the interaction of filler particles with binder macromolecules with the formation of physical bonds. It is also possible that some part of the absorbed moisture occurs in the interfacial layer [27]. With increasing degree of filling, the influence of moisture on the viscoelastic properties of the binder in the CM grows, and at c = 6% it becomes equal to that of the binder in a block. The filler particles loosen the binder structure in the NC, and the rate of relaxation processes in the region of great times decreases.

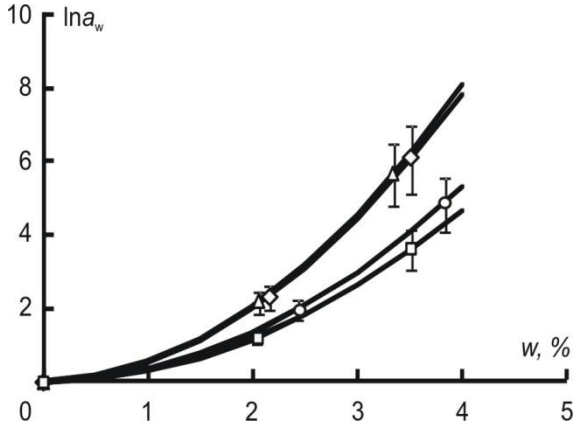

Figure 6.4. Functions of moisture-time reduction of the NC at c = 0 (◊), 2 (□), 4 (Δ), and 6% (○) obtained by approximating the families of creep recovery curves of the material with different moisture content by using Eqs. (6.6) and (6.7).

The influence of the equilibrium moisture content in the NC on its viscoelastic properties is expressed as a changing limit of forced elasticity in quasi-static tests (see Figure 5.2*b*). According to the Eyring equation, the relation between the limit of forced elasticity and strain rate has the form

$$\sigma_{v.e.} = A + B \ln \dot{\varepsilon} . \tag{6.8}$$

Taking into account the relaxation nature of viscoelasticity, $\dot{\varepsilon}\tau_i = const_w$,

$$\ln \frac{\dot{\varepsilon}_1}{\dot{\varepsilon}_0} = \ln \frac{\tau_i^0}{\tau_i^1} = -\ln a_w , \tag{6.9}$$

i.e., the variation in the limit of forced elasticity must correlate with the reduction function. Such a correlation does exist: for NC with different filler content, the variation in the limit of forced elasticity is directly proportional to the value of the function of moisture-time reduction (Figure 6.5). This correlation can serve as a basis for an alternative determination of the function of moisture-time reduction, namely by using the results of quasi-static tests in the mode of constant strain rate.

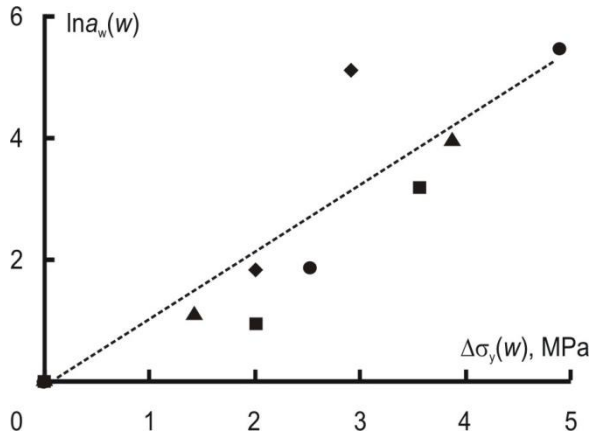

Figure 6.5. Correlation between the function of moisture-time reduction (6.7) and changes in the limit of forced elasticity in quasi-static tests for the NC at c = 0 (♦), 2 (■), 4 (▲), and 6% (●).

There is another way for determining the reduction function - according to the volumetric strain [39]. Assuming the binder in a block to be isotropic, the volumetric swelling strain $\frac{\Delta V}{V_0} = 3\varepsilon_h$ can be calculated and using the relation between the reduction function and the change in volume [40]

$$\ln a_w = \frac{1}{f_0^2}\frac{\Delta V}{V_0}\frac{1}{1+\frac{1}{f_0}\frac{\Delta V}{V_0}}, \qquad (6.10)$$

the function of moisture-time reduction is derived (Figure 6.4), which coincides with that determined from creep experiments with f_0 = 0.062.

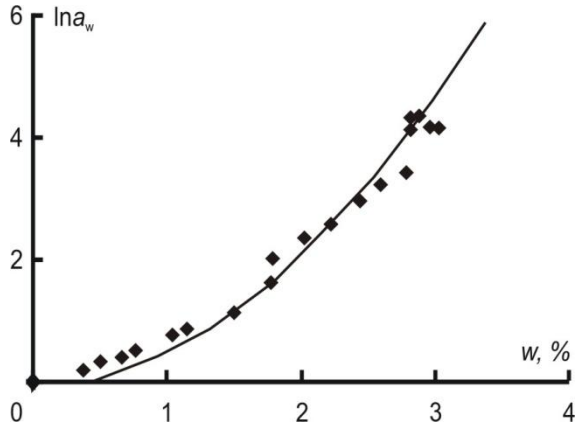

Figure 6.6. Function of moisture-time reduction of the epoxy binder: dots - calculation by Eq. (6.10) with the use of relation between the swelling strain and the relative moisture content; the line - approximation of the family of creep recovery curves given in Figure 6.4.

Thus, based on the principle of moisture-time analogy the function of moisture-time reduction of epoxy resin was derived which correlates with varying volume of specimens upon moistening that allows estimating the function by the results of swelling. In turn the revealed correlation function of moisture-time reduction with the change of limit of forced elasticity indicated viscoelastic character of deformation of NC specimens at different moisture content.

Viscoelastic properties of polymer based composites are fully connected to environmental conditions (temperature, moisture) since with the increase of temperature the frequency of molecular rearrangements increases but delay time decreases. Thus NC specimens having absorbed moisture behave differently due to distinction in glass transition temperature. The features of thermophysical characteristics and their interrelation with structural changes of epoxy-based NC under moistening are explicitly discussed in the next chapter.

7. Thermophysical characteristics and structural changes under moistening of epoxy-based nanocomposites

[P5], [C3]

The features of the phase and relaxation transitions in heating the NC specimens have been studied by the method of thermomechanical analysis (TMA) in the absence of external load. The typical TMA curves of the NC specimens held in an atmosphere with a relative humidity of 24 and 98% until they reached the equilibrium state are presented in Figure 7.1. The general rule for all NC modifications, including those held in an atmosphere with a humidity of 77%, is the presence on the thermal expansion curves of a narrow (5–10°C) temperature range of a sharp change in the character of deformability when in the course of heating the expansion at T_1 is replaced by a shrinkage, and then at T_2 a new growth of deformation begins just as quickly. Such dependences are characteristic of amorphized polymers in which, after passing through glass transition temperature T_g, crystallization occurs very quickly to cause hardening of the material. Then, also spontaneously, melting of the crystallites formed in them begins, which just causes a rise on the TMA curve.

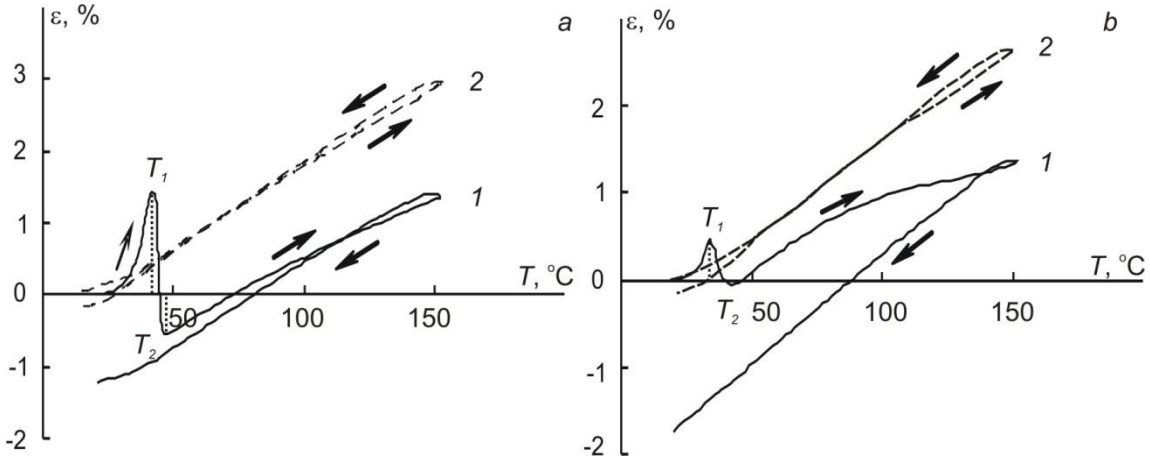

Figure 7.1. TMA curves of NC specimens with c = 4%, φ = 24% (*a*) and 98% (*b*) (number of heating–cooling cycle (*1, 2*)).

The fact that the process of shrinkage of the binder in the NC is caused by crystallization is confirmed by experiments with multiple heating of specimens to 70°C and their cooling to 20°C. Figure 7.2 gives the thermomechanical curves for three heating-cooling cycles and shows that the crystallization process was accompanied each time by shrinkage and the melting process — by spontaneous extension. Consequently, in the 20–70°C temperature range the restructuring process in the binder appears to be reversible; crystallization begins at T_1 = 41–45°C, and melting at T_2 = 46–50°C.

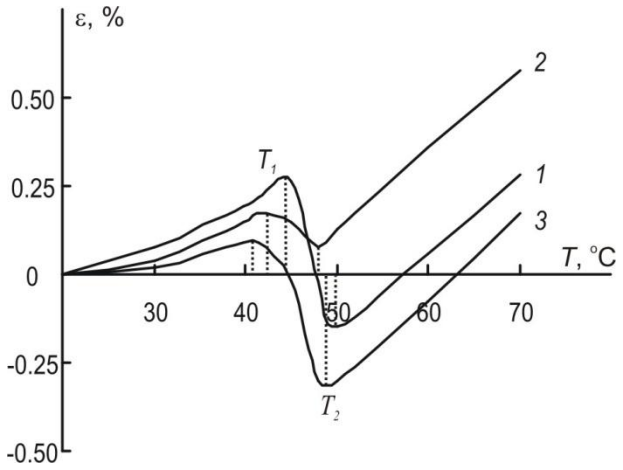

Figure 7.2. TMA curves of the binder at φ = 24% (number of heating–cooling cycle (*1*, *2*, *3*)).

X-ray structural analysis also confirms that upon preliminary annealing of specimens at 80 ^{o}C and subsequent drying in a medium of humidity 24% in the binder the crystalline phase is preserved (Figure 7.3, diffractogram *1*). The introduction into the NC composition of MMT nanoparticles (diffractogram *2*) leads to a change in the parameters of the crystalline reflex of the binder, for example, an increase in the interplanar spacing *d* and, accordingly, a change in the internal stress in the NC.

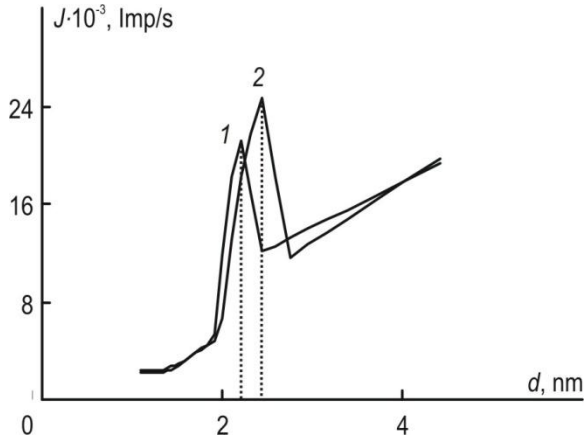

Figure 7.3. Diffractograms of NC specimens with *c* = 0% (*1*) and 6% (*2*).

It was somewhat difficult to determine T_g from the TMA curves since the attaining by it of the glass transition temperature served as a prerequisite to the binder crystallization in the NC. It was assumed that both processes (devitrification and onset of crystallization) proceeded practically simultaneously. Therefore, the deformation maximum temperature T_1 on the TMA curves (Figure 7.1) was assumed to correspond to the crystallization temperature, and the T_g value was assumed to be slightly different from it. Thus application of thermomechanical analysis to NC with different filler content under moisture effect has shown the following (Figure 7.4): glass transition temperature of NC decreases from 45 to 35 °C with the increase of moisture content in NC; the change of glass transition temperature of NC in relation to filler content is insignificant (lies within scattering of experimental data) within atmosphere of equal humidity.

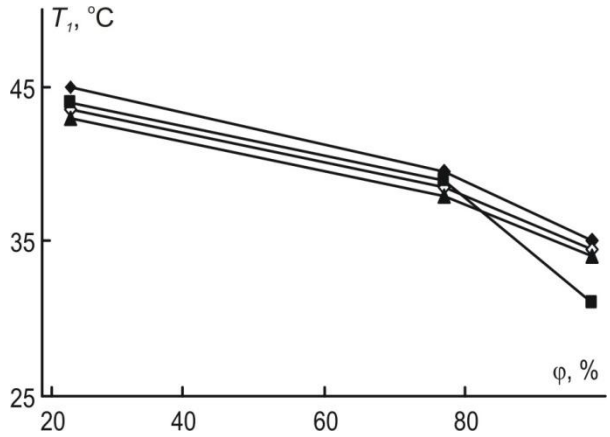

Figure 7.4. Glass transition temperature as a function of the atmospheric humidity for NC at c = 0 (♦), 2 (◊), 4 (▲), and 6% (■).

The weak strengthening effect of filler probably is associated with low cross-linking density of polymer's macromolecules located around filler particles and also with possible agglomeration of filler particles [14]. In turn reduction of glass transition temperature of epoxy resin and NC with the increase of moisture content (Figure 7.4) indicates that absorbed moisture softens the materials, i.e. facilitates reduction of intensity interaction between polymer macromolecules and mobility increment of the segments which results in acceleration of relaxation processes. Glass transition temperature of epoxy resin and NC is shifted to temperature region which is only 10-20 °C above room temperature, i.e. temperature during mechanical tests. Therefore loading can lead to transition of epoxy resin to viscoelasticity region which is characterized by large deformations. At least considered epoxy resin with the raised moisture content belongs to transition region from glassy to viscoelastic state.

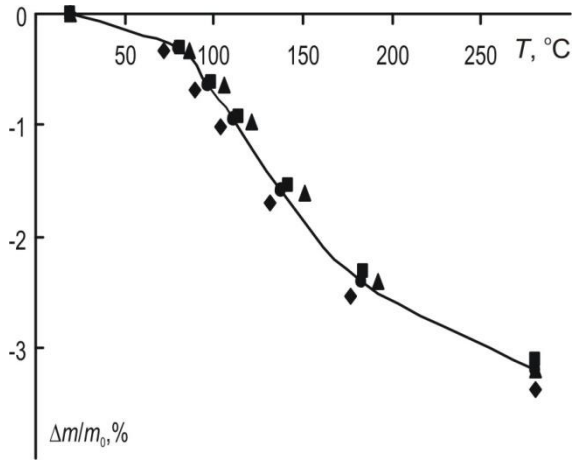

Figure 7.5. Mass loss curves of NC specimens at φ = 98% with c = 0 (♦), 2 (■), 4 (▲), and 6% (●).

From the mass loss curves of the thermogravimetric analysis (Figure 7.5) it is seen that in the 80–170^{o}C temperature range the mass loss process is the fastest, which agrees with the decrease in the thermal expansion coefficient. The maximum mass loss is observed in specimens held in an atmosphere with humidity of 98%. For instance, at clay content of 6% the NC mass

loss at 150°C is 1.5%, and in the binder it is 2% under the same conditions; however, no strict dependence on the degree of filling is observed. A further increase in the temperature leads to a decrease in the mass loss rate. Proceeding from the practically linear interrelation between the moisture content and the mass loss (Figure 7.6), it may be stated that upon heating the NC up to 280°C the moisture desorption process prevails.

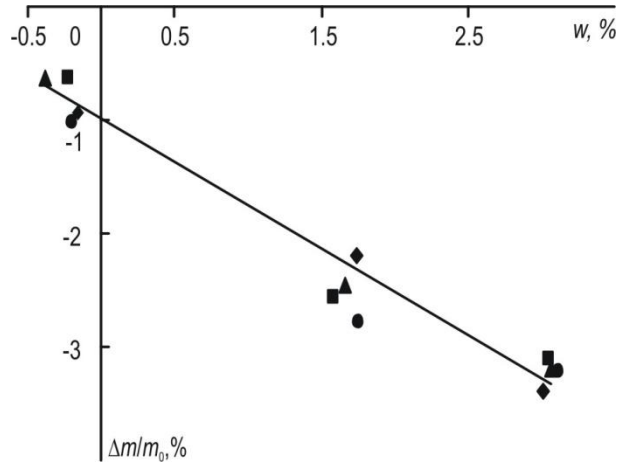

Figure 7.6. Moisture content of NC specimens with c = 0 (♦), 2 (■), 4 (▲), and 6% (●) in relation to the mass loss in heating.

In order to establish the relationship between the thermal characteristics and the structural changes attending the NC deformation process TMA analysis has been applied to epoxy-based NC specimens after quasistatic (Figure 5.1) and creep tension experiments (Figure 6.1). For these purpose moist specimens from atmosphere with φ = 98% RH were pre-deformed in the air in the regime of quasi-static tension with $\dot{\varepsilon}$ = const and creep with σ = const until the whole of the working part material went into the "neck." Then the specimens were cut along and across the direction of stretching. From the analysis of the TMA curves (Figure 7.7*a*) it is seen that the thermal expansion of the NC specimens cut in mutually perpendicular directions differs markedly and there are anisotropic changes in the thermomechanical characteristic. Analogous laws have also been obtained for specimens upon creep tests. For heated NC specimens cut along the stretching direction, in both quasi-static tension and creep experiments, their clear similarity to the TMA curves is observed (Figure 7.7*b*). For instance, in the glass transition temperature range their linear sizes sharply decrease. However, specimens oriented in the creep regime (curve *2*) shrink to a greater extent and the process proceeds in a narrower temperature range than for specimens oriented under quasi-static tension (curve *1*). Next, when temperatures of 37 °C (under creep) and 64 °C (under quasi-static tension) are attained, the process of their spontaneous stretching begins as sharply as shrinkage.

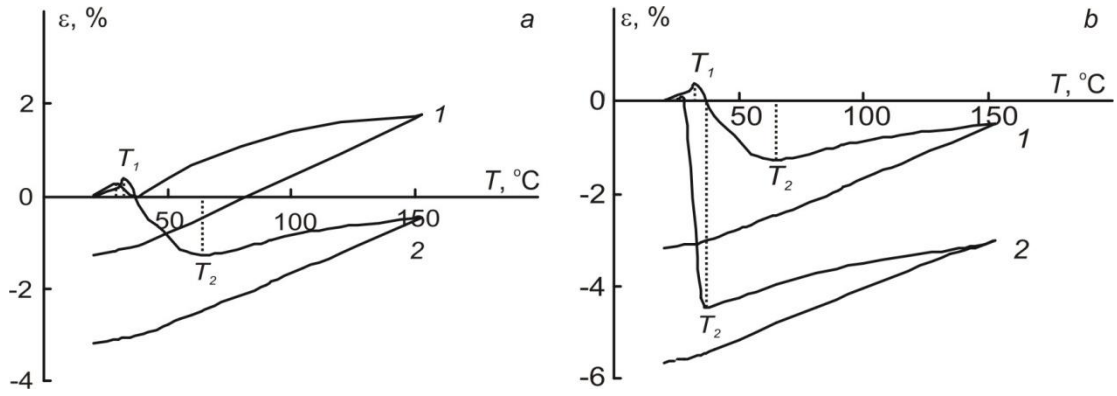

Figure 7.7. TMA curves of NC specimens cut across (*1*) and along (*2*) the stretching directions under quasi-static tension (*a*) and specimens cut along the stretching direction under quasi-static tension (*1*) and creep (*2*) (*b*).

From a comparison with the TMA curves of unloaded NC specimens (Figure 7.1*b*), it is seen that crystallization of oriented specimens begins at lower temperatures, and the shrinkage value (assumed to be proportional to the degree of crystallinity) is much larger than that for loaded specimens. This is explained by the fact that at orientation a considerable ordering of the NC structure occurs, which is a kind of a crystalline "blank," and therefore its transition to the crystalline structure is considerably facilitated. As a consequence of the crystallization of fibrillar aggregates the NC specimens do not completely regain their sizes either. At the same time, the TMA curves of the specimens cut across the orientation, as the results of quasi-static tension and creep experiments show, practically coincide in terms of the character of the change in the deformability and in its value. The TMA curves of the second heating cycle of specimens reflect, as for unloaded specimens, only one transition connected with the NC devitrification.

The data of X-ray structural analysis correlate well with the assumptions about structural changes in the NC at its deformations to high values. Figure 7.8 presents meridian and equatorial diffraction patterns of NC specimens pre-stretched to failure. It is seen that in the region of small angles on the equatorial diffraction pattern a peak caused by the crystalline phases is present, while it is absent from the meridian diffraction pattern. This effect can be explained by the fact that at large stretches the material acquires an almost completely fibrillated oriented structure, which leads to the disappearance of interfaces characteristic of microcrack walls. Apparently, joining of microcrack walls occurs and, therefore, no diffuse scattering is observed on the diffraction pattern meridian.

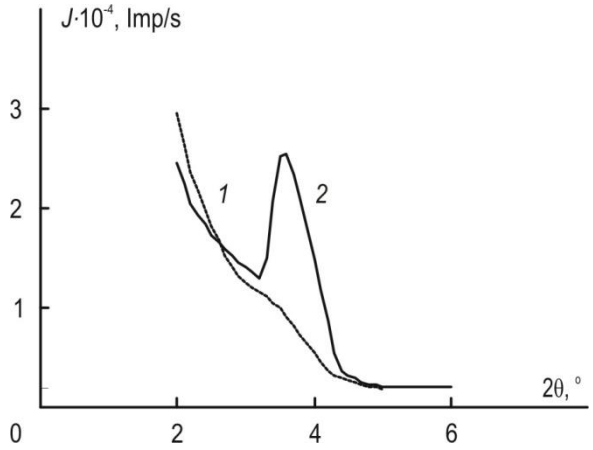

Figure 7.8. Diffraction patterns of a tension pre-deformed NC specimen with c = 6% cut from the "neck" region: meridian (*1*); equator (*2*).

Thus, from the above data it follows that the specific features of the thermomechanical behavior of the non-equilibrium structure of the NC upon stretching is largely determined by the quantity of the initial binder, which has gone to the oriented state, from which fibrillar aggregates of microcracks have been constructed. Changes take place in the region of T_g and, consequently, they have a supermolecular character. In heating, the fibrils acquire a greater mobility, and the coagulation process proceeds. This leads to a disorientation of fibrils with respect to one another and a decrease in the interface area, which shows up macroscopically as shrinkage of the NC.

This chapter concludes the description of complex investigation of mechanical and thermophysical properties of epoxy-based NC filled with nanoparticles of MMT platelets under effect of moisture. The interrelation of thermophysical and mechanical behavior with the structural changes accompanying deformation of epoxy-based NC specimens having absorbed moisture is established in the thesis at various schemes of loading and temperatures. The main conclusions and results, as well as practical importance and scientific novelty of the complex investigation are discussed and analyzed in the next chapter of the thesis.

8. General conclusions, practical importance, and scientific novelty of the work

The results of complex investigation on sorption, mechanical and thermophysical properties of various epoxy resins and epoxy-clay nanocomposite are summarized as follows:

1. Sorption process of investigated epoxy-nanoclay composite was described by Fick's model with good agreement for filler content 0-6% wt. and atmospheres 24, 77, and 98%RH. It was experimentally confirmed that sorption process in NC passed more slowly than in pure epoxy resin, and for the composite with highest filler content diffusivity reduces about half of diffusivity as for epoxy resin. The clay nanoparticles act as efficient barriers against moisture transport. The increase in equilibrium moisture content observed with the increase of clay weight content in NC was explained by growth of interphase content. The specific sorption capacity of interphase in NC per 1% of filler was determined and the sorption isotherm of interphase was derived.

2. Substantial effect of moisture on mechanical properties was shown. Absorbed moisture essentially plasticized the composite changing its fracture character. Tensile strength of moistened composite decreased twice. Elastic modulus both of moistened pure epoxy resin and NC was reduced approximately 1/3 in comparison to initial state.

   2.1. In order to estimate effect of filler morphological peculiarities on elastic properties of NC Halpin-Tsai equations were modified for the case of layered silicate platelets and applied to estimate effective elastic modulus of NC conditioned in atmospheres of different relative humidity. The equation parameters obtained for specimens conditioned in dry atmosphere were used for moistened NC and provided opportunity to estimate structural changes of the polymer resin because of moisture absorption.

   2.2. In order to estimate effect of interphase on elastic properties of NC the expressions for the bulk and shear moduli of epoxy-clay NC were derived by modification of Norris expressions for randomly oriented platelets. The properties of quasi-particle were estimated at nanolevel considering efficiency of adhesion at different filler contents. Epoxy resin was further filled with these quasi-particles and micro-model was applied to quantify elastic properties of epoxy-clay NC. This analysis at nano- and microlevels provided possibility to estimate the effect of filler and interphase properties and content on effective properties of NC in whole.

3. Viscoelastic properties of epoxy resin and NC in relation to absorbed moisture content were described on the basis of the principle of moisture-time analogy.

3.1. The spectrum of delay times for NC with filler content 6% differed from a spectrum of delay times for epoxy resin: delay times increased, the intensity decreased slightly. Value of moisture-time reduction function for NC with filler content 2% was smaller in comparison with epoxy resin. The further increase in filler content leaded to increase in parameters of reduction function.

3.2. It was established that moisture-time reduction function correlated with change of upper yield point of NC that indicated viscoelastic character of NC specimens' deformation having different moisture content.

3.3. Presence of correlation between moisture-time reduction function and volume change of epoxy resin upon moistening allowed its estimating based on the data on swelling.

4. Moisture sorption caused plasticization of NC and leaded to decrease of glass transition temperature by 10 ^{o}C. The deformation mechanism of NC changed significantly under affect of moisture. Large plastic deformations and formation of transition regions to orientated state ("necking") revealed during tension of moistened specimens of NC. Thermal expansion of the NC specimens cut in mutually perpendicular directions after tensile quasitatic and creep tests differed markedly and there were anisotropic changes in the thermomechanical characteristic. The data of X-ray structural analysis correlated well with the assumptions about structural changes in the NC at its deformations to high values.

5. Incorporation of impenetrable clay nanoparticles with high mechanical characteristics didn't reduce the negative effect of absorbed moisture on mechanical properties of NC. But since the value of elastic modulus of epoxy resin was improved with respect to filler content up to 20% epoxy resin modified by impenetrable stiff montmorillonite clay nanoparticles could be applied in environments with higher-operating relative humidity.

The **practical importance** of the complex investigation of sorption, mechanical and thermophysical properties of various epoxy resins and composites on their basis rests in the obtained results of steadiness to different environmental factors (temperature, humidity, loading, etc.) determination for novel composite materials. These results will allow estimating possible applications of nanoclay composite materials under influence of environment factors (moisture, temperature, constant and time-varying loading) that will facilitate expanding a scope of polymer composite materials in civil engineering and technological sectors. Since the use of composites in different spheres of life becomes inevitable due to loss of nonrenewable natural resources the efficiency and safety of composites' applications should be guaranteed by correct research of operational properties under the influence of different factors.

Following theses having **scientific novelty** are defended within the work:

1. The account of heterogeneity and formation of the interphase is significant upon modeling of moisture absorption of and determination of sorption characteristics of epoxy-clay NC;
2. Modification of Halpin-Tsai equations for isotropic polymer matrix filled with coplanar transversally isotropic cylindrical particles of arbitrary aspect ratio and Norris equations for polymers filler with randomly oriented platelets for the bulk and shear moduli allowed to determine effective elastic moduli of epoxy-clay NC taking into account filler morphological peculiarities (layered structure of filler particles and formation of inhomogeneous interphase);
3. The correlation between moisture-time reduction function with the change of upper yield point and volume change of NC specimens upon moistening was established which indicates viscoelastic character of NC specimens' deformation having different moisture content and allowed its estimating based on the data on swelling.
4. Anisotropic changes in the thermomechanical characteristic of the NC in mutually perpendicular directions after tensile quasistatic and creep tests were revealed. These results correlated well with data of X-ray structural analysis.

Main results of doctoral thesis are published in 6 scientific articles [P] and 3 conference proceedings [C], and also reported at 12 international conferences (the conference theses are not included in the thesis).

9. References

1. *Fornes T. D., Yoon P. J., Hunter D. L., Keskkula H., Paul D. R.* Effect of organoclay structure on nylon 6 nanocomposite morphology and properties. Polymer, 2002, Vol. 43, No. 22, p. 5915-5933.
2. *LeBaron P., Wang Z., Pinnavaia T. J.* Polymer-layered silicate nanocomposites: an overview. Applied Clay Science, 1999, Vol. 15, No. 1, p. 11-29.
3. *Gay D., Hoa A., Tsai S.* Composite materials. Design and applications. CRC Press, 2003, 503 p.
4. Roco M. Broader social issues of nanotechnology. Journal of Nanoparticle Research, 2003, Vol. 5, No. 3-4, p. 181-189.
5. *Aniskevich K., Glaskova T., Janson Yu.* Elastic and sorption characteristics of an epoxy binder in a composite during its moistening. Mechanics of Composite Materials, N. Y., Kluwer Academic/Plenum Publishers, 2005, Vol. 41, No. 4, p. 341-350.
6. *Vlasveld D., Groenevold J., Bersee H., Mendes E., Pichen S. J.* Analysis of the modulus of polyamide-6 silicate nanocomposites using moisture controlled variation of the matrix properties. Polymer, 2005, Vol. 46, No. 16, p. 6102-6113.
7. *Kim J.-K., Hu Ch., Woo R. S. C., and Sham M.-L.* Moisture barrier characteristics of organoclay-epoxy nanocomposites. Composites Science and Technology, 2005, Vol. 65, No. 5, p. 805-813.
8. *Crank J.* The Mathematics of Diffusion, Oxford, 1956, 224 p.
9. *Maggana C. and Pissis P.* Water sorption and diffusion studies in an epoxy resin system. Journal of Polymer Science. Part B — Polymer Physics, 1999, Vol. 37, No. 11, p. 1165-1182.
10. *Andrikson G. A., Mochalov V. P., and Aniskevich A. N.* Principle of modified time scale for tasks of nonstationary moisture diffusion in polymer materials. Mekh. Kompoz. Mater., 1980, Vol. 16, No. 1, p. 153-170.
11. *Xiao G. Z. and Shanahan M. E. R.* Swelling of DGEBA/DDA epoxy resin during hygrothermal ageing. Polymer, 1998, Vol. 39, No. 14, p. 3253-3260.
12. *Koo J. H.* Polymer nanocomposites. McGraw-Hill, 2006.
13. *Ajayan P. M., Schadler L. S., Braun P. V.* Nanocomposite science and technology. Wiley, 2003.
14. *Yasmin A., Luo J. J., Abot J. L., Daniel I. M.* Mechanical and thermal behaviour of clay/epoxy nanocomposites. Composites Science and Technology, 2006, Vol. 66, No. 14, p. 2415-2422.
15. *Maksimov R. D., Gaidukov S., Zicans J., and Jansons J.* Moisture permeability of a polymer nanocomposite containing unmodified clay. Mechanics of Composite Materials, 2008, Vol. 44, No. 5, p. 505-514.
16. *Glaskova T., Aniskevich A.* Moisture effect on deformability of epoxy/montmorillonite nanocomposite. Journal of Applied Polymer Science, 2010, Vol. 116, No. 1, p. 493-498.
17. *Wang J., Pyrz R.* Prediction of the overall moduli of layered silicate-reinforced nanocomposites – part I: basic theory and formulas. Composites Science and Technology, 2004, Vol. 64, No.7-8, p. 925-934.
18. *Christensen R. M.* A critical evaluation for a class of micromechanics models. Journal of Mechanics and Physics of Solids, 1990, Vol. 38, p. 379-404.
19. *Norris A. N.* The mechanical properties of platelet reinforced composites. International Journal of Solids and Structures, 1990, Vol. 26, p. 663-674.
20. *Odegard G. M., Clancy T. C., Gates T. S.* Modeling of the mechanical properties of nanoparticle/polymer composites. Polymer, 2005, Vol. 46, p. 553-562.
21. *Wang J., Pyrz R.* Prediction of the overall moduli of layered silicate-reinforced nanocomposites-part II: analyses. Composites Science and Technology, 2004, Vol. 64, p. 935-944.

22. *Bicerano J.* Prediction of polymer properties. 3d ed., Marcel Dekker, 2002, 756 p.
23. *Giannelis E.* Polymer layered silicate nanocomposites. Advanced materials, 1996, Vol. 8, p. 29-35.
24. *Pal R.* Mechanical properties of composite of randomly oriented platelets. Composites: Part A, 2008, Vol. 39, p. 1496-1502.
25. *Maksimov R. D., Gaidukov S., Kalnins M., Zicans J., Plume E.* A nanocomposite based on styrene-acrylate copolymer and native montmorillonite clay. Part 2. Modeling of the elastic properties. Mechanics of Composite Materials, 2006, 42, p. 163-172.
26. *Halpin J. C., Kardos J. L.* The Halpin-Tsai equations: a review. Polymer Engineering and Science, 1976, Vol. 16, No. 5, p. 344-352.
27. *Glaskova T., Aniskevich A.* Moisture absorption by epoxy/montmorillonite nanocomposite. Composites Science and Technology, 2009, Vol. 69, No.15-16, p. 2711-2715.
28. *Ferry J. D.* Viscoelastic properties of polymers. John Wiley & Sons. New York, 1961, 218 p.
29. *Perez C. J., Alvarez V. A., Vazquez A.* Creep behaviour of layered silicate/starch-polycaprolactone blends nanocomposites. Materials Science and Engineering A, 2008, Vol. 480, No. 1-2, p. 259-265.
30. *Glaskova T. I., Guedes R. M., Morais J. J., Aniskevich A. N.* A comparative analysis of moisture transport as applied to an epoxy binder. Mechanics of Composite Materials, 2007, Vol. 43, No. 4, p. 377-388.
31. *Bond D. A.* Moisture diffusion in a fiber-reinforced composite. Pt.I. Non-Fickian transport and the effect of fiber spatial distribution. Journal of Composite Materials, 2005, Vol. 39, No. 23, p. 2113-2129.
32. *Weitsman Y.* Diffusion with time-varying diffusivity with application to moisture sorption in composites. Journal of Composite Materials, 1976, Vol. 10, p. 193-204.
33. *Masenelli-Varlot K., Chazeau L., Gauthier C., Bogner A., Cavaillé J.Y.* The relationship between the electrical and mechanical properties of polymer–nanotube nanocomposites and their microstructure. Composites Science and Technology, 2009, Vol. 69, p. 1533-1539.
34. *Tsai J., Sun T.* Effect of platelet dispersion on the load transfer efficiency in nanoclay composites. Journal of Composite Materials, 2004, Vol. 38, p. 567-579.
35. *Chen B., Evans J. R. G.* Elastic moduli of clay platelets. Scripta Materialia, 2006, Vol. 54, p. 1581-1585.
36. *Anthoulis G. I., Kontou E.* Micromechanical behavior of particulate polymer nanocomposites. Polymer, 2008, Vol. 49, p. 1934-1942.
37. *Luo J.-J., Daniel I. M.*. Characterization and modeling of mechanical behavior of polymer/clay nanocomposites. Composites Science and Technology, 2003, Vol. 63, p. 1607–1616.
38. *Starkova O., Yang J., Zhang Zh.* Application of time-stress superposition to non-linear creep of polyamide 66 filled with nanoparticles of various sizes. Composites Science and Technology, 2007, Vol. 67, p. 2691-2698.
39. *Aniskevich K., Krastev R., Hristova Yu.* Effect of long-term exposure to water on viscoelastic properties of an epoxy-based composition. Mechanics of Composite Materials, 2009, Vol. 45, No. 2, p. 137-144.
40. *Aniskevich A. N., Yanson Yu. O., Aniskevich N. I.* Creep of epoxy binder in a humid atmosphere. Mechanics of Composite Materials, 1992, Vol. 28, No.1, p. 12-18.

10. List of publications and conference theses

10.1. Papers in journals included in the thesis

[P1] *Aniskevich K., Glaskova T., Janson Yu.* Elastic and sorption characteristics of an epoxy binder in a composite during its moistening. Mechanics of Composite Materials, N. Y., Kluwer Academic/Plenum Publishers, 2005, Vol. 41, No. 4, p. 341-350.

[P2] *Glaskova T. I., Guedes R. M., Morais J. J., Aniskevich A. N.* A comparative analysis of moisture transport models applied to epoxy binder. Mechanics of Composite Materials, N. Y., Kluwer Academic/Plenum Publishers, 2007, Vol. 43, No. 4, p. 377-388.

[P3] *Glaskova T., Aniskevich A.* Moisture absorption by epoxy/montmorillonite nanocomposite. Composites Science and Technology, 2009, Vol. 69, p. 2711-2715.

[P4] *Glaskova T., Aniskevich A.* Moisture effect on deformability of epoxy/montmorillonite nanocomposite. Journal of Applied Polymer Science, 2010, Vol. 116, No. 1, p. 493-498.

[P5] *Faitel'son E. A., Glaskova T. I., Korkhov V. P., Aniskevich A. N.* Structural changes in a clay-containing nanocomposite with a different moisture content caused by its deformation. Journal of Engineering Physics and Thermophysics, 2010, Vol. 83, No. 3, p. 443-451.

[P6] *Aniskevich K. K., Glaskova T. I., Aniskevich A. N., and Faitelson Ye. A.* Effect of moisture on the viscoelastic properties of epoxy-clay nanocomposite. Mechanics of Composite Materials, 2010, in press.

10.2. Conference proceedings included in the thesis

[C1] *Aniskevich A., Glaskova T., Spacek V., Sviglerova P.* Effect of moisture sorption on deformability of epoxy/montmorillonite nanocomposite. Proceedings of European conference on Composite Materials, 2006, CD, No. 90.

[C2] *Glaskova T., Aniskevich A.* Modeling of effective elastic properties of composite material containing nanoparticles with an inhomogeneous interphase. Proceedings of European Conference on Composite Materials, 2008, CD, No. 1454.

[C3] *Glaskova T., Aniskevich A.* Creep behavior of epoxy/clay nanocomposite. Proceedings of International Conference on Composite Materials, 2009, CD, No. F1:14.

10.3. Conference theses

1. *Glaskova T., Aniskevich K., Korkhov V.* Structure and properties of epoxy resin in filled composite during its moistening. Baltic Polymer Symposium, November 24-25, 2004, Kaunas, Lithuania. Book of abstracts p. 28.
2. *Glaskova T., Aniskevich A., Spacek, V., Sviglerova P*. Effect of moisture sorption on the mechanical properties of epoxy/montmorillonite nanocomposite. Mechanics of Composite Materials, May 29-June 2, 2006, Riga, Latvia. Book of abstracts p. 58.
3. *Aniskevich A., Glaskova T., Spacek V., Sviglerova P.* Effect of moisture sorption on deformability of epoxy/montmorillonite nanocomposite. 12-th European conference on Composite Materials, August 29 – September 1, 2006, Biarritz, France. Book of abstracts p. 101.
4. *Glaskova T., Aniskevich A., Starkova O., Merijs Meri R., Zicans J.* Mechanical performance of organo-clay-epoxy nanocomposite under moisture effect. Baltic Polymer Symposium, September 20-22, 2006, Riga, Latvia. Book of abstracts p. 51.
5. *T. Glaskova, A. Aniskevich, Yu. Jansons.* Organoclay-epoxy nanocomposite: properties modeling including interphase layer. ICSAM - The international Conference on Structural

Analysis of Advanced Materials, September 2-6, 2007, Patras, Greece. Book of abstracts p. 42.

6. *T. Glaskova, A. Tuchs, A. Aniskevich.* Modeling of volume-dependent properties of disperse filled composite material considering inhomogeneous interphase. Baltic Polymer Symposium, May 13-16, 2008, Otepaa, Estonia. Book of abstracts p. 65.
7. *E. A. Faitelson,T. I. Glaskova, A. N. Aniskevich, and V. P. Korhov.* Thermomechanical properties of epoxy/clay nanocomposite depending on filler and moisture content. Mechanics of Composite Materials, May 26-30, 2008, Riga, Latvia. Book of abstracts p. 84.
8. *T. Glaskova, A. Aniskevich*. Modeling of effective elastic properties of composite containing nanoparticles with an inhomogeneous interphase. European Conference on Composite Materials, June 2-5, 2008, Stockholm, Sweden. CD, No. 1454.
9. *T. Glaskova, A. Aniskevich, R. M. Guedes, and J. J. Morais*. Application of moisture absorption theories for epoxy resin system. Duracosys'08 (Durability Analysis of Composite Systems), July 16-18, 2008, Porto, Portugal. Book of abstracts p. 119, 120.
10. *T. Glaskova, A. Tuchs, A. Aniskevich.* Modeling of nanocomposite scalar properties taking into account inhomogeneity of the interphase. Functional materials and nanotechnologies, March 31-April 3, 2009, Riga, Latvia. Book of abstracts p. 190.
11. *T. Glaskova, A. Aniskevich.* Creep behavior of epoxy/clay nanocomposite. 17th International Conference on Composite Materials, July 27-31, 2009, Edinburgh, United Kingdom. CD.
12. *T. Glaskova, K. Aniskevich, A. Aniskevich*. Creep behavior of epoxy/clay nanocomposite. Mechanics of Composite Materials, May 24-28, 2010, Riga, Latvia. Book of abstracts p. 71.

11. Participation in research projects

1. "Development of modern functional and constructive materials and corresponding technologies for microelectronics, nanoelectronics, photonics, biomedicine". State research program in Material Science, 2005-2008 yrs. The head of project Dr. Sc. Ing. *Juris Jansons*, full member of Latvian Academy of Science.
2. "Investigation of deformation and strength properties of nanocomposites with non-elastic matrices". Grant of Latvian Scientific Council No. 05.1933, 2006-2010 yrs. The head of project Dr. Sc. Ing. *Juris Jansons*, full member of Latvian Academy of Science.
3. "Foundation of young scientist group for investigation of mechanical and physical properties at nano-, meso- and microlevel of modern polymer composite materials with a disperse filler". Research project of the University of Latvia No. Y2-ZP119-100, 01.06.-30.11.2009. The head of the project Dr. Phys. *Olesja Starkova*.
4. "Support for doctoral studies at University of Latvia". Project of European Social Fund No. 20092009/0138/1DP/1.1.2.1.2/09/IPIA/VIAA/004, 01.10.2009.-31.09.2010.
5. "Involvement of human resources to complex investigation of modern composite materials". Project of European Social Fund No. 2009/0209/1DP/1.1.1.2.0/09/APIA/VIAA/114, 2009-2012 yrs. The head of project Dr. Sc. Ing. *Juris Jansons*, full member of Latvian Academy of Science.

Acknowledgments

I would like to express my sincere thanks to my scientific supervisor Dr. Sc. Ing. *Andrey Aniskevich,* to director of Institute of Polymer Mechanics (IPM), head of our laboratory Dr. Habil. Sc. Ing *Juris Jansons,* Dr. Phys. *Olesja Starkova* and Dr. Sc. Ing. *Mauro Zarrelli* and the rest non-mentioned but really close colleagues from IPM and CNR for their guidance and encouragement throughout this work.

I am also grateful to L`ORÉAL Baltic (scholarship for „Women in science" with the support of Latvian National Committee of UNESCO and Latvian Academy of Sciences) and European Social Fund (project „Support for doctoral studies at University of Latvia" and project „Involvement of human resources to complex investigation of modern composite materials") for the financial support of this research.

And finally last but HUGE thanks I would like to express to my family and friends for their invaluable support and infinite patience. Owing to my elder brother whose first education is physics I've done my choice once. As a result I still do research with gusto. My parents and my husband have also stimulated me a lot to work as good as possible and make them really happy with me ☺.

Publikācija 1

Elastic and sorption characteristics of an epoxy binder in a composite during its moistening

Aniskevich K., Glaskova T., Janson Yu.

Institute of Polymer Mechanics, University of Latvia, Riga, Latvia

Mechanics of Composite Materials, 2005, Vol. 41, No. 4, p. 341-350.

Mechanics of Composite Materials, Vol. 41, No. 4, 2005

ELASTIC AND SORPTION CHARACTERISTICS OF AN EPOXY BINDER IN A COMPOSITE DURING ITS MOISTENING

K. Aniskevich, T. Glaskova, and J. Jansons

Keywords: *filled composite, epoxy binder, sorption, elastics characteristics*

Results of an experimental investigation into the elastic and sorption characteristics of a model composite material (CM) — epoxy resin filled with LiF crystals — during its moistening are presented. Properties of the binder in the CM with different filler contents (v_f = 0, 0.05, 0.11, 0.23, 0.28, 0.33, 0.38, and 0.46) were evaluated indirectly by using known micromechanical models of CMs. It was revealed that, for the CM in a conditionally initial state, the elastic modulus of the binder in it and the filler microstrain (change in the interplanar distance in the crystals, measured by the X-ray method) as functions of filler content had the same character. The elastic modulus of the binder in the CM with a low filler content was equal to that for the binder in a block; the elastic modulus of the binder in the CM decreased with increasing filler content. The maximum (corresponding to water saturation of the CM) stresses in the binder and the filler microstresses as functions of filler content were of the same character. Moreover, the absolute values of maximum stresses in the binder and of filler microstresses coincided for high and low contents of the filler. At v_f = 0.2-0.3, the filler microstrains exceeded the stresses in the binder. The effect of moisture on the epoxy binder in the CM with a high filler content was not entirely reversible: the elastic characteristics of the binder increased, the diffusivity decreased, and the ultimate water content increased after a moistening–drying cycle.

Introduction

Filling a polymer with more rigid particles and/or a powder allows one to obtain a composite material (CM) with a necessary complex of elastic and strength properties, which depend on the properties of the filler and the binder (polymer), the coefficient of filling, and the manufacturing technology of the CM.

A change in the structure and properties of a polymer with time, because of physical and chemical transformations under the influence of external factors (temperature, humidity, loading, etc.), leads to changes in the structure and properties of the CM. These changes have to be predicted based on the results of investigating the variability of the structure and the properties of the binder with time. However, this information can be insufficient, since the structure and properties of the polymer in the composite and in a block, as well as the character of their variation with time, can differ. The binder in a CM can be inhomogeneous [1], forming a layer with a more or less expressed boundary at the interface with the filler. The density of this layer and/or the binder in the CM may be higher or lower than that of the binder in a block, owing to distinctions in the degree of

Institute of Polymer Mechanics, University of Latvia. Translated from Mekhanika Kompozitnykh Materialov, Vol. 41, No. 4, pp. 499-511, July-August, 2005. Original article submitted April 18, 2005.

0191-5665/05/4104-0341

TABLE 1. Density (g/cm^3), Coefficient of Filling, and Porosity of CMs

Initial			After a sorption–desorption cycle		
ρ	v_f	v_p	ρ	v_f	v_p
1.103	0	0.06	1.261	0	0.09
1.193	0.05	0.05	1.316	0.05	0.09
1.440	0.11	0.06	1.545	0.11	0.10
1.398	0.23	0.14	1.608	0.25	0.10
1.522	0.28	0.14	1.657	0.30	0.10
1.610	0.33	0.16	1.786	0.35	0.10
1.672	0.38	0.15	1.813	0.39	0.10
1.762	0.46	0.19	1.951	0.48	0.11

cross-linking and porosity. The presence of the boundary layer and pores affects the properties of the composite, such as its elastic characteristics, strength, kinetics of moisture sorption, swelling, and character of failure. If the composite is subjected to a long-term action of external factors, the structure and properties of this layer can change as a result of aftercure of the polymer, relaxation of technological stresses, swelling, etc.

The purpose of the present study is to reveal the features of the structure and properties of an epoxy binder in a CM and their changes with time under a long-term action of a moist atmosphere. To do this, we estimated and compared the theoretical and experimental values of elastic and sorption characteristics of the binder in the CM and in a block.

2. Materials and Experiments

A model composite based on an epoxy binder filled with LiF crystals was investigated. This composite is characterized by a good adhesion between the filler and the binder [2]. The crystal structure of the filler makes it possible to estimate its deformation in a CM, both in conditionally initial and moistened states, by using the X-ray method [2, 3]. The results of preliminary experiments show that the filler does not absorb moisture.

We used series of CM specimens with different filler contents: μ = 0, 0.10, 0.20, 0.42, 0.48, 0.54, 0.59, and 0.68 wt.% (four specimens for each value of μ), made by using the technique described in detail in [3]. The linear sizes of the specimens were measured by a micrometer, and their weight m was found on a VLR-200 analytical balance. Then, we calculated the density ρ and, taking into account the value of μ, the relative volume content of the filler v_f in the CM. The porosity v_p was determined by the method of hydrostatic weighing. The values of ρ, v_f, and v_p are given in Table 1.

The specimens were moistened in a desiccator above a saturated solution of K_2SO_4 at a relative humidity of ϕ = 98%. At certain time intervals, we removed the specimens from the desiccator, measured their linear sizes, weighed, and, using an IChZ-9F unit, measured the resonant frequencies of longitudinal and torsional vibrations to determine the elastic E and shear G moduli [4]. As soon as the specimens were completely saturated, they were placed in a desiccator with silica gel to desorb moisture from the CM.

The experimental values of the elastic modulus of CMs with different coefficients of filling are presented in Fig. 1. As seen from the figure, an increase in the modulus E with increasing v_f is observed for the CM in a conditionally initial state at $v_f \le 0.33$, in the saturated state at all the values of v_f considered, and after a moistening–drying cycle at $v_f \le 0.38$. The relations between the shear modulus G and the quantity v_f have the same character.

Figure 2 shows a typical — of the CM examined and the binder in a block — experimental relative weight of a specimen $w = \dfrac{m - m_0}{m_0}$ (m_0 is the weight of the specimen in a conditionally initial state) vs. time t during the sorption and subsequent

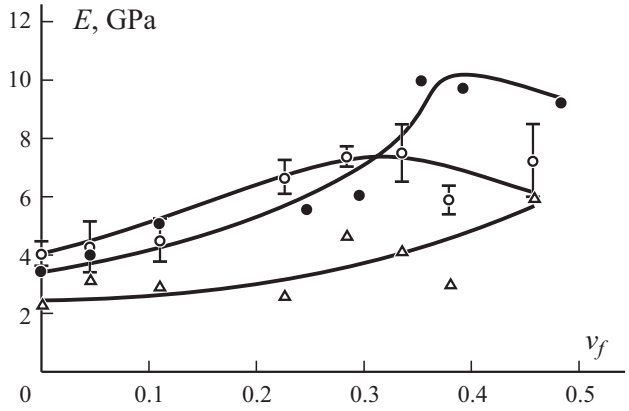

Fig. 1

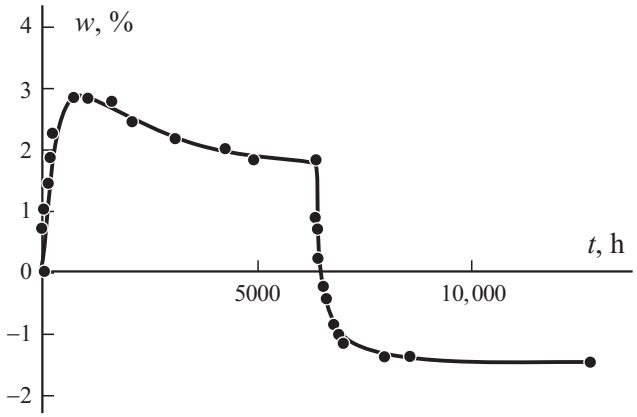

Fig. 2

Fig. 1. Experimental elastic moduli E of the CM in the initial (○) and water-saturated (△) states and after a moistening–drying cycle (●) in relation to the filler content v_f.

Fig. 2. Change in the weight w of CM (v_f = 0.11) specimens with time t during moistening and subsequent drying (experiment).

desorption. As is seen, the weight of the dried specimen is less than that of the initial one. This is explained in particular by the fact that, before the beginning of tests, the specimens were not dried [they were in equilibrium with the environment (laboratory): T_l = 20°C and ϕ_l = 59%]. In addition, the decrease in specimen weight after a moistening–drying cycle is also caused by mass losses, as clearly seen from the sorption curve after the achievement of the saturated state. The weight losses can be caused by volatilization of low-molecular substances from the binder and/or "squeezing of moisture" from the binder as a result of its aftercure [3].

For a quantitative comparison of experimental results on moisture sorption and desorption from the CM, the initial moisture content in specimens was estimated by additional tests. We used twin CM specimens in a conditionally initial state, which were held in a desiccator with silica gel at T_l = 20°C for a long time. During this time, the specimens were repeatedly weighed until their weight reached the limiting value m_0'. The difference $\Delta m = m_0 - m_0'$ was used as a correction in experiments on moisture desorption from the CM.

Figure 3 shows the initial sections of sorption curves in the coordinates $w_m - \sqrt{t}$, (where $w_m = w/(1-\mu)$), characterizing moisture sorption by the binder in the CM. It is seen that, for a CM with a small content of filler, the sorption curves for the binder in the CM and in a block practically coincide, while in the case of a high filler content they differ noticeably. This means that the structure and properties of the binder in a CM with a high content of filler and in a block are different.

Figures 4 and 5 present the coefficients of swelling α and α_m and the ultimate moisture content of CM w^∞ and the binder in the CM $w_m^\infty = w_\infty/(1-\mu)$ as functions of the coefficient of filling. As follows from the data in Fig. 5, in sorption, the value of w_m^∞ is practically constant at $\mu \le 0.54$ ($v_f \le 0.33$) and decreases noticeably at high filler concentrations in the CM. In desorption, the w_m^∞-dependence of μ appears already at $\mu = 0.48$ ($v_f < 0.28$). The difference between the values of w_m^∞ in sorption and desorption increases in absolute value with growing μ. This cannot be explained by the presence of moisture in the conditionally initial specimens, since, in this case, the experiment gives a value ~1%, which does not depend on μ.

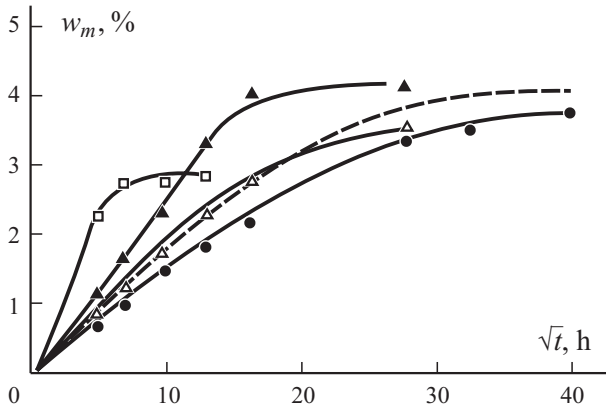

Fig. 3. Change in the binder weight w_m with time t in specimens of CM with v_f = 0.05 (●), 0.11 (△), 0.38 (▲), and 0.46 (□) and in a block (- - -) (calculation).

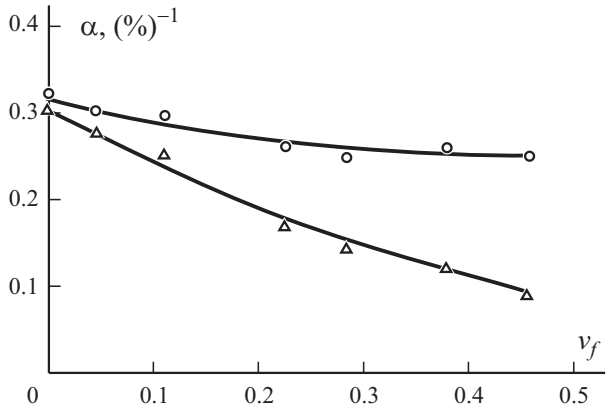

Fig. 4. Coefficient of swelling of the CM (△) and binder (○) in the CM in relation to v_f.

3. Calculation Models

3.1. Micromechanical model of a filled composite. The effect of volume content of filler on the mechanical properties of composites has been much studied and is taken into account in numerous mathematical models. Well-known are models considering a spherical inclusion surrounded by a matrix layer in an equivalent homogeneous medium with unknown effective characteristics. These are three-phase models, containing a particle, the surrounding matrix (the continuous phase), and the composite itself with averaged properties. The external radius of the matrix layer, *b*, is found from the condition that the concentration of inclusions v_f satisfies the relation $(a/b)^3 = v_f$, where a is the radius of the spherical inclusion. The effective bulk K and shear G moduli are calculated from continuity conditions for displacements at the interface, assuming that the bulk and shear moduli of the inclusion and matrix are known. According to this scheme, simple formulas for a composite with a small volume fraction of inclusions were derived in [5]:

$$K = K_m + v_f \frac{K_f - K_m}{1 + (1 - v_f)\dfrac{K_f - K_m}{K_m + \dfrac{4}{3}G_m}}, \qquad (1)$$

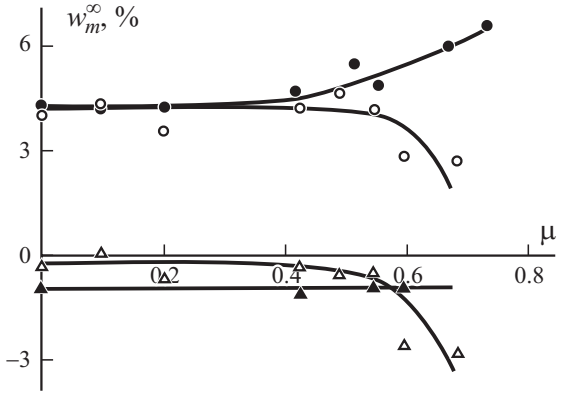

Fig. 5. Ultimate moisture content w_m^∞ in the CM, related to the weight content of binder, upon sorption (○) and desorption (●), their difference (△), and the weight losses of initial specimens dried in a desiccator (▲) in relation to μ.

$$G = G_m + v_f \frac{G_f - G_m}{1 + (1 - v_f)(G_f - G_m)\dfrac{6(K_m + 2G_m)}{5G_m(3K_m + 4G_m)}}, \tag{2}$$

where K_m, G_m, and K_f, G_f are the bulk and shear moduli of the matrix and filler, respectively. The elastic modulus E of the CM in tension (compression) is equal to $E = \dfrac{9KG}{3K + G}$.

We should note that the above-mentioned theories are linear, i.e., they are valid in the case of small pressure and/or small shear forces. Thus, in shear, the spherical form of inclusions must be retained. Although these theories have been developed for a certain geometry of inclusions, the resulting formulas are simple and convenient in use, in particular for comparing theoretical and experimental data.

Since the rigidity of the filler of the CM examined is much higher than that of the binder (matrix), i.e., $K_m / K_f << 1$ and $G_m / G_f << 1$, formulas (1) and (2) become much simpler and take the form

$$K = K_m \frac{1 + \nu_m + 2v_f(1 - 2\nu_m)}{(1 - v_f)(1 + \nu_m)}, \tag{3}$$

$$G = G_m \frac{2(4 - 5\nu_m) + v_f(7 - 5\nu_m)}{2(1 - v_f)(4 - 5\nu_m)}. \tag{4}$$

Hereinafter, ν_m and ν are the Poisson ratios of the binder and CM, respectively.

The influence of porosity on the elastic characteristics of a CM can be modeled by using the same equations (1) and (2) provided the rigidity of the filler (pores) is much lower than the rigidity of the binder: $K_f / K_m << 1$ and $G_f / G_m << 1$. Then, relations (1) and (2) take the form

$$K = K_m r \frac{(1 - v_p)}{(r + v_p)}, \tag{5}$$

$$G = G_m \frac{(1-v_p)(3+2r)}{3+2r+v_p(2+3r)}, \tag{6}$$

where v_p is the relative volume content of pores; $r = \frac{4G_m}{3K_m} = \frac{2(1-2\nu_m)}{1+\nu_m}$.

From Eqs. (5) and (6), we derive expressions for calculating the elastic modulus and Poisson ratio of a CM filled with air bubbles (pores):

$$E = \frac{6E_m}{1+\nu_m} \cdot \frac{(1-v_p)(3+2r)}{12+11(r+v_p)+2r(r+7v_p)}, \tag{7}$$

$$\nu = \frac{6+r+v_p+2r(2v_p-r)}{12+11(r+v_p)+2r(r+7v_p)}. \tag{8}$$

3.2. Moisture sorption by a quasi-homogeneous material. The moisture sorption by the epoxy binder and composites based on it is usually described by the Fick equation [6], which, for the case of one-dimensional diffusion, has the form

$$\frac{\partial c}{\partial t} = D\frac{\partial^2 c}{\partial x^2}, \tag{9}$$

where $c(x,t)$ is the concentration of diffusing moisture at a point x at a moment of time t; D is the diffusivity. For a plane-parallel plate of thickness h, at the initial $c(x,t=0)=c_0$ and boundary $c(x=0, x=h, t)=c_\infty$ conditions, the solution to Eq. (9) is the series [7]

$$c(x,t) = c_\infty - 2\frac{(c_\infty - c_0)}{\pi}\sum_{k=1}^{\infty}\frac{(1-(-1)^k)}{k}\sin\left(\frac{\pi k}{h}x\right)\exp\left[-\left(\frac{\pi k}{h}\right)^2 Dt\right]. \tag{10}$$

Integrating Eq. (10) across the plate thickness, we obtain an expression for the relative moisture content in a specimen:

$$w(t) = w_\infty - 2\frac{(w_\infty - w_0)}{\pi^2}\sum_{k=1}^{\infty}\frac{(1-(-1)^k)^2}{k^2}\exp\left[-\left(\frac{\pi k}{h}\right)^2 Dt\right]. \tag{11}$$

Here, w_∞ is the ultimate (equilibrium) moisture content in the specimen.

The diffusivity is determined from the slope of the initial section of the sorption curve [8]

$$D = \frac{\pi h^2}{16t}F^2, \tag{12}$$

where $F = \frac{w(t)-w_0}{w_\infty - w_0}$ is the relative change in the moisture content $w(t)$ in the specimen from w_0 to w_∞. The value of w_∞ is found experimentally. Both the parameters D and w_∞ depend on the surrounding temperature and humidity [8].

The Fick model is the simplest and, at the same time, the most widespread for describing the process of moisture sorption. However, it does not describe the decrease in weight with time observed in experiments (see Fig. 2).

In [9], an approach is presented where it is assumed that the diffusion is accompanied by volatilization of the low-molecular-weight components unreacted during curing of resin or formed as a result of a possible chemical interaction between the water and polymer. The total change in the specimen weight is

$$w(t) = w_d(t) - w_w(t). \tag{13}$$

Here, $w_d(t)$ is the change in weight due to diffusion described by Eq. (11); $w_w(t)$ is the change in weight due to the volatilization of low-molecular-weight components, determined by the differential equation of first order

$$\frac{dw_w}{dt} = \gamma(w_W - w_w), \tag{14}$$

where w_W is the maximum change in weight of the CM due to the escape of all low-molecular-weight substances, and γ is the factor of proportionality.

With the initial condition $w_w(0) = 0$, Eq. (14) has the solution

$$w_w(t) = w_W[1 - \exp(-\gamma t)]. \tag{15}$$

3.3. Moisture sorption by a composite. The kinetics of moisture sorption by a composite in which the filler does not absorb moisture depends on the sorption characteristics of the binder, its relative content in the CM, and the presence of pores in it. The diffusion processes are described by the same equations as the heat and electric conduction. Therefore, the diffusivity D of a composite with a given coefficient of filling v_f can be calculated from the known diffusivities of the binder D_m and filler D_f by the formulas derived in solving the problem of heat conduction for a heterogeneous material. For example, in [10], polymer blends were calculated by the relation

$$D = \frac{\sum\limits_{i=m,f} D_i V_i \, 3D_f / (D_i + 2D_f)}{\sum\limits_{i=m,f} V_i \, 3D_f / (D_i + 2D_f)}, \tag{16}$$

derived by Kerner.

For the CM examined, $D_f \approx 0$. At $D_f / D_m \to 0$, relation (16) takes the form

$$D = D_m\left(1 + \frac{v_f}{3v_m}\right), \tag{17}$$

where $v_m = 1 - v_f - v_p$.

4. Calculation Results and Discussion

For an indirect evaluation of the elastic E_m and shear G_m moduli of the binder in a composite, according to the experimentally determined elastic E and shear G moduli of the CM with the known coefficient of filling (see Fig. 1), we used relations (3) and (4). The values of E_m calculated for the CM in conditionally initial and water-saturated states, as well as for the CM after a moistening–drying cycle, are presented in Fig. 6a. As follows from the data in the figure, for the CM in the conditionally initial state, the elastic moduli of the binder in the CM and in a block are equal at $v_f \le 0.33$; with increasing v_f, E_m decreases. In its character, the dependence $E_m(v_f)$ is similar to the relation between the filler (LiF crystals) microstrain in the CM and the coefficient of filling [2]. This is obviously caused by the fact that the higher the rigidity of the binder, the more it "stretches" the filler particles because of its shrinkage during the manufacture of a CM. At $v_f > 0.33$, the state of binder in the CM differs from that in a block: it is characterized by a smaller elastic modulus. This can be explained by insufficient curing of the binder, the porosity, and the presence of an interphase layer with characteristics different from those of the binder in a block.

For the CM in the saturated state, we obtained a rather wide scatter of E_m values, which lie around the straight line E_m = 2.2 GPa. For the CM after a moistening–drying cycle, $E_m(v_f)$ = 3.8 GPa. Thus, the effect of moistening the CM up to saturation and the subsequent drying is expressed by an increase in the elastic modulus of the binder E_m in the CM at high coefficients of filling $v_f > 0.33$.

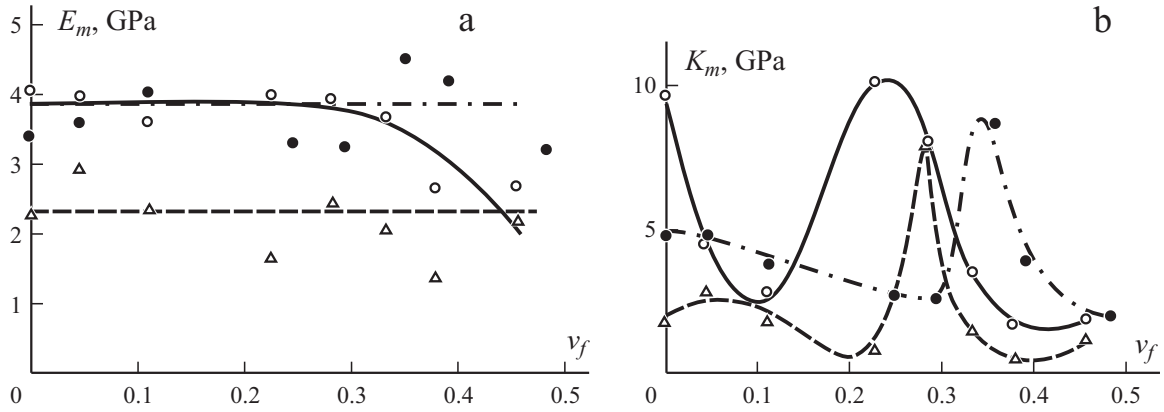

Fig. 6. Elastic E_m (a) and bulk K_m moduli of binder (b) in the CM in relation to v_f for CMs in the initial (○) and water-saturated (△) states and after a moistening–drying cycle (●), calculated from elastic characteristics of the CM by Eqs. (3) and (4).

Since two independent elastic characteristics of the binder, K_m and G_m, were optimized in approximating the elastic modulus of the composite, let us consider the bulk modulus in hydrostatic compression $K_m = \frac{E_m G_m}{3(3G_m - E_m)}$, in relation to the coefficient of filling. The dependences $K_m(v_f)$ for the CM in the conditionally initial and water-saturated states, as well as after a moistening–drying cycle (Fig. 6b), have an extreme character. Their maximum occurs at $v_f = 0.23$ for the CM in the conditionally initial state and at $v_f = 0.28$ in the water-saturated state. For the latter state, the maximum is more pronounced. The subsequent drying leads to a shift of the maximum toward great values of v_f ($v_f = 0.33$), with practically no changes in its magnitude. If the maximum is caused by the presence of a denser and more rigid binder layer at the boundary with the filler, the parameters of this layer in the water-saturated state of the CM and after a moistening–drying cycle differ from those of the boundary layer in the initial CM.

Figure 7 shows the results of indirectly evaluating — by Eq. (17) — the diffusivity D_m of the binder in the composite from the experimentally determined value of D (see Fig. 3) of a CM with a known coefficient of filling. As follows from these data, in sorption, the value of D_m of the binder in the CM grows with v_f; at $v_f \geq 0.33$, this value is several times higher than that in a block. In desorption, the values of D_m of the binder in the CM and in a block at $v_f \leq 0.33$ practically coincide. At $v_f > 0.33$, the diffusivity D_m of the binder in the CM is several times higher than in a block, but this difference is less than in the case of sorption. At high coefficients of filling ($v_f \geq 0.33$), after a moistening–drying cycle, the decrease in the diffusivity of the binder in the CM correlates with the increase in its elastic modulus E_m. The change in both the parameters indicates that the structure of the binder in the CM is improved after the moistening–drying cycle.

Thus, the results of comparing the elastic characteristics of the binder in the CM in a conditionally initial state and after a moistening–drying cycle (see Fig. 6), as well as the characteristics of moisture sorption and desorption from the binder in the CM (see Fig. 7), show that the effect of moisture on the binder in the CM has an irreversible character mainly at high filler concentrations.

Using the dependences $E_m(v_f)$ (see Fig. 6a), $\alpha_m(v_f)$ (see Fig. 4), and $w_m^\infty(v_f)$ (see Fig. 5), we calculated the maximum stresses of swelling in the binder $\sigma_{\max}^m$ in the CM for different values of v_f (Fig. 8). As seen from the graph, $\sigma_{\max}^m$ decreases with increasing v_f; the dependence $\sigma_{\max}^m(v_f)$ is practically linear. For comparison, the maximum changes in the tensile microstresses $\sigma_{\max}^f$ in LiF crystals in the CM due to its moistening up to the water-saturated state, calculated from the results of X-ray analysis [3], are also given here. A quantitative estimation of the microstresses in LiF crystals in the CM was

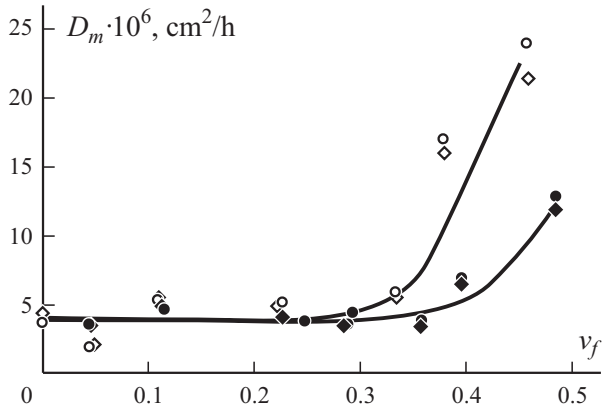

Fig. 7

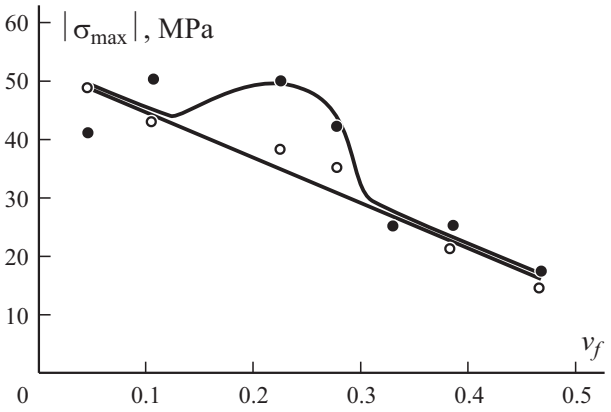

Fig. 8

Fig. 7. Diffusivity D_m of binder in the CM in relation to v_f, calculated from the sorption (○) and desorption (●) curves of CM by Eq. (17).

Fig. 8. Maximum stresses in the binder (●) and microstresses in LiF crystals (○) [3] upon moistening the CM in relation to v_f.

carried out on the assumption that $E_f = 86$ GPa. The absolute values of σ^m_{max} and σ^f_{max} coincide in the region of small v_f, and, within the limits of scatter, they also coincide for great values of v_f. In the region $v_f = 0.2\text{-}0.3$, $\left|\sigma^m_{max}\right| > \left|\sigma^f_{max}\right|$. Compared with the volume-average changes in stresses in the binder, the greater — in absolute value — changes in the filler stresses are obviously caused by the presence of a more rigid binder layer at the filler boundary. The effect of the boundary layer is also expressed by the extremum of the dependence $K_m(v_f)$ at $v_f = 0.2\text{-}0.3$ (see Fig. 6b).

With increasing coefficient of filling, practically all the binder is concentrated in a thin layer around the filler particles. However, the elastic characteristics of the binder in the CM (E_m and K_m), calculated from the properties of a CM with a known coefficient of filling, decrease. This can be explained by the influence of porosity on the elastic characteristics of the binder in the CM. With increasing v_f, the relative volume content of pores v_p in the CM increases (see Table 1), and thus the relative volume content of pores v_p in the binder of the CM also increases. The elastic characteristics of a binder with pores in the CM were evaluated with the use of Eqs. (7) and (8). It was found that, in the absence of pores, the value of E_m increased with v_f, and, at great v_f, it could reach 5 GPa in the initial CM and 8-10 GPa in the CM after a moistening–drying cycle.

5. Basic Results and Conclusions

It is established experimentally that the processes of moisture sorption by the binder in a CM with a small filler content ($\mu = 0.10$, 0.20, 0.42, and 0.48) and in a block differ; at high filler contents ($\mu = 0.54$, 0.59, and 0.68), the sorption process proceeds faster.

The results of comparing the theoretical and experimental data obtained show that, for the CM in a conditionally initial state, the relation between the elastic modulus of the binder in the CM and the coefficient of filling μ has the same character as that between the filler microstrain (changes in the interplanar distance in the crystals, measured by the X-ray method) and μ in the CM. The elastic moduli of the binder in a CM with a small filler content ($\mu = 0.10$, 0.20, 0.42, and 0.48) and in a block are equal; with increasing coefficient of filling, the elastic modulus of the binder in the CM decreases.

The relation between the maximum stresses (corresponding to the ultimate water saturation) in the binder in the CM and the coefficient of filling μ has the same character as the relation between the filler microstrain in the CM and μ. Moreover, the absolute values of maximum stresses in the binder and filler coincide at high and low coefficients of filling. At v_f = 0.2-0.3, the maximum stresses in the filler are higher than those in the binder.

The effect of moisture on the epoxy binder in the CM with a high coefficient of filling, μ = 0.54, 0.59, and 0.68, is not entirely reversible: after a moistening–drying cycle, the elastic characteristics of the binder in the CM increase, the diffusivity decreases, and the ultimate moisture content increases.

The correlations obtained between the calculated elastic characteristics of the binder in the CM, as well as the stress levels in the binder in the CM, and the microstrains in filler crystals, measured by the X-ray method, confirm that the structural (Kerner) model can be used to calculate the elastic characteristics of the composite from the properties of its components for all the coefficients of filling considered.

The low elastic moduli and the high diffusivity of the binder in the CM, compared with the characteristics of the binder in a block, as well as the improvement of these parameters after a moistening–drying cycle, indicate that, in the binder of the CM with a high filler content, structural changes (possibly, aftercure) occur during moistening the CM.

REFERENCES

1. Yu. S. Lipatov, F. G. Fabulyak, and N. G. Popova, "Investigation of molecular mobility in epoxy polymers at various stages of curing in the bulk and at the interface," Vysokomol. Soed., **A13,** No. 11, 2601-2606 (1971).
2. V. P. Korkhov, M. G. Kamenskii, and E. A. Faitel'son, "Effect of the adhesion interaction and the degree of filling on the internal stresses in finely divided crystalline fillers of epoxy composites," Mech. Compos. Mater., **35**, No. 6, 527-534 (1999).
3. V. P. Korkhov, E. A. Faitel'son, T. I. Glaskova, and Yu. O. Janson, "Influence of moisture on the structure and properties of the interphase layer of a composite based on an epoxy binder with a disperse filler," Mech. Compos. Mater. (2005) (in press).
4. V. A. Latyshenko, Diagnostics of the Rigidity and Strength of Materials [in Russian], Zinatne, Riga (1968).
5. E. H. Kerner, "The elastic and thermoelastic properties of composite media," Proc. Phys. Soc., **29**, No. 440B, 808-813 (1956).
6. G. Z. Xiao and M. E. R. Shanahan, "Swelling of DGEBA/DDA epoxy resin during hygrothermal ageing," Polymer, **39**, No. 14, 3253-3260 (1998).
7. J. Crank, The Mathematics of Diffusion, Oxford (1956).
8. R. D. Stepanov and O. F. Shlenskii, Strength Calculations for Plastic Structures Operating in Liquid Media [in Russian], Moscow (1981).
9. M. E. R. Shanahan and Y. Auriac, "Water absorption and leaching effects in cellulose diacetate," Polymer, **39**, No. 5, 1155-1164 (1998).
10. J. A. Manson and L. H. Spearling, Polymer Blends and Composites, Premium Press, New York (1981).

Publikācija 2

A comparative analysis of moisture transport models applied to epoxy binder

Glaskova T. I.[1], Guedes R. M.[2], Morais J. J.[3], Aniskevich A. N.[1]

[1]Institute of Polymer Mechanics, University of Latvia, Riga, Latvia

[2]University of Porto, Porto, Portugal

[3]University Tras-os-Montes and Alto Douro, Vila Real, Portugal

Mechanics of Composite Materials, 2007, Vol. 43, No. 4, p. 377-388.

Mechanics of Composite Materials, Vol. 43, No. 4, 2007

A COMPARATIVE ANALYSIS OF MOISTURE TRANSPORT MODELS AS APPLIED TO AN EPOXY BINDER

T. I. Glaskova,* R. M. Guedes,**
J. J. Morais,* and A. N. Aniskevich***

Keywords*: epoxy binder, moisture sorption, multiphase sorption, sorption models*

The results of experimental and theoretical investigations into the kinetics of moisture sorption by a neat epoxy resin obtained from RAE Industries (Reapox 520, D523) are reported. The sorption process was realized in atmospheres with a constant relative humidity of 33, 53, 75, 84, and 97% and a temperature of 50°C. The results obtained showed that the diffusion behavior of epoxy resin did not obey Fick's law under the experimental conditions considered. Consequently, the application of a non-Fickian diffusion model was necessary. For this purpose, two-phase moisture sorption models, a model with a time-dependent diffusivity, a two-phase material model, as well as relaxation and convection models of anomalous diffusion, were considered. The model parameters were obtained from the approximation of experimental sorption data. A comparative analysis of the sorption models was performed, and the specific features of their applications were estimated. The two-phase material model and the model with varying diffusivity were found to be the most suitable ones due to a good agreement between calculation results and experimental data and the rather small (three or four) number of parameters, which make them more flexible and physically more justified than the classical Fick's model with its two parameters.

Introduction

The extensive application of epoxy resins is explained by their structural features and high operational properties, the ability to be cured in a wide temperature interval, the insignificant shrinkage, the non-toxicity in the cured state, the high values of adhesion and cohesion strength, and the chemical stability. In this connection, epoxy resins are used as binders to create materials with good physicomechanical properties. However, epoxy binders, as well as the majority of other ones, have a considerable drawback, namely a rather high moisture sorption, which noticeably degrades their functional, structural, and mechanical properties [1, 2].

Materials based on polymers are frequently exposed to a humid environment. Water molecules, as well as low-molecular substances, are able to move in a polymeric binder and change its physical properties. The key parameters determining the mechanism of moisture sorption are the chemical composition and microstructure of the polymers.

The moisture sorption in epoxy binders and composites based on them is investigated rather well. Different models have been suggested for describing the water sorption kinetics [3-10]. It is usually assumed that the moisture sorption in epoxy

*Institute of Polymer Mechanics, University of Latvia, Riga, Latvia. **University of Porto, Porto, Portugal. ***University Tras-os-Montes and Alto Douro, Vila Real, Portugal. Translated from Mekhanika Kompozitnykh Materialov, Vol. 43, No. 4, pp. 555-570, July-August, 2007. Original article submitted March 12, 2007.

0191-5665/07/4304-0377

binders proceeds by diffusion according to Fick's law [3, 11]. Such a model, which suits well the initial stage of moisture sorption, is often inadequate for describing the moisture sorption process as a whole. The moisture sorption can activate different processes in a material, which, in turn, affect the water sorption kinetics (chemical reactions, leaching of low-molecular components, etc.). Therefore, the purpose of this study is to estimate the applicability of different moisture transport models to describing experimental data on water sorption in epoxy binders and to determine the most adequate ones.

Materials and the Experimental Procedure

We investigated a Reapox 520 epoxy binder presented by the RAE Industries company. The cure process was performed in four steps. First, the binder was cured at 20°C for 7 days. Then, the material was held for 24 h at a temperature of 40°C, annealed at 130°C, and rapidly cooled down to 50°C.

The specimens were made in the form of thin plates 50 20 2 mm in size, so that to favor the one-dimensional diffusion. They were moistened in atmospheres with various humidity = 34, 53, 75, 84, and 97%, at a temperature of 50°C, which were created by using saturated solutions of $MgCl_2$, $Mg(NO_3)_2$, NaCl, KCl, and K_2SO_4.

The specimens were weighed periodically, and their mass increment $m(t)$ m_0 against the initial mass m_0 was used to find the moisture content during sorption

$$w(t) \quad \frac{m(t) \quad m_0}{m_0}.$$

Sorption Models

Let us clear up the applicability of basic sorption models to describing the moisture sorption process in the epoxy binder.

Classical model with a constant diffusivity

In this model [3], it is assumed that moisture sorption occurs only by diffusion. According to the first Fick's law, the diffusant flow density j is directly proportional to the gradient of its concentration c:

$$j \quad D \operatorname{grad} c, \tag{1}$$

where D is the diffusivity, describing the rate of moisture sorption, which is independent of moisture concentration. For a nonstationary state, with account of the mass conservation law, the second Fick's equation is valid. For the case of a one-dimensional diffusion along the x axis, when the specimen thickness is smaller than its length and width, it has the form

$$\frac{c}{t} \quad D \frac{^2 c}{x^2}, \tag{2}$$

where c is the moisture concentration in the specimen at the instant of time t.

The solution to Eq. (2) for a plane-parallel plate of thickness h, with initial $c(0 \quad x \quad h, t \quad 0) = c_0$ and boundary $c(x \quad 0, x \quad h, t \quad 0) = c$ conditions, is the series [3]

$$c(x,t) \quad c \quad 2\frac{(c \quad c_0)}{k \quad 1} \frac{[1 \quad (\ 1)^k]}{k} \sin \frac{k}{h} x \ \exp \quad \frac{k}{h}^2 Dt \ . \tag{3}$$

Integrating Eq. (3) across the plate thickness, we come to an expression for determining the moisture content in the specimen:

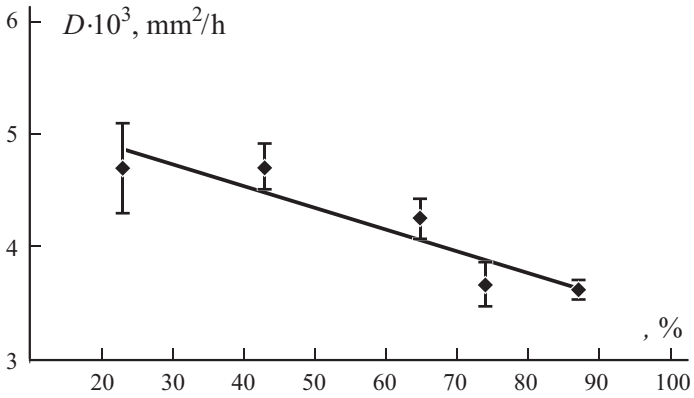

Fig. 1. Diffusivity D vs. the relative humidity of environment.

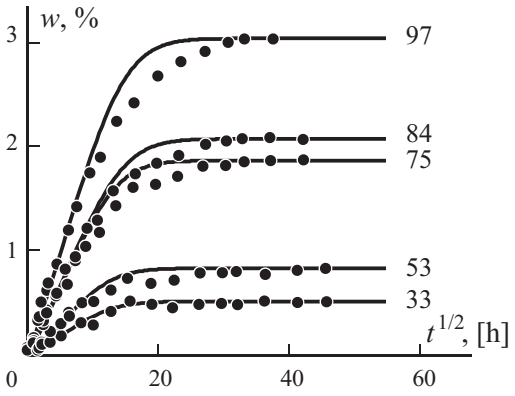

Fig. 2. Changes in the specimen mass with time at different values of (numbers next to the curves): experimental data (dots) and calculations by Fick's model (4) (curves).

$$w(t) \quad w \quad 2\frac{(w \quad w_0)}{^2} \quad _{k\ 1} \frac{[1 \quad (\ 1)^k\ ]^2}{k^2} \exp \quad \frac{k}{h}^{\ 2} Dt \quad . \tag{4}$$

Here, w is the equilibrium moisture content in the specimen. Thus, the model considered contains two material characteristics as parameters: the diffusivity D and the equilibrium moisture content w . In numerous studies (e.g., [3]), it is shown that, if the sorption curve is drawn on a diagram whose abscissa axis is $\sqrt{t}$, the initial section of this diagram will be a straight line passing through the origin of coordinates. Then, using experimental data, the diffusivity can be determined from its inclination:

$$D \quad \frac{h^2}{16t} L^2, \tag{5}$$

where $L \quad \frac{w(t) \quad w_0}{w \quad w_0}$ is the change in the moisture content $w(t) \quad w_0$ in the specimen by the instant of time t, normalized to its maximum value. The second parameter of the model — the equilibrium moisture content — as a rule, is found experimentally as the maximum moisture content achieved in the specimen. We should note here that, according to Eq. (4), this maximum is achieved only asymptotically at t , which in practice leads to an error in determining w . The relation between the diffusivity found by Eq. (5) and of the environment is shown in Fig. 1.

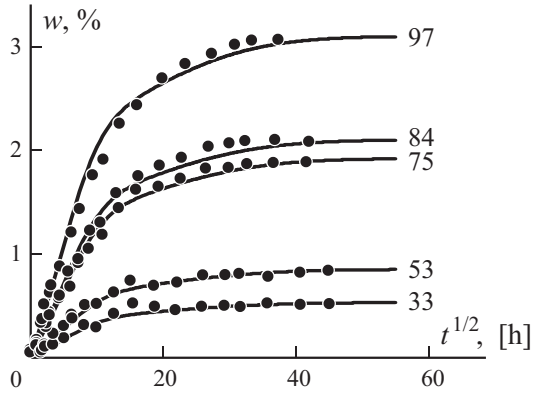

Fig. 3. Changes in the specimen mass with time at different values of (numbers next to the curves): experimental data (dots) and calculations by Eq. (6) (curves).

The results from calculating the moisture content by Eq. (4) and experimental data for atmospheres with various humidity are shown in Fig. 2. It is clear that the Fick's model describes well the process of moisture sorption in a low-humidity atmosphere, but when the relative humidity exceeds 75%, the moisture sorption process slows down in the middle part of sorption curve.

In other words, the value of moisture sorption rate used in the calculation is overestimated, since the model disregards the processes of interaction between the moisture and polymer, swelling, etc., which accompany the process of moisture sorption. It is seen that the adequacy of Fick's model declines with increasing relative humidity of environment, since the diffusion mechanism becomes less dominating, and other mechanisms, such as the interaction between the polymer and the diffusant and/or relaxation processes, start to affect the moisture transport in the polymer [12]. The alternative models of moisture sorption which can be used to explain the deviation of moisture transport in polymers from the classical diffusion mechanism with a diffusivity independent of moisture concentration, take into account different subtle differences in the moisture sorption process in each particular case.

A model taking into account the two-phase state of absorbed moisture in the material

This model, known as the Langmuir model, is described, for example, in [4, 5]. According to this model, the anomalous moisture sorption in epoxy binders can be explained on the assumption that the absorbed moisture exists in two — free and bound — phases. The free-phase molecules diffuse with a diffusivity independent of diffusant concentration and are absorbed (become bound) with a probability in a unit time. The molecules leave the bound state with a probability in a unit time. Therefore, the process of diffusion is described by the same equation of diffusion (2), which is only modified and now takes into account the two-phase state of moisture in the material.

According to this model, the moisture content in a material, as a function of time $w(t)$, depends on four parameters: D, w , and the probabilities and and is expressed by the formula

$$w(t) \quad w \quad 1 \quad \frac{}{} \exp(\quad t) \quad \frac{}{} \quad \frac{2}{2} \quad {}_{k \ 0} \quad \frac{[1 \quad (\ 1)^k]^2 \exp \quad \left(\frac{k}{h}\right)^2 Dt}{k^2} \ . \tag{6}$$

The results of calculations by the Langmuir model, depicted in Fig. 3, show a better description of the sorption curve with account of the two-phase nature of moisture in the epoxy binder. This in turn means that, although the moisture sorption process could proceed by diffusion, some part of the water molecules absorbed was connected with polymer molecules, but some part was free.

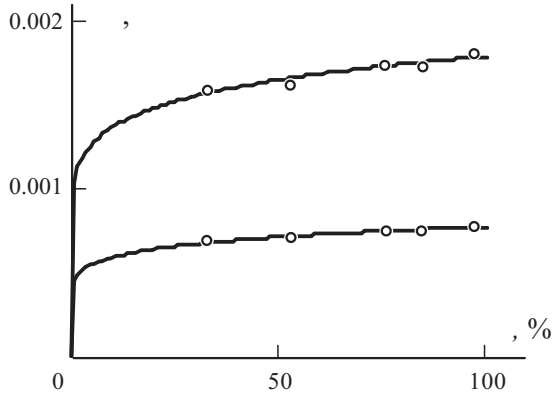

Fig. 4. Probabilities and vs. .

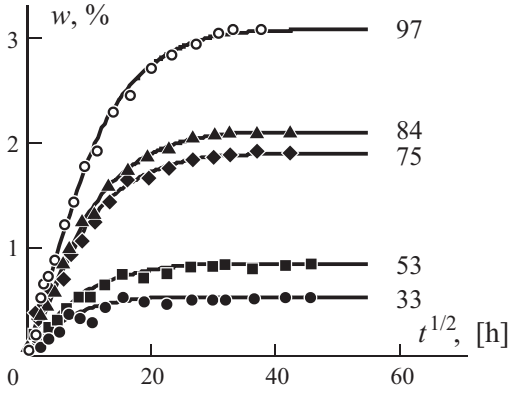

Fig. 5. Changes in the mass of specimens with time at different values of (numbers next to the curves): experimental data (dots) and calculations by Eq. (7) (curves).

The growing values of the parameters and with increasing humidity of environment, shown in Fig. 4, points to the increased possibility of transition of water molecules from the bound state into the free one and back. It is seen that, since the possibility for water molecules to become bound is much lower than to become free, the process of interaction between water and polymer can be presented as a constant migration of diffusant molecules from the bound state into the free one.

A model taking into account the two-phase nature of the material

In the model known as the Jacob's–Jones model [6], it is assumed that the material consists of two phases of different density and, accordingly, different sorption properties. It is assumed that the moisture sorption process in both the phases proceeds simultaneously and obeys Fick's law. The possibility of formation of chemical bonds between water and polymer molecules is neglected.

The moisture content in each phase of the material is expressed by the formulas

$$w_1(t) \quad w_{\ 1} \quad 2\frac{(w_{\ 1} \quad w_0)}{2} \quad \underset{k\ 1}{} \quad \frac{[1 \quad (\ 1)^k\ ]^2}{k^2}\exp \quad \left(\frac{k}{h}\right)^{\ 2} D_1 t \ ,$$

$$w_2(t) \quad w_{\ 2} \quad 2\frac{(w_{\ 2} \quad w_0)}{2} \quad \underset{k\ 1}{} \quad \frac{[1 \quad (\ 1)^k\ ]^2}{k^2}\exp \quad \left(\frac{k}{h}\right)^{\ 2} D_2 t \ ,$$

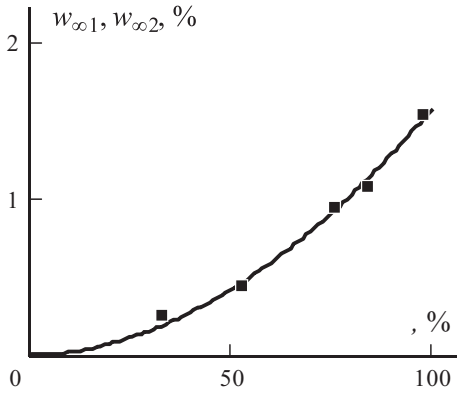

Fig. 6. Sorption isotherms of two phases. The values of w_1 and w_2 (dots) are obtained by approximating the sorption curve by Eq. (8) at $w_1 = 2.55$, $k = 0.73$, and $f = 0.59$ (see Fig. 5).

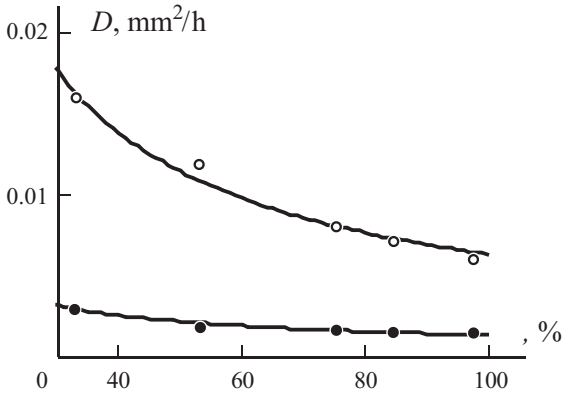

Fig. 7. Diffusivity of the phases D_1 (○) and D_2 (●) vs. .

which contain four unknown parameters, namely the equilibrium moisture content and the diffusivity of each of the phases. The total moisture content in the specimen is

$$w(t) \quad w_1(t) \quad w_2(t), \tag{7}$$

where $w_1(t) \quad \frac{m_1}{m_0}$ and $w_2(t) \quad \frac{m_2}{m_0}$; m_1 and m_2 are the mass increments of the phases with respect to the specimen mass.

The calculation by Eq. (7), presented in Fig. 5, agrees with experimental data rather well for all the values of , which means that the epoxy binder can be two-phase. It is known that epoxy resins contain both areas with a sufficiently perfect and dense spatial network and poorly cross-linked regions, which can be regarded as a two-phase structure of the material. This model does not take into account possible changes in the material microstructure during the sorption process, which can be expressed in a worse description of sorption curves with increasing relative humidity of the environment, as seen from Fig. 5. Nevertheless, it can be used for an objective estimation of sorption characteristics of materials with a nonuniform structure.

An advantage of the given model is the possibility of describing the equilibrium moisture content by the Guggenheim–Anderson–De Boer equation [6]

$$w \quad w_1 \frac{kf}{(1 \quad f)[1 \quad (k \quad 1)f]}, \tag{8}$$

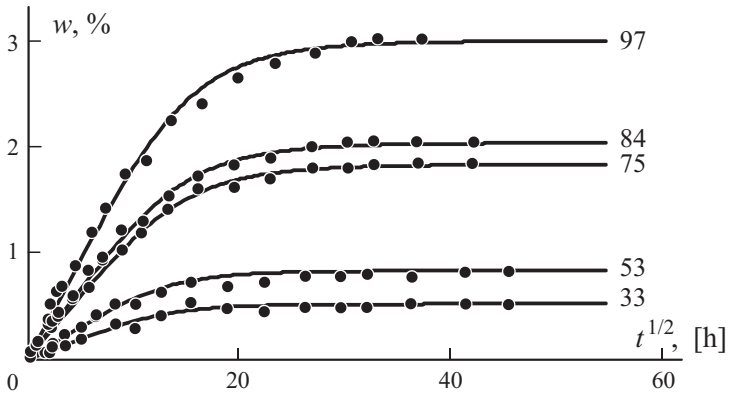

Fig. 8. Approximation of experimental sorption data according to the model with a time-variable diffusivity for different (numbers next to the curves).

where w_1 is the moisture content connected with the more hydrophilic phase, k is the factor of bond strength between water and polymer molecules, and f is the ratio between the chemical potentials of an indirectly bound diffusant molecule and a diffusant molecule in the free liquid state. The low values of f (f l) indicate that the polymer is hydrophobic. It is assumed in this case that sorption ability of both material phases is equal, $w_1 \quad w_2$.

As seen from Fig. 6, formula (8) is good for describing the sorption isotherm. In turn, it follows from Fig. 7 that the diffusivity in the different phases differs several times. Probably, this reflects the real material structure, with areas of relatively small and high permeabilities. The account of two-phase nature of the system allows one to improve the description of the sorption curve.

A model with a time-dependent diffusivity [7]

According to this model, owing to the physical processes going on in the material (primarily, the plasticization and associate changes in the relaxation character, as well as aging, aftercure, etc.), the diffusivity decreases with time in proportion to its current value:

$$\frac{dD}{dt} \quad D(t).$$

The solution of this equation is $D \quad D_0 e^{\ t}$. This model contains three parameters — the diffusivity at the initial instant of time D_0, the equilibrium moisture content w , and the coefficient describing the rate of change in diffusivity.

To reduce the diffusion equation to Eq. (2) with a constant diffusivity D, we use the principle of modified time, by analogy with the change in D under a nonstationary temperature [13]:

$$dt \quad e^{\ t} dt, \quad t \quad \int_0^t e^{\ t} dt \quad \frac{1 \quad e^{\ t}}{}. \tag{9}$$

Then, the diffusion equation takes the form

$$\frac{C}{t} \quad D_0 \quad C. \tag{10}$$

Using the earlier-found solution (4) to Eq. (2) and replacing t with t , according to Eq. (9), the solution to Eq. (10) for the one-dimensional case has the form

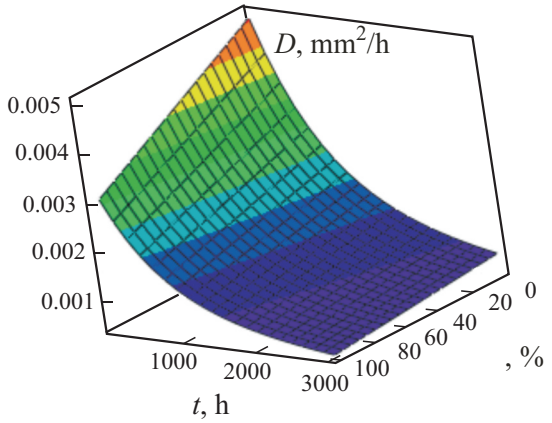

Fig. 9. Diffusivity D as a function of time t and the relative humidity of environment.

$$w \quad w \quad \frac{2(w \quad w_0)}{2} \quad _{k\ 1} \quad \frac{[1 \quad (\ 1)^k]^2}{k^2} e \quad ^{2}_{k}F, \tag{11}$$

where $F \quad \frac{D_0}{}[1 \quad \exp(\quad t)]$; $_k \quad \frac{k}{a}$; F is the Fourier criterion, $\quad 1/$, and is the characteristic time of relaxation. A description of the sorption curve by Eq. (11) is shown in Fig. 8.

The diffusivity D as a function of time and the relative humidity of environment is shown in Fig. 9. It is seen that, at great times, the diffusivity tends to an infinitesimal value, which describes the saturated state of the system. During moisture sorption (for about 450 h) at $= 98\%, D_0 = 3.61\ 10^{\ 3}$ cm^2/h, and $= 0.002$, the diffusivity decreased 4-6 times. In general, due to the presence of three parameters, the model is relatively flexible and can describe the sorption curves rather well (Fig. 8).

Relaxation model of anomalous diffusion

This model [9] considers the time-dependent boundary conditions

$$(t) \quad m_1 \quad (\ _0 \quad _1)\exp(\ rt), \quad r \quad 0, \tag{12}$$

where and are the initial and limiting moisture concentrations and r is the constant of relaxation. The quantity is a characteristic of the supermolecular structure, reflecting the diffusant-caused structural transformations in the polymer. These transformations can be described by changing the equilibrium boundary conditions, i.e., by regarding them variable. Thus, for the boundary conditions $c(x,0) \quad c_0$ and $c(0,t) \quad c(h,t) \quad (t)$, the moisture content in a plane-parallel plate of thickness h is calculated by the formula

$$w(t) \quad M_1 \quad (M_0 \quad M_1)\exp(\ rt) \quad 8 \quad _{k\ 0} S_k, \tag{13}$$

where

$$S_k \quad \frac{V_0 n_k^2 \frac{D}{h^2} \quad V_1 r \ \exp \quad n_k \frac{Dt}{h^2} \quad r(M_1 \quad M_0)\exp(\ rt)}{n_k^2 \quad n_k^2 \frac{D}{h^2} \quad r},$$

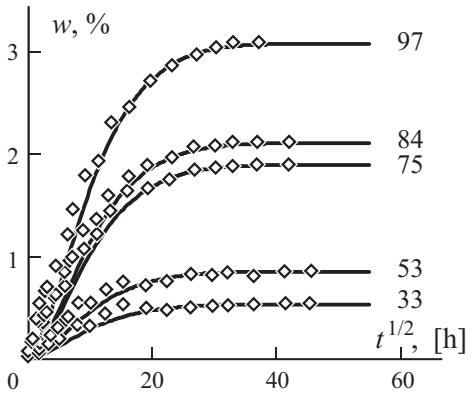

Fig. 10. Changes in the mass of specimens with time at different values of (numbers next to the curves): experimental data (dots) and calculations by relaxation model (13) (curves).

$$V_0 \quad M_0 \quad C_0,\ V_1 \quad M_1 \quad C_0,\ n_k \quad (2k \quad 1),\ M_0 \quad h \quad _0,\ M_1 \quad h \quad _1,\ C_0 \quad hc_0.$$

The calculation according to model (13), shown in Fig. 10, describes the sorption curves at great times rather well, but underestimates the rate of moisture sorption at the initial stage. Another drawback of this model is the presence of a great (five) number of coefficients, which complicate calculations and, in this case, have no exact physical meaning. Therefore, although this model accounts for the relaxation in materials which occurs under any boundary conditions, it is more suitable for describing the process of moisture sorption under a nonstationary humidity. An example of nonstationary humidity is a seasonally varying humidity of the environment.

Convection model of anomalous diffusion

Upon nonuniform moisture sorption, layers with different moisture contents can arise in the material, which leads to the appearance of a diffusant flow through the material. The process of moisture convection can be taken into account by supplementing the equation of diffusion (2) with an additional term:

$$\frac{c}{t} \quad D\frac{^2c}{x^2} \quad v\left|\frac{c}{x}\right|, \tag{14}$$

which describes the diffusant flow at a rate v. The solution of Eq. (14) is found for the initial and boundary conditions

$$c(x,0) \quad 0 \quad \text{and} \quad c(0) \quad c(l,t) \quad _0. \tag{15}$$

For the equilibrium state, we have

$$D\frac{^2c}{x^2} \quad v\left|\frac{c}{x}\right| \quad 0, \tag{16}$$

where $c \quad (0) \quad c \quad (l,t) \quad _0$. The solution to Eq. (16) is

$$c \quad (x) \quad \frac{_0\ 1 \quad \exp \quad \frac{v}{D}\left|x \quad \frac{h}{2}\right|}{1 \quad \exp \quad \frac{vh}{2D}}. \tag{17}$$

As a result of integrating Eq. (17) across the specimen thickness, we find the limiting moisture content in the specimen

$$w \quad \frac{M_0}{1 \quad \exp} \quad \frac{\exp}{} \quad 1\ , \tag{18}$$

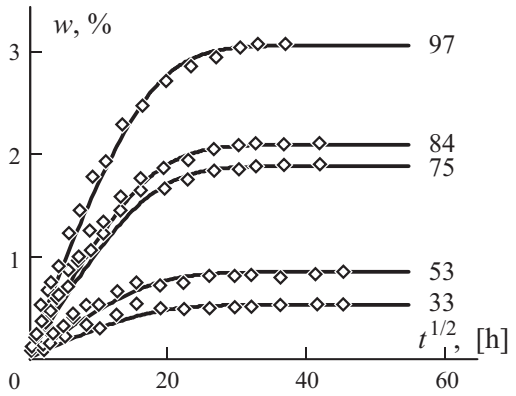

Fig. 11. Changes in the mass of specimens with time at different values of (numbers next to the curves): experimental data (dots) and calculations by convection model Eq. (19) (curves).

where M_0 h $_0$ and $\frac{vl}{2D}$ is the parameter determining the convection rate. It is logical that the solution of Eq. (14), with account of Eq. (15), at great times tends to solution (18).

Integrating the solution of Eq. (14) across the specimen thickness h, we come to the expression for moisture content in the specimen

$$w(t) \quad w \quad \frac{16M_0 \coth 0.5}{1 \quad \exp}$$

$$\underset{k \quad 0}{} \frac{n_k[n_k \exp 0.5 \quad {}^{k \quad 1}]}{(\quad n_k^2)^2} \exp \quad (n_k^2 \quad {}^2)\frac{D}{h^2} t \quad , \tag{19}$$

where n_k $(2k \quad 1)$.

The results of calculations by Eq. (19), shown in Fig. 11, point to a rather good description of sorption curves at all stages of moisture sorption for all the atmospheres considered, but the great (five) number of coefficients complicates the calculation. Therefore, the application of the given model is justified only in the case of heavily swelling polymers, whose sorption capacity is high [9].

Comparison of Models

The sorption models considered in the present study reflect the process of moisture sorption in different ways, taking into account certain additional processes occurring in a material. These models describe experimental data rather well, but not always can we agree with the physical meaning laid in them for describing some particular situation, as in the case of convection and relaxation models of anomalous diffusion. Therefore, in each specific case, one must be guided not only by the results of good approximation, but also by the physical interpretation of the complex process of moisture sorption included in the models.

Figure 12 presents a comparison between all the models examined in this study for an atmosphere with the maximum relative humidity = 97%. To evaluate the correspondence between the calculations and experimental results, the sum of all absolute deviations $s \quad \underset{i}{} \left| w_i^e \quad w_i \right|$ of the calculation results w_i from the experimental data w_i^e was determined. It is seen that the presence of a greater number of parameters leads to a better description of experimental data. However, in choosing a suitable model, the number of parameters used in the model should also be considered.

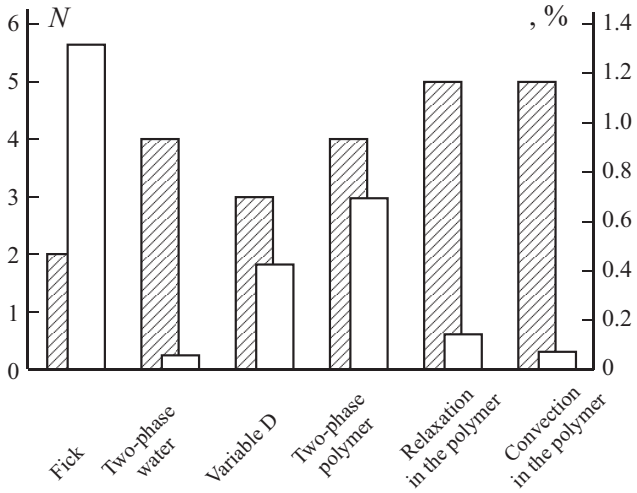

Fig. 12. Comparison of moisture sorption models at = 97%. N is the number of parameters (▨), and is the absolute deviation, % (□).

Consequently, the models most suitable for describing the kinetics of moisture sorption for the particular epoxy binder are the two-phase model taking into account the two-phase nature of materials and the model with a variable diffusivity. The latter one has only three parameters and agrees well with experimental results. The model with a two-phase material, in turn, is characterized by four independent parameters, but it has a good physical basis — the two-phase nature of the system, with corresponding values of diffusivity and equilibrium moisture content for each phase.

Conclusions

In this study, a comparative analysis of various moisture sorption models, based on different assumptions and boundary conditions and distinct physical interpretations of the process of moisture sorption, as applied to an epoxy binder moistened in atmospheres with different relative humidity has been carried out. It is shown that, with increased environmental humidity, the classical Fick's model is unable to adequately describe the process of moisture sorption, since it takes into account only the diffusion mechanism. In such cases, it is also necessary to consider the additional processes arising during moisture sorption in the material.

It is shown that a good approximation of experimental data not always evidence the validity of a model, even in the case where they are physically substantiated. For example, the Langmuir model and the model with a two-phase material are based on different physical interpretations of the process, each of them is physically admissible, and both give good approximations of experimental data. Consequently, the true applicability of a model can be confirmed by check tests including sorption–desorption cycles or sorption under nonstationary environmental conditions.

Most suitable for describing the sorption kinetics are found to be the model taking into account the two-phase nature of materials and the model with a variable diffusivity. These models give results agreeing rather well with experimental data and, in addition, contain a relatively small number of parameters, which make them more acceptable in practical applications.

References

1. P. S. Theocaris, G. C. Papanicolaou, and E. A. Kontou, "Interrelation between moisture absorption, mechanical behavior, and extent of the boundary interphase in particulate composites," J. Appl. Polym. Sci., **28**, 3145-3153 (1983).
2. J.-K. Kim, Ch. Hu, R. S. C. Woo, and M.-L. Sham, "Moisture barrier characteristics of organoclay-epoxy nanocomposites," Compos. Sci. Technol., **65**, 805-813 (2005).

3. J. Crank, The Mathematics of Diffusion, Oxford (1956).
4. P. Bonniau and A. R. Bunsell, "A comparative study of water absorption theories applied to glass epoxy composites," J. Compos. Mater., **15**, 272-293 (1981).
5. H. G. Carter and K. G. Kibler, "Langmuir-type model for anomalous moisture diffusion in composite resins," J. Compos. Mater., **12**, 118-131 (1978).
6. C. Maggana and P. Pissis, "Water sorption and diffusion studies in an epoxy resin system," J. Polym. Sci., Pt B, Polym. Phys., **37**, No. 11, 1165-1182 (1999).
7. G. A. Andrikson, V. P. Mochalov, and A. N. Aniskevich, "Principle of modified time scale for tasks of nonstationary moisture diffusion in polymer materials," Mekh. Kompoz. Mater., **16**, No. 1, 153-170 (1980).
8. S. Roy, W. X. Xu, and S. J. Park, "Anomalous moisture diffusion in viscoelastic polymers: modelling and testing," J. Appl. Mech., Trans. ASME, **67**, No. 2, 391-396 (2000).
9. A. L. Pomerantsev, "Phenomenological modelling of anomalous diffusion in polymers," J. Appl. Polym. Sci., **96**, No. 4, 1102-1114 (2005).
10. L.-W. Cai and Y. Weitsman, "Non-Fickian moisture diffusion in polymeric composites," J. Compos. Mater., **28**, No. 2, 130-154 (1994).
11. G. Z. Xiao and M. E. R. Shanahan, "Swelling of DGEBA/DDA epoxy resin during hygrothermal ageing," Polymer, **39**, No. 14, 3253-3260 (1998).
12. D. A. Bond, "Moisture diffusion in a fiber-reinforced composite. Pt. I. Non-Fickian transport and the effect of fiber spatial distribution," J. Compos. Mater., **39**, No. 23, 2113-2129 (2005).
13. Y. Weitsman, "Diffusion with time-varying diffusivity with application to moisture sorption in composites," J. Compos. Mater., **10**, 193-204 (1976).

Publikācija 3

Moisture absorption by epoxy/montmorillonite nanocomposite

Glaskova T., Aniskevich A.

Institute of Polymer Mechanics, University of Latvia, Riga, Latvia

Composites Science and Technology, 2009, Vol. 69, p. 2711-2715.

Composites Science and Technology 69 (2009) 2711–2715

Contents lists available at ScienceDirect

Composites Science and Technology

journal homepage: www.elsevier.com/locate/compscitech

Moisture absorption by epoxy/montmorillonite nanocomposite

T. Glaskova *, A. Aniskevich

Institute of Polymer Mechanics, University of Latvia, Aizkraukles Str. 23, LV-1006 Riga, Latvia

ARTICLE INFO

Article history:
Received 9 January 2009
Received in revised form 18 August 2009
Accepted 20 August 2009
Available online 23 August 2009

Keywords:
A. Nanoclays
A. Polymer-matrix composites (PMCs)
B. Transport properties
C. Fickian diffusion
B. Interphase

ABSTRACT

The peculiarities of moisture absorption of epoxy–nanoclay composite are estimated in the paper. Second Fick's law of diffusion was used to predict moisture diffusivity and equilibrium moisture content using accelerated analytical procedure. It was experimentally confirmed that sorption process in NC passes more slowly than in pure epoxy resin, for the highest filler content diffusivity reduces about half of diffusivity as for epoxy resin. The deviation from mixture rule was obtained for the equilibrium moisture content and the estimation of interphase content in composite was undertaken. It was determined that the higher content of interphase consistently leads to greater moisture absorption.

1. Introduction

The scientific and industrial interest devoted to polymer/layered silicate nanocomposites (NC) due to their outstanding properties and possible novel applications have resulted in numerous studies [1–5,8–11,18,19]. Polymer NC are polymers (thermoplastic, thermosets, or elastomers) filled with small quantity (less than 6% by weight) of nanosized particles.

These materials promise improvements over conventional composites in mechanical, thermal, electrical and barrier properties. Furthermore, they can significantly reduce flammability and maintain the transparency of the polymer matrix. In the case of layered nanoclay filler contents of 2–5% by weight result in mechanical properties (tensile elastic modulus and strength, fracture toughness) similar to those achieved in conventional composites with 30–40% filler content [5].

The attractive characteristics suggest a variety of possible industrial applications for NC: automotive (gas tanks, bumpers, interior and exterior panels), constructions (building sections and structural panels), aerospace (flame retardant panels and high performance components), electrical applications and electronics (electrical components and printed circuit boards), food packaging (containers and wrapping films) [6,7].

The key to such performance rests in the ability to exfoliate and disperse individual, high shape-anisotropic silicate particles within the polymer matrix [8,9]. The complete dispersion of clay nanolayers in a polymer optimizes the number of available reinforcing elements for carrying an applied load and deflecting cracks. The coupling between the tremendous specific surface area of the clay ($S \approx 800\ m^2/g$) and a polymer matrix facilitates stress transfer to the reinforcement phase, allowing for such tensile and toughening improvements [10].

Apart from the mechanical properties, the excellent barrier capability with significantly reduced permeability of moisture and gases is one of the most attractive and useful properties that have not been fully explored in the past [11,12]. The enhanced gas barrier properties of NC are now finding some limited application in packaging material and containers for a wide variety of food and beverage products. Meanwhile, the moisture barrier properties of NC are yet to be exploited.

While epoxy resins are very attractive due to their high strength and stiffness, high temperature resistance, low volatility, creep and shrinkage, good adhesion to metal and ceramic substrates. Nevertheless epoxy resins have a major drawback of high moisture absorption, which in turn degrades the functional, structural and mechanical properties of the composites [13–18].

Because of the high shape-anisotropy and surface of the exfoliated silicate layers they act as efficient barriers against transport through the material. The transport speed of gases and vapors through the polymer is reduced because the impenetrable silicate layers cause an increase in the path length for molecules diffusing through the polymer. Because absorption of water reduces the elastic characteristics of hydrophilic polymers, the addition of nanoparticles to minimize the negative effects of water uptake is particularly useful [17–21]. The reduction of moisture absorption in turn can suppress the internal damage and progress to improved long-term performance of the NC.

* Corresponding author. Tel.: +371 67543120; fax: +371 67820467.
E-mail address: Tatjana.Glaskova@pmi.lv (T. Glaskova).

0266-3538/$ - see front matter © 2009 Elsevier Ltd. All rights reserved.
doi:10.1016/j.compscitech.2009.08.013

The objective of this paper is to establish peculiarities of moisture sorption of epoxy–nanoclay composite. For this purpose the moisture diffusion behavior in atmospheres with different relative humidity of the NC containing different clay contents has to be investigated.

2. Experimental

The investigated material was provided by Research institute SYNPO, Pardubice, Czech Republic. It was received in the shape of thin and wide plates with dimensions $2.0 \times 200.0 \times 200.0$ (±0.2) mm and then cut accordingly into bars with dimensions $2.0 \times 8.0 \times 100.0$ (±0.1) mm.

The NC consisted of bisphenol-A epoxy resin and octadecylamine modified montmorillonite (MMT)-based organoclay. Four filler weight fractions $c = 0\%$, 2%, 4% and 6% were used in order to study kinetics of moisture absorption of NC.

Specimens in the form of thin plates were used in order to measure the percentage of weight change due to moisture absorption as a one-dimensional diffusion mode. Specimens were dried in an oven at 80 °C to remove internal stresses which appeared during their production before starting the tests. The specimens were placed then into the humid atmospheres at room temperature, were periodically removed, wiped, air dried for 5 min, and then weighed with accuracy 0.00005 g using Mettler Toledo XS205DU balance. It was experimentally confirmed that the duration of 5 min is sufficient to remove the extraneous moisture and does not cause significant desorption from the bulk of the NC specimens. In this way the data obtained during the experiments on moisture absorption could be accurately compared for all the NC specimens.

Moisture sorption was performed in atmospheres with relative humidity $\phi = 24\%$, 77%, and 98% using desiccators with silica gel and saturated solution of salts NaCl and K_2SO_4, respectively. Kinetics of moisture sorption was experimentally investigated using sorption method. Four specimens per each filler mass fraction were tested and the values given correspond to their arithmetic mean value.

Thus the peculiarities of moisture absorption of epoxy/MMT NC were determined.

3. Results and discussion

The percent weight gain of the composite $w(t)$ may be defined as the difference in weights of the time-varying moistened w_t and initial w_0 specimens, normalized to initial weight of specimens according to relation:

$$w(t) = \frac{w_t - w_0}{w_0} \times 100. \quad (1)$$

A series of measurements of moisture content of the specimens were executed at different time intervals. The experimental values of moisture content for NC with filler weight fraction $c = 0\%$ were plotted in Fig. 1 versus the square root of time.

Moisture sorption by epoxies is usually [22–24] described by Fick's equation, which for the case of one-dimensional diffusion, i.e. if there is a gradient of concentration only along the x axis, is given by

$$\frac{\partial C}{\partial t} = D\frac{\partial^2 C}{\partial x^2}, \quad (2)$$

where $C(x, t)$ is the concentration of diffusing substance in point x at time moment t, D is the diffusion coefficient. The diffusion is considered in a medium bounded by two parallel planes (planes at $x = 0$ and $x = h$, where h is the thickness of the specimen under initial $C(x, t = 0) = C_0$ and boundary conditions $C(x = 0, x = h, t) = C_\infty$ according to [25]. The total amount of diffusing substance is obtained by integration the solution of Eq. (2) by the thickness of specimen

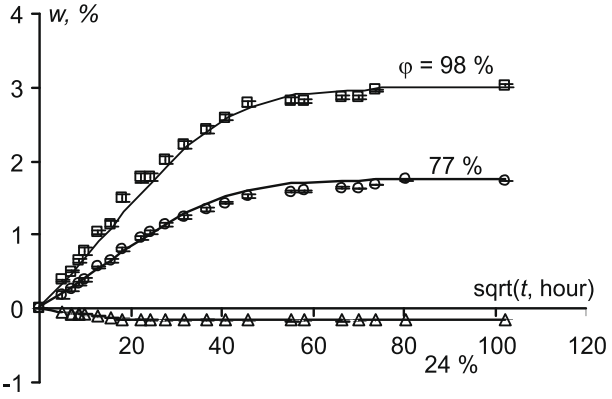

Fig. 1. The percentage of experimental weight gain (dots) versus square root of time in hours for NC with $c = 0\%$ in atmospheres with ϕ (numbers on the curves) and evaluation by Fick's model (solid lines).

$$w(t) = w_\infty - 2\frac{(w_\infty - w_0)}{\pi^2}\sum_{k=1}^{\infty}\frac{(1-(-1)^k)^2}{k^2}\exp\left[-\left(\frac{\pi k}{h}\right)^2 Dt\right], \quad (3)$$

where w_∞ is equilibrium moisture content in specimen.

From Fig. 1 it is clear that sorption process could be described with good agreement for NC $c = 0\%$ in all considered atmospheres. Similar results were obtained for epoxy resin filled with 2%, 4%, and 6% by weight. Moisture diffusivity and equilibrium moisture content of composite could be determined using accelerated analytical procedure [26]. The proposed method allows shortening the time needed for correct prediction of the two unknown parameters of Eq. (3) as diffusivity and equilibrium moisture content and further could be compared with experimental results obtained by Eq. (1).

The general idea is that for large values of time its enough to describe sorption curve with first term of series in Eq. (3) ($k = 1$). Hence by assuming that initial moisture content in the specimen $w_0 = 0$, moisture content takes form

$$w(t) = w_\infty - 8\frac{w_\infty}{\pi^2}\exp\left[-\left(\frac{\pi}{h}\right)^2 Dt\right]. \quad (4)$$

Accordingly the time derivative of moisture content in Eq. (4) represents the rate of moisture sorption and is determined by formula

$$\frac{dw}{dt} = 8\frac{w_\infty \cdot D}{h^2}\cdot\exp\left[-\left(\frac{\pi}{h}\right)^2 Dt\right]. \quad (5)$$

Further expressing $8w_\infty \exp\left[-\left(\frac{\pi}{h}\right)^2 Dt\right] = (w_\infty - w(t))\pi^2$ from Eq. (4) and substituting it in Eq. (5) results in following formula for evaluation the rate of moisture absorption:

$$\frac{dw}{dt} = \frac{\pi^2 \cdot D}{h^2}\cdot(w_\infty - w(t)). \quad (6)$$

Consequently, for large values of time $\frac{dw}{dt}$ is linearly dependent on $w(t)$ and the interception point with w axis corresponds to equilibrium moisture content w_∞. It is shown in Fig. 2 as an example for NC with filler content 4% and atmosphere 98% RH. Accordingly the inclination angle of this curve allows determining diffusion coefficient, which is found by relation

$$D = -\frac{4\cdot\left(\frac{h}{2}\right)^2}{\pi^2}\frac{\Delta\left(\frac{dw}{dt}\right)}{\Delta w}. \quad (7)$$

It should be mentioned that the diffusion coefficients of NC obtained by (7) are independent on relative humidity of atmosphere. The scattering within the atmosphere of equal humidity

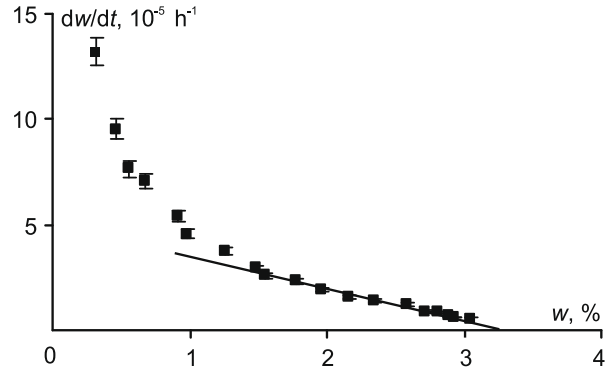

Fig. 2. The rate of moisture absorption versus moisture content in NC with $c = 4\%$ and atmosphere $\phi = 98\%$.

does not exceed 10% of average value. The diffusion coefficients were determined using the above mentioned procedure and are presented in Fig. 3. It was experimentally confirmed that sorption process in NC passes much more slowly than in pure epoxy resin (as shown in Fig. 3), for the highest filler content diffusivity reduces about half of diffusivity as for neat epoxy resin. As it was mentioned above this phenomenon takes place owing to the extremely high aspect ratio of clay platelets, which increased the tortuosity of the water molecules' path of while moisture diffuses into the NC. According to the tortuous path model and since the moisture permeability is a function of volume fraction and aspect ratio of the platelets the exfoliated NC is more preferred to conventional or intercalated composites in terms of the barrier characteristics [11].

The equilibrium moisture content of NC w_∞^{NC} involves the equilibrium moisture content of the NC components: of polymer resin w_∞^{ep} and of filler w_∞^{f}, accordingly:

$$w_\infty^{NC} = w_\infty^{ep} \cdot (1 - c) + w_\infty^{f} \cdot c. \quad (8)$$

The use of mass was chosen as a reference in the rule of mixture instead of volume since all the NC specimens revealed swelling of about 3% by volume at the end of the saturation. It is considered that hydrophilic epoxy resin has the main contribution to the moisture uptake and equilibrium moisture content of the filler w_∞^{f} is close to zero since naturally hydrophilic MMT clay has been organically treated.

The increase of equilibrium moisture content with the increase of clay weight content in NC (shown in Fig. 4) could be caused by growth of interphase weight content. The estimation of interphase moisture sorption characteristics can be created using modified rule of mixture for equilibrium moisture content

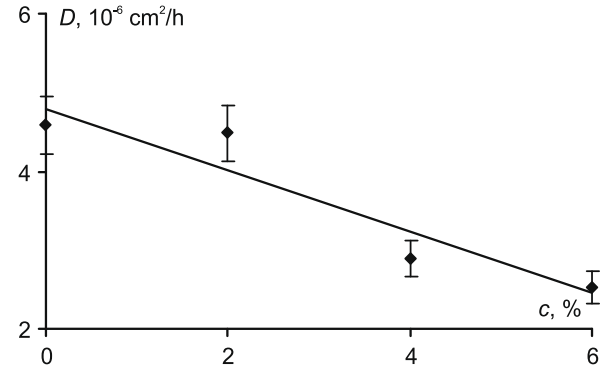

Fig. 3. Diffusion coefficient of NC evaluated by Eq. (5) versus filler weight fraction in atmosphere with $\phi = 98\%$.

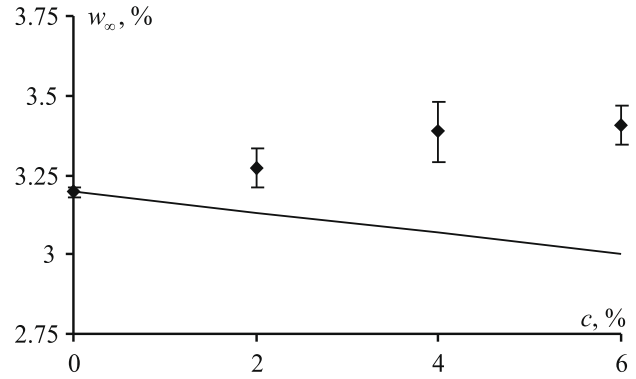

Fig. 4. Equilibrium moisture content versus filler mass fraction in atmosphere with 98% RH (dots – result of extrapolation of experimental data, line – evaluation by (8)).

$$w_\infty^{NC} = w_\infty^{ep} \cdot (1 - c - b) + w_\infty^{i} \cdot b, \quad (9)$$

where w_∞^{i} is equilibrium moisture contents of interphase, b is interphase fraction by weight. Such addition of interphase around the filler particles allows preventing the deviation of evaluation by mixture rule (8) from results of extrapolation using experimental data. Nevertheless the mixture rule (9) contains two unknown parameters (w_∞^{i} and b), that cannot be determined independently. That's why the proper analysis is based on the attributing capacity of moisture absorption of the interphase to the deviation between evaluation by (8) and experimental results.

Moreover it should be expected that for atmosphere with higher relative humidity (higher content of absorbed moisture) the difference between the amount of absorbed moisture content measured by experiments and predicted by (8) should increase. This observation was further supported by experiments as shown in Fig. 5. The higher content of filler leads to greater moisture absorption and greater deviation from estimation by mixture rule without consideration of sorption characteristics of interphase layer. The general idea is that this deviation that represents moisture content in interphase is linear proportional on filler content (as shown in Fig. 5). It means that coefficients of proportionality correspond to sorption capacity of interphase in NC with 1% of filler.

At equilibrium the relationship between moisture content in material and equilibrium relative humidity of surrounding atmosphere can be displayed by sorption isotherm. It is estimated that the total moisture content is distributed homogeneously by the

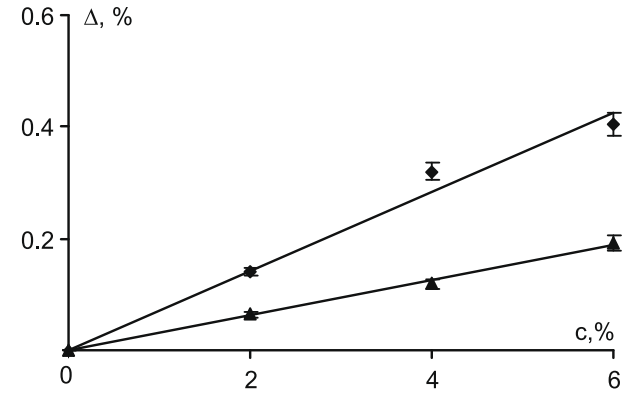

Fig. 5. Deviation between experimental data of equilibrium moisture content of NC and estimation of it by mixture rule (8) for atmosphere with $\phi = 77$ (▲) and 98 (♦) % RH.

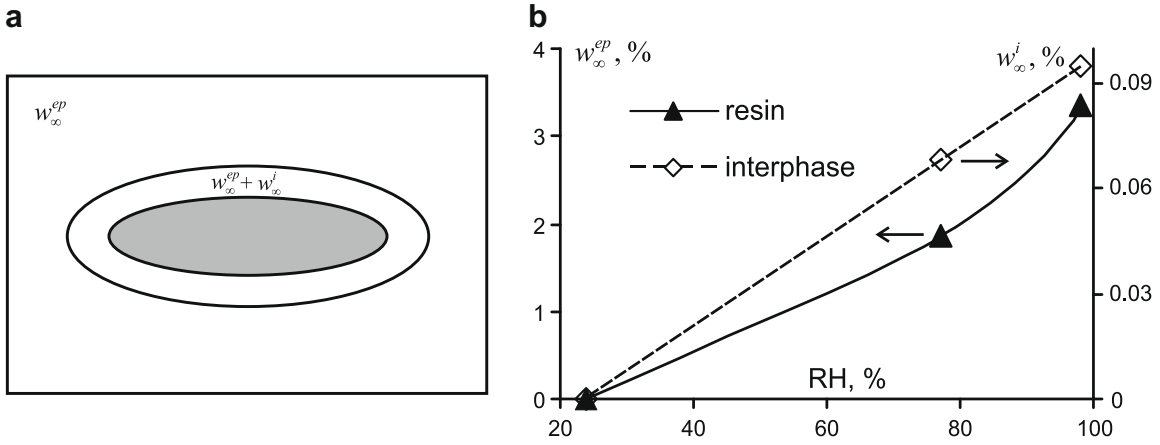

Fig. 6. Schematic representation of equilibrium moisture content distribution within composite system of one particle (a) and sorption isotherm of epoxy resin and interphase in NC with 1% of clay by weight (b).

section of the NC specimens and according to sorption isotherm for the moisture concentration in NC. For each humidity value, a sorption isotherm indicates the corresponding moisture content at a given, constant temperature. Because of the complexity of sorption processes in composite materials, the isotherms traditionally deviate from Henry's law, exhibit nonlinear behavior and should be measured experimentally.

The sorption isotherm of interphase layer in NC with 1% of clay could be estimated from Fig. 6. As it was mentioned before the content of interphase in NC could not be predicted independently from the rule of mixture for equilibrium moisture content (9). Nevertheless its possible to estimate the effect of the interphase on sorption properties of NC in whole. These results could be used for further analysis of the moisture effect on mechanical and thermal properties of NC. Respectively moisture content which exists both in matrix and in interphase of NC could be predicted instead of (9) for given composite system

$$w_\infty^{NC} = w_\infty^{ep} \cdot (1 - c) + w_\infty^{i} \cdot c, \tag{10}$$

where both w_∞^{ep} and w_∞^{i} are determined from Fig. 6, which represents the sorption isotherm of epoxy resin and interphase layer. This sorption isotherm and formula (10) allow approximate estimation of additional moisture content of NC in atmosphere of any relative humidity and any filler content.

4. Conclusions

In the present paper the moisture absorption by epoxy/MMT NC was examined. From the above investigation the following conclusions may be derived:

- Sorption process could be described by Fick's model with good agreement for all contents of clay and all atmospheres. The diffusion coefficient and equilibrium moisture content of NC has been evaluated by Fick's model using accelerated procedure.
- It was experimentally confirmed that sorption process in NC passes more slowly than in pure epoxy resin, for the highest filler content diffusivity reduces about half of diffusivity as for epoxy resin. It could be caused by clay nanoparticles as they act as efficient barriers against moisture transport.
- The increase in equilibrium moisture content observed with the increase of clay weight content in NC is explained by growth of interphase layer content. The sorption capacity of interphase layer in NC with 1% of filler was determined and the sorption isotherm of interphase was derived.
- Interphase should be taken into account when properties of composite are calculated using properties of components. The higher content of interphase consistently leads to greater moisture absorption.
- Based on the results obtained by relating moisture on properties of NC it could be concluded that the addition of impenetrable clay nanoparticles is useful for the reduction of negative effect of moisture on properties of NC allowing the application of modified epoxy resin in environments with higher-operating relative humidity.

References

[1] Koo JH. Polymer nanocomposites. McGraw-Hill; 2006.
[2] Mai YW, Zhen Yu Zhong. Polymer nanocomposites. Woodhead Publishing; 2006.
[3] Friedrich K, Fakirov S, Zhang Zh. Polymer composites from nano- to macro-scale. Springer; 2005.
[4] Ajayan PM, Schadler LS, Braun PV. Nanocomposite science and technology. Wiley; 2003.
[5] Yasmin A, Luo JJ, Abot JL, Daniel IM. Mechanical and thermal behavior of clay/epoxy nanocomposites. Compos Sci Technol 2006;66(14):2415–22.
[6] Gay D, Hoa A, Tsai S. Composite materials. Design and applications. CRC Press; 2003.
[7] Roco M. Broader social issues of nanotechnology. J Nanopart Res 2003;5:181–9.
[8] Fornes T, Yoon P, Hunter DL, Keskkula H, Paul DR. Effect of organoclay structure on nylon 6 nanocomposite morphology and properties. Polymer 2002;43(22):5915–33.
[9] Zelenkova Myshkova M, Zelenka J, Scpachek V, Socha F. Properties of epoxy systems with clay nanocomposites. Mech Compos Mater 2003;39(2):119–22.
[10] LeBaron P, Wang Z, Pinnavaia TJ. Polymer-layered silicate nanocomposites: an overview. Appl Clay Sci 1999;15(1–2):11–29.
[11] Kim JK, Hu C, Woo RSC, Sham ML. Moisture barrier characteristics of organoclay–epoxy nanocomposites. Compos Sci Tech 2005;65(5):805–13.
[12] Choudalakis G, Gotsis AD. Permeability of polymer/clay nanocomposites: A review. Eur Polym J 2009;45:967–84.
[13] Theocaris P, Kontou E. The effect of moisture absorption on the thermomechanical properties of particulates. Colloid Polym Sci 1983;261:394–403.
[14] Ishisaka A, Kawagoe M. Examination of the time water content superposition on the dynamic viscoelasticity of moistened polyamide 6 and epoxy. J Appl Polym Sci 2004;93(2):560–7.
[15] Theocaris P, Papanicolaou G. Interrelation between moisture absorption, mechanical behavior, and extent of boundary interface in particulate composites. J Appl Polym Sci 1983;28(10):3145–53.
[16] Aniskevich K, Glaskova T, Janson Yu. Elastic and sorption characteristics of an epoxy binder in a composite during its moistening. Mech Compos Mater 2005;41(4):341–50.
[17] Glaskova T. Analysis of filler and interphase influence on properties of epoxy/clay nanocomposite. Master Thesis, University of Latvia; 2007.
[18] Vlasveld D, Groenevold J, Bersee HEN, Mendes E, Picken SJ. Analysis of the modulus of polyamide-6 silicate nanocomposites using moisture controlled variation of the matrix properties. Polymer 2005;46(16):6102–13.

[19] Maksimov RD, Gaidukov S, Zicans J, Jansons J. Moisture permeability of a polymer nanocomposite containing unmodified clay. Mech Compos Mater 2008;44(5):505–14.
[20] See SC, Zhang ZY, Richardson MOW. A study of water absorption characteristics of a novel nano-gelcoat for marine application. Prog Org Coat 2009;65:169–74.
[21] Liu W, Hoa SV, Pugh M. Water uptake of epoxy–clay nanocomposites: experiments and model validation. Compos Sci Technol 2008;68:2066–72.
[22] Xiao G, Shanahan M. Swelling of DGEBA/DDA epoxy resin during hygrothermal ageing. Polymer 1998;39(14):3253–60.
[23] Glaskova TI, Guedes RM, Morais JJ, Aniskevich AN. A comparative analysis of moisture transport as applied to an epoxy binder. Mech Compos Mater 2007;43(4):377–88.
[24] Maggana C, Pissis P. Water sorption and diffusion studies in an epoxy resin system. J Polym Sci: Part B 1999;37(11):1165–82.
[25] Crank J. The mathematics of diffusion. Oxford; 1956.
[26] Aniskevich A. Experimental investigation of moisture sorption by epoxy resin EDT-10. Mech Compos Mater 1985;20(6):670–4.

Publikācija 4

Moisture effect on deformability of epoxy/montmorillonite nanocomposite

Glaskova T., Aniskevich A.

Institute of Polymer Mechanics, University of Latvia, Riga, Latvia

Journal of Applied Polymer Science, 2010, Vol. 116, No. 1, p. 493-498.

Moisture Effect on Deformability of Epoxy/ Montmorillonite Nanocomposite

T. Glaskova, A. Aniskevich

Institute of Polymer Mechanics, University of Latvia, Riga LV-1006, Latvia

Received 26 June 2009; accepted 8 October 2009
DOI 10.1002/app.31575
Published online 1 December 2009 in Wiley InterScience (www.interscience.wiley.com).

ABSTRACT: In this article the moisture effect on deformability of epoxy/montmorillonite nanocomposite was investigated. The change of fracture character and drop of elastic characteristics due to moisture absorption was observed. The estimation of filler morphological peculiarities (platelet stack constitution) in composite and its effect on nanocomposite elastic properties was undertaken. It is shown that the higher number of filler platelet per stack consistently leads to the decrease of nanocomposite elastic properties. Nevertheless prediction by micromechanical model is rough for moistened nanocomposite because of resin structural changes. © 2009 Wiley Periodicals, Inc. J Appl Polym Sci 116: 493–498, 2010

Key words: nanoclay-composite; deformability; moisture effect; modeling

INTRODUCTION

The peculiarities of moisture absorption by epoxy/ montmorillonite (MMT) nanocomposite (NC) were discussed in.[1] The enhanced barrier properties referred in the literature[2–8] were revealed. The sorption process in NC passed more slowly, for the highest filler content diffusivity was reduced about twice. This could be described by large aspect ratio and surface of the exfoliated silicate layers as they act as efficient barriers against moisture transport through the material and cause an increase in the path length for molecules diffusing through the polymer.[9]

Epoxy resins are quite attractive for structural applications because of their relatively high strength and stiffness, low creep, and shrinkage. However they have a major drawback of high moisture absorption, which in turn degrades the functional, structural and mechanical properties of the composites.[10–15] Since absorption of water reduces the elastic characteristics of hydrophilic polymers, the addition of nanoparticles to minimize the negative effects of water uptake is particularly useful.[5,14,15]

The emphasis of this article is made mainly to establish effect of moisture on deformability of epoxy/ MMT NC taking into account filler morphological peculiarities and to verify if the negative effect of moisture on deformability of NC is minimized by introducing MMT clay nanoparticles.

Correspondence to: T. Glaskova (Tatjana.Glaskova@pmi.lv).

Journal of Applied Polymer Science, Vol. 116, 493–498 (2010)

EXPERIMENTAL

The investigated material was provided by research institute SYNPO, Pardubice, Czech Republic. It was received in the shape of thin and wide plates with dimensions 2.0 × 130.0 × 130.0 (± 0.2) mm and then cut into bars with dimensions 2.0 × 8.0 × 130.0 (± 0.1) mm.

The NC consisted of bisphenol-A epoxy resin and octadecylamine modified MMT-based organoclay. Four filler weight fractions $c = 0$, 2, 4, and 6% were used to study the effect of moisture and filler weight fraction on the mechanical behavior of NC.

The homogeneity of the filler particles' dispersion could be approved by the transparency of all NC specimens. Additional microscopy methods, scanning electron (SEM) and transmission electron microscopy (TEM), were applied for the analysis.

Moisture sorption was performed in atmospheres with relative humidity $\varphi = 24$, 77, and 98% using desiccators with silica gel and saturated solution of salts NaCl and K_2SO_4, respectively.[1] According to the results obtained in Ref. 1, the average equilibrium moisture content reached in 437 days for NC was approximately −0.4, 1.7, and 3.2% for $\varphi = 24$, 77, and 98% with increase by approximately 7% for filler content changing from 0 to 6 wt %. It was experimentally confirmed that sorption process in NC passed more slowly than in pure epoxy resin, for the highest filler content diffusivity reduced about half of diffusivity as for epoxy resin. It could be caused by clay nanoparticles as they act as efficient barriers against moisture transport. The increase in equilibrium moisture content observed with the increase of clay weight content in NC was

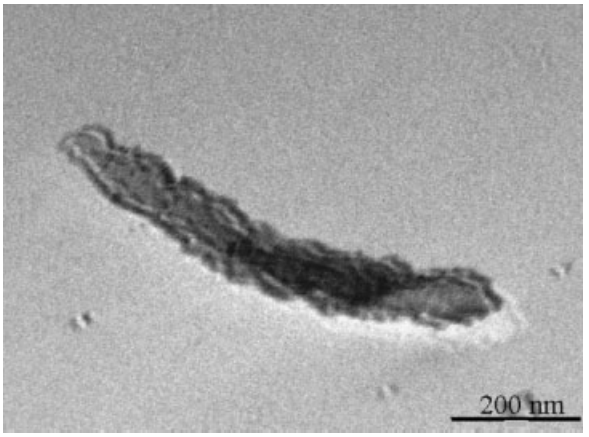

Figure 1 Typical TEM image of acetone suspension of clay nanoparticle. The nanoclay appears in black.

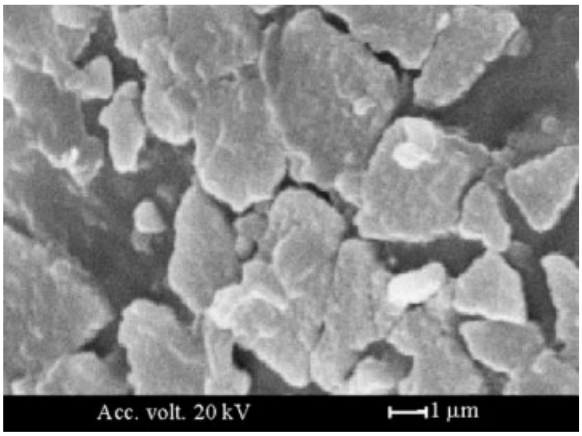

Figure 2 SEM micrograph of fracture surface of NC with $c = 2\%$.

explained by growth of interphase layer content. The sorption capacity of interphase layer in NC with 1% of filler was determined and the sorption isotherm of interphase was derived.

Quasi static tensile tests were performed on the specimens with different clay content in dry and wet state using Zwick 2.5 testing machine with a crosshead speed of 5 mm/min at room temperature. Tensile strength is defined as the maximal achieved value of stress in the specimen, and elastic modulus is calculated from the slope of a secant line between 0.05% and 0.25% strain on a stress–strain plot. Four specimens per each filler mass fraction were tested and the values given correspond to their arithmetic mean value.

RESULTS AND DISCUSSION

Microstructural characterization

The behavior and properties of NC are dependent not only on properties of its structural components but also on the material microstructure: the dispersion and orientation of filler particles, and the interactions between filler particles and polymer matrix.[16]

Nevertheless one of the main parameters that affect the behavior of the nanosystem is the effectiveness of dispersion of filler particles within the polymer matrix.[17]

One way to check the morphological peculiarities of clay nanoparticles in a solvent, before incorporating them to a matrix, is to observe their dispersion by TEM. A typical image of acetone suspension of clay nanoparticles is shown in Figure 1.

It is obvious from Figure 1 that the observed aggregate should be a stack of clay platelets having layered structure and high aspect (diameter to thickness) ratio (50). The aspect ratio of the platelet stack as observed from Figure 1 is about 7.

Moreover the platelet shape of the filler particles could be confirmed by SEM micrograph of fracture surface of NC specimen with $c = 2\%$ (Fig. 2). It could be seen that the transversal dimension of the filler aggregates is much smaller than longitudinal ones.

Mechanical properties

Experimentally measured stress–strain curves of NC with $c = 6\%$ moistened at $\varphi = 24$, 77, and 98% RH are shown in Figure 3. From these curves it could be observed that the effect of moisture on mechanical behavior is substantial. Absorbed moisture essentially plasticizes the NC and changes its fracture character from brittle in dry atmosphere to plastic one in wet atmospheres.

To examine the effect of organoclay content on mechanical properties, elastic modulus and tensile strength were plotted versus filler mass fraction (Figs. 4 and 5). From these figures it is clear that elastic modulus increases up to 20% and tensile strength of the NC decreases about the same value with the increase of organoclay content to 6%.

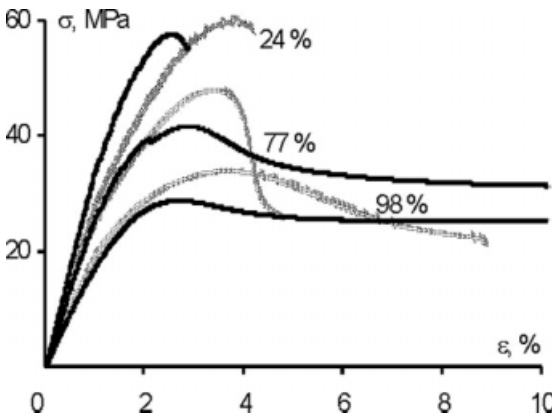

Figure 3 Typical stress–strain curves at a fixed rate of deformation ($v = 5$ mm/min) for neat epoxy resin (gray curves) and NC with $c = 6\%$ (black curves) and $\varphi = 24$, 77, and 98% RH.

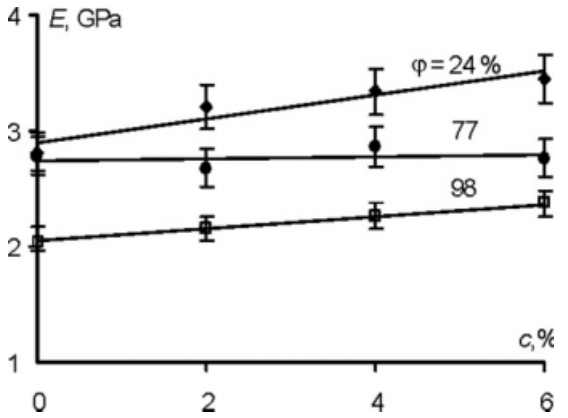

Figure 4 Elastic modulus of NC in atmospheres with different relative humidity versus filler weight fraction.

Figures 2 and 3 also show the quantitative effect of moisture on tensile strength and elastic modulus of NC. Tensile strength of moistened composite drops twice. Elastic modulus both of moistened pure epoxy resin and NC is reduced approximately 1/3 in comparison to initial state. Consequently, due to absorbed moisture both pure resin and NC with $c =$ 6% show almost same degradation as for elastic modulus 1 GPa and for tensile strength 25 MPa, respectively. It should be noted that although the values themselves of elastic modulus and strength are improved with respect to filler content, the positive effect as moisture content increases (in atmosphere from 24% RH till 98% RH) was not revealed.

Efforts were being made to relate effective tensile elastic modulus of moistened NC with properties of its structural components. It should be emphasized that taking into account complicated structure of real composite material, only evaluative results could be obtained theoretically.[18]

The majority of micromechanical models are limited to characterization of linear elastic behavior of composites during static loading.[19–27] Another assumption is that the components are also linear elastic, and the composite is represented as nonhomogeneous linear-elastic medium.

In the structural hierarchy of polymer-clay NC at least two states can be assigned: (1) state of total exfoliation of clay platelets with characteristic parameters as thickness and dimensions in the plane of platelets, and (2) state of incomplete exfoliation of clay platelets and characteristic parameters as thickness and dimensions in the plane of intercalated layered stacks.[28] The aspect ratio and orientation of anisometric particles determine their reinforcement degree. Nevertheless, it is difficult to control the orientation of plane particles during processing of composite and the real distribution of their orientation could be rather complex, the determination of the effective elastic constants of transversely isotropic layers of a NC with coplanar orientation of such particles is of great importance. The data obtained in this case could serve as initial for a further analysis of the elastic properties of a composite with disoriented nanoparticles taking into account their orientational distribution in the material.[27]

Halpin-Tsai equations[27,25] obtained for isotropic polymer matrix filled with coplanar transversally isotropic cylindrical particles of arbitrary aspect ratio (Fig. 6) were used for the case of exfoliated NC. The elastic solution was obtained for the composite consited of a single fiber encased in a cylinder of matrix, both embedded in an unbounded homogeneous medium, which is macroscopically indistinguishable from the composite. The relations between the stress and strain components were averaged throughout the composite. The obtained formulas were curve fitted to exact elasticity solutions and confirmed by experimental measurements in order to get the solution for composite filled with particles of arbitrary aspect ratio.

If the exfoliation of filler platelets is incomplete the composite system is considered to consist of matrix and pseudoparticles (stacks of individual platelets). Figure 7 shows sheme of filler particles that are forming a stack (a pseudoparticle). N is the number

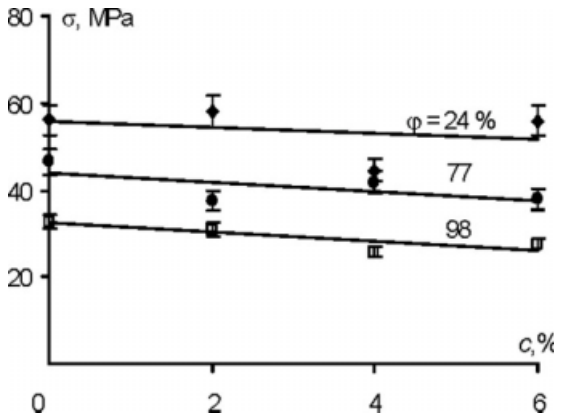

Figure 5 Tensile strength of NC in atmospheres with different relative humidity versus filler weight fraction.

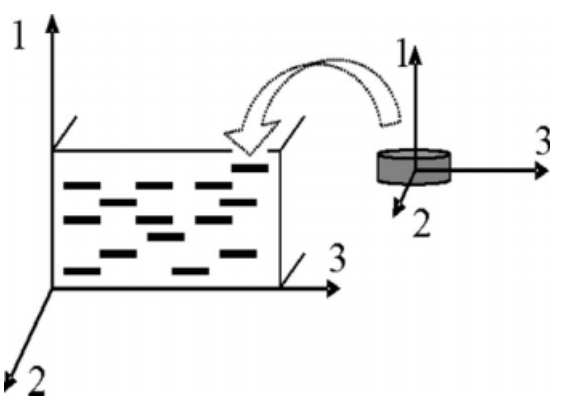

Figure 6 Schematic representation of cylindrical filler particles embedded in polymer matrix.

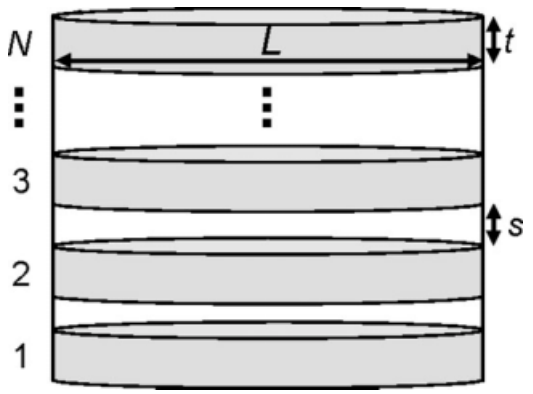

Figure 7 Representation of pseudoparticle (platelet stack).

of platelets per stack, L – length (width), t – thickness of the platelet, s – interplatelet spacing.

The Halpin-Tsai equations that were used[27] to characterize the case of incomplete exfoliation of filler platelets within the composite are as follows

$$E_1 = E_m \frac{1 + 2\eta_1' \phi'}{1 - \eta_1' \phi'}, \quad (1)$$

where

$$\eta_1' = \frac{R_1' - 1}{R_1' + 2},\ R_1' = \frac{E_{p1}}{E_m}, E_{p1} = \frac{E_{f1} E_m (Nt + (N-1)s)}{E_m N t + E_{f1}(N-1)s},$$
$$\phi' = \phi\left(1 + \left(1 - \frac{1}{N}\right)\frac{s}{t}\right).$$

Here E_1, E_m, E_{p1}, E_{f1} are elastic moduli of given composite, matrix, filler platelet stack and single filler platelet, accordingly, for axis direction shown in Fig. 6; φ and φ′ are the volume fraction of filler particles and filler platelets. The case of complete exfoliation of filler platelets within composite could be easily obtained for $N = 1$, $s = 0$.

Taking into account the anisotropy of considered filler particles and as consequence of the composite material two additional Halpin-Tsai equations could be applied

$$E_2 = E_3 = E_m \frac{1 + 2A_f' \eta_2' \phi'}{1 - \eta_2' \phi'}, \quad (2)$$

where

$$\eta_2' = \frac{R_2' - 1}{R_2' + 2A_f'},\ R_2' = \frac{E_{p2}}{E_m}, E_{p2} = \frac{E_{f2} N t + E_m (N-1)s}{N t + (N-1)s},$$
$$A_f' = \frac{A_f}{N}\left(\frac{1}{1 + \left(1 - \frac{1}{N}\right)\frac{s}{t}}\right).$$

In these equations E_{p2},E_{f2} are elastic moduli of filler platelet stack and single filler platelet for the axis direction shown in Figure 6. A_f and A_f' are the aspect ratios of single filler platelet and platelet stack (>1 since it equals to the diameter divided by thickness for cylindrical platelets). Again the case of complete exfoliation of filler platelets within composite could be easily obtained assuming that $N = 1$, $s = 0$.

Using known values of elastic modulus of matrix in atmospheres with different relative humidity it is possible to determine elastic moduli of NC by equations (1) and (2). The elastic moduli of montmorillonite clay platelets are ranging from 40 GPa[29] to 180 GPa[23,30–32] based on the literature values for layered-structure clay minerals, an empirical modulus-density relation for alumina, silica and their compounds and values obtained by simulation for the product of elastic modulus and thickness of the platelets. In this study elastic moduli of filler are assumed to be $E_{f1} = 55$ GPa, $E_{f2} = E_{f3} = 178$GPa, aspect ratio of filler platelet $A_f = 50$, number of platelets per stack N is changed from 1 to 6, $s/t = 1$.

Comparing results of evaluation by eq. (1) with experimental data of quasistatic tensile tests of specimens conditioned in dry atmosphere (φ = 24% RH) provided in Figure 8 it is obvious that evaluation results for elastic modulus of NC with exfoliated filler particles are higher than experimental ones. Increasing the number of platelets per stack gives the opportunity to get better agreement between them. Although it is rather arguable, as it is assumed in the model that filler particles obey coplanar orientation in polymer matrix. On the other hand evaluation by eq. (2) (low bound) is much lower than experimental results even for the case of exfoliated platelets. It means that real orientation distribution of clay platelets is somewhere in between these limits and could be rather complicated.

Nevertheless using obtained results (the same parameters N, t, s) for moistened NC it is possible to estimate structural changes of the polymer resin because of moisture absorption.

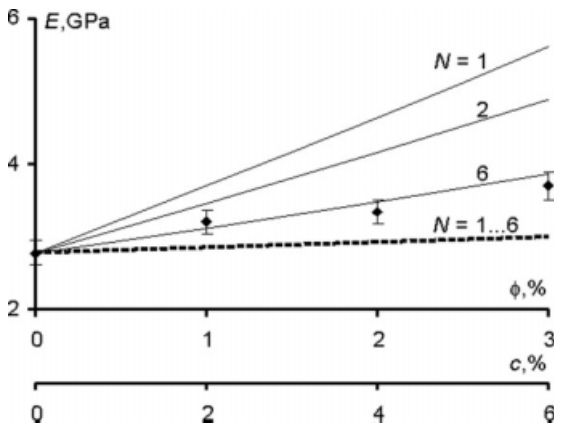

Figure 8 Elastic modulus of NC versus filler volume content. Evaluation by (1) (solid line) and (3) (dashed line) for different number of elementary layers N (numbers on the curves) in a platelet stack. Dots – experimental data for φ = 24% RH.

The resulting evaluation of elastic modulus of moistened NC by eq. (1) shows the deviation from results obtained experimentally (Fig. 9). As it can be seen taking into account platelet stack layered structure (increasing the number of platelets in stack till 6) improves the congruence of results with experimental data. Apparently it could be described by the change of elastic properties of the platelet stacks. It should be emphasized that while elastic modulus of impermeable clay platelets is not dependent on moisture content, the matrix phase that is located in the interplatelet spacing absorbs moisture. Therefore, the elastic properties of the platelet stacks are dependent on absorbed moisture content and cause more significant decrease of moistened NC elastic modulus as presented in Figure 9.

The change of elastic modulus under effect of moisture e.g. NC with $c = 6\%$ proves that moisture which exists in the interplatelet spacing significantly influences the elastic modulus. Logically enough, the higher content of filler leads to higher content of interplatelet spacing and as a result to greater moisture absorption and greater change of NC properties that are sensitive to moisture.

The isotherm shown in Figure 10 concludes the proposed analysis of moisture and filler effect on deformability of epoxy/MMT NC taking into account filler morphological peculiarities. Using this figure it is possible to estimate NC elastic modulus of any filler content in atmosphere with any relative humidity. It is obvious that because of moisture absorption elastic modulus of NC is substantially decreased. Since the value of elastic modulus of epoxy resin is improved with respect to filler content in spite of no positive effect for the decrease of elastic modulus of NC, due to moisture absorption (in atmosphere from 24% RH till 98% RH) epoxy resin modified by impenetrable stiff MMT clay nanoparticles could be applied in environments with higher-operating relative humidity.

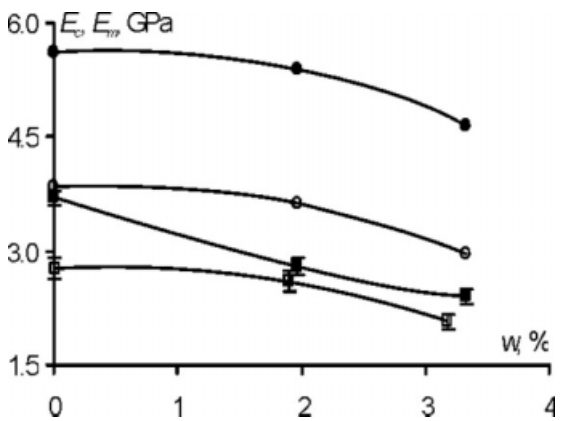

Figure 9 Elastic modulus of epoxy resin and NC with $c = 6\%$ versus absorbed moisture content. Experimental data (NC with $c = 6\%$ (–■–), epoxy resin (–□–)), evaluation by (3) for NC with $c = 6\%$ and $N = 1$ (–●–) and $N = 6$(–○–).

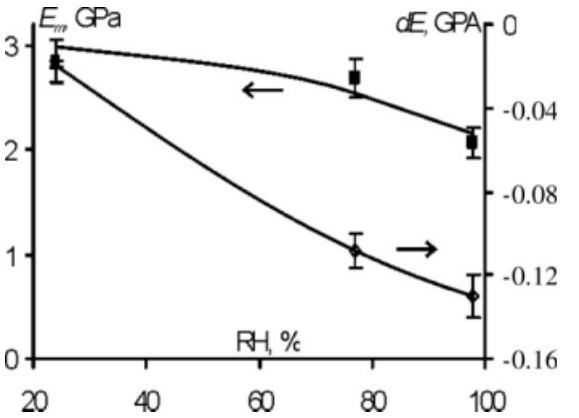

Figure 10 Elastic modulus of epoxy resin (■) and normalized to 1 wt % of filler deviation of NC elastic modulus (◇) versus relative humidity of the atmosphere.

CONCLUSIONS

In this article the effect of moisture absorption on the mechanical properties of NC was examined. Quasistatic tensile tests were carried out for evaluation of the mechanical properties. Finally, an attempt was made to estimate the effect of moisture on elastic modulus of platelet stack and moistened NC. From the above investigation the following conclusions may be derived:

- Shown effect of moisture on mechanical properties is substantial. Absorbed moisture essentially plasticizes the composite changing the fracture character. Tensile strength of moistened composite drops twice. Elastic modulus both of moistened pure epoxy resin and NC is reduced approximately 1/3 in comparison to initial state.
- Halpin-Tsai equations were applied to estimate effective elastic modulus of NC conditioned in atmospheres of different relative humidity. The results obtained for specimens conditioned in dry atmosphere were used for moistened NC and provided opportunity to estimate structural changes of the polymer resin because of moisture absorption.
- Based on obtained results it could be concluded that incorporation of impenetrable clay nanoparticles with high mechanical characteristics did not reduce the negative effect of absorbed moisture on mechanical properties of NC. But since the value of elastic modulus of epoxy resin is improved with respect to filler content up to 20% epoxy resin modified by impenetrable stiff

MMT clay nanoparticles could be applied in environments with higher-operating relative humidity.

References

1. Glaskova, T.; Aniskevich, A. Compos Sci Technol 2009, 69, 2711.
2. Friedrich, K.; Fakirov, S.; Zhang, Zh. Polymer composites from nano-to macro-scale; Springer: New York, New York, 2005; 373 p.
3. Lebaron, P.; Wang, Z.; Pinnavaia, T. Appl Clay Sci 1999, 15, 11.
4. Kim, J.-K.; Hu, C.; Woo, R.; Sham, M.-L. Compos Sci Technol 2005, 65, 805.
5. Maksimov, R. D.; Gaidukov, S.; Zicans, J.; Jansons, J. Mech Composite Mater 2008, 44, 505.
6. Koo, J. H. Polymer nanocomposites; McGraw-Hill: New York, New York, 2006; 273 p.
7. Mai, Y.-W.; Yu, Zh. Zh Polymer nanocomposites; Woodhead publishing: Cambridge, England, 2006; 613 p.
8. Ajayan, P. M.; Schadler, L. S.; Braun, P. V. Nanocomposite science and technology; Wiley: Weinheim, Germany, 2003; 236 p.
9. Fornes, T.; Yoon, P.; Hunter, D.; Keskkula, H.; Paul, D. Polymer 2002, 43, 5915.
10. Theocaris, P.; Kontou, E. Colloid Polym Sci 1983, 394.
11. Ishisaka, A.; Kawagoe, M. J Appl Polym Sci 2004, 93, 560.
12. Theocaris, P.; Papanicolaou, G. J Appl Polym Sci 1983, 28, 3145.
13. Aniskevich, K.; Glaskova, T.; Janson, Yu. Mechanics of Composite Materials; Kluwer Academic/Plenum Publishers: New York, 2005; Vol 41, pp 341–350.
14. Glaskova, T. Analysis of filler and interphase influence on properties of epoxy/clay nanocomposite, Master thesis, supervisors: Dr. Sc. Ing. A. Aniskevich, Dr. Sc. Ing. M. Zarrelli, University of Latvia, Riga, 2007 p.
15. Vlasveld, D.; Groenevold, J.; Bersee, H.; Mendes, E.; Picken, S. Polymer 2005, 46, 6102.
16. Masenelli-Varlot, K.; Chazeau, L.; Gauthier, C.; Bogner, A.; Cavaillé, J. Y. Compos Sci Technol 2009, 69, 1533.
17. Tsai, J.; Sun, T. J Composite Mater 2004, 38, 567.
18. Christensen, R. M. Mechanics of composite materials, 2nd ed; Dover Publications: New York, 2005; 348 p.
19. Eshelby, J. D. Proc R Soc Lond Ser A: Math Phys Sci 1957, 241, 376.
20. Wu, T. T. Int J Solids Struct 1966, 2, 1.
21. Lee, K. Y.; Paul, D. R. Polymer 2005, 46, 9064.
22. Pal, R. Composites Part A 2008, 39, 1496.
23. Maksimov, R. D.; Gaidukov, S.; Kalnins, M.; Zicans, J.; Plume, E. Mech Composite Mater 2006, 42, 163.
24. Wang, J.; Pyrz, R. Compos Sci Technol 2004, 64, 925.
25. Halpin, J. C.; Kardos, J. L. Polym Eng Sci 1976, 16, 344.
26. Bicerano, J. Prediction of polymer properties, 3rd ed.; Marcel Dekker: New York, New York, 2002; 756 p.
27. Brune, D.; Bicerano, J. Polymer 2002, 43, 369.
28. Plume, E.; Maksimov, R. D.; Lagzdins, A. Mech Composite Mater 2008, 44, 341.
29. Chen, B.; Evans, J. R. G. Scr Mater 2006, 54, 1581.
30. Anthoulis, G. I.; Kontou, E. Polymer 2008, 49, 1934.
31. Thostenson, E. T.; Li, Ch; Chou, T.-W. Compos Sci Technol 2005, 65, 491.
32. Luo, J.-J.; Daniel, I. M. Compos Sci Technol 2003, 63, 1607.

Publikācija 5

Structural changes in a clay-containing nanocomposite with a different moisture content caused by its deformation

Faitel'son E. A., Glaskova T. I., Korkhov V. P., Aniskevich A. N.

Institute of Polymer Mechanics, University of Latvia, Riga, Latvia

Journal of Engineering Physics and Thermophysics, 2010, Vol. 83, No. 3, p. 443-451.

Journal of Engineering Physics and Thermophysics, Vol. 83, No. 3, 2010

STRUCTURAL CHANGES IN A CLAY-CONTAINING NANOCOMPOSITE WITH A DIFFERENT MOISTURE CONTENT CAUSED BY ITS DEFORMATION

E. A. Faitel'son, T. I. Glaskova, V. P. Korkhov, and A. N. Aniskevich

UDC 539.431:678.067

This paper presents the results of an investigation of the properties of a clay-containing nanocomposite with an epoxy binder under moisture-temperature and mechanical action. It has been established that whatever the moisture content, the nanocomposite crystallizes under the thermomechanical action (upon reaching the glass-transition temperature). When the nanocomposite is heated to 70°C, the restructuring process is reversible, and its heating to above 150°C leads to its amorphization. The presence of clay nanoparticles (up to 6 mass percent) does not influence the temperature of structural transitions of the nanocomposite and does not cause a substantial strengthening effect. The sorbed moisture plasticizes the nanocomposite and decreases its glass-transition temperature by 10°C. The specific features of the thermomechanical behavior of nanocomposites upon their tensile prestrain or creep are due to the formation of an oriented structure. Their crystallization begins at lower temperatures and with a higher degree of crystallinity than that of unloaded nanostructures.

Keywords: *adsorption-active medium, microheterogeneity, X-ray structural analysis, morphological changes, induced elasticity.*

Introduction. In modern thermal physics of polymer materials, along with the development of phenomenological notions, the thermophysical properties and the processes proceeding in them connected with structural changes are being studied extensively. Such an approach appears to be particularly important, since it is necessary to take into account the microheterogeneity of polymer bodies due to the presence in them of regions with different types of elasticity, as well as the morphological changes caused by strains with energy transformations. In this connection, the question of the interrelationship between the mechanical characteristics of composite materials (CM) and the structural changes accompanying the deformation process in adsorption-active media and of establishing general laws for them is of great importance. The mechanical phenomena taking place in the process of sorption and swelling in polymer CMs, while being of certain theoretical and practical interest, have been studied very little, especially in nanocomposites (NC) that are of interest in developing high-efficiency materials. For example, for clay-containing NCs exhibiting improved mechanical, thermal, and barrier properties compared to unfilled polymers, the majority of papers [1–5] presented results without conclusions about the processes proceeding in them.

Resistance to various kinds of action is a characteristic of the material in the unloaded state whereas the fracture strength under load under service conditions characterizes the material in the stressed state. In this case, the structure inhomogeneity of NCs is one of the necessary conditions providing their plastic deformation ability at temperatures below the glass transition temperature T_g [6, 7]. But even in the absence of stresses applied from the outside, internal stresses may arise in the material as a result of the swelling inhomogeneity. The swelling accompanying the sorption is inhomogeneous due to the presence in the material of parts not affected by this process, and it is only when the whole of the material is saturated with moisture that it becomes heterogeneous again. The concentration of internal stresses upon swelling and the degree of swelling of the NC depend strongly on the strength of the binder-filler interaction, as well as on the plasticizing action of the substance sorbed by the NC [6, 8, 9].

The aim of the present work is to establish the relation between the thermophysical and mechanical characteristics of the clay-containing nanocomposite that has sorbed the moisture and the structural changes attending the deformation process under different kinds of load and at different temperatures.

Institute of Polymer Mechanics, Latvian University, 23 Aizkraukles Str., Riga, LV-1006, Latvia. Translated from Inzhenerno-Fizicheskii Zhurnal, Vol. 83, No. 3, pp. 421–429, May–June, 2010. Original article submitted October 5, 2009; revision submitted November 10, 2009.

Objects and Methods of Investigation. We have investigated a nanocomposite whose composition included epoxy resin, a hardener — polyoxypropylene with end amine groups (Jeffamine® D-400), and a filler — clay nanoparticles (content c = 2, 4, 6 mass %).

Epoxy resin based on epichlorohydrin and diphenylolpropane (bisphenol A) contains end epoxy groups:

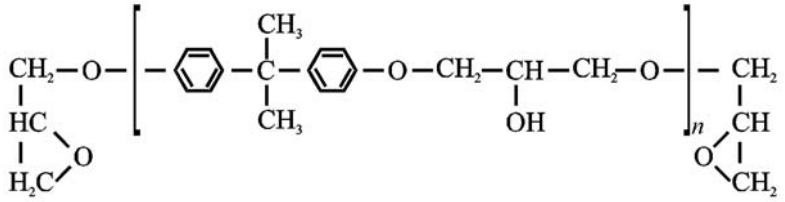

Polyoxypropylene

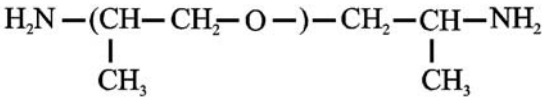

has a high degree of crystallinity (~95%), an amorphous phase T_g equal to ~75°C, and a glass transition temperature of the crystalline phase ~60–65°C. It has a fairly close molecular packing since the bond between carbon and oxygen atoms is shorter than between carbon atoms, is easy to orient in tension, and, when heated, is destroyed with the formation of low-molecular-weight products [10].

The clay is montmorillonite having the composition

$$[(Mg_{0.33}Al_{1.67})Si_4O_{10}(OH)_2]Na_{0.33},$$

which crystallizes in a monoclinic system in the form of scales of thickness ~1 nm and diameter ~100 nm. The presence of hydroxyl groups on its surface determines the strengthening properties. Octadecylamine served as the surface modifier.

Specimens of the unfilled binder and the NC were held in atmospheres with humidity φ = 24, 77, and 98% until they reached the equilibrium state. The equilibrium moisture content in the specimens at 20°C was attained after 270 days and equaled w = 0.2, 1.7, and 3.0%, respectively.

Thermomechanical investigations were carried out with the use of an UIP-70M device with specimens heated to 150°C at a rate of 20°C/min with subsequent cooling.

The mass loss kinetics at physical and chemical transformations in the NC was investigated by the thermogravimetric (TG) method. Measurements were made on a "Mettler" TA3000 instrument in the temperature range 20–280°C; the heating rate was 10°C/min.

The structure was investigated by the X-ray diffraction method on a DRON-3M device with photography "in transmitted light" on CuK_α radiation. Scanning of angular intervals was carried out with a 0.1°C step and with a pulse collection time in each step of 90 sec.

Quasi-static tension tests were carried out with the aid of a Zwick 2.5 machine at 20°C with a deformation rate of 5 mm/min.

Creep studies were made at tensile stresses $\sigma = 0.5\sigma_{max}$ on wet specimens; the duration of the experiment was 7.5 h for forward and 17 h for backward creep.

Results and Discussion. The features of the phase and relaxation transitions in heating the NC specimens have been studied by the method of thermomechanical analysis (TMA) in the absence of external load. The typical TMA curves of the NC specimens held in an atmosphere with a relative humidity of 24 and 98% until they reached the equilibrium state are presented in Fig. 1.

The general rule for all NC modifications, including those held in an atmosphere with a humidity of 77%, is the presence on the thermal expansion curves of a narrow (5–10°C) temperature range of a sharp change in the character of deformability when in the course of heating the expansion at T_1 is replaced by a shrinkage, and then at T_2 a new growth of deformation begins just as quickly. Such dependences are characteristic of amorphized polymers [11] in which, after passing through T_g, crystallization occurs very quickly to cause hardening of the material. Then, also

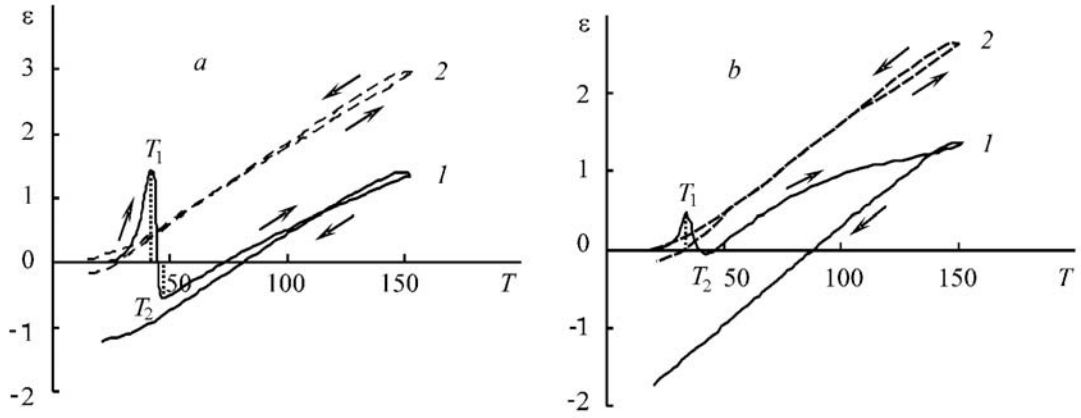

Fig. 1. TMA curves of NC specimens with c = 4%, φ = 24% (a) and 98% (b): 1, 2) heating–cooling cycles.

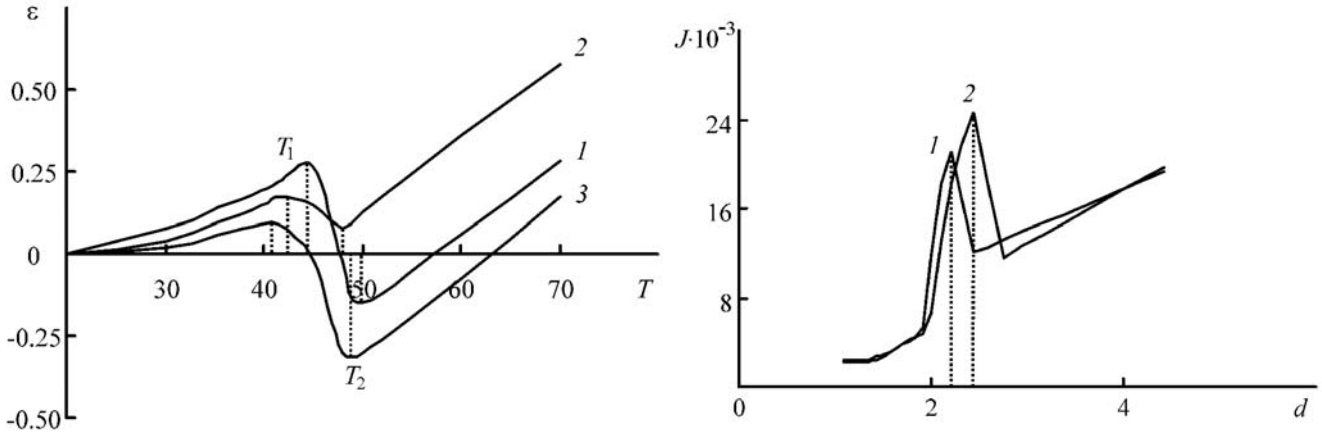

Fig. 2. TMA curves of the binder at φ = 24%: 1–3) heating–cooling cycles.

Fig. 3. Diffractograms of NC specimens with c = 0% (1) and 6% (2).

spontaneously, melting of the crystallites formed in them begins, which just causes a rise on the TMA curve. The fact that the process of shrinkage of the binder in the NC is caused by crystallization is confirmed by experiments with multiple heating of specimens to 70°C and their cooling to 20°C. Figure 2 gives the thermomechanical curves for three heating-cooling cycles and shows that the crystallization process was accompanied each time by shrinkage and the melting process — by spontaneous extension. Consequently, in the 20–70°C temperature range the restructuring process in the binder appears to be reversible; crystallization began at T_1 = 41–45°C, and melting at T_2 = 46–50°C.

X-ray structural analysis also confirms that upon preliminary annealing of specimens at 80°C and subsequent drying in a medium of humidity 24% in the binder the crystalline phase is preserved (Fig. 3, diffractograms 1).

The introduction into the NC composition of clay nanoparticles (diffractogram 2) leads to a change in the parameters of the crystalline reflex of the binder, for example, an increase in the interplanar spacing d and, accordingly, a change in the internal stress in the NC.

It was somewhat difficult to determine T_g from the TMA curves since the attaining by it of the glass transition temperature served as a prerequisite to the binder crystallization in the NC. We assumed that both processes (devitrification and onset of crystallization) proceeded practically simultaneously. Therefore, the deformation maximum temperature T_1 on the TMA curves (Fig. 1) was assumed to correspond to the crystallization temperature, and the T_g value was assumed to be slightly different from it. Comparison of the values of T_1 (T_g) (Fig. 4) of the investigated modifications has made it possible to establish that as a result of moisture sorption, the glass transition temperature of the specimens in a medium with a humidity of 98% decreases by about 10°C compared to the dried specimens. This fact proves that the moisture in the NC acts as a plasticizer.

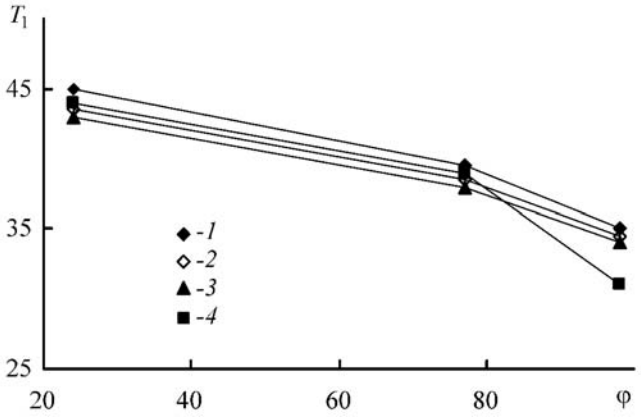

Fig. 4. Glass transition temperature as a function of the atmospheric humidity for NCs with different filling: 1) 0%; 2) 2; 3) 4; 4) 6.

TABLE 1. Values of the Thermal Expansion Coefficients of NCs with Different φ and *c*

φ, %	*c*, %	$\alpha_1 \cdot 10^{-5}$, °C^{-1} $T \in$ (20–35) °C	$\alpha_2 \cdot 10^{-5}$, °C^{-1} $T \in$ (35–50) °C	$\alpha_3 \cdot 10^{-5}$, °C^{-1} $T \in$ (50–70) °C	$\alpha_4 \cdot 10^{-5}$, °C^{-1} $T \in$ (100–150) °C
24	0	11.9	–123.0	21.4	21.6
	2	7.6	–200.0	25.6	20.1
	4	8.0	–130.0	19.4	19.0
	6	5.3	–65.0	23.9	18.3
77	0	6.5	–68.8	20.0	15.2
	2	7.9	–50.0	20.1	13.3
	4	7.3	–38.0	21.7	12.6
	6	10.7	–16.0	18.4	13.0
98	0	11.8	–128.0	23.9	6.7
	2	9.7	–159.0	21.3	9.7
	4	8.0	–79.0	20.6	7.2
	6	5.2	–91.0	27.1	3.6

An increase in the filler content from 2 to 6 mass % practically does not affect the temperature values of the structural transitions in the NC within the atmosphere with equal humidity (Fig. 4). Apparently, shielding the clay surface by an ODA modifier decreases access to the surface hydroxyl groups. Therefore, the conditions for the formation of hydrogen bonds with an epoxy binder worsen. The weak strengthening effect from the filling is possibly associated with both the low mechanical strength of clay nanoparticles and their possible agglomeration [12, 13].

We have also determined by the TMA curves the temperature ranges of a sharp change in the NC deformation rate. For the quantitative characteristic, we took the thermal expansion coefficient (TEC). The table gives the TEC values for four temperature ranges corresponding to the vitreous state of the NC α_1, as well as to its states of crystallization α_2, recrystallization α_3, and additional structuring α_4. From the analysis of the table it is seen that the NC specimens, both dried and wet, with a temperature below T_g are characterized by practically equal values of α_1 which, however, decrease with increasing degree of filling with clay. In the T_1–T_2 temperature range, the process is characterized by negative values of α_2, which also change with increasing degree of filling with clay. Characteristically, α_3 in all NC modifications and degrees of their moistening is practically the same. Upon reaching a temperature of 80°C in moist specimens the physicochemical processes lead to a significant rigidification of the structure and to a decrease in α_4 to values corresponding to the vitreous state. The decrease in the TEC of moist specimens can be due to at least two processes — loss of moisture and structurization. In so doing, a significant increase in the hysteresis effects is observed (Fig. 1b).

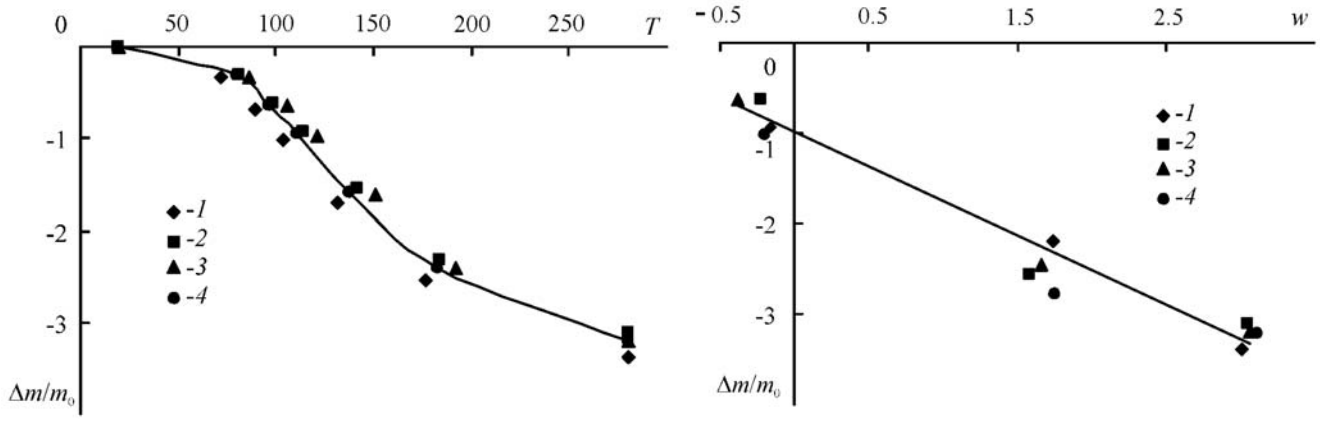

Fig. 5. Mass loss curves of NC specimens at φ = 98% with different filling: 1) 0%; 2) 2; 3) 4; 4) 6.

Fig. 6. Interrelation between the moisture content and the mass loss in heating NC specimens with different filling. Designations 1–4 are same as in Fig. 5.

From the mass loss curves of the thermogravimetric analysis (Fig. 5) it is seen that in the 80–170°C temperature range the mass loss process is the fastest, which agrees with the decrease in the TEC. The maximum mass loss is observed in specimens held in an atmosphere with a humidity of 98%. For instance, at a clay content of 6% the NC mass loss at 150°C is 1.5%, and in the binder it is 2% under the same conditions; however, no strict dependence on the degree of filling is observed. A further increase in the temperature leads to a decrease in the mass loss rate. Proceeding from the practically linear interrelation between the moisture content and the mass loss (Fig. 6), it may be stated that upon heating the NC up to 280°C the moisture desorption process prevails.

Thus, the thermal history of the first cycle of heating to 150°C and cooling to 20°C led to irreversible structural changes in the NC in the course of the TMA. Repeated studies enabled us to make certain of irreversible thermal processes in the NC. The TMA curves of the second cycle upon heating consists now of two portions connected at the point corresponding to T_g (curves 2 in Fig. 1). Hysteresis effects are practically absent, i.e., the TMA curves reflect a state of the composite close to equilibrium. Thus, combining the conditions of heating and cooling NC specimens, we can realize in them various structural transitions leading to complete amorphization. Accordingly, the crystalline phase too can not only be present in them in different quantities but be also represented by formations differing in the degree of perfection and sizes [7, 11].

The experiments described above were performed on unloaded NC specimens. To establish the relationship between the thermal characteristics and the structural changes attending the NC deformation process, we investigated their mechanical behavior under quasi-static tension. Figure 7 shows the deformation curves of an NC (c = 6%) whose specimens were held in atmospheres with a humidity of 24, 77, and 98% until they attained the equilibrium state. The deformation curves of the binder and an NC with a clay content of 2 and 4% have a similar character.

It has been established that as the degree of filling increases, there is an increase in the elastic modulus of the NC by about 30%, whereas with increasing moisture content its decrease is noted (Fig. 8). In turn, as is seen from Fig. 7, dried specimens fail in the air brittely, and their maximum strength is twice that of specimens held at a humidity of 98%. Intermediate strength values are observed in specimens held at a humidity of 77%. Characteristically, whatever the moisture content, maximum strength values are attained at a 2.5–3% deformation of the NC. These values should obviously be considered as corresponding to the limit of induced elasticity of the NC in a given atmosphere. Exceeding this limit in the process of extension of moist specimens leads to the initiation of transverse growth of microcracks. This conclusion is based on the fact that on the working part of the specimens whitening of the material and a loss of their transparency were observed. Such changes appear when the refractive indices of the microcrack material and of the block material of the NC differ [7, 15]. In [7, 11, 14, 15]; it has been shown that the microcracking effect manifests itself only when glassy- or crystal-state materials are loaded. Microcracks differ fundamentally from breaking macrocracks in that that they contain a material able to transfer stresses. In [7, 15], it has been

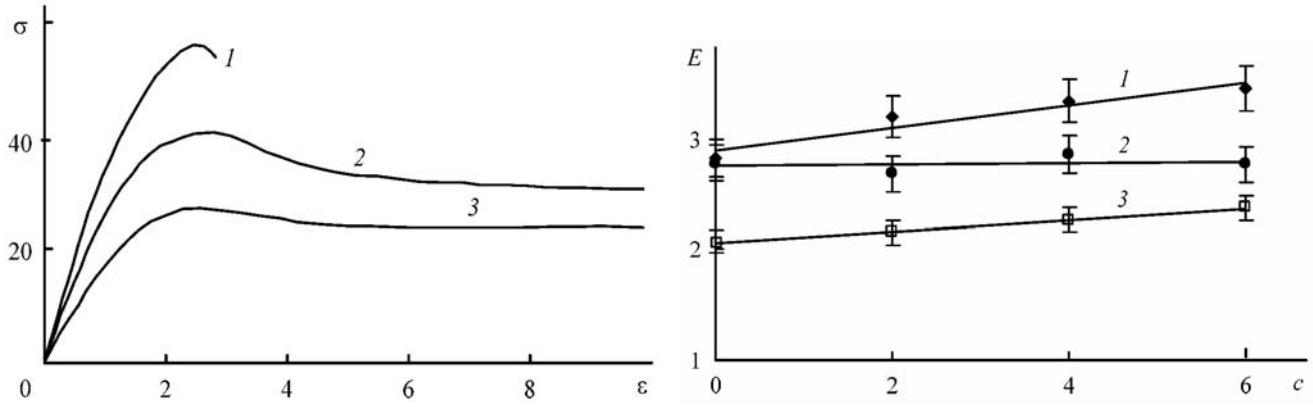

Fig. 7. Deformation curves of NC specimens at c = 6% and various values of φ: 1) 24%; 2) 77; 3) 98.

Fig. 8. Elastic modulus of the NC depending on the nanofiller concentration for various φ values. Designations 1–3 are same as in Fig. 7.

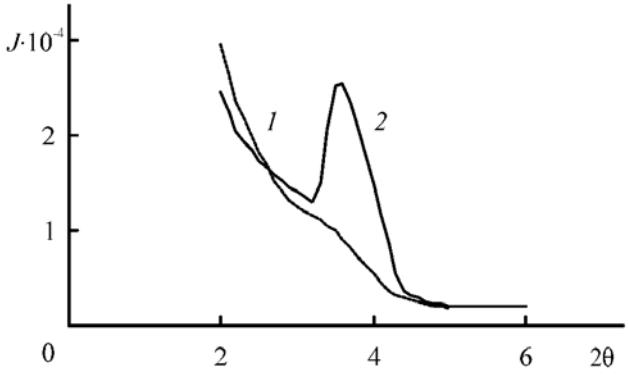

Fig. 9. Diffractograms of a tension predeformed NC specimen cut from the "neck" region: 1) meridian; 2) equator.

shown that the edges of microcracks are connected by thin fibrillas (~10 nm) whose length increases in tension and, therefore, the interface area increases. Consequently, in moist NC specimens at deformations exceeding the induced elasticity limit, specific zones of plastic deformation and microcracking are formed. With increasing deformation the curve goes to a plateau and a "neck" is formed. In so doing, the breaking deformation reaches ~60%, whereas in dry specimens it reaches no more than 3–4%. Apparently, the "neck" is formed when certain critical conditions are attained. The influence of such factors as plastification and orientation of the polymer in the NC should be considered simultaneously. Their role reduces to changing the position of the working test temperature with respect to the temperatures of transitions, which leads to changes in the strength — its increase due to the orientation and decrease due to the plasticization. Meanwhile, in [11] it was noted that the "necking" is not connected with plastic deformations, and the role of moistening is to facilitate significantly the development of induced-elastic deformation of the material. Then the tension-induced "necking" should be considered as a relaxation process of the localized nonoriented-oriented transition of the polymer inside the microcracks.

The data of X-ray structural analysis correlate well with the assumptions about structural changes in the NC at its deformations to high values. Figure 9 presents meridional and equatorial diffractograms of NC specimens prestretched to failure. It is seen that in the region of small angles on the equatorial diffractogram a peak caused by the crystalline phases is present, while it is absent from the meridional diffractogram. This effect can be explained by the fact that at large stretches the material acquires an almost completely fibrillized oriented structure, which leads to the disappearance of interfaces characteristic of microcrack walls. Apparently, joining of microcrack walls occurs and, therefore, no diffuse scattering is observed on the diffractogram meridian.

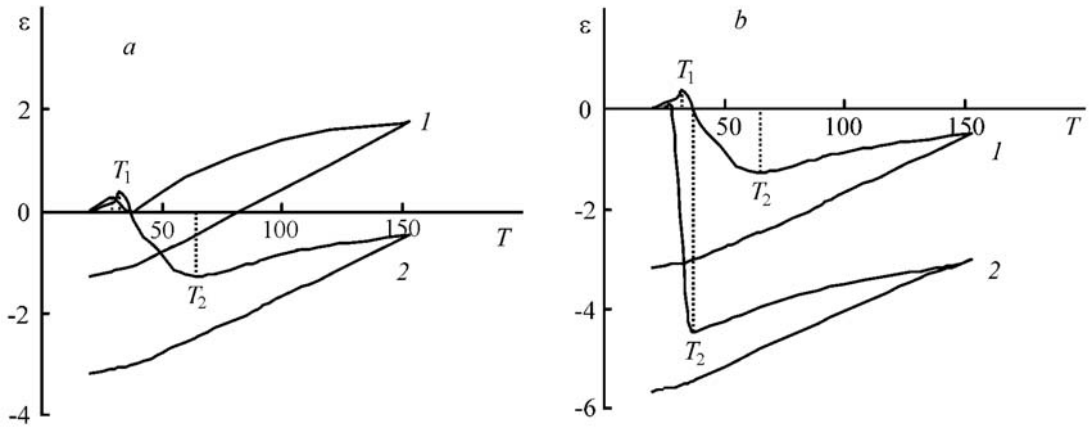

Fig. 10. TMA curves of NC specimens cut across (1) and along (2) the stretching directions under quasi-static tension (a) and specimens cut along the stretching direction under quasi-static tension (1) and creep (2) (b).

It is interesting to compare the deformation and "necking" mechanisms depending on the NC loading conditions and the plasticizing effect of moisture. Moist specimens (φ = 98%) were predeformed in the air in the regime of quasi-static tension ($\dot{\varepsilon}$ = const) and creep (σ = const) until the whole of the working part material went into the "neck." Then we cut from them specimens along and across the direction of stretching. From the analysis of the TMA curves (Fig. 10a) it is seen that the thermal expansion of the NC specimens cut in mutually perpendicular directions differs markedly and there are anisotropic changes in the thermomechanical characteristic. Analogous laws have also been obtained for specimens upon creep tests. For heated NC specimens cut along the stretching direction, in both quasi-static tension and creep experiments, their clear similarity to the TMA curves is observed (Fig. 10b). For instance, in the glass transition temperature range their linear sizes sharply decrease. However, specimens oriented in the creep regime (curve 2) shrink to a greater extent and the process proceeds in a narrower temperature range than for specimens oriented under quasi-static tension (curve 1). Next, when temperatures of 37°C (under creep) and 64°C (under quasi-static tension) are attained, the process of their spontaneous stretching begins as sharply as shrinkage. From a comparison with the TMA curves of unloaded NC specimens (Fig. 1b), it is seen that crystallization of oriented specimens begins at lower temperatures, and the shrinkage value (assumed to be proportional to the degree of crystallinity) is much larger than that for loaded specimens. This is explained by the fact that at orientation a considerable ordering of the NC structure occurs, which is a kind of a crystalline "blank," and therefore its transition to the crystalline structure is considerably facilitated. As a consequence of the crystallization of fibrillar aggregates the NC specimens do not completely regain their sizes either. At the same time, the TMA curves of the specimens cut across the orientation, as the results of quasi-static tension and creep experiments show, practically coincide in terms of the character of the change in the deformability and in its value. The TMA curves of the second heating cycle of specimens reflect, as for unloaded specimens, only one transition connected with the NC devitrification. Thus, from the above data it follows that the specific features of the thermomechanical behavior of the nonequilibrium structure of the NC upon stretching is largely determined by the quantity of the initial binder, which has gone to the oriented state, from which fibrillar aggregates of microcracks have been constructed. Their strength determines the macroscopic strength of the material at "cold" stretching. With heating, the fibrillas acquire a greater mobility; they become able to coalesce, and the coagulation process occurs. This leads to a disorientation of fibrils with respect to one another, which shows up macroscopically as a shrinkage of the NC. The process proceeds in the region of the glassy state and, consequently, it is supermolecular in nature, i.e., it is not accompanied by a disorientation of molecules inside a fibril. Above T_g complete disorientation of the NC structure occurs and, as a consequence, "healing" of microcracks occur [7, 9]. It is possible that additional stitching of the NC also leads to a suppression of microcracks already in the first cycle upon heating to higher temperatures.

Conclusions. Investigation of clay-containing NC points to a complex influence of adsorption effects on its properties, which hampers obtaining a material exhibiting a wide variety of thermomechanical properties. The general rule for all NC modifications is crystallization that takes place in the course of the TMA. Restructuring begins in the

region of reaching T_g. In repetitive heating to 70°C, crystallization and melting of crystallites in the NC binder are reversible. However, upon heating to 150°C the structure becomes completely amorphized and the TMA curves of the second heating cycle reflect an NC state close to equilibrium.

An increase in the content of clay nanoparticles to 6 mass % practically does not change the temperature values of the structural transitions in the NC and does not lead to a strengthening effect. Sorbed moisture plays the role of a plasticizer in the NC. A content of 3% of moisture in it leads to a decrease in T_g by about 10°C. The practically linear interrelation between the moisture content in the NC and the mass loss upon its heating to 280°C points to the prevalence of the moisture desorption processes.

The thermomechanical behavior of the NC depends not only on the moistening and thermal history, but also on the regime of their preloading. For instance, dried specimens fail brittely under tension. In moist specimens above the limit of induced elasticity, a plastic deformation (microcrak zone) is formed, "necking" occurs, and deformations reach ~60%. The data of X-ray structural analysis confirm that in the course of the stretching process almost the whole of the NC acquires a fibrillized oriented structure. Crystallization of oriented specimens begins in the course of the TMA at higher temperatures and their degree of crystallinity is much higher than in unloaded specimens. The features of the thermomechanical behavior of the NC upon quasi-static pretension or creep are largely determined by the quantity of the binder, which has gone to the oriented state, from which fibrillar aggregates of microcracks have been constructed. Changes take place in the region of T_g and, consequently, they have a supermolecular character. In heating, the fibrils acquire a greater mobility, and the coagulation process proceeds. This leads to a disorientation of fibrils with respect to one another and a decrease in the interface area, which shows up macroscopically as a shrinkage of the NC.

NOTATION

c, mass content of the filler, %; d, interplanar spacing, nm; E, elastic modulus, GPa; J, intensity of X-rays, pulse/sec; m, mass, g; T, temperature, °C; T_g, glass transition temperature, °C; w, relative moisture content, %; α, thermal expansion coefficient, $^oC^{-1}$; ε, deformation, %; $\dot{\varepsilon}$, deformation rate, mm/sec; θ, stress, MPa; θ, scattering angle, deg; φ, relative humidity of the air, %. Subscripts: 0, initial; 1, 2, 3, 4, subsequent values; max, maximum; g, glass transition.

REFERENCES

1. A. Yasmin, J. J. Luo, J. L. Abot, and I. M. Daniel, Mechanical and thermal behavior of clay/epoxy nanocomposites, *Compos. Sci. Technol.*, **66**, 2415–2422 (2006).
2. P. J. Yoon, T. D. Fornes, and D. R. Paul, Thermal expansion behavior of nylon 6 nanocomposites, *Polymer*, **43**, 6727–6741 (2002).
3. F. Hussain, J. Chen, and M. Hojjati, Epoxy-silicate nanocomposites: cure monitoring and characterization, *Mater. Sci. Eng. A*, **445–446**, 467–476 (2007).
4. D. R. Paul and L. M. Robeson, Polymer nanotechnology: nanocomposites, *Polymer*, **49**, 3187–3204 (2008).
5. T. Glaskova and A. Aniskevich, Moisture absorption by epoxy/montmorillonite nanocomposite, *Compos. Sci. Technol.*, **69**, 2711–2715 (2009).
6. V. P. Korhov, E. A. Faitelson, T. I. Glaskova, and Yu. O. Janson, Influence of moisture on the structure and properties of the interphase layer of a composite based on an epoxy binder with disperse filler, *Mech. Compos. Mater.*, **41**, No. 4, 365–370 (2005).
7. A. L. Volynskii and N. F. Bakeev, *Highly Dispersed Oriented State of Polymers* [in Russian], Khimiya, Moscow (1984).
8. M. O. Richardson (Ed.), *Polymer Engineering Composites* [Russian translation], Khimiya, Moscow (1980).
9. A. E. Bar (Ed.), *Structural Properties of Plastics* [Russian translation], Khimiya, Moscow (1967).
10. I. P. Losev and E. B. Trostyanskaya, *Chemistry of Synthetic Polymers* [in Russian], Khimiya, Moscow (1971).
11. B. Ya. Teitel'baum, *Thermomechanical Analysis of Polymers* [in Russian], Nauka, Moscow (1979).
12. A. A. Berlin and V. E. Basin, *Principles of the Adhesion of Polymers* [in Russian], Khimiya, Moscow (1974).

13. F. R. Eirich and T. L. Smith, Molecular-mechanical aspects of the isothermal rupture of elastomers, in: H. Liebowitz (Ed.), *Fracture*, Vol. 7, Pt. 1, *Fracture of Nonmetals and Composite Materials* [Russian translation], Mir, Moscow (1976), pp. 104–469.
14. G. A. Andrianova, *Physicochemistry of Polyolefins* (*Structure and Properties*) [in Russian], Khimiya, Moscow (1974).
15. J. P. Berry, Destruction of glassy polymers, in: H. Liebowitz (Ed.), *Fracture*, Vol. 7, Pt. 1, *Fracture of Nonmetals and Composite Materials* [Russian translation], Mir, Moscow (1976), pp. 7–66.

Publikācija 6

Effect of moisture on the viscoelastic properties of epoxy-clay nanocomposite

Aniskevich K. K., Glaskova T. I., Aniskevich A. N., and Faitelson Ye. A.

Institute of Polymer Mechanics, University of Latvia, Riga, Latvia

Mechanics of Composite Materials, 2010, Vol. 46, No. 6, p. 839-852.

МЕХАНИКА КОМПОЗИТНЫХ МАТЕРИАЛОВ.— 2010.— Т. 46, № 6. — С. 839—852
MECHANICS OF COMPOSITE MATERIALS. — 2010.— Vol. 46, No. 6. — P. 839—852

К. К. Анискевич, Т. И. Гласкова, А. Н. Анискевич, Е. А. Файтельсон*

Латвийский университет, Институт механики полимеров, Рига, LV-1006 Латвия

ВЛИЯНИЕ ВЛАГИ НА ВЯЗКОУПРУГИЕ СВОЙСТВА ГЛИНОСОДЕРЖАЩЕГО НАНОКОМПОЗИТА НА ОСНОВЕ ЭПОКСИДНОГО СВЯЗУЮЩЕГО

K. K. Aniskevich, T. I. Glaskova, A. N. Aniskevich, and Ye. A. Faitelson*

EFFECT OF MOISTURE ON THE VISCOELASTIC PROPERTIES OF AN EPOXY-CLAY NANOCOMPOSITE

Keywords: epoxy binder, montmorillonite, viscoelastic properties, moisture, moisture-time analogy

The results of a complex study on the viscoelastic behavior of an epoxy-clay nanocomposite after a long-term exposure to moisture are presented. The main laws of variation in the glass-transition temperature of the nanocomposite in relation to the different content of filler and absorbed moisture were determined by using a thermomechanical analysis. The loading levels in creep experiments were chosen according to the results of quasi-static tensile tests. The sets of creep and creep recovery curves obtained were approximated by the Boltzmann–Volterra linear integral equation with account of the principle of moisture-time analogy. The variation in the spectrum of retardation time of the epoxy resin with introduction of the nanofiller was estimated. It is shown that the moisture-time reduction function correlates with changes in the forced rubber-like elasticity and the volume of nanocomposite specimens upon their moistening.

Ключевые слова: связующее эпоксидное, монтмориллонит, свойства вязкоупругие, влага, аналогия влаго-временная

Представлены результаты комплексного исследования вязкоупругого поведения глиносодержащего нанокомпозита на основе эпоксидного связующего после длительного воздействия влаги. Применение метода термомеханического анализа позволило установить основные закономерности для температуры стеклования нанокомпозита с разным содержанием наполнителя и сорбированной влаги. По результатам экспериментов на квазистатическое растяжение были выбраны уровни нагрузки для экспериментов

*Автор, с которым следует вести переписку: Tatjana.Glaskova@pmi.lv
Corresponding author: Tatjana.Glaskova@pmi.lv

на ползучесть. Полученные семейства кривых ползучести и обратной ползучести были аппроксимированы с помощью линейного интегрального уравнения Больцмана—Вольтерра с учетом принципа влаго-временной аналогии. Проведена оценка изменения спектра времен запаздывания и функции редукции эпоксидной смолы при введении в нее частиц нанонаполнителя. Показано, что функция влаго-временной редукции коррелирует с изменением предела вынужденной высокоэластичности и изменением объема образцов нанокомпозита при увлажнении.

Введение

Использование новых материалов — нанокомпозитов (НК) на основе полимерной матрицы — в разных областях техники, конструкциях, а также в электронике требует оценки их длительной деформативности и прочности в условиях воздействия разных факторов окружающей среды (нагрузок, повышенной и/или переменной температуры и/или влажности). Для прогнозирования длительной деформативности и прочности традиционных композитных материалов (КМ) — полимеров, наполненных микрочастицами минералов, а также армированных стекло-, угле- и органоволокнами, — применяется метод аналогий [1—3]: напряженно-временной, температурно-временной и влаго-временной. В основе этого метода лежит редуцирование времени посредством ускорения релаксационных процессов при увеличении уровня нагрузки, температуры и относительного влагосодержания в материале, характеризуемое функцией редукции.

Релаксационные процессы в полимере обусловлены его молекулярной и надмолекулярной структурой. При введении микронаполнителя структура полимера изменяется преимущественно в пограничном с частицей наполнителя слое. Толщина пограничного слоя и его относительное объемное содержание в микрокомпозите невелики. Поэтому релаксационные процессы в связующем в КМ и в блоке протекают одинаково и их функции редукции совпадают. Введение в полимер наночастиц, имеющих огромную удельную поверхность (~800 $м^2/г$), может оказать влияние на его надмолекулярную структуру в силу образования новых связей и/или уменьшения свободного объема. Это в свою очередь может привести к изменению скорости и интенсивности релаксационных процессов и, как следствие, — к изменению спектра времен релаксации и функции редукции. Основываясь на том, что вязкоупругие свойства полимера, в частности ползучесть, имеют релаксационную природу, можно ожидать, что изменение характера кривых ползучести полимера после введения в него частиц нанонаполнителя даст информацию об изменении его спектра времен запаздывания или релаксации. Таким образом, сравнительное изучение ползучести нанокомпозита и базового полимера в условиях воздействия повышенной температуры и/или влажности будет полезно не только с точки зрения составления прогноза длительной деформативности, но и с точки зрения возможности оценки изменения спектра времен запаздывания (релаксации) полимера в КМ по сравнению с полимером в блоке в расширенном временном диапазоне.

В работах [4, 5] было выявлено снижение податливости при ползучести термопластов (полиамида и поликапролактона) после введения в них наночастиц органомодифицированной глины. Для прогнозирования длительной деформативности НК в [5] использовали принцип температурно-временной аналогии. Значения функции температурно-временной редукции, характеризующей изменение скорости ползучести при изменении температуры, для НК с содержанием наполнителя = 1 и 2,5% по массе были выше, чем для связующего в блоке, а при увеличении содержания нанонаполнителя до 7,5% — уменьшались.

Ранее в [6] было изучено влияние наполнения эпоксидного связующего плоскими частицами монтмориллонита (ММТ) на его сорбционные свойства. Благодаря существенному увеличению извилистости пути диффундирующих молекул воды процесс сорбции влаги в НК протекает медленнее, чем в ненаполненном полимере [7]. Так, при = 6% коэффициент диффузии влаги в НК уменьшается вдвое [6]. Однако предельное (равновесное) влагосодержание в НК выше, чем в базовом полимере. Оно увеличивается с увеличением содержания наполнителя. Избыточная по сравнению со связующим в блоке влага в НК может находиться в пограничном слое или в самом связующем НК, которое может отличаться от связующего в блоке плотностью упаковки макромолекул, т.е. свободным объемом. Особенности структуры связующего в КМ могут быть выявлены при исследовании вязкоупругих свойств НК и их изменении после увлажнения НК.

Исходя из сказанного цели настоящей работы можно сформулировать следующим образом: изучение возможности применения метода влаго-временной аналогии к прогнозированию длительной ползучести нанокомпозита на примере наполненной наночастицами ММТ эпоксидной смолы и оценка изменения спектра времен запаздывания и функции редукции эпоксидной смолы при введении в нее частиц нанонаполнителя.

Материал и методы исследования

Исследовали нанокомпозит, в состав которого входили эпоксидная смола на основе эпихлоргидрина и дифенилолпропана (бисфенол А), отвердитель — полиоксипропилен с концевыми аминовыми группами (Jeffamine® D-400) и наполнитель — наночастицы глины (= 2, 4, 6% по массе). Глина — монтмориллонит, имеющая состав $[(Mg_{0,33}Al_{1,67})Si_4O_{10}(OH)_2]Na_{0,33}$, кристаллизуется в моноклинной системе в форме чешуек толщиной ~1 нм, диаметром ~100 нм [8]. Наличие гидроксильных групп на поверхности частиц наполнителя определяет эффект армирования. Модификатором поверхности являлся октадециламин. Материал предоставлен исследовательским институтом SYNPO (Пардубице, Чехия).

Призматические образцы размером 2,0 8,0 100,0 (±0,1) мм вырезаны из тонких пластин размером 2 200 200 мм^3. Для снятия технологических напряжений произведен отжиг образцов в термошкафу при 80 C в течение 3 ч. После отжига образцы ненаполненного связующего и НК были выдержаны до равновесного состояния в атмосферах с влажностью = 24, 77 и

98% при температуре 20 C. В процессе увлажнения периодически измеряли массу и длину образцов для определения в них влагосодержания и деформации набухания. Равновесное влагосодержание в образцах достигнуто за 270 сут и было равным $w = 0{,}2,\ 1{,}7,\ 3{,}0 \pm 0{,}05\%$ соответственно [6].

Для определения температуры стеклования НК проведены термомеханические испытания [9] при нагревании образцов до 150 °C со скоростью 2 C/мин и последующем охлаждении с помощью прибора УИП-70М.

Испытания на квазистатическое растяжение [10] проводили на машине Zwick 2.5 при 20 °C со скоростью перемещения верхней траверсы 5 мм/мин, что соответствует скорости деформации 1,2 10 ^{3} $с^{-1}$.

Исследование ползучести осуществляли при постоянных растягивающих нагрузках, составляющих 50% от разрушающей для каждого НК и каждого значения равновесного влагосодержания. Испытания проводили при комнатной температуре 20 ± 3 °C. Длительность эксперимента на ползучесть 7,5 ч, на обратную ползучесть — 17 ч.

Результаты экспериментов

Термомеханический анализ. Применение метода термомеханического анализа к НК с разным содержанием наполнителя и влаги [9] показало следующее (рис. 1): а) с увеличением влагосодержания в НК его температура стеклования понижается от 45 до 35 °C; б) изменение температуры стеклования НК в зависимости от содержания наполнителя в пределах атмосферы с одинаковой влажностью невелико (лежит в пределах разброса экспериментальных данных).

Слабый усиливающий эффект наполнения, возможно, связан с низкой плотностью сшивания макромолекул связующего, расположенных вокруг частиц наполнителя, а также с возможной агломерацией частиц наполнителя

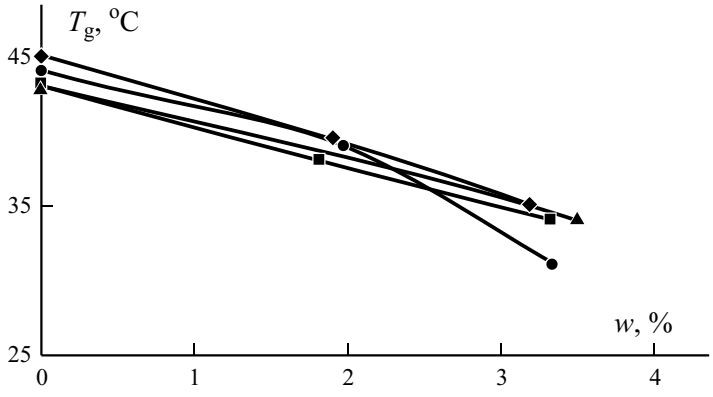

Рис. 1. Зависимость температуры стеклования T_g от влагосодержания w для НК при = 0 (◆); 2 (■); 4(▲); 6% по массе (●).

[11, 12]. В свою очередь снижение температуры стеклования эпоксидного связующего и НК на его основе с увеличением влагосодержания (см. рис. 1) свидетельствует о том, что сорбированная влага является пластификатором, т.е. способствует уменьшению интенсивности взаимодействия между макромолекулами и облегчению подвижности их сегментов, что приводит к ускорению релаксационных процессов. Температура стеклования эпоксидного связующего в блоке и НК смещается в область температур, которые лишь на 10—20 °С выше комнатной, т.е. температуры, при которой проводились механические испытания. Поэтому приложение нагрузки может привести к тому, что эпоксидное связующее перейдет в область высокоэластичности, характеризуемую большими деформациями. По крайней мере, рассматриваемое здесь эпоксидное связующее с повышенным влагосодержанием находится в области перехода из стеклообразного состояния в высокоэластическое.

Набухание. Известно, что процессу влагопоглощения в полимерах сопутствует набухание, которое обязательно связано с изменением структуры полимера и приводит к увеличению объема образцов [13]. Среди факторов, определяющих набухание полимеров, таких, как природа полимера и растворителя, гибкость полимерных цепей, молекулярная масса и химический состав полимера, наличие поперечных связей между цепями и температура, немаловажное значение имеют особенности надмолекулярной структуры полимера, в частности, плотность упаковки макромолекул. Таким образом, исследуя особенности кинетики набухания НК с разным содержанием наполнителя, можно получить необходимую информацию о структурных изменениях, происходящих в образцах НК при их увлажнении.

Зависимости деформации набухания НК от содержания влаги в связующем для всех рассматриваемых НК приведены на рис. 2. Как видно из данных рисунка, для всех материалов наблюдается ограниченное набухание с

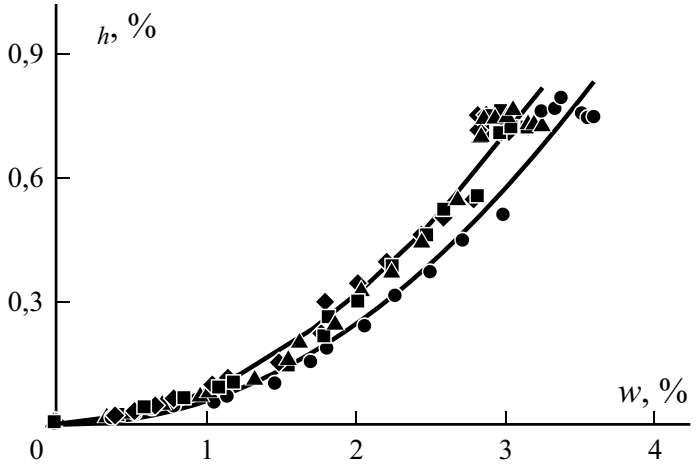

Рис. 2. Зависимость деформации набухания $_h$ образцов НК от величины w при 0 (◆); 2 (■); 4 (▲); 6% по массе (●).

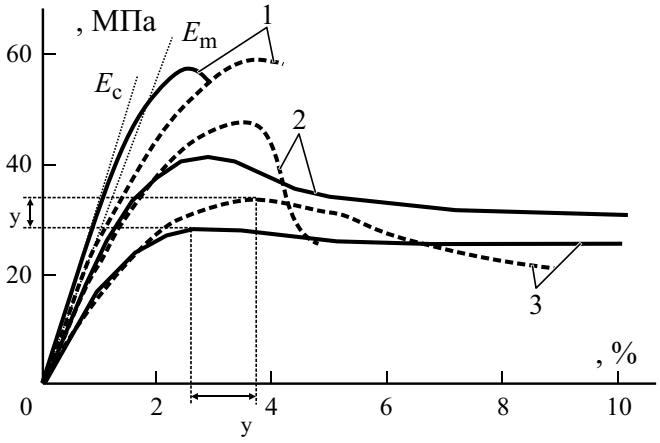

Рис. 3. Кривые деформирования эпоксидного связующего (- - -) и НК при = 6% (——) и = 24 (*1*); 77 (*2*); 98% (*3*).

возрастающей скоростью. Для НК при = 2 и 4% и связующего в блоке зависимости деформации набухания от содержания влаги одинаковы, т.е. набухание НК обусловлено набуханием связующего. Для НК с бо́льшим содержанием наполнителя (= 6%) набухание связующего в КМ меньше, чем в блоке. Очевидно, часть молекул воды, сорбированной НК, находится не в связующем, а в пограничном с частичками наполнителя слое (или ввиду менее плотной упаковки макромолекул связующего в НК часть молекул воды находится в его свободном объеме).

Растяжение в режиме квазистатики. Для оценки влияния содержания наполнителя и сорбированной влаги на модуль упругости и прочность материала было изучено поведение образцов эпоксидного связующего и НК при квазистатическом деформировании [10]. Для примера на рис. 3 приведены кривые деформирования эпоксидного связующего и НК при = 6%, образцы которых были предварительно выдержаны до равновесного состояния в атмосферах с влажностью 24, 77 и 98%. Кривые деформирования НК с содержанием наполнителя 2 и 4% имеют аналогичный характер с ярко выраженным пределом вынужденной эластичности (на рисунке не приведены).

Как видно из данных рис. 4, наполнение эпоксидного связующего частицами ММТ приводит к увеличению модуля упругости сухого материала примерно на 30% и к уменьшению предела вынужденной эластичности и деформации, соответствующей этому пределу, примерно на 1/3. Увеличение влагосодержания в материале, как в эпоксидном связующем, так и НК, обусловливает уменьшение модуля упругости и предела вынужденной эластичности; деформация, соответствующая этому пределу, практически не изменяется при изменении влагосодержания в материале. Сухие (выдержанные в атмосфере при = 24%) образцы разрушаются более хрупко, чем увлажненные (при = 98%). Прочность первых в два раза превышает прочность вторых. Промежуточные значения прочности наблюдаются у образцов, выдержанных в атмосфере при = 77%.

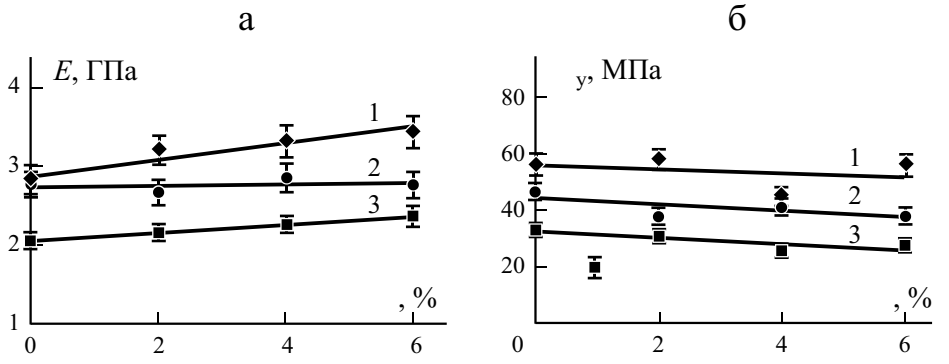

Рис. 4. Зависимость модуля упругости E (*а*) и предела вынужденной эластичности $_y$ (*б*) от величины для НК, увлажненного до равновесного состояния при 24 (*1*); 77 (*2*); 98% (*3*).

Ползучесть и обратная ползучесть. Результаты испытаний на кратковременную (7,5 ч) ползучесть сухого материала показывают, что кривые податливости при ползучести (за исключением мгновенной податливости I_0 $1/E$) НК без наполнителя и при = 4% практически совпадают (рис. 5—*а*), т.е. эффект влияния наполнителя выражен в зависимости мгновенной податливости (или модуля упругости) от содержания наполнителя. Увлажнение материала приводит к заметному увеличению податливости при ползучести (рис. 5—*а*). Это, очевидно, обусловлено тем, что состояние материала близко к высокоэластическому.

Эксперименты на обратную ползучесть показали, что деформации не возвращаются в нуль после 17 ч наблюдения, однако тенденция уменьшения деформаций во времени сохраняется (рис. 5—*б*).

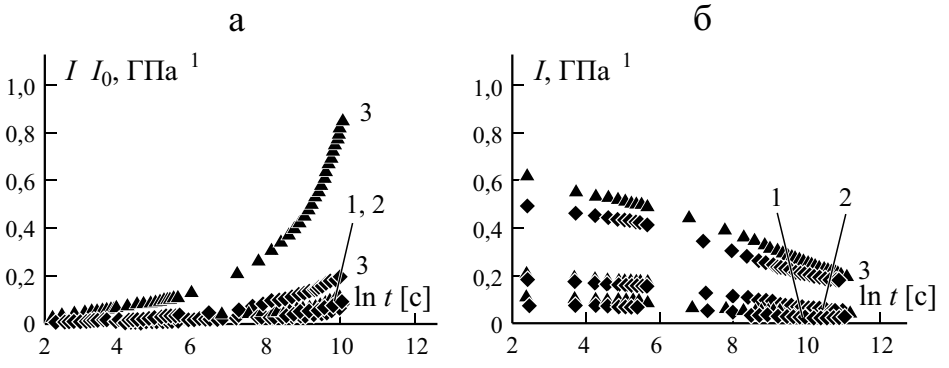

Рис. 5. Кривые податливости НК при = 0 (◆) и 4% (▲) и = 24 (*1*), 77 (*2*) и 98% (*3*) для прямой (*а*) и обратной ползучести (*б*).

Описание ползучести и обратной ползучести

Для описания семейства кривых ползучести и обратной ползучести НК с разным содержанием наполнителя при разных значениях w использовали линейное интегральное уравнение Больцмана—Вольтерра

$$(t) \quad \frac{(t)}{E} \quad \frac{1}{E}\int_0^t K(t \quad s)\ (s)ds \tag{1}$$

с ядром ползучести в виде суммы экспонент

$$K(t) \quad \sum_{i\ 1}^{n} \frac{b_i}{\ \ i} e^{t/\ \ i}. \tag{2}$$

Здесь $_i$, b_i, $i = 1,..., n$, — спектр времен запаздывания. Согласно принципу влаго-временной аналогии

$$t \quad t\, a_w, \tag{3}$$

где $a_w(w)$ — функция влаго-временной редукции, характеризующая изменение спектра времен запаздывания при изменении относительного влагосодержания в материале.

Для напряжения, меняющегося по закону

$$(t) \qquad {}_0H(t) \qquad {}_0H(t \quad t_0), \tag{4}$$

где $t = 0$ — момент приложения нагрузки, t_0 — момент разгрузки, $H(t)$ — функция Хевисайда, податливость $I(t) \quad \frac{(t)}{\ \ 0}$ будет иметь следующую зависимость от времени:

для ползучести при $t \quad t_0$

$$I(t) \quad \frac{1}{E} \quad \frac{1}{E}\sum_{i\ 1}^{n} b_i(1 \quad e^{\ ta_w/\ \ i}), \tag{5}$$

для обратной ползучести при $t \quad t_0$

$$I(t) \quad \frac{1}{E}\sum_{\ \ i}^{n} b_i e^{\ ta_w/\ \ i}(e^{t_0 a_w/\ \ i} \quad 1). \tag{6}$$

Функция влаго-временной редукции выбрана в виде

$$\ln a_w \qquad {}_1 w \qquad {}_2 w^2. \tag{7}$$

Такие формы зависимости использовали ранее для эпоксидных связующих и композитов на их основе [2, 14, 15].

Как уже было отмечено, после 17 ч наблюдения тенденция уменьшения во времени деформации при обратной ползучести сохраняется. Иными сло-

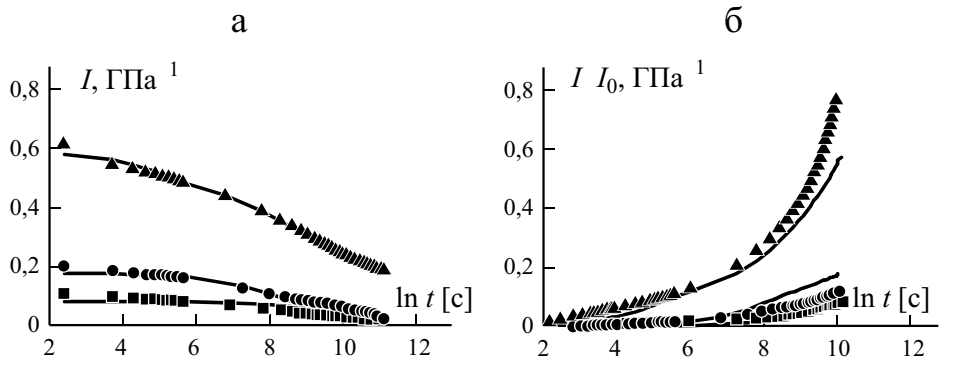

Рис. 6. Кривые податливости при обратной ползучести (*а*) и ползучести (*б*) НК (4%), полученные экспериментально при $w = 0$ (■); 2,04 (●); 3,52% (▲). Линии — аппроксимация эксперимента формулой (6) с учетом (7) (*а*) и расчет по формуле (5) с учетом (7) (*б*).

вами, есть основание предполагать, что деформации ползучести обратимы. Для проверки этого предположения необходимо параметры модели, определенные по результатам испытаний на ползучесть, применить для случая обратной ползучести или наоборот.

Для определения спектров времен запаздывания $_i$, b_i, $i = 1,..., n$ (2) и функции влаго-временной редукции (7) НК с разным содержанием наполнителя воспользуемся результатами испытаний на обратную ползучесть. Для каждого значения семейство кривых податливости при обратной ползучести, соответствующих разным уровням влагосодержания w, аппроксимировали выражением (6) с учетом (7). Задачу аппроксимации решали с использованием SIMPLEX алгоритма, реализованного на языке FORTRAN. Целевая функция задавалась в виде среднеквадратичного отклонения расчета от эксперимента. Начальные значения времен запаздывания выбирали с равномерным шагом в логарифмическом масштабе, т.е. 1, 10, 100 и т. д.; число экспонент n в ядре ползучести (2) равно семи. В процессе минимизации целевой функции слагаемые со значением предэкспоненциального множителя порядка 10^{-3} и менее отбрасывали. Экспонент в ядре ползучести (2) осталось четыре.

В качестве примера на рис. 6—*а* приведены результаты аппроксимации кривых податливости при обратной ползучести в полулогарифмических координатах для НК с содержанием наполнителя 4%. Проверка применимости изложенной модели показала удовлетворительное описание экспериментов на ползучесть (рис. 6—*б*). Полученные в результате аппроксимации спектры времен запаздывания и функции влаго-временной редукции НК с разным содержанием наполнителя приведены на рис. 7 и 8 соответственно. Спектры времен запаздывания для НК при = 2 и 4% (рис. 7) практически не отличаются от спектра для связующего в блоке: они имеют единую ампли-

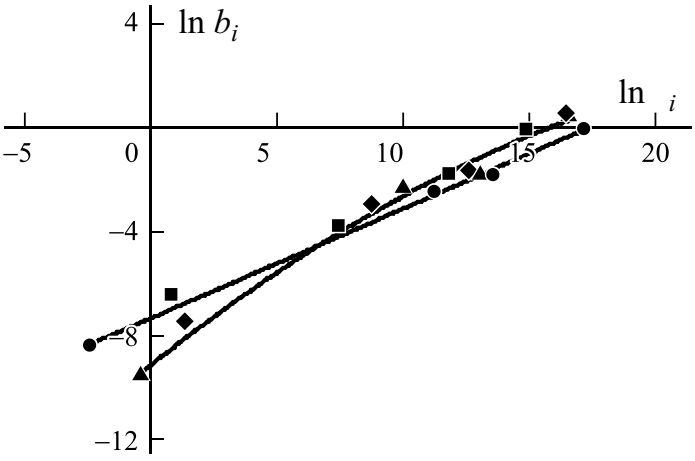

Рис. 7. Спектры времен запаздывания НК при = 0 (◆); 2 (■); 4 (▲); 6% (●).

тудную огибающую. В случае же = 6% эти спектры различаются: времена запаздывания увеличиваются, интенсивность несколько уменьшается. В результате огибающая спектра является более пологой, чем для связующего в блоке и НК при < 6%.

Функции влаго-временной редукции НК с разным содержанием наполнителя (рис. 8) нелинейны, их графики — вогнутые линии, характеризующие усиление влияния сорбированной влаги при увеличении ее содержания в материале. Сравнение функций влаго-временной редукции НК при разных значениях показало, что введение малого количества наполнителя (= 2%) ослабляет влияние влаги на вязкоупругие свойства связующего в КМ. Воз-

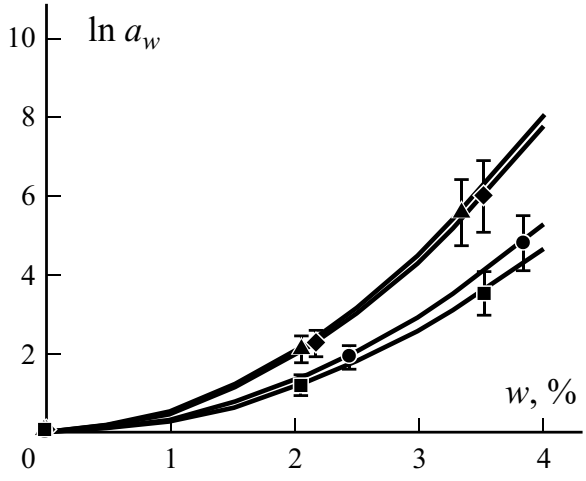

Рис. 8. Функции влаго-временной редукции НК при = 0 (◆); 2 (■); 4 (▲); 6% (●), полученные путем аппроксимации семейства кривых обратной ползучести материала с разным влагосодержанием формулами (6), (7).

можно, это вызвано взаимодействием частиц наполнителя с макромолекулами связующего с образованием физических связей. Возможно также, что часть сорбированной влаги находится в межфазном слое [6]. С увеличением коэффициента наполнения влияние влаги на вязкоупругие свойства связующего в КМ усиливается и при = 6% это влияние такое же, как для связующего в блоке. Частицы наполнителя разрыхляют структуру связующего в НК, скорость релаксационных процессов в области больших времен уменьшается.

Влияние равновесного влагосодержания в НК на его вязкоупругие свойства выражено в изменении предела вынужденной эластичности в квазистатических испытаниях (см. рис. 4—*б*). В соответствии с уравнением Эйринга зависимость предела вынужденной эластичности от скорости деформации имеет вид

$$_{\text{y}} \quad A \quad B \ln \dot{}. \tag{8}$$

Учитывая релаксационную природу вязкоупругости $\dot{}_{i}$ const(w), имеем

$$\ln \frac{\dot{}_{1}}{\dot{}_{0}} \quad \ln \frac{{}^{0}_{i}}{{}^{1}_{i}} \qquad \ln a_w, \tag{9}$$

т. е. изменение предела вынужденной эластичности должно коррелировать с функцией редукции. Такая корреляция существует: для НК с разным содержанием наполнителя изменение предела вынужденной эластичности прямо пропорционально значению функции влаго-временной редукции (рис. 9). Выявленная корреляция может служить основой для альтернативного определения функции влаго-временной редукции по результатам квазистатических испытаний в режиме постоянной скорости деформирования.

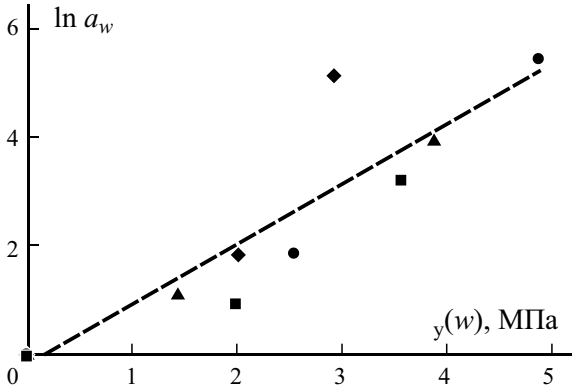

Рис. 9. Корреляция функции влаго-временной редукции (7) и изменения предела вынужденной эластичности в квазистатических испытаниях для НК при = 0 (◆); 2 (■); 4 (▲); 6% (●).

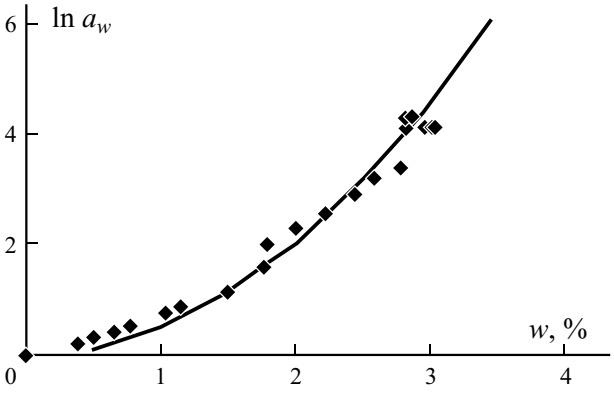

Рис. 10. Функция влаго-временной редукции эпоксидного связующего: точки — расчет по формуле (10) с использованием зависимости деформации набухания от относительного влагосодержания (см. рис. 2); линия — аппроксимация семейства кривых обратной ползучести на рис. 8.

Существует еще один альтернативный способ определения функции редукции — по объемной деформации [15]. К сожалению, при увлажнении образцов измеряли лишь деформацию, характеризующую изменение толщины. Набухание НК с разным содержанием наполнителя иллюстрируют данные рис. 2. Полагая, что связующее в блоке изотропно, вычислим объемную деформацию набухания $\frac{V}{V_0}$ 3 $_h$ и, используя зависимость функции редукции от изменения объема [14]

$$\ln a_w \quad \frac{1}{f_0^2}\frac{V}{V_0}\frac{1}{1 \quad \frac{1}{f_0}\frac{V}{V_0}}, \tag{10}$$

получим функцию влаго-временной редукции (рис. 10), совпадающую с определенной из экспериментов на ползучесть в случае $f_0 = 0{,}062$.

Таким образом, корреляция функции влаго-временной редукции связующего в блоке с изменением объема образцов при увлажнении позволяет провести ее оценку по результатам набухания.

Выводы

1. Наполнение эпоксидного связующего наночастицами модифицированного ММТ увеличивает жесткость (модуль упругости) примерно на 30%, на 1/3 уменьшает предел вынужденной эластичности и деформацию, соответствующую этому пределу, практически не изменяет температуру стеклования сухого материала. Слабый усиливающий эффект наполнения, возможно, связан с низкой плотностью сшивания эпоксидного связующего

вокруг частиц наноглины из-за взаимодействия полимерных цепей с поверхностью частиц и формированием межфазного слоя.

2. С ростом влагосодержания в НК до 3% по массе модуль упругости снижается при всех рассмотренных значениях . Характерно, что независимо от влагосодержания максимальные значения предела вынужденной эластичности достигаются при деформировании НК до 2,5—3%. По-видимому, эти значения следует рассматривать как соответствующие пределу вынужденной эластичности НК в данной среде.

3. Зависимость вязкоупругих свойств НК от влагосодержания в материале, так же как и базового полимера, описывается на основе принципа влаго-временной аналогии. Спектры времен запаздывания НК при $< 6\%$ практически совпадают, а при $= 6\%$ отличаются от спектра времен запаздывания связующего в блоке. Функция влаго-временной редукции, характеризующая влияние влагосодержания в материале на его вязкоупругие свойства, имеет минимальные значения параметров для НК с содержанием наполнителя 2%. Дальнейшее увеличение содержания наполнителя приводит к увеличению параметров функции редукции, и при $= 6\%$ их значения совпадают с таковыми для базового полимера.

4. Корреляция функции влаго-временной редукции с изменением предела вынужденной эластичности свидетельствует о вязкоупругом характере деформирования НК с разным влагосодержанием. Корреляция функции влаго-временной редукции связующего в блоке с изменением объема образцов при увлажнении позволяет провести ее оценку по результатам набухания.

Работа выполнена при финансовой поддержке Европейского социального фонда (проект № 2009/0209/1DP/1.1.1.2.0/09/APIA/VIAA/114 и проект № 2009/0138/1DP/1.1.2.1.2/09/IPIA/VIAA/004).

СПИСОК ЛИТЕРАТУРЫ

1. *Ferry J. D.* Viscoelastic Properties of Polymers. — N. Y.: John Wiley & Sons, 1961. — 218 p.

2. *Уржумцев Ю. С., Максимов Р. Д.* Прогностика деформативности полимерных материалов. — Рига, 1975. — 416 с.

3. *Максимов Р. Д.* Прогнозирование длительного сопротивления полимерных композитов // Механика композит. материалов. — 1984. — № 3. — С. 376—388.

4. *Vlasveld D. P. N., Bersee H. E. N., and Picken S. J.* Creep and physical ageing of PA6 // Polymer. — 2005. — Vol. 46, No. 26. — P. 12539—12545.

5. *Perez C. J., Alvarez V. A., and Vazquez A.* Creep behaviour of layered silicate/starch-polycaprolactone blends nanocomposites // Materials Sci. Eng. A. — 2008. — Vol. 480, Nos. 1—2. — P. 259—265.

6. *Glaskova T. and Aniskevich A.* Moisture absorption by epoxy/montmorillonite nanocomposite // Composite Sci. Technology. — 2009. — Vol. 69, Nos. 15—16. — P. 2711—2715.

7. *Maksimov R. D., Gaidukov S., Zicans J., and Jansons J.* Moisture permeability of a polymer nanocomposite containing unmodified clay // Mechanics of Composite Materials. — 2008. — Vol. 44, No. 5. — P. 505—514.

8. *LeBaron P. C., Wang Zh., and Pinnavaia T. J.* Polymer-layered silicate nanocomposites: an overview // Appl. Clay Sci. — 1999. — Vol. 15, Nos. 1-2. — P. 11—29.

9. *Faitel'son E. A., Glaskova T. I., Korkhov V. P., and Aniskevich A. N.* Structural changes in a clay-containing nanocomposite with a different moisture content caused by its deformation // J. Engineering Phys. Thermophys. — 2010. — Vol. 83, No. 3. — P. 443—451.

10. *Glaskova T. and Aniskevich A.* Moisture effect on deformability of epoxy/montmorillonite nanocomposites // J. Appl. Polymer Sci. — 2010. — Vol. 116, No. 1. — P. 493—498.

11. *Yasmin A., Luo J. J., Abot J. L., and Daniel I. M.* Mechanical and thermal behavior of clay/epoxy nanocomposite // Composites Sci. a.Technology. — 2006. — Vol. 66, No. 14. — P. 2415—2422.

12. *Yoon P. J., Fornes T. D., and Paul D. R.* Thermal expansion behavior of nylon 6 nanocomposite // Polymer. — 2002. — Vol. 43, No. 25. — P. 6727—6741.

13. *Тагер А. А.* Физико-химия полимеров. — М.: Химия, 1968. — 536 с.

14. *Анискевич А. Н., Янсон Ю. О., Анискевич Н. И.* Ползучесть эпоксидного связующего во влажной атмосфере // Механика композит. материалов. — 1992. — № 1. — С. 17—24.

15. *Анискевич К., Крастев Р., Христова Ю.* Вязкоупругие свойства эпоксидной композиции после длительной выдержки в воде // Механика композит. материалов. — 2009. — Т. 45, № 2. — С. 201—210.

Поступила в редакцию 04.08.2010
Received Aug. 4, 2010

Konferences materiāls 1

Effect of moisture sorption on deformability of epoxy/montmorillonite nanocomposite

Aniskevich A.[1], Glaskova T.[1], Spacek V.[2], Sviglerova P.[2]

[1]Institute of Polymer Mechanics, University of Latvia, Riga, Latvia

[2]Research Institute SYNPO, Pardubice, Czech Republic

Proceedings of European conference on Composite Materials, 2006, CD, No. 90.

EFFECT OF MOISTURE ON DEFORMABILITY OF EPOXY/MONTMORILLONITE NANOCOMPOSITE

A. Aniskevich[1], T. Glaskova[1], V. Spacek[2], P. Sviglerova[2]

[1]Institute of Polymer Mechanics, University of Latvia,
Aizkraukles Str. 23, LV-1006, Riga, Latvia
andrej@pmi.lv
[2]Research institute SYNPO, Pardubice, Czech Republic

ABSTRACT

The effect of moisture on mechanical characteristics of epoxy-nanoclay composite is established in the paper. Second Fick's law of diffusion was used to predict moisture diffusivity and equilibrium moisture content using accelerated analytical procedure. The change of the elastic modulus, tensile stress, breaking strain due to moisture absorption was examined. Finally, the estimation of boundary interlayer content in composite and its effect on nanocomposite elastic properties was done. The higher content boundary interlayer consistently leads to greater moisture absorption and as a result the greater change of nanocomposite properties is observed.

1. INTRODUCTION

Interest in polymer layered silicate nanocomposites (NC) is driven by the possibility of exceptional physical property enhancements, e.g. increased elastic modulus and improved barrier properties, at low filler levels. The key to such performance rests in the ability to exfoliate and disperse individual, high-aspect ratio (L/h>300) silicate platelets within the polymer matrix [1]. The complete dispersion of clay nanolayers in a polymer optimizes the number of available reinforcing elements for carrying an applied load and deflecting cracks. The coupling between the tremendous surface area of the clay (~760 m^2/g) and a polymer matrix facilitates stress transfer to the reinforcement phase, allowing for such tensile and toughening improvements [2].

Apart from the mechanical properties, the excellent barrier capability with significantly reduced permeability of moisture and gases is one of the most attractive and useful properties that have not been fully explored in the past [3]. The enhanced gas barrier properties of polymer nanocomposites are now finding some limited application in packaging material and containers for a wide variety of food and beverage products. Meanwhile, the moisture barrier properties of nanocomposites are yet to be exploited.

While epoxy resins are very attractive due to their high strength and stiffness, high temperature resistance, low volatility, low creep, low shrinkage, good adhesion to metal and ceramic substrates, they have a major drawback of high moisture absorption, which in turn degrades the functional, structural and mechanical properties of the composites [4-6].

Because of the large aspect ratio and surface area of the exfoliated silicate layers they act as efficient barriers against transport through the material. The transport speed of gases and vapors through the polymer is reduced because the impenetrable silicate layers cause an increase in the path length for molecules diffusing through the polymer. The reduced transport rate reduces the rate of moisture uptake in hydrophilic polymers. Because

absorption of water reduces the elastic characteristics of hydrophilic polymers, the addition of nanoparticles to reduce the negative effects of water uptake is particularly useful [7].
The objective of this paper is to establish peculiarities of moisture sorption and to show the influence of moisture on deformability of epoxy-nanoclay composite. For this purpose the moisture diffusion behavior in atmospheres with different relative humidity of the nanocomposite containing different clay contents was investigated. The influences of moisture on the change of mechanical properties, such as tensile modulus and strength are also studied.

2. EXPERIMENTAL

Bisphenol A epoxy resin was used as a matrix of the composite. The filler was intercalated octadecylamine modified montmorillonite-based organoclay. The filler content was varied from 0 till 6% by mass.
Specimens in the form of thin plates were used in order to measure the percentage of weight change due to moisture absorption as a one-dimensional diffusion mode. The dimensions of these orthogonal plates were in all our tests 2.0 × 8.0 × 130.0 (± 0.1) mm. Specimens were dried in an oven at 80ºC to remove internal stresses which appeared during their production before starting the tests. The specimens were placed then into the humid atmospheres at room temperature, were periodically removed, wiped, air dried for 5 min, and then weighed with accuracy 0.00005 g.
Moisture sorption was performed in atmospheres with relative humidity φ = 24, 77, and 98% using desiccators with silica gel and saturated solution of salts NaCl and K_2SO_4. Kinetics of moisture sorption was experimentally investigated using sorption method. Specimen swelling was also measured during moisture sorption.
On the other hand, elastic properties during sorption process were determined by using measured specimens eigenfrequences. The method is fully described in [8].
Quasi static tensile tests were performed on the specimens with different clay content in dry and wet state using Zwick testing machine with a crosshead speed of 5 mm/min at room temperature. Four filler mass concentrations c = 0, 2, 4 and 6% were used in order to study the effect of moisture and filler mass fraction on the mechanical behavior of NC under investigation. Four specimens per each filler mass fraction were tested and the values given correspond to their arithmetic mean value.
Thus the effect of moisture on the mechanical properties of epoxy/montmorillonite NC was determined.

3. RESULTS AND DISCUSSION

3.1- Sorption kinetics of NC

The percent weight gain of the composite $w(t)$ may be defined as the difference in weights of the time-varying moistened w_t and initial w_0 specimens, normalized to initial weight of specimens according to relation:

$$w(t) = \frac{w_t - w_0}{w_0} \times 100 . \qquad (1)$$

A series of measurements of moisture content of the specimens was executed at different time intervals. The experimental values of moisture content for nanocomposite with filler

mass fraction c = 0% were plotted in figure 1 versus the square root of time. Each of these data points corresponds to the average value of 4 specimens.

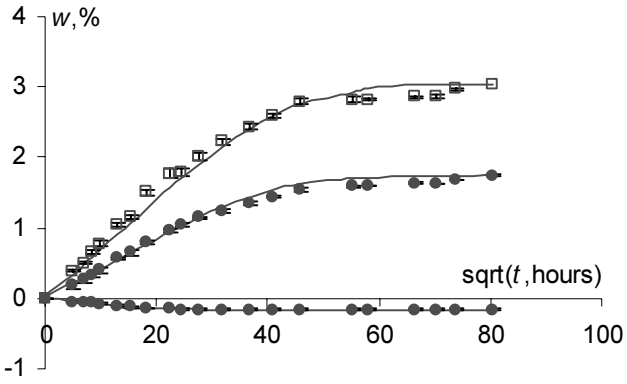

Figure 1: The percentage of experimental weight gain (dots) for NC with c = 0% at atmospheres with φ = 24, 77 and 98% and evaluation by Fick's model (solid lines).

Moisture sorption by epoxy-based adhesives and composites is usually [9] described by Fick's equation, which for the case of one-dimensional diffusion, i.e. if there is a gradient of concentration only along the x axis, is given by

$$\frac{\partial c}{\partial t} = D\frac{\partial^2 c}{\partial x^2}, \tag{2}$$

where $c(x, t)$ is the concentration of diffusing substance in point x at time moment t, D is the diffusion coefficient. We consider the diffusion in a medium bounded by two parallel planes (planes at x = 0 and $x = h$, where h is the thickness of the specimen. The total amount of diffusing substance obtained by integration the solution of equation (2) $c(x, t)$ by the thickness of specimen with initial conditions $c(x, t = 0) = c_0$ and boundary conditions $c(x = 0, x = h, t) = c_\infty$ according to [10] is in the form of trigonometrical series

$$w(t) = w_\infty - 2\frac{(w_\infty - w_0)}{\pi^2}\sum_{k=1}^{\infty}\frac{(1-(-1)^k)^2}{k^2}\sin\left(\frac{\pi k}{h}x\right)\exp\left[-\left(\frac{\pi k}{h}\right)^2 Dt\right], \tag{3}$$

where w_∞ is equilibrium moisture content in specimen.

By the example of NC with c = 0% in figure 1, it is obvious that sorption process is described by Fick's model with good agreement for all concentrations of clay and all atmospheres. Moisture diffusivity and equilibrium moisture content of composite could be determined using accelerated analytical procedure [11]. The general idea is that for large values of time it's enough to describe sorption curve with first term of series in equation (3) (k=1). It means that the rate of moisture sorption becomes

$$\frac{dw}{dt} = \frac{\pi^2 \cdot D}{4 \cdot \left(\frac{h}{2}\right)^2} \cdot (w_\infty - w). \tag{4}$$

Consequently, for large values of time $\frac{dw}{dt}$ is linear-dependent on w and the interception point with w axis corresponds to equilibrium moisture content w_∞. Accordingly the

inclination angle of this curve allows determining diffusion coefficient, which is found by relation

$$D = -\frac{4 \cdot \left(\frac{h}{2}\right)^2}{\pi^2} \frac{\Delta\left(\frac{dw}{dt}\right)}{\Delta w}. \qquad (5)$$

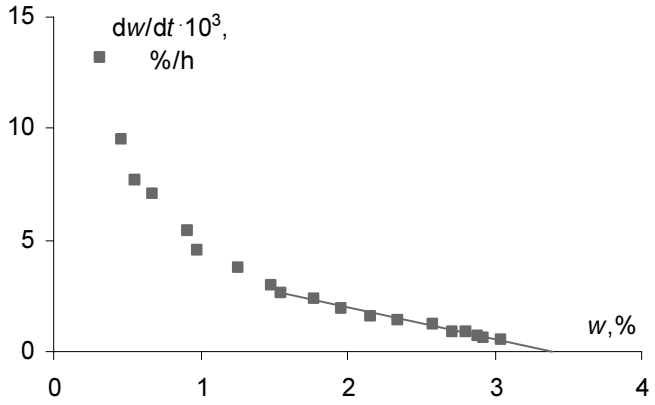

Figure 2: The rate of moisture absorption versus moisture content in NC with c = 4% and atmosphere φ = 98%.

Diffusion coefficients were determined using the above mentioned procedure and are presented in figure 3. It was experimentally confirmed that sorption process in NC passes much more slowly than in pure epoxy resin (as shown in figure 3), for the highest filler content diffusivity reduces about twice. As it was mentioned above this phenomenon takes place owing to the large aspect ratio and surface area of the exfoliated silicate layers, because they act as efficient barriers against transport through the material.

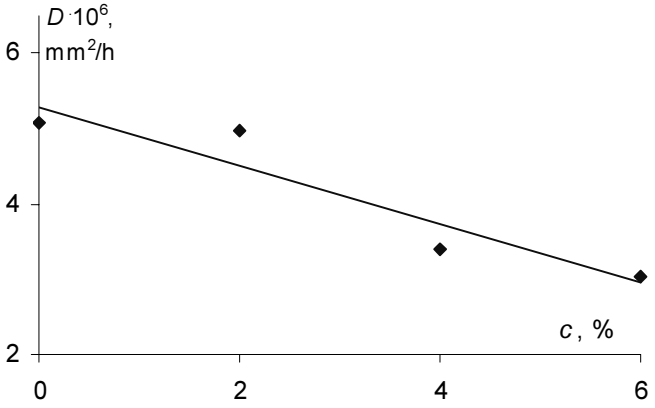

Figure 3: Diffusion coefficient of NC evaluated by equation (5) versus filler mass fraction.

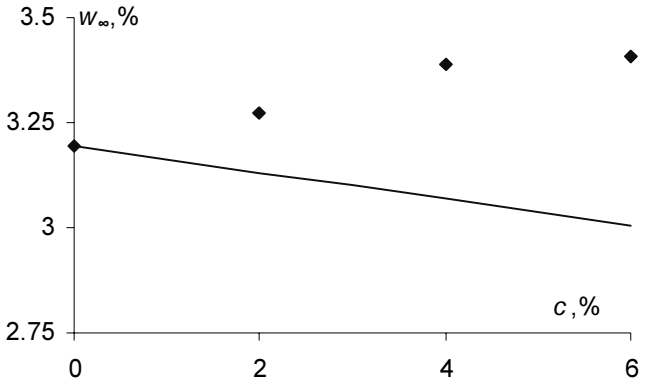

Figure 4: Equilibrium moisture content versus filler mass fraction (dots – result of extrapolation of experimental data, line – evaluation by mixture rule).

The increase of equilibrium moisture content with the increase of clay mass content in NC (shown in figure 4) could be caused by growth of boundary interface mass content. The estimation of interface moisture sorption characteristics can be created using rule of mixture for equilibrium moisture content

$$w_{\infty}^{NC} = w_{\infty}^{ep} \cdot (1 - c - b) + w_{\infty}^{b.l.} \cdot b + w_{\infty}^{f} \cdot c, \quad (6)$$

where $w_{\infty}^{NC}, w_{\infty}^{ep}, w_{\infty}^{b.l.}$ and w_{∞}^{f} are equilibrium moisture contents of NC, epoxy resin, boundary layer and filler accordingly, *c*, *b* are mass filler and boundary layer fractions. It is considered that $w_{\infty}^{f} \to 0$. Such addition of boundary layer around the filler particles allows preventing the deviation of evaluation by mixture rule (6) from results of extrapolation using experimental data.

3.2- Mechanical characteristics

Of the various mechanical properties determined, elastic modulus is one of the possible indicators of clay platelet exfoliation and could be weighted for gauging effects of modifier structure on exfoliation [2].

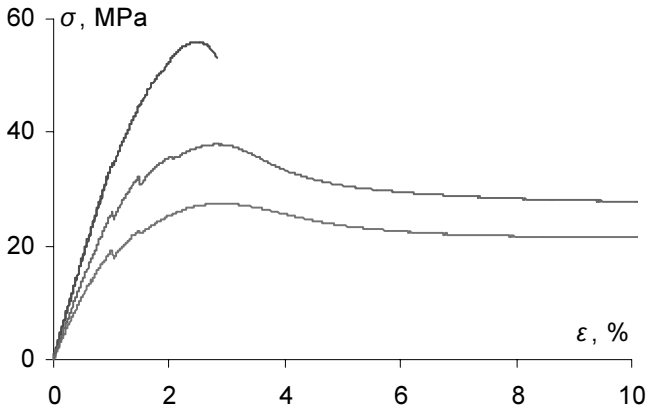

Figure 5: Typical stress-strain curves at a fixed rate of deformation (v = 5 mm/min) for NC with c = 6% and φ = 24, 77 and 98% RH.

Stress-strain curves of NC are shown in figure 5. To examine the effect of organoclay content on mechanical properties, elastic modulus and tensile strength were plotted versus filler mass fraction (figures 6, 7). From these figures it could be observed that elastic modulus increases up to 20% and tensile strength of the nanocomposite decreases about the same value with the increase of organoclay content to 6%.
It was experimentally confirmed that the effect of moisture on the mechanical behavior of NC is substantial. Absorbed moisture essentially plasticizes the composite and changes rupture character from brittle in dry atmosphere to plastic in humid atmospheres. Tensile strength of moistened composite drops twice. Elastic modulus both of moistened pure epoxy resin and nanocomposite is reduced approximately 1/3 in comparison to initial state.

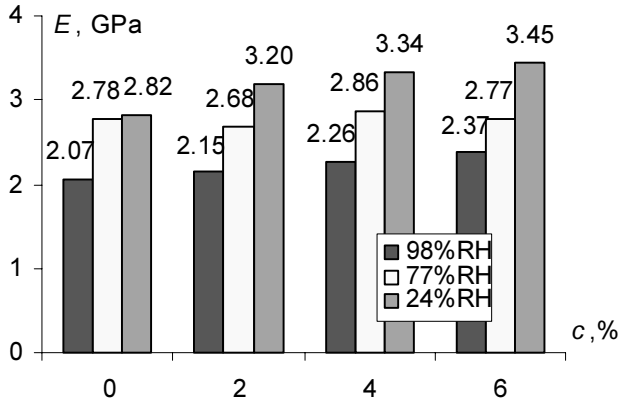

Figure 6: Elastic modulus of NC in atmospheres with different relative humidity versus filler mass fraction.

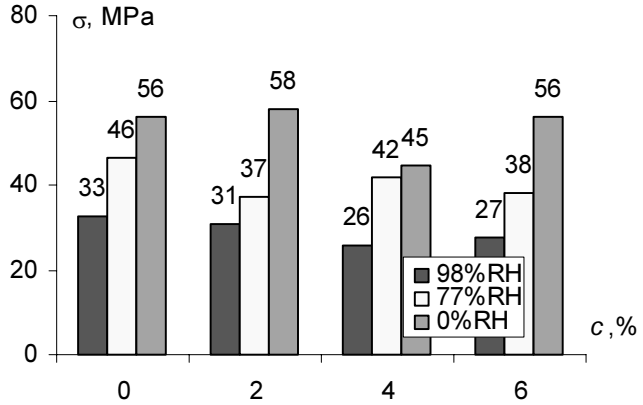

Figure 7: Tensile strength of NC in atmospheres with different relative humidity versus filler mass fraction.

The relative change of elastic modulus for different filler fractions and atmospheres with different humidity was evaluated using measured specimens eigenfrequencies during sorption process. Figure 8 illustrates observed reduction of elastic modulus of NC in

atmosphere with relative humidity 98%. Appreciably, the negative effect on elastic modulus of NC is reduced at high filler mass fractions.

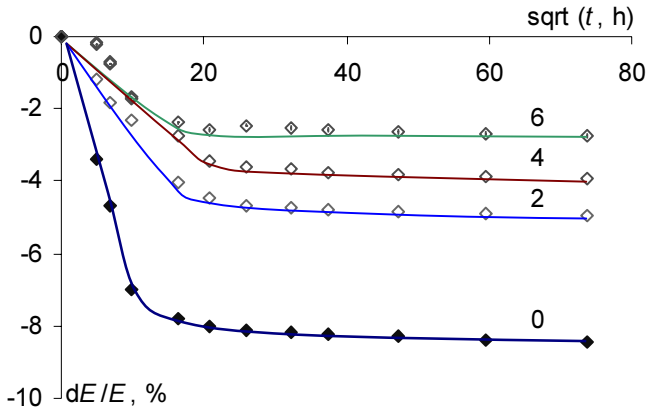

Figure 8: Relative change of elastic modulus of NC with different clay content (numbers above curves) with time in atmosphere φ = 98%.

The efforts were being made to estimate the effect of boundary layer sorption characteristics on nanocomposite elastic properties. As it was argued in figure 4 mixture rule could not describe equilibrium moisture content of NC without including the third phase – boundary layer. The same deviation in evaluation by mixture rule from results obtained experimentally concerns dependence of elastic modulus on absorbed moisture content as presented in figure 9.

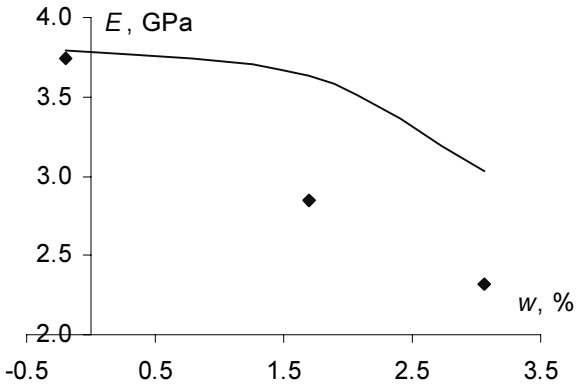

Figure 9: Elastic modulus of NC with c = 6% versus absorbed moisture content (dots – experimental data, line – evaluation by mixture rule).

The change of elastic modulus under effect of moisture by example of NC with filler mass fraction 6% proves that moisture which exists in boundary layer significantly influences the elastic modulus. As a result the effect of moisture on elastic modulus predicted by mixture rule, where moisture content by boundary layer wasn't taken into account is hardly underestimated. Logically enough, the higher content of boundary layer consistently leads to greater moisture absorption and consequently the greater change of nanocomposite properties which are sensitive to moisture.

4. CONCLUSIONS

In the present paper the effect of moisture absorption on the mechanical properties of NC was examined. The second Fick's law of diffusion was used for the evaluation of the diffusion coefficient and equilibrium moisture content of the materials tested. Moreover, tensile tests and measurements of specimens' eigenfrequencies were carried out for evaluation of the mechanical properties. Finally, an attempt was made to estimate the effect moisture in boundary layer on elastic modulus of NC. From the above investigation the following conclusions may be derived

- As the filler mass fraction is increased the equilibrium moisture content increases. It can be described by the increase of boundary layer content around filler particles which has an additional possibility to absorb moisture.
- It was experimentally confirmed that sorption process in NC passes much more slowly than in pure epoxy resin. Diffusion coefficient for high filler fractions reduces about twice.
- Shown effect of moisture on mechanical properties is substantial. Absorbed moisture essentially plasticizes the composite changing the rupture character. Tensile strength of moistened composite drops twice. Elastic modulus both of moistened pure epoxy resin and nanocomposite is reduced approximately 1/3 in comparison to initial state.
- Boundary layer should be taken into account when properties of composite are calculated using properties of components. The higher content of boundary layer consistently leads to greater moisture absorption and as a result the greater change of nanocomposite properties.

References:

1. **Fornes, T., Yoon, P.** etc., "Effect of organoclay structure on nylon 6 nanocomposite morphology and properties", *Polymer*, **43** (2002), 5915-5933.
2. **LeBaron, P., Wang, Z.** etc.,"Polymer-layered silicate nanocomposites: an overview", *Applied Clay Science*, **15** (1999)**,** 11-29.
3. **Kim, J.-K., Hu, C.** etc., "Moisture barrier characteristics of organoclay – epoxy nanocomposites", *Composites Science and Technology*, **65** (2005), 805-813.
4. **Theocaris, P., Kontou, E.,** "The effect of moisture absorption on the thermomechanical properties of particulates", *Colloid and Polymer Science*, **261** (1983), 394-403.
5. **Ishisaka, A., Kawagoe, M.,** "Examination of the time - water content superposition on the dynamic viscoelasticity of moistened polyamide 6 and epoxy", *Journal of Applied Polymer Science*, **93** (2004), 560-567.
6. **Theocaris, P., Papanicolaou, G.,** "Interrelation between moisture absorption, mechanical behavior, and extent of boundary interface in particulate composites", *Journal of Applied Polymer Science*, **28** (1983), 3145-3153.
7. **Vlasveld, D., Groenevold, J.** etc, "Analysis of the modulus of polyamide-6 silicate nanocomposites using moisture controlled variation of the matrix properties", *Polymer*, **46** (2005), 6102-6113.
8. **Latishenko, V.,** "Diagnostics of rigidity and strength of materials" (in Russian), *Zinatne* (1968), 319 p.
9. **Xiao, G., Shanahan, M.,** "Swelling of DGEBA/DDA epoxy resin during hygrothermal ageing", *Polymer*, **39**/14 (1998), 3253-3260.
10. **Crank, J.,** "The mathematics of diffusion", O*xford*, (1956), 347 p.
11. **Aniskevich, A.,** "Experimental investigation of moisture sorption by epoxy resin EDT-10", *Mechanics of Composite Materials*, 6 (1984), 670-673.

Konferences materiāls 2

Modeling of effective elastic properties of composite material containing nanoparticles with an inhomogeneous interphase

Glaskova T., Aniskevich A.

Institute of Polymer Mechanics, University of Latvia, Riga, Latvia

Proceedings of European Conference on Composite Materials, 2008, CD, No. 1454.

MODELING OF EFFECTIVE ELASTIC PROPERTIES OF COMPOSITE CONTAINING NANOPARTICLES WITH AN INHOMOGENEOUS INTERPHASE

T. Glaskova, A. Aniskevich

Institute of Polymer Mechanics, University of Latvia, Aizkraukles St. 23, LV-1006, Riga, Latvia

ABSTRACT

In the current study the effect of filler and interphase on elastic properties of epoxy/clay nanocomposite is estimated at nano- and macrolevels.

The interphase was introduced as a region with gradient of properties nearby the interface of matrix and filler particles. At nanolevel the elastic properties of one single particle containing interphase were considered. The effect of adhesion efficiency was taken into account in the region of the interphase. At macrolevel elastic properties of nanocomposite were described analytically considering the structural components of the nanocomposite: previously calculated effective elastic properties of filler particle containing interphase and elastic properties of the matrix. The results of calculated elastic properties of nanocomposite at macrolevel were compared with results of quasistatic tensile tests and good correlation was found.

It was shown that the thickness of the interphase and the adhesion efficiency should be considered due to their high influence on overall behavior of the nanocomposite. This analysis at nano- and microlevels provides possibility to estimate the effect of filler and interphase properties and content on effective elastic properties of nanocomposite in whole.

1. INTRODUCTION

Due to unique platelet-like layered structure, relatively high elastic modulus and surface of clay nanoparticles it's possible to enhance mechanical and barrier properties of polymers at low filler content (less than 6% by mass) comparing with conventional composites filled with micro-sized inclusions [1-7]. Generally layered silicate-filled composites could be divided into three groups: conventional composites filled with silicate aggregates and no matrix intercalated inside the aggregate stacks; intercalated nanocomposites where matrix material is located in the galleries between the clay platelets but layered structure remains and exfoliated nanocomposites where the filler platelets are divided and separated within the polymer matrix. It should be mentioned that these three cases are just idealization of possible state in composite. Real NC can contain all the structures mentioned above. The predominance of a particular type of structure mainly depends on the manufacturing method of a composite and the degree of dispersion of the filler in it.

Although there have been numerous material syntheses, tests and characterizations of layered silicate-filled nanocomposites in the literature, the fundamental mechanisms are not fully clear and are rarely discussed [2]. Therefore a better understanding and prediction ability is significant in accelerating development and application of nanocomposites.

It should be emphasized that effective properties of two-phase composites have been extensively studied and various micromechanical models have been developed [8-12]. It is well known that the basis of these micromechanics models is elastic solution of an infinite matrix containing one inclusion. Nevertheless many authors proposed that apart from two

base phases there is an interphase layer between particle and matrix and its properties should be taken into account [13-16].
Another point is that anisotropy of the layered silicate should be considered. A single layer of montmorillonite clay is a monoclinic crystal composed of two silica tetrahedral sheets and a central octahedral sheet [17]. Such a monoclinic sheet has 13 independent elastic constants. Taking into account the hexagonal configuration of the tetrahedrons in the two tetrahedral sheets and layered structure of montmorillonite clay it could be assumed that a stack of the silicate layers is a transversely isotropic medium. For the case of intercalated silicate in composite, the layered structure remains while the galleries between layers are filled with polymer. This case also could be represented as transversally isotropic medium from an overall point of view.
In current work the formulas for the composite filled with transversally isotropic spheroidal inhomogeneities with a zero aspect ratio (platelets) will be used. The interphase will be introduced as a region with gradient of properties nearby the interface of filler particle and matrix. At nanolevel the elastic properties of one single particle containing interphase are considered. The effect of adhesion efficiency is taken into account in the region of interphase. At macrolevel elastic properties of nanocomposite are described analytically considering the structural components of the nanocomposite: previously calculated effective properties of filler particle containing interphase and elastic properties of matrix.

2. EXPERIMENTAL

Bisphenol A epoxy resin was used as a matrix of the composite. The filler was intercalated octadecylamine modified montmorillonite-based organoclay. The filler content was varied from 0 till 6% by mass.
The dimensions of these orthogonal plates were in all our tests 2.0 × 8.0 × 130.0 (± 0.1) mm. Specimens were dried in an oven at 80ºC to remove internal stresses which appeared during their production before starting the tests.
Quasi static tensile tests were performed on the specimens with different clay content using Zwick testing machine with a crosshead speed of 5 mm/min at room temperature. Four filler mass concentrations c = 0, 2, 4 and 6% were used in order to study the effect of filler mass fraction on the mechanical behavior of NC under investigation. Four specimens per each filler mass fraction were tested and the values given correspond to their arithmetic mean value.
Thus the effective elastic properties of epoxy/montmorillonite NC were determined.

3. MODELING

Since special attention is given to the evaluation of interphase problem and efficiency of adhesion in nanocomposite appropriate formulas for the elastic properties of nanocomposite filled with randomly oriented transversally isotropic spheroids with zero small aspect ratio will be applied. Wang [2] showed that for the small filler volume fractions Norris approximate expressions [12] for bulk and shear moduli of composite material reinforced with isotropic oblate spheroids with small aspect ratio agree well with explicit Mori-Tanaka expressions which are widely applied for the prediction of nanocomposite properties. These approximate expressions can be written as

$$K = K_1 + \frac{4}{9}\cdot c_f \cdot \left(\chi \frac{\pi}{8} \frac{3-4\cdot\nu_1}{\mu_1\cdot(1-\nu_1)} + \frac{1}{\mu_2}\frac{1-\nu_2}{1+\nu_2} \right)^{-1}, \tag{1}$$

$$\mu = \mu_1 + \frac{1}{15}\cdot c_f \cdot \left(\chi \frac{\pi}{8} \frac{3-4\cdot\nu_1}{\mu_1\cdot(1-\nu_1)} + \frac{1}{\mu_2}\frac{1-\nu_2}{1+\nu_2} \right)^{-1} + \frac{2}{5}\cdot c_f \cdot \left(\chi \frac{\pi}{16} \frac{7-8\nu_1}{\mu_1\cdot(1-\nu_1)} + \frac{1}{\mu_2} \right)^{-1}, \tag{2}$$

where c_f is filler volume fraction, χ is aspect ratio of filler, K, μ and ν are the bulk, shear moduli and Poisson ratio of composite, respectively. Indices 1 and 2 represent matrix and filler properties. The aspect ratio χ is defined as filler particle's thickness related to its length and is for the case of nanocomposite filled with clay platelets much smaller than 1.

In the numerical calculations, the bulk and shear moduli of the matrix and filler are chosen in such way that they reflect the typical properties of epoxy resin and montmorillonite silicate, respectively. Therefore, the Young's modulus and Poisson ratio of the matrix are considered to be $E_1 = 3.45$ GPa and $\nu_1 = 0.35$. The elastic modulus is also experimentally determined value. Unfortunately there is lack of the complete elastic constants of montmorillonite silicate. In the literature it is usually assumed that elastic modulus in the longitudinal direction is ranging from 140 GPa [2] to 175 GPa [18]. In this work it is assumed that $E_2 = 168$ GPa and $\nu_2 = 0.2$. The aspect ratio is chosen to be about 0.015.

Then the calculated values of formulas (1) and (2) are used to evaluate the elastic modulus by the equation

$$E = \frac{9\cdot K\cdot\mu}{3\cdot K+\mu}. \tag{3}$$

The interphase was introduced as a region with gradient of properties nearby the interface of matrix and filler particles. At nanolevel the elastic properties of one single particle containing interphase were considered. The effect of adhesion efficiency was taken into account in the region of the interphase. In our previous investigation [1] it was shown that existence of interphase results in increase of equilibrium moisture content during sorption experiments and as a result a significant decrease of elastic moduli was observed. Since the analytical evaluation for both elastic and sorption properties was higher than that for experimental results it was concluded that interphase has elastic properties lower than the matrix and this conclusion will be used in current work.

The expression of the bulk modulus for the system of filler particle-interphase-matrix is assumed to follow the formula

$$K(x,k,R_f) = \begin{cases} K_2 \text{ if } 0 \le x \le R_f \\ K_1 \cdot \left(1 - \dfrac{(K_2-K_1)}{K_2} \cdot \exp\left(\dfrac{-(x-R_f)}{k\cdot R_f} \right) \right) \text{if } R_f \le x \le R_i(k,R_f), \\ K_1 \text{ otherwise} \end{cases} \tag{4}$$

where x is the coordinate in one-dimensional approach, k is the efficiency of adhesion, R_f is the thickness of the filler particle. The adhesion efficiency is varying from 0 to 1 and expresses the strength of interaction between filler and matrix. The thickness of interphase R_i is denoted as the distance from filler particle to the matrix material with the deviation from matrix properties $\delta = 0.1$ % and is evaluated by formula

$$R_i(k, R_f) = R_f - R_f \cdot k \cdot \ln\left(\delta \frac{\delta \cdot K_2}{(K_2 - K_1)}\right).$$

The similar formulas could be written for the shear modulus.

Figure 1 shows the change of bulk modulus within the system of filler-interphase-matrix material. Four different filler contents corresponding to experimental ones are used in the analysis. It is evident from the figure that increasing filler radius the thickness of the interphase increases. This leads to decrease of effective bulk modulus for the system in whole.

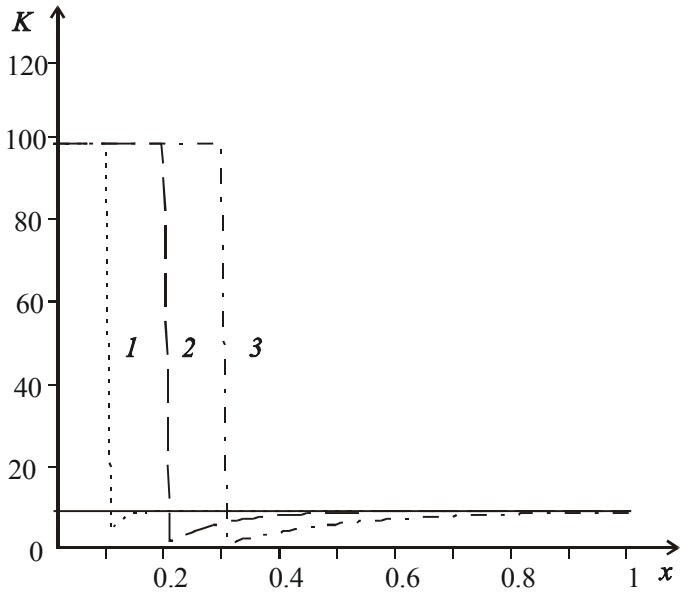

Figure 1: Bulk modulus of the 3-phase system for different filler contents R_f = 1, 2 and 3 % (numbers on the curves) and constant line – pure resin, k = 0.3.

Moreover the adhesion efficiency strongly influences the thickness of the interphase and in this way lowers the value of the elastic moduli with the increase of R_i. The dependence of interphase thickness on the filler thickness and adhesion efficiency is shown in Figure 2. It is clearly seen that with the increase of filler content or thickness of filler particle the thickness of interphase layer increases reaching maximal value for the highest adhesion efficiency (k = 1).

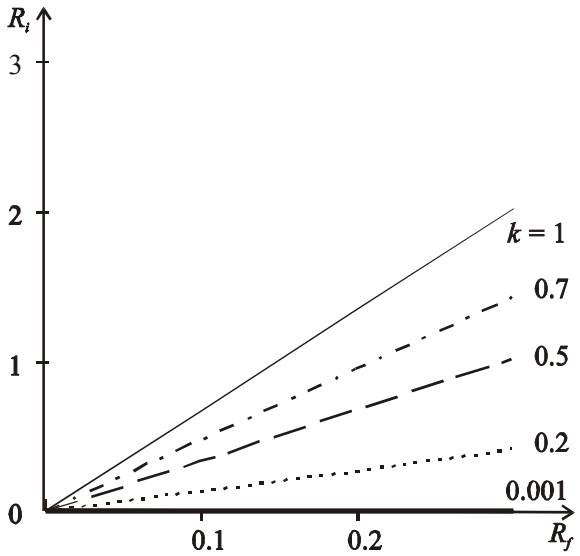

Figure 2: Thickness of the interphase vs. thickness of filler particle for different values of adhesion efficiency.

Then the derived variations of moduli were averaged for system of filler particle-interphase in order to get quasi-particle with constant properties using formulas

$$\overline{K}(k,R_f)=\frac{1}{x_{\max}}\cdot\int_0^{R_i(k,R_f)}K(x,k,R_f)dx,$$

(5)

$$\overline{\mu}(k,R_f)=\frac{1}{x_{\max}}\cdot\int_0^{R_i(k,R_f)}\mu(x,k,R_f)dx.$$

(6)

These elastic characteristics were used to evaluate the elastic modulus of nanocomposite taking into account degree of adhesion and presence of quasi-particles with averaged properties. The elastic modulus is determined by well known relation between elastic characteristics

$$\overline{E}(k,R_f)=\frac{9\cdot\overline{K}(k,R_f)\cdot\overline{\mu}(k,R_f)}{3\cdot\overline{K}(k,R_f)+\overline{\mu}(k,R_f)}.$$

(7)

The final result for the elastic modulus of the composite is showed in Figure 3. As it was mentioned before the elastic moduli in the interphase were assumed to be lower than that of the matrix. As seen from the figure adhesion efficiency greatly influences elastic properties of the composite and lowers the effective elastic modulus. It is interesting to notice that with the increase of adhesion efficiency the thickness of the interphase increases and so the content of the quasi-filler particles grows as well. Nevertheless the averaging by the diameter of the particle gives results which are monotonically growing functions in dependence of filler content.

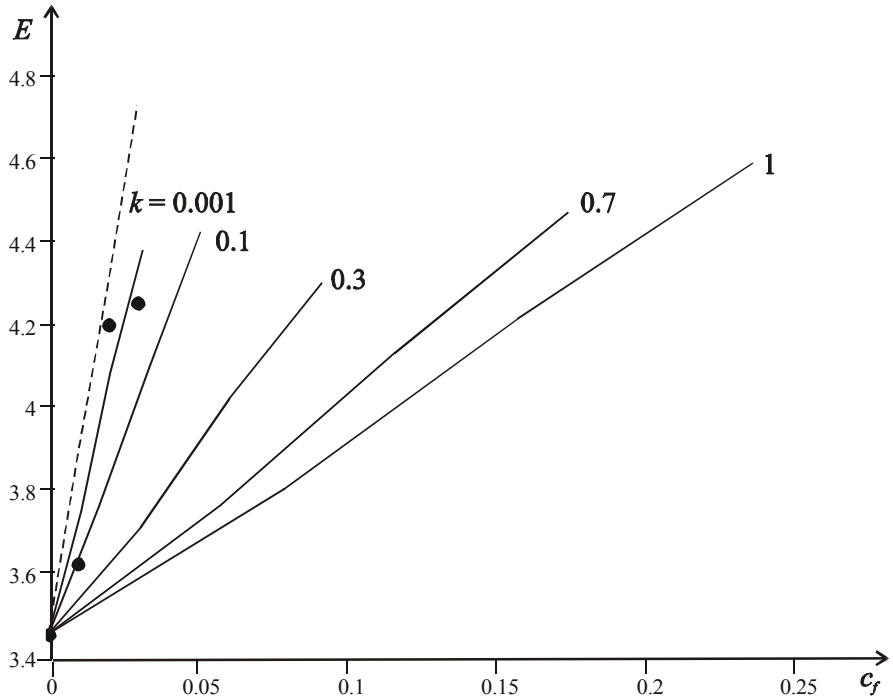

Figure 3. Effective elastic modulus vs. filler volume content (dots – experimental data, dotted line - evaluation by formula (3), solid lines – evaluation by formula (7).

4. COMPARISON BETWEEN MODEL PREDICTION AND EXPERIMENTS AND CONCLUSIONS

As pointed out before the silicate platelets could be dispersed in the polymer in three ways: in aggregates, as in intercalated layered nanocomposite and in exfoliated platelets. In the current work only the last case was considered due to primary emphasis on the interphase problem. The exfoliated platelets were represented as transversally isotropic spheroids with low aspect ratio (0.015). The expressions for the bulk and shear moduli of the composite were presented using expressions of Norris for randomly oriented platelets which are suitable for low filler contents. First the properties of quasi-particle were estimated at nanolevel considering efficiency of adhesion at different filler contents. It should be noted that the stiffness of filler particles in the direction of major axis is the dominating parameter in these calculations. Since the literature data for the elastic constants of montmorillonite is incomplete it could be concluded that these values could be varied in order to get better agreement with the experimental data.

According to the results obtained in the work the theoretical prediction using expressions of Norris agree quite well with the results of quasistatic tensile test. Nevertheless the results of this prediction are higher which can be described by the lack of precise values of parameters like elastic constants and aspect ratio of montmorillonite clay. Another possibility to describe this deviation is to introduce interphase layer. It is clear that taking into account adhesion efficiency and high surface of filler particles quite high content of quasi-particles is obtained in the case of nanocomposite. That's why the thickness of the interphase and adhesion efficiency can greatly influence the mechanical behavior of the nanocomposite and should be considered. This analysis at nano- and microlevels provides

possibility to estimate the effect of filler and interphase properties and content on effective properties of nanocomposite in whole.

ACKNOWLEDGEMENTS

The work presented in this paper has been funded by European Social Fund (ESF) and grant of Latvian Scientific Council Nr. 2005/9.

REFERENCES

1 -Aniskevich A., Glaskova T., Spacek V., Sviglerova P., "Effect of moisture sorption on deformability of epoxy/montmorillonite nanocomposite", *Proceedings of European Conference on Composite Materials*, 2005; CD, No. 091.
2 -Wang J., Pyrz R., "Prediction of the overall moduli of layered silicate-reinforced nanocomposites – part I: basic theory and formulas", *Composites Science and Technology,* 2004; 64: 925-934.
3 –Wetzel B., Haupert F., Zhang M. Q., "Epoxy nanocomposite with high mechanical and tribological performance", *Composites Science and Technology,* 2003; 63: 2055-2067.
4 –Xiong J., Zheng Z., Jiang H., Ye S., Wang X., "Reiforcement of polyurethane composite with an organically modified montmorillonite", *Composites: Part A*, 2007; 38: 132-137.
5 –Weon J. I., Sue H. J., "Effects of clay orientation and aspect ratio on mechanical behavior of nylon-6 nanocomposite", *Polymer*, 2005; 46:6325-6334.
6 –Yasmin A., Luo J. J., Abot J. L., Daniel I. M., "Mechanical and thermal behavior of clay/epoxy nanocomposite", *Composites Science and Technology*, 2006; 66: 2415-2422.
7 –Brechet Y., Cavaile J.-Y. Y., Chabert E., Chazeau L., Dendievel R., Flandin L., Gauthier C., "Polymer based nanocomposites: effect of filler-filler and filler-matrix interactions", *Advanced Engineering Materials*, 2001; 3, No. 8: 571-577.
8 –Hashin Z., "Analysis of composite materials—a survey", *Journal of Applied Mechanics,* 1983; 50: 481–505.
9 -Christensen R. M., "A critical evaluation for a class of micromechanics models", *Journal of Mechanics and Physics of Solids*, 1990; 38: 379-404.
10 -Weng G. J. "Some elastic properties of reinforced solids with special reference to isotropic ones containing spherical inclusion", *International Journal of Engineering Science*, 1984; 22: 845-856.
11 –Mori T., Tanaka K., "Average stress in matrix and average elastic energy of materials with misfitting inclusions", *Acta Metallurgica*, 1973; 21: 571-574.
12 -Norris A. N., "The mechanical properties of platelet reinforced composites", *International Journal of Solids and Structures*, 1990; 26: 663-674.
13 -Papanicolaou G. C, Anifantis N. K., Keppas L. K., Kosmidou Th. V., "Stress analysis of short fiber-reinforced polymers incorporating a hybrid interphase region", *Composite Interfaces*, 2007; 14: 131-152.
14 -Shen L., Li J., "Effective elastic moduli of composite reinforced by particle or fiber with an inhomogenous interphase", *International Journal of Solids and Structures*, 2003; 40: 1393-1409.

15 -Odegard G. M., Clancy T. C., Gates T. S., “Modeling of the mechanical properties of nanoparticle/polymer composites”, *Polymer,* 2005; 46: 553-562.
16 -Wang J., Pyrz R., “Prediction of the overall moduli of layered silicate-reinforced nanocomposites-part II: analyses”, *Composites Science and Technology*, 2004; 64: 935-944.
17 -Giannelis E., “Polymer layered silicate nanocomposites”, *Advanced materials*, 1996; 8: 29-35.
18 -Maksimov R. D., Gaidukov S., Kalnins M., Zicans J., and Plume E., “A nanocomposite based on a styrene-acrylate copolymer and native montmorillonite clay. Part 2. Modeling the elastic properties”, *Mechanics of Composite Materials*, 2006; 42: 163- 172.

Konferences materiāls 3

Creep behavior of epoxy/clay nanocomposite

Glaskova T., Aniskevich A.

Institute of Polymer Mechanics, University of Latvia, Riga, Latvia

Proceedings of International Conference on Composite Materials, 2009, CD, No. F1:14.

CREEP BEHAVIOUR OF EPOXY/CLAY NANOCOMPOSITE

T. Glaskova, A. Aniskevich
Institute of Polymer Mechanics, University of Latvia
23, Aizkraules Str., Riga, LV-1006, Latvia
Tatjana.Glaskova@pmi.lv

SUMMARY

In the current study the peculiarities of creep behaviour of epoxy/clay nanocomposite (NC) under effect of moisture are estimated. The viscoelastic properties of NC were investigated experimentally and their dependence on filler and moisture effect was determined. The obtained results of uniaxial quasistatic tensile tests and creep tests were compared and effect of moisture and filler on NC and matrix properties was analyzed.

Keywords: nanoclay composites, moisture effect, viscoelastic properties, creep, tension

INTRODUCTION

Recently several works have been devoted to the investigation of creep behaviour of NC such as polyamide 66 filled with TiO_2 nanoparticles [1-3], polyamide 6 filled with layered silicate [4], starch-polycaprolactone blend filled with montmorillonite modified by quaternary ammonium salt [5] and polypropylene filled with shorter and longer aspect ratio multiwalled carbon nanotubes [6]. Creep behaviour is rather important property of polymer composites that determines their dimensional stability especially in applications where material should support loads for a long period of time [5].

It has been shown in the literature that the use of polymers filled with exfoliated layered silicate platelets instead of unfilled polymers can give an advantage - appreciable improvement in creep resistance [4, 5]. Due to large length to thickness ratio and high stiffness of the particles, the optimal properties could be reached at lower filler content than with the use of traditional minerals or fibre fillers [5]. Nevertheless the effect of moisture on creep behaviour of polymer containing nanoparticles is still unclear and hardly published. Due to moisture absorption glass transition temperature T_g can be reduced below the operating temperature and this strongly increases the creep compliance [4].

Therefore the aim of current investigation is to estimate peculiarities of tensile quasistatic and creep behaviour of epoxy/clay NC under effect of moisture. The creep behaviour of this NC is of crucial interest because it is investigated also close to its glass transition temperature.

EXPERIMENTAL

Bisphenol A epoxy resin was used as a matrix of the composite. The filler was intercalated octadecylamine modified montmorillonite-based organoclay. The filler content was varied from 0 till 6% by weight.

Moisture sorption experiments [7, 8] were performed in atmospheres with relative humidity φ = 24, 77, and 98% using desiccators with silica gel and saturated solution of salts NaCl and K_2SO_4. The moisture kinetics was measured until specimens reached the saturation level. The average equilibrium moisture content for NC was app. -0.4, 1.7 and 3.2 % for φ = 24, 77, and 98% with increase by app. 7 % for filler content changing from 0 to 6 % wt. At least four specimens of the same compositions were tested for each test. All the experiments were carried out at room conditions.

Quasi static tensile tests were performed with Zwick 2.5 at speed of 5 mm/min and creep tests at stress level equal to half of tensile strength for 7 h and recovery tests for 17 h for the specimens at room temperature. The decrease of tensile strength with increase of absorbed moisture content was taken into account. In order to estimate T_g of NC for all filler and moisture contents differential scanning calorimetry (DSC) analysis was applied using Mettler Toledo DSC device for temperature range from -50 to 150°C at heating rate 10°C/min.

RESULTS AND DISCUSSION

Thermal analysis

Using DSC analysis glass transition temperature of moistened NC with different filler content was determined. The results of the effect of filler and moisture content on T_g are given in Fig. 1. As seen from this figure glass transition temperature of NC remains nearly constant within one atmosphere and is about 50±0.4, 46±0.5 and 40±0.4 ºC in atmospheres with φ = 24, 77 and 98% RH.

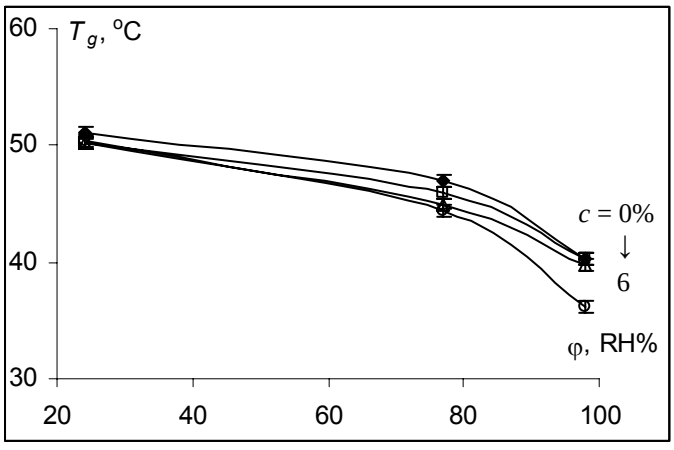

Fig. 1. Glass transition temperature versus relative humidity of atmosphere of NC with different filler content (numbers on the curves).

The slight reduction of NC T_g with increase of clay content indicates a possible lower crosslink density around the clay particle, perhaps due to the perturbing effects of the clay [11, 12] or/and interaction between polymer chains with the surface of the particles and consequent interphase formation between the silicate layers [13, 14].

Since glass transition temperature of moistened NC is rather close to room temperature and temperature of mechanical tests of NC peculiarities for short- and long-term deformability is of current interest.

Quasistatic tensile tests

Experimentally measured stress-strain curves of NC with c = 6% moistened at φ = 24, 77 and 98% RH are shown in Fig. 2. From these curves it could be observed that the effect of moisture on mechanical behaviour is substantial. Absorbed moisture essentially plasticizes the NC and changes its fracture character from brittle in dry atmosphere to plastic one in wet atmospheres.

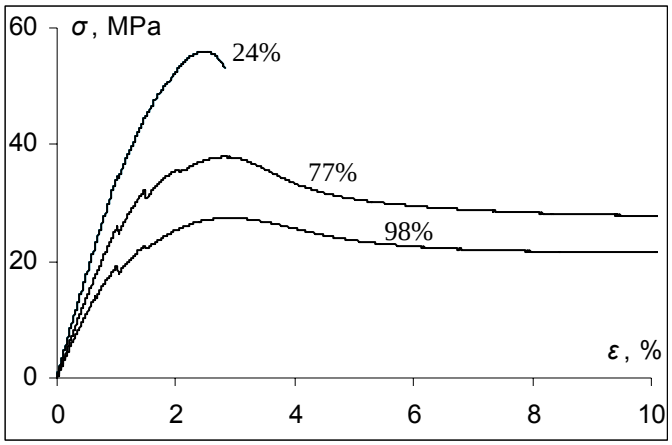

Fig. 2. Typical stress-strain curves at a fixed rate of deformation (v = 5 mm/min) for NC with c = 6% and φ = 24, 77 and 98% RH.

In order to examine the effect of organoclay content on mechanical properties, elastic modulus and tensile strength were plotted versus filler mass fraction (Fig. 3, 4). Tensile strength is defined as the maximal achieved value of stress in the specimen, and elastic modulus is calculated from the slope of a secant line between 0.05% and 0.25% strain on a stress-strain plot. It is clear from these figures that elastic modulus increases up to 20% and tensile strength of the NC decreases about the same value with the increase of organoclay content to 6% for atmosphere with 24% RH. The reduction of tensile strength in epoxy/clay systems could be attributed to the stress concentration effect of clay agglomerates [15]. The point is that non-exfoliated clay particles can form large agglomerates and as a result clay-matrix interactions decrease as clay content increase [15, 16]. In other words the reduction in interfacial interactions lowers the efficiency of the clay in strengthening of epoxy.

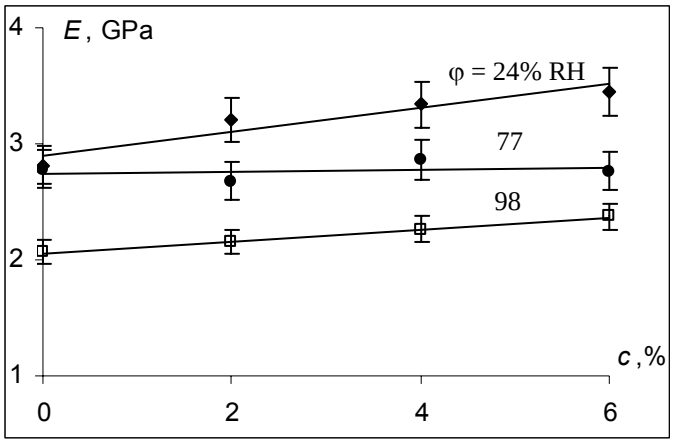

Fig. 3. Elastic modulus of NC in atmospheres with different relative humidity versus filler weight fraction.

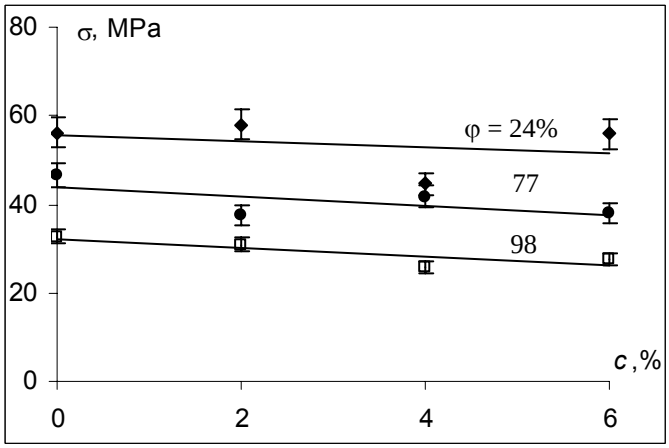

Fig. 4. Tensile strength of NC in atmospheres with different relative humidity versus filler weight fraction.

Figures 3 and 4 also show the quantitative effect of moisture on tensile strength and elastic modulus of NC. Tensile strength of moistened composite drops twice. Elastic modulus both of moistened pure epoxy resin and NC is reduced approximately 1/3 in comparison to initial state.

Creep tests

Creep performance is commonly represented by creep compliance *J(t)* and

$$J(t) = \frac{\varepsilon(t)}{\sigma},$$

where ε*(t)* is creep strain and σ is applied stress.

For dry atmosphere and NC with different filler content the creep compliance curves are given in Fig. 5. As seen from the figure the inclusion of clay nanoparticles into epoxy resin led to a sufficient reduction of creep compliance of NC specimens dried in atmosphere of 24% RH. Nevertheless for humid atmospheres absorbed moisture significantly affected creep behaviour, leading to high deformability.

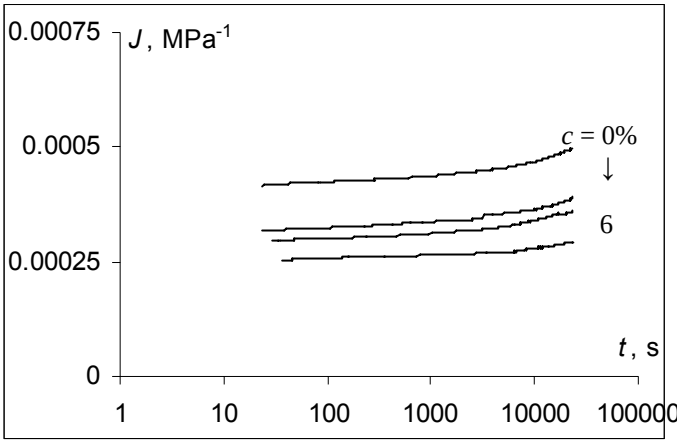

Fig. 5. Creep compliance curves of NC specimens saturated in atmosphere with 24% RH.

In Fig. 6 the creep curves for dried and moistened NC are superimposed on one reference curve by shifts along the time axis from the compliance curve obtained in dry atmosphere. The figure shows the reference curves for all filler contents. It can be seen that the curves have different shape. Obviously the creep compliance of NC in dry atmosphere is reduced in comparison with unfilled epoxy but with the increase of absorbed moisture content the plastization of the resin occurs (the mobility of polymer chains increases). The change of creep behaviour that led to increase of creep compliance with increase of filler content was possibly caused by morphological peculiarities of filler particles (the layered structure and the initial formation of aggregated stacks). Due to these factors the creep compliance could be increased by additional “sliding” of silicate nanoparticles within the layered stacks.

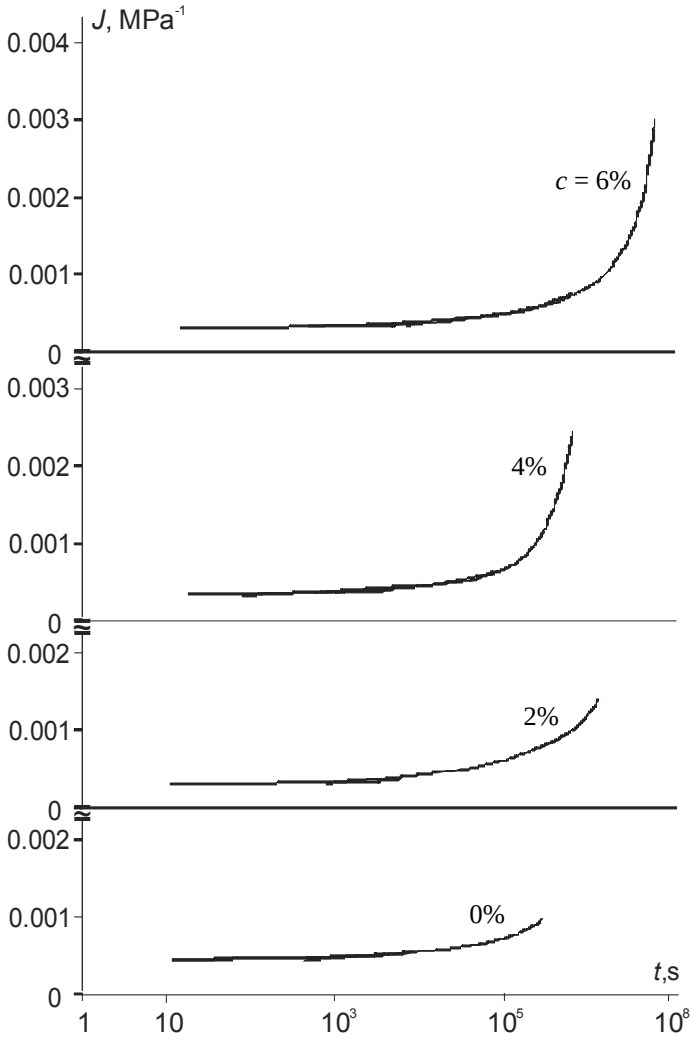

Fig. 6. Creep compliance for NC of different filler content (numbers on the curves) as a function of time. The overlapped curves represent the curves shifted over the time axis.

In order to estimate the effect of moisture on long-term deformability of NC the creep parameters should be clearly denoted. Fig. 7 shows a standard creep-recovery test with time-dependent deformation. The initial data obtained from creep curves are maximal deformation ε_{max}, elastic deformation ε_{el}, viscoelastic jump ε_{vej} and residual deformation ε_{res} after recovery test.

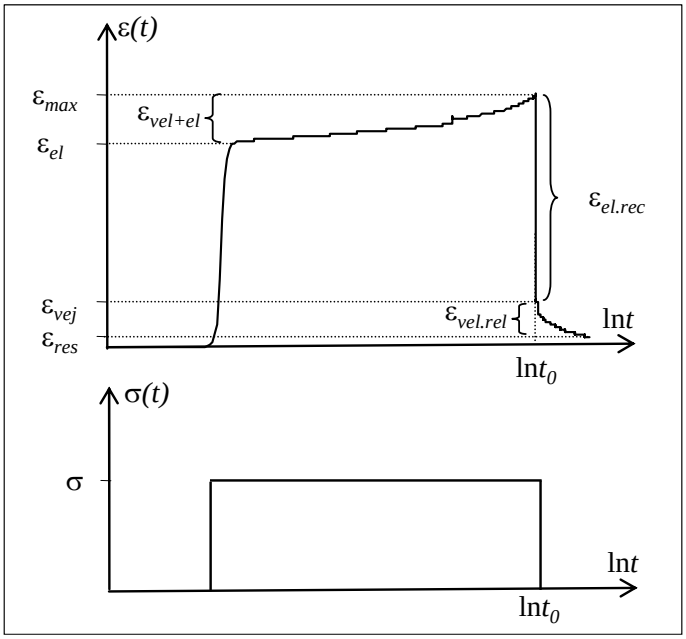

Fig. 7. A standard creep-recovery test.

Further calculations provide additional data such as viscoelastic and plastic deformation $\varepsilon_{vel+pl} = \varepsilon_{\max} - \varepsilon_{el}$, elastic recovery $\varepsilon_{el.rec} = \varepsilon_{\max} - \varepsilon_{vej}$, viscoelastic relaxation $\varepsilon_{vel.rel} = \varepsilon_{vep} - \varepsilon_{res}$, elastic modulus of composite at loading $E_l = \frac{\sigma}{\varepsilon_{el}}$ and unloading $E_{ul} = \frac{\sigma}{\varepsilon_{el.rec}}$.

It is obvious from Fig. 2 that the stress level (0.5 of tensile strength) used for creep tests is relatively far from yield stress of the NC at room temperature. At this case the dominant deformation mechanism of the polymers during creep is assumed to be mainly viscoelastic if T_g of NC is higher than test temperature [2].

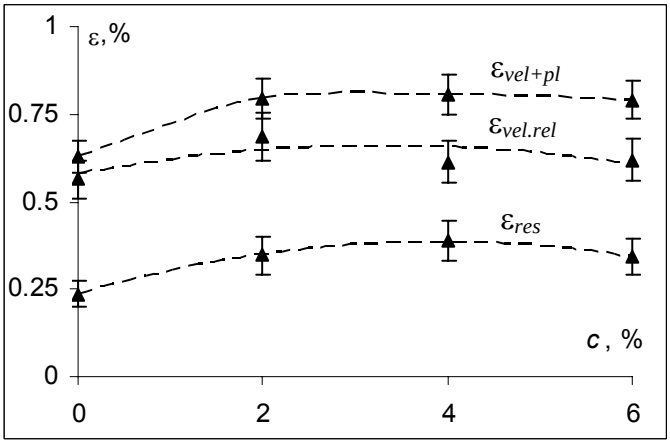

Fig. 8. Deformations - ε_{vel+pl}, $\varepsilon_{vel.rel}$ and ε_{res} versus filler content for atmosphere with 98% RH.

Since the most essential creep deformations were observed for NC specimens moistened in atmosphere with 98% RH, the special attention is given to estimate peculiarities of NC creep behaviour at these conditions. Fig. 8 shows the dependence of three creep parameters – viscoelastic plus plastic deformation, viscoelastic relaxation and residual (plastic) deformation on filler content. It can be observed that there is a good correlation between them. All the deformations increase with the increase of filler content till 6 %. Therefore it was confirmed that inclusion of clay nanoparticles to epoxy resin restricts the mobility of polymer chains in dry atmosphere and improves creep resistibility of the polymer, but absorbed moisture drastically plasticized the polymer (lowering T_g by 10 ^{o}C) and changed creep behaviour leading to the increase of creep compliance with the increase of filler content. Particularly high deformations were observed for the highest filler content in atmosphere with highest humidity which can be explained by additional "sliding" of silicate nanoparticles within the layered stacks.

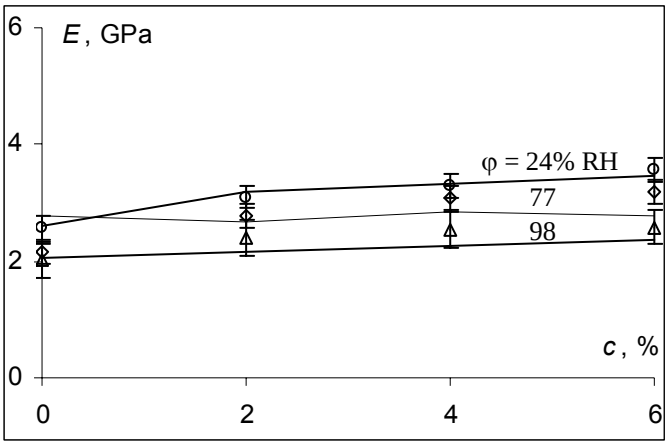

Fig. 9. Elastic modulus versus filler content (symbols – results of creep tests, curves – results of quasistatic tensile tests).

The results for elastic modulus obtained from quasistatic tensile tests and creep tests are compared in Fig. 9. It should be noted that elastic modulus for creep and recovery experiments almost coincide. It can be seen that results of quasistatic tensile tests and creep tests resemble. Elastic modulus in these tests increases by app. 30 (25)% with increase of filler content and decreases by app. 45 (40)% with increase of moisture content. As it was shown and discussed before in both tests moisture significantly affects behaviour of deformation, leading to high deformability especially in atmosphere with 98% RH.

CONCLUSIONS

In the present paper the effect of moisture absorption on the quasistatic tensile and creep behaviour of epoxy/clay NC was examined. From the above investigation the following conclusions may be derived:

- Results of quasistatic tensile tests and creep tests resemble. Elastic modulus in these tests increases by app. 30 (25)% with increase of filler content and decreases by app. 45 (40)% with increase of moisture content. In both tests

moisture significantly affects behaviour of deformation, leading to high deformability especially in atmosphere with 98% RH.

- Particularly high deformations were observed for the highest filler content in atmosphere with highest humidity which can be explained by "sliding" of clay platelets induced by plasticization of epoxy resin.
- It has been experimentally testified that inclusion of nanoparticles to polymer restricts the mobility of polymer chains in dry atmosphere and improves creep resistibility of the polymer, but moisture drastically plasticized polymer (by lowering its T_g by 10 ºC) and changed creep behaviour leading to increase of creep compliance with increase of filler content.
- The change of creep behaviour that led to increase of creep compliance with increase of filler content is possibly caused by morphological peculiarities of filler particles (the layered structure and the initial formation of aggregated stacks). Due to these factors the creep compliance could be increased by additional "sliding" of silicate nanoparticles within the layered stacks.

References

1. Zhang Zh., Yang J. –L., Friedrich K. Creep resistant polymeric nanocomposites, *Polymer*, 45, 2004, p. 3481-3485.
2. Starkova O., Yang J., Zhang Zh. Application of time-stress superposition to non-linear creep of polyamide 66 filled with nanoparticles of various size, Composites Science and Technology, 67, 2007, p. 2691-2698.
3. Yang J.-L., Zhang Zh., Schlarb A. K., Friedrich K. On the characterization of tensile creep resistance of polyamide 66 nanocomposites. Part II. Modelling and prediction o long-term performance, *Polymer*, 47, 2006, p. 6745-6758.
4. Vlasveld D. P. N., Bersee H. E. N., Picken S. J. Creep and physical ageing of PA6, *Polymer*, 46, 2005, p. 12539-12545.
5. Perez C. J., Alvarez V. A., Vazquez A. Creep behaviour of layered silicate/starch-polycaprolactone blends nanocomposites, *Materials Science and Engineering A*, 480, 2008, p.259-265.
6. Yang J.-L., Zhang Zh., Friedrich K., Schlarb A. K. Creep resistant polymer nanocomposites reinforced with multiwalled carbon nanotubes, *Macromolecular Rapid Communications*, 28, 2007, p.955-961.
7. Aniskevich A., Glaskova T., Spacek V., Sviglerova P. Effect of moisture sorption on deformability of epoxy/montmorillonite nanocomposite, *Proceedings of European Conference on Composite Materials*, 2005, CD, No. 091.
8. Glaskova T., Aniskevich A. Moisture absorption by epoxy/montmorillonite nanocomposite, submitted to *Composites Science and Technology*, 2009.
9. Zhou T. H., Ruan W. H., Yang J. L., Rong M. Zh., Zhang M. Q., Zhang Zh. A novel route for improving creep resistance of polymers using nanoparticles, *Composites Science and Technology*, 67, 2007, p. 2297-2302.

10. Wang Z. D., Zhao X. X. Modelling and characterization of viscoelasticity of PI/SiO2 nanocomposite films under constant and fatigue loading, *Materials Science and Engineering A*, 486, 2008, p. 517-527.

11. Liu, W., Hoa, S., Pugh, M. Organoclay-modified high performance epoxy nanocomposites. Composites Science and Technology, 2005, N 62, N 2, p. 307-316.

12. Jordan, J., Jacobs, K., Tannenbaum, R., Sharam, M., Jasiuk, I. Experimental trends in polymer nanocomposites – a review. *Materials Science and Engineering A*, 2004, Vol. 393, N 1, p.1 - 11.

13. Yasmin A., Luo J. J., Abot J. L., Daniel I. M. Mechanical and thermal behaviour of clay/epoxy nanocomposite, *Composites Science and Technology*, 66, 2006, p. 2415-2422.

14. Yoon P. J., Fornes T. D., Paul D. R. Thermal expansion behaviour of nylon 6 nanocomposite, *Polymer*, 43, 2002, p. 6727-6741.

15. Akbari bB., Bagheri R. Deformation mechanism of epoxy/clay nanocomposite, *European Polymer Journal*, 43, 2007, p. 782-788.

16. Isik I., Yilmazer U., Bayram G. Impact modified epoxy/montmorillonite nanocomposites: synthesis and characterization, *Polymer*, 44, 2003, p. 6371-6377.